



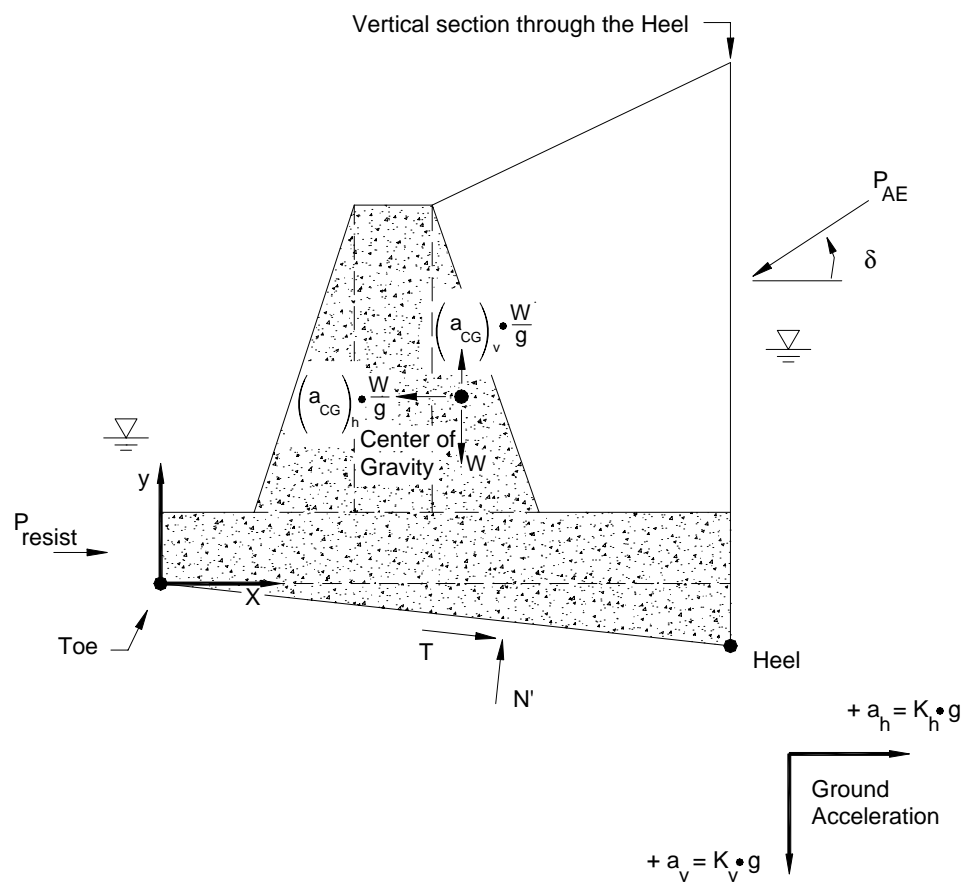
**US Army Corps  
of Engineers®**  
Engineer Research and  
Development Center

*Infrastructure Technology Research Program  
Navigation Systems Research Program*

## **Translational Response of Toe-Restrained Retaining Walls to Earthquake Ground Motions Using CorpsWallSlip (CWSlip)**

Robert M. Ebeling, Amos Chase, and Barry C. White

June 2007



# **Transitional Response of Toe-Restrained Retaining Walls to Earthquake Ground Motions Using Corps WallSlip (CWSlip)**

Robert M. Ebeling

*Information Technology Laboratory  
U.S. Army Engineer Research and Development Center  
3909 Halls Ferry Road  
Vicksburg, MS 39180-6199*

Amos Chase

*Science Applications International Corporation  
3532 Manor Drive, Suite 4  
Vicksburg, MS 39180*

Barry C. White

*Information Technology Laboratory  
U.S. Army Engineer Research and Development Center  
3909 Halls Ferry Road  
Vicksburg, MS 39180-6199*

Final report

Approved for public release; distribution is unlimited.

Prepared for U.S. Army Corps of Engineers  
Washington, DC 20314-1000

Under Work Unit 4402JC

**Abstract:** This research report describes the engineering formulation and corresponding software developed for the translational response of rock-founded retaining walls buttressed at their toe by a reinforced concrete slab to earthquake ground motions. The PC software CorpsWallSlip (sometimes referred to as CWSlip) was developed to perform an analysis of the permanent sliding displacement response for each proposed retaining wall section to either a user-specified earthquake acceleration time-history via a Complete Time-History Analysis or to user-specified peak ground earthquake response values via a Simplified Sliding Block Analysis. The resulting engineering methodology and corresponding software is applicable to a variety of retaining walls that are buttressed at their toe by a structural feature (e.g., navigation walls retaining earth, spillway chute walls, spillway discharge channel walls, approach channel walls to outlet works structures, highway and railway relocation retaining walls, and floodwall channels). CorpsWallSlip is particularly applicable to L-walls and T-walls (usually referred to as cantilever retaining walls). It may also be used to predict permanent seismically induced displacements on retaining walls without a toe restraint. Companion PC software, CorpsWallRotate, was developed to perform an analysis of permanent wall rotation. Both CorpsWallSlip and CorpsWallRotate software perform engineering calculations that help the engineer in assessment of the tendency for a retaining wall to slide or to rotate during earthquake shaking.

Formal consideration of the permanent seismic wall displacement in the seismic design process for Corps-type retaining structures is given in Ebeling and Morrison (1992). The key aspect of the engineering approach presented in this 1992 document is that simplified procedures for computing the seismically induced earth loads on Corps retaining structures are also dependent upon the amount of permanent wall displacement that is expected to occur for each specified design earthquake. The Ebeling and Morrison simplified engineering procedures for Corps retaining structures, including waterfront retaining structures, are geared towards hand calculations. The engineering formulation and corresponding PC software CorpsWallSlip discussed in this report extend these simplified procedures to walls that slide during earthquake shaking and make possible the use of acceleration time-histories in the Corps design/analysis process when time-histories are made available on Corps projects. The engineering methods contained in this report and implemented within CorpsWallSlip allow the engineer to rapidly determine if a given retaining wall system has a tendency to slide or to rotate for a specified seismic event.

**DISCLAIMER:** The contents of this report are not to be used for advertising, publication, or promotional purposes. Citation of trade names does not constitute an official endorsement or approval of the use of such commercial products. All product names and trademarks cited are the property of their respective owners. The findings of this report are not to be construed as an official Department of the Army position unless so designated by other authorized documents.

**DESTROY THIS REPORT WHEN NO LONGER NEEDED. DO NOT RETURN IT TO THE ORIGINATOR.**

# Contents

<b>Figures and Tables.....</b>	<b>vii</b>
<b>Preface.....</b>	<b>x</b>
<b>Considerations for Assigning Shear Strength Parameters.....</b>	<b>xii</b>
<b>Assumption Made for the Soil Driving Wedge in a Cohesive Soil .....</b>	<b>xiii</b>
<b>1 Introduction to Translational Response of Toe-Restrained Retaining Walls to Earthquake Ground Motions.....</b>	<b>1</b>
1.1 Introduction .....	1
1.1.1 Pseudo-static methods with a preselected seismic coefficient.....	4
1.1.2 Stress-deformation methods.....	7
1.1.3 Sliding block methods.....	11
1.2 New rotational analysis model based on a rigid block problem formulation .....	21
1.3 Tendency of a retaining wall to slide or to rotate during earthquake shaking .....	24
1.4 Seismic design criteria for Corps retaining structures .....	25
1.5 Axial load capacity of spillway invert slabs.....	27
1.6 Background and research objective.....	28
1.7 Organization of report .....	30
<b>2 New Translational Block Analysis Model of a Retaining Structure Buttressed by a Reinforced Concrete Slab .....</b>	<b>32</b>
2.1 Introduction .....	32
2.2 Contrasting a translational with the rotational analysis of a rigid block .....	33
2.3 Maximum transmissible acceleration .....	34
2.4 Time-history of permanent wall displacement.....	40
2.4.1 Introduction to a step-by-step solution scheme .....	40
2.4.2 Positive relative accelerations $relA0$ and $relA1$ at times $t_i$ and $t_{i+1}$ .....	44
2.4.3 Positive relative acceleration $relA0$ at time $t_i$ and negative relative acceleration $relA1$ at $t_{i+1}$ .....	46
2.4.4 Negative relative accelerations $relA0$ and $relA1$ at times $t_i$ and $t_{i+1}$ .....	52
2.4.5 Positive relative acceleration $relA0$ at time $t_i$ and negative relative acceleration $relA1$ at $t_{i+1}$ .....	56
2.4.6 Starting the $C_{CorpsWallSlip}$ analysis and the initiation of wall translation during a DT time-step .....	61
2.4.7 Cessation of wall translation .....	62
2.5 New translational analysis model of a wall retaining a partially submerged backfill and buttressed by a reinforced concrete slab.....	63
2.5.1 Introduction .....	63
2.5.2 Threshold value of acceleration corresponding to incipient lateral translation of the retaining wall – partially submerged backfill .....	65

2.5.3 Numerical method for computing the translational time-history of a rigid block retaining structure.....	71
2.6 Vertical acceleration in the new translational analysis model of a wall retaining a partially submerged backfill and buttressed by a reinforced concrete slab.....	71
2.7 Simplified Newmark sliding block permanent displacement analysis .....	74
2.7.1 Ambraseys and Menu (1988) mean and 95% confidence relationships.....	75
2.7.2 Cai and Bathurst (1996) mean upper bound relationship for the Franklin and Chang (1977) data.....	76
2.7.3 Cai and Bathurst (1996) mean upper bound relationship for the Newmark (1965) data .....	77
2.7.4 Whitman and Liao (1985a and 1985b) mean and 95 percent confidence relationships.....	77
2.7.5 Richards and Elms (1979) upper bound relationship for the Franklin and Chang (1977) data.....	78
2.7.6 Makdisi and Seed (1978) range in displacements for (Richter) magnitude 6.5, 7.5, and 8.25 events.....	79
<b>3 Threshold Value of Acceleration Corresponding to Incipient Lift-Off of the Base of the Wall in Rotation .....</b>	<b>80</b>
3.1 Introduction .....	80
3.2 Threshold value of acceleration corresponding to incipient lift-off of the base of a wall, retaining moist backfill, in rotation.....	81
3.3 Threshold value of acceleration corresponding to incipient lift-off of the base of a wall, retaining a partially submerged backfill, in rotation.....	85
3.3.1 Water pressures acting on the structural wedge .....	86
3.3.2 Threshold value of acceleration corresponding to incipient lift-off of the base of the wall in rotation – partially submerged backfill .....	88
<b>4 The Visual Modeler and Visual Post-Processor – Corps WallSlip .....</b>	<b>91</b>
4.1 Introduction .....	91
4.2 Visual modeler and visual post-processor .....	91
4.2.1 Introduction to the visual modeling environment.....	91
4.2.2 Earthquake time-history input.....	93
4.2.3 Selection of the simplified sliding block methods of analysis and peak ground motion parameter input data .....	96
4.2.4 Structural geometry input.....	99
4.2.5 Structural wedge data.....	110
4.2.6 Driving wedge data .....	113
4.2.7 Analysis results and visual post-processor.....	116
4.2.8 Example 1 – Earth retaining wall at a dry soil site – No reinforced concrete slab buttress at the wall’s toe .....	120
4.2.9 Example 2 – Earth retaining wall at a dry soil site – 1-foot-thick reinforced concrete slab buttress at the wall’s toe.....	129
4.2.10 Example 3 – Earth retaining wall at a dry soil site – No reinforced concrete slab buttress at the wall’s toe (no time-histories).....	133

<b>5 Summary, Conclusions, and Recommendations.....</b>	<b>140</b>
5.1 Summary and conclusions.....	140
5.2 Recommendations for future research .....	142
<b>References.....</b>	<b>145</b>
<b>Appendix A: Computation of the Dynamic Active Earth Pressure Forces for a Partially Submerged Retained Soil Using the Sweep-Search Wedge Method.....</b>	<b>150</b>
A.1 Introduction .....	150
A.2 Dynamic Active Earth Pressure Force, $P_{AE}$ — Effective Stress Analysis.....	152
A.2.1 Calculation of Water Pressure Forces for a Hydrostatic Water Table .....	154
A.2.2 Static Water Pressure Forces Acting on the Wedge.....	154
A.2.3 Equilibrium of Vertical Forces.....	155
A.2.4 Equilibrium of Forces in the Horizontal Direction.....	155
A.3 Static Active Earth Pressure Force, $P_A$ — Effective Stress Analysis .....	157
A.4 Dynamic Active Earth Pressure Force, $P_{AE}$ — Total Stress Analysis .....	160
A.5 Static Active Earth Pressure Force, $P_A$ — Total Stress Analysis .....	161
A.6 Weight Computation of a Soil Wedge with a Bilinear Ground Surface .....	164
A.6.1 $\alpha$ greater than $\alpha_{corner}$ .....	164
A.6.2 $\alpha_{corner}$ greater than $\alpha$ .....	169
<b>Appendix B: Dynamic Active Earth Pressure Force, <math>P_{AE}</math> and its Point of Application, <math>h_{PAE}</math> .....</b>	<b>177</b>
<b>Appendix C: An Approach for Computing the Dynamic Active Earth Pressure Distribution for a Partially Submerged Retained Soil .....</b>	<b>183</b>
C.1 Earth Pressure Distribution for the Dynamic Active Earth Pressure Force, $P_{AE}$ , of a Partially Submerged, Cohesionless, Level Backfill – Effective Stress Analysis with $c'$ Equal to Zero .....	183
Step 1: Convert the static active earth pressure force, $P_A$ , into an equivalent active earth pressure diagram .....	184
Step 2: Create an incremental dynamic force component pressure diagram .....	188
Step 3: Create the dynamic active earth pressure diagram.....	189
Step 4: Complete the pressure diagram by adding in the pore water pressure distribution.....	189
C.2 Earth Pressure Distribution for the Static Active Earth Pressure Force, $P_A$ , Component of $P_{AE}$ of a Cohesionless, Backfill with a Sloping or a Bilinear Ground Surface – Effective Stress Analysis with $c'$ Equal to Zero.....	191
C.2.1 Basic Procedure to Compute the Active Effective Stress Distribution Corresponding to $P_A$ for a Moist Retained Soil with a Sloping Ground Surface .....	191
C.2.2 Basic Procedure to Compute the Active Effective Stress Distribution Corresponding to $P_A$ for a Partially Submerged Retained Soil with a Sloping Ground Surface .....	193
C.2.3 Basic Procedure to Compute the Active Effective Stress Distribution Corresponding to $P_A$ for a Partially Submerged Retained Soil with a Bilinear Ground Surface .....	195

C.3 Earth Pressure Distribution for the Dynamic Active Earth Pressure Force $P_{AE}$ for a Backfill with Mohr-Coulomb Shear Strength Parameters $c'$ and $\phi'$ - Effective Stress Analysis .....	197
C.3.1 Basic Procedure to Compute the Active Effective Stress Distribution Corresponding to $P_A$ for a Partially Submerged Retained Soil with a Sloping Ground Surface .....	204
C.3.2 Basic Procedure to Compute the Active Effective Stress Distribution Corresponding to $P_A$ for a Partially Submerged Retained Soil with a Bilinear Ground Surface .....	206
C.4 Earth Pressure Distribution for the Dynamic Active Earth Pressure Force, $P_{AE}$ , for a Backfill with Mohr-Coulomb Shear Strength Parameters, $S_u$ - Total Stress Analysis .....	208
C.4.1 Basic Procedure to Compute the Active Total Stress Distribution Corresponding to $P_A$ for a Partially Submerged Retained Soil with a Sloping Ground Surface .....	213
C.4.2 Basic Procedure to Compute the Active Total Stress Distribution Corresponding to $P_A$ for a Partially Submerged Retained Soil with a Bilinear Ground Surface .....	215
<b>Appendix D: Water Pressures Acting on a Partially Submerged Structural Wedge .....</b>	<b>218</b>
D.1 Steady-State Water Pressures Acting on the Structural Wedge.....	218
D.2 Westergaard Procedure for Computing Hydrodynamic Water Pressures .....	223
<b>Appendix E: Structural Wedge Rigid Body Mass and Mass Moment of Inertia Computations .....</b>	<b>227</b>
E.1 Mass and Center of Gravity of the Structural Wedge.....	227
E.2 Mass Moment of Inertia of the Structural Wedge .....	229
E.2.1 Mass Moment of Inertia of a Rectangle.....	231
E.2.2 Mass Moment of Inertia of a Triangle .....	232
E.2.3 Mass Moment of Inertia of the Structural Wedge .....	234
<b>Appendix F: Listing and Description of CorpsWallSlip ASCII Input Data File (filename: CWROTATE.IN).....</b>	<b>235</b>
<b>Appendix G: Listing of CorpsWallSlip ASCII Output Files .....</b>	<b>247</b>
<b>Appendix H: Earth Pressure Distribution and Depth of Cracking in a Cohesive Retained Soil – Static Active Earth Pressures .....</b>	<b>250</b>
H.1 Example No. 1: Effective Stress Analysis of a Cohesive Soil.....	251
H.2 Example No. 2: Total Stress Analysis of a Cohesive Soil .....	253

# Figures and Tables

## Figures

Figure 1.1. Translational response of a cantilever retaining wall with a permanent earthquake-induced sliding displacement, $\Delta_s$ .....	2
Figure 1.2. Rotational response of a cantilever retaining wall with a permanent earthquake induced rotation, $\theta_r$ .....	3
Figure 1.3. Rock-founded cantilever retaining wall bordering a spillway channel. ....	3
Figure 1.4. Gravity retaining wall and driving soil wedge treated as a rigid body.....	5
Figure 1.5. Simplified driving wedge method of analysis and the Mononobe-Okabe active earth pressure force relationship. ....	7
Figure 1.6. Elements of the Newmark (rigid) sliding block method of analysis. ....	14
Figure 1.7. Gravity retaining wall and failure wedge treated as a sliding block.....	18
Figure 1.8. Incremental failure by base sliding. ....	18
Figure 1.9. Permanent, seismically induced displacement of a rock-founded cantilever wall retaining moist backfill and with toe restraint, computed using CorpsWallSlip. ....	20
Figure 1.10. Idealized permanent, seismically induced displacement due to the rotation about the toe of a rock-founded wall retaining moist backfill, with toe restraint, computed using CorpsWallRotate.....	22
Figure 1.11. Permanent, seismically induced displacement due to the rotation about the toe of a rock-founded, partially submerged cantilever retaining wall and with toe restraint, computed using CorpsWallRotate. ....	23
Figure 1.12. Structural wedge with toe resistance retaining a driving soil wedge with a bilinear moist slope (i.e., no water table) analyzed by effective stress analysis with full mobilization of $(c', \phi')$ shear resistance within the backfill. ....	24
Figure 2.1. Permanent, seismically induced displacement of a rock-founded cantilever wall retaining moist backfill and with toe restraint, computed using CorpsWallSlip. ....	33
Figure 2.2. Inertia forces and resultant force vectors acting on a rigid block model of a cantilever wall retaining moist backfill with sliding along its base during horizontal and vertical shaking of the inclined rigid base. ....	36
Figure 2.3. Complete equations for relative motions over time increment $\Delta T$ based on linearly varying acceleration.....	42
Figure 2.4. Relative velocity and displacements at the end of time increment $\Delta T$ based on linearly varying relative acceleration. ....	45
Figure 2.5. Two possible outcomes for the case of a negative relative acceleration at time $t_i$ and a positive relative acceleration at time $t_{i+1}$ . ....	47
Figure 2.6. Two possible outcomes for the case of negative relative accelerations at times $t_i$ and $t_{i+1}$ . ....	52
Figure 2.7. Two possible outcomes for the case of a positive relative acceleration at time $t_i$ and a negative relative acceleration at time $t_{i+1}$ . ....	57
Figure 2.8. Control points, water pressures, and corresponding resultant forces acting normal to faces of the three regions of a structural wedge sliding along its base – effective stress analysis.....	64



Figure 2.9. Inertia forces and resultant force vectors acting on a rigid block model of a (inclined base) cantilever wall retaining a partially submerged backfill with sliding along the base of the wall during earthquake shaking of the inclined rigid base – effective stress analysis. ....	65
Figure 3.1. Idealized permanent, seismically induced displacement due to the rotation about the toe of a rock-founded wall retaining moist backfill, with toe restraint, computed using CorpsWallRotate.....	81
Figure 3.2. Free-body and kinetic diagrams of a rigid block model of a cantilever wall retaining moist backfill with rotation about the toe of the wall during horizontal and vertical shaking of the rigid level base. ....	84
Figure 3.3. Inertia forces and resultant force vectors acting on a rigid block model of a cantilever wall retaining moist backfill with rotation about the toe of the wall during horizontal and vertical shaking of the rigid level base. ....	84
Figure 3.4. Control points, water pressures, and corresponding resultant forces acting normal to faces of the three regions of a structural wedge rotating about its toe – effective stress analysis. ....	87
Figure 3.5. Inertia forces and resultant force vectors acting on a rigid block model of a (inclined base) cantilever wall retaining a partially submerged backfill with rotation about the toe of the wall during horizontal and vertical shaking of the inclined rigid base – effective stress analysis.....	88
Figure 4.1. The <b>Introduction</b> tab features and idealized structural wedge diagram – complete time-history analysis.....	93
Figure 4.2. A strong earthquake time-history ground motion shown in the <b>Earthquake</b> tab.....	94
Figure 4.3. The <b>Introduction</b> tab features and idealized structural wedge diagram – simplified sliding block method of analysis. ....	97
Figure 4.4. Simplified sliding block method of <b>Analysis</b> tab.....	98
Figure 4.5. Dynamic forces acting on the free-body section of the structural wedge and its material regions.....	100
Figure 4.6. Examples of width and height definition for each of the ten structural wedge material regions.....	101
Figure 4.7. Examples of structural wedge material regions. ....	102
Figure 4.8. The input <b>Geometry</b> tab in action. ....	107
Figure 4.9. Boundary water pressure diagram – full contact along the base of the retaining wall with its foundation in a sliding block analysis.....	109
Figure 4.10. Summary of the user-defined geometry and computed weight, mass, and moments of inertia for the structural wedge as defined in the <b>Geometry</b> tab. ....	109
Figure 4.11. Defining the material properties of the <b>Structural Wedge</b> tab for an effective stress analysis. ....	111
Figure 4.12. Defining the material properties of the <b>Structural Wedge</b> tab for a total stress analysis. ....	112
Figure 4.13. Defining the material properties in the <b>Driving Wedge</b> tab - effective stress method of analysis.....	114
Figure 4.14. Defining the material properties in the <b>Driving Wedge</b> tab - total stress method of analysis.....	115
Figure 4.15. The <b>Analysis</b> tab.....	117
Figure 4.16. Rock-founded earth retaining wall for Example 1. ....	121

Figure 4.17. Data contained within the input <b>Geometry</b> tab for Example 1. ....	122
Figure 4.18. The final <b>Analysis</b> tab for Example 1. ....	124
Figure 4.19. Time-history of the evaluation of the effective vertical acceleration. ....	125
Figure 4.20. Newmark sliding block time-history results for Example 1.....	127
Figure 4.21. Rock-founded earth retaining wall buttressed at the toe of the wall by a 1-ft thick reinforced concrete slab for Example 2. ....	129
Figure 4.22. The input <b>Geometry</b> tab for Example 2.....	130
Figure 4.23. The final <b>Analysis</b> tab for Example 2.....	132
Figure 4.24. Simplified sliding block method of <b>Simplified Analysis</b> tab for Example 3.....	135
Figure 4.25. <b>Analysis</b> tab for Example 3 simplified sliding block analysis.....	136

## Tables

Table 1.1. Approximate magnitudes of movements required to reach minimum active earth pressure conditions (after Clough and Duncan (1991)). ....	6
Table 4.1. Assessment of <b>Constant Y Acceleration</b> , the effective vertical acceleration for Example 1.....	123
Table 4.2. Assessment of <b>Constant Y Acceleration</b> , the effective vertical acceleration for Example 2. ....	132

## Preface

This research report describes the engineering formulation and corresponding software developed for the translational response of retaining walls buttressed at their toe by a reinforced concrete slab to earthquake ground motions. The PC software *CorpsWallSlip* (sometimes referred to as *CWSlip*) was developed to perform an analysis of the permanent sliding displacement response for each proposed retaining wall section to either a user-specified earthquake acceleration time-history via a Complete Time-History Analysis or to user-specified peak ground earthquake response values via a Simplified Sliding Block Analysis. Funding to initiate research and software development was provided by Headquarters, U.S. Army Corps of Engineers (HQUSACE), as part of the Infrastructure Technology Research Program. Funding to conclude this research task, including software development, was provided by the Navigation Systems Research Program. The research was performed under Work Unit 4402JC, entitled “Soil-Structure Interaction for Seismic Evaluation of Earth-Retaining Lock and Cantilever Walls,” for which Dr. Robert M. Ebeling, Engineering Informatics Systems Division (EISD), Information Technology Laboratory (ITL), U.S. Army Engineer Research and Development Center (ERDC), Vicksburg, MS, was the Principal Investigator. The HQUSACE Technical Monitor was Anjana Chudgar.

James E. Clausner, Coastal and Hydraulics Laboratory, ERDC, was the Navigation Systems Research Program Manager. Dr. Michael K. Sharp, Geotechnical and Structures Laboratory, ERDC, was the Acting Technical Director for Navigation. Angela Premo, U.S. Army Engineer Division, South Atlantic, was the Navigation Business Line Leader, HQUSACE.

The resulting engineering methodology and corresponding software is applicable to a variety of retaining walls that is buttressed at their toe by a structural feature (e.g., navigation walls retaining earth, spillway chute walls, spillway discharge channel walls, approach channel walls to outlet works structures, highway and railway relocation retaining walls, and flood wall channels). *CorpsWallSlip* is particularly applicable to L-walls and T-walls (usually referred to as cantilever retaining walls). It may also be used to predict permanent seismically induced displacements on retaining walls without a toe restraint. Companion PC software, *CorpsWallRotate*, was

developed to perform an analysis of permanent wall rotation. Both CorpsWallSlip and CorpsWallRotate software performs engineering calculations that help the engineer in their assessment of the tendency for a retaining wall to slide or to rotate during earthquake shaking.

This report was prepared by Dr. Ebeling, Amos Chase, Science Applications International Corporation, Vicksburg, MS, and by Barry C. White, Computational Science and Engineering Branch, ITL. Dr. Ebeling was author of the scope of work for this research. The report was prepared by Dr. Ebeling under the supervision of Dr. Cary D. Butler, Chief, EISD, and Dr. Jeffery P. Holland, Director, ITL. During the publication of this report John E. West was Acting Assistant Director of ITL, and Dr. Deborah F. Dent was Acting Director.

COL Richard B. Jenkins was Commander and Executive Director of ERDC. Dr. James R. Houston was Director.

### Considerations for Assigning Shear Strength Parameters

A key item in the permanent deformation and permanent rotation analysis of a Corps earth retaining structure using the PC-based software, CorpsWallSlip, described in this report, is the selection of suitable shear strength parameters. In an effective stress analysis, the issue of the suitable friction angle is particularly troublesome when the peak friction angle is significantly greater than the residual friction angle. In the displacement controlled approach examples given in Section 6.2 of Ebeling and Morrison (1992), effective stress based shear strength parameters (i.e., effective cohesion  $c'$  and effective angle of internal friction  $\phi'$ ) were used to define the shear strength of the dilative granular backfills, *with  $c'$  set equal to zero in all cases due to the level of deformations anticipated in a sliding block analysis during seismic shaking.* In 1992 Ebeling and Morrison concluded that it is conservative to use the residual friction angle in a sliding block analysis, and this should be the usual practice for displacement based analysis of granular retained soils. The primary author of this report would broaden the concept to the assignment of effective (i.e.,  $c'$  and  $\phi'$ ) or total (i.e., undrained  $S_u$ ) shear strength parameters for the retained soil be consistent with the level of shearing-induced deformations encountered for each design earthquake in a rotational analysis and note that active earth pressures are used to define the loading imposed on the structural wedge by the driving soil wedge. (Refer to Table 1.1 in this report for guidance regarding wall movements required to fully mobilize the shear resistance within the retained soil during earthquake shaking.) In an effective stress analysis, engineers are cautioned to carefully consider the reasonableness of including a nonzero value for effective cohesion  $c'$  in their permanent deformation and permanent rotation analyses.

### Assumption Made for the Soil Driving Wedge in a Cohesive Soil

C<sub>orps</sub>W<sub>all</sub>Slip performs a permanent displacement analysis of a retaining wall due to earthquake shaking. Reversal in the direction of the horizontal component of the time-history of earthquake ground shaking occurs many times during the typical tens of seconds of ground motion. Consequently, a reversal in direction of the inertial force imparted to the structural wedge and to the soil driving wedge occurs many times during the course of the analysis using C<sub>orps</sub>W<sub>all</sub>Slip. In a traditional soil wedge formulation for static loading, a crack is typically considered to exist within the upper portion of the soil driving wedge for a cohesive soil (with shear strength,  $S_u$ , specified in a total stress analysis or  $c'$  specified in an effective stress analysis) and the planer wedge slip surface is terminated when it intersects the zone of cracking at a depth,  $d_{\text{crack}}$ , below the ground surface (e.g., see Appendix H in EM 1110-2-2502). This assumption is not made in the C<sub>orps</sub>W<sub>all</sub>Slip formulation for *dynamic loading*. Instead, it is assumed that in the dynamic wedge formulation, the crack within the zone of cracking at the top of the retained cohesive soil of the driving wedge will not remain open during earthquake shaking *due to the inertial load direction reversals* during this time-history based C<sub>orps</sub>W<sub>all</sub>Slip analysis. So, even for cohesive soils the planar slip surface, obtained from the sweep-search method of analysis of the driving wedge used by C<sub>orps</sub>W<sub>all</sub>Slip to obtain a value for the earthquake induced resultant driving force  $P_{AE}$  (acting on the structural wedge), extends uninterrupted within the driving soil wedge (in the retained soil) to the ground surface and is not terminated by a vertical crack face to the ground surface when it enters the zone of cracking.

In order to assign a location to  $P_{AE}$ , the static value for active earth pressure force,  $P_A$ , is needed (refer to Equation B.2 in Appendix B for the level ground, moist backfill case and to Appendix C for all other cases). C<sub>orps</sub>W<sub>all</sub>Slip proceeds with the computation of  $h_{PAE}$ , the location of the resultant force  $P_{AE}$ , using the value for  $P_A$  computed by procedure discussed in Appendix A. The computation of  $h_{PAE}$  by C<sub>orps</sub>W<sub>all</sub>Slip is described in Appendix C.

In a traditional soil wedge formulation for static loading, a crack is typically considered to exist within the upper portion of the soil driving wedge for a cohesive soil and the planer wedge slip surface is terminated when it intersects the zone of cracking at a depth,  $d_{\text{crack}}$ , below the ground surface (e.g., see Appendix H in EM 1110-2-2502). This assumption is made in the C<sub>orps</sub>W<sub>all</sub>Slip formulation for static loading force  $P_A$  (but not when computing  $P_{AE}$  for dynamic loading). A sweep-search wedge method of analysis as discussed in Appendix A is used by the C<sub>orps</sub>W<sub>all</sub>Slip to determine the value of the active earth pressure force,  $P_A$ .

Earth pressure distributions and depth of cracking: The earth pressure distribution applied to the structural wedge by the driving soil wedge in a CorpsWallSlip analysis is made up of two components, the earth pressure distribution due to the static active earth pressures and a trapezoidal earth pressure distribution due to the incremental dynamic force component,  $\Delta P_{AE}$  (with  $\Delta P_{AE} = P_{AE} - P_A$ ). The methodologies discussed in Appendix A are used by CorpsWallSlip to first determine the resultant earth pressure forces  $P_A$  and  $P_{AE}$  and then the methodologies discussed in Appendix C are used to compute the resulting earth pressure distributions for  $P_A$  and  $\Delta P_{AE}$ , respectively. In order to compute values of  $P_{AE}$  and  $P_A$  by the dynamic and static sweep-search solutions of trial soil wedges, a depth of cracking needs to be specified in each sweep-search analysis made by CorpsWallSlip of a cohesive soil. Initial sweep-search soil wedge solutions are always made assuming a zero depth of crack. This is deemed sufficient for all  $P_{AE}$  computations, as discussed previously. However, an iterative procedure is used to determine the value for the depth of cracking in the analysis of  $P_A$  in cohesive soils and the corresponding earth pressure distribution (which includes both compression as well as tensile stresses). After the resulting static earth pressure force,  $P_A$ , computation is completed, a resulting earth pressure distribution is constructed and new depth of cracking for static loading is determined. CorpsWallSlip then proceeds with second sweep-search trial wedge analysis of the retained soil for a new value for  $P_A$  corresponding to this new, nonzero crack depth value. A new static earth pressure distribution and a third value for crack depth is then determined. The process is repeated until the depth of cracking used in the sweep-search trial wedge analysis and the depth of cracking determined from the static active earth pressure distribution are nearly the same value.

In the special case of cohesive soils, the CorpsWallSlip analysis disregards the tensile stresses when defining the static active earth pressures and the corresponding resulting static active earth pressure force to be applied to the structural wedge, as well as when computing the resulting force location  $h_{PA}$  of this modified stress distribution. A trapezoidal earth pressure distribution is used to define  $\Delta P_{AE}$  for cohesive as well as cohesionless soils.

# **1 Introduction to Translational Response of Toe-Restrained Retaining Walls to Earthquake Ground Motions**

## **1.1 Introduction**

Engineering formulations and software provisions based on sound seismic engineering principles are needed for a wide variety of the Corps retaining walls that (1) rotate or (2) slide (i.e., translate) during earthquake shaking and (3) for massive concrete retaining walls constrained to rocking. The engineering formulation discussed in this report was developed to address the second of these three different modes of retaining wall responses to earthquake shaking.

This research report describes the engineering formulation developed for the permanent translational response, including permanent displacement, of rock-founded retaining walls to earthquake ground motions as idealized in Figure 1.1. The corresponding PC software, *CorpsWallSlip*, developed to perform a sliding block analysis of each user-specified retaining wall section is also discussed. When acceleration time-histories are used as input to the *CorpsWallSlip* complete time-history sliding block analysis to represent the earthquake ground motions, baseline-corrected, horizontal and vertical acceleration time-histories are to be specified as input. A particular formulation of the rotational analysis model for computing the threshold value of acceleration corresponding to lift-off from the base of the wall in rotation (Figure 1.2) is also described. (Note that a more versatile, complete time-history based formulation for computing earthquake-induced, permanent wall rotations using the PC-based software *CorpsWallRotate* has also been developed and is discussed in Ebeling and White (2006).) Additionally, a simplified sliding block formulation that eliminates the need for an acceleration time-history to characterize earthquake shaking is discussed in this report and incorporated within *CorpsWallSlip*. Ground motion parameters such as peak ground acceleration and velocity and earthquake magnitude values are all that are required in this formulation.



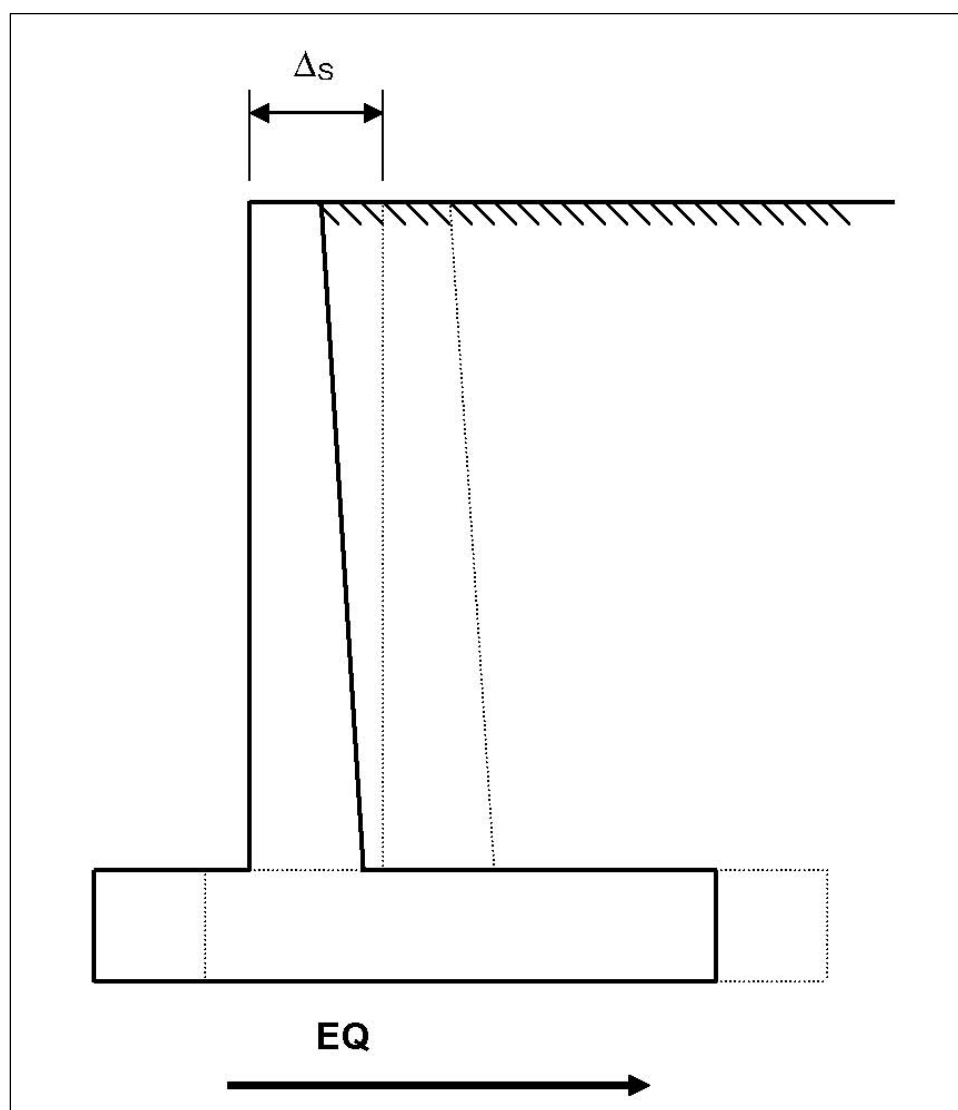


Figure 1.1. Translational response of a cantilever retaining wall with a permanent earthquake-induced sliding displacement,  $\Delta_s$ .

The engineering methodology and software are particularly applicable to rock-founded L-walls and T-walls (usually referred to as cantilever retaining walls) and semi-gravity walls. Figure 1.3 shows an example of retaining walls that border a spillway channel in which the base slab will act as a strut during a seismic event. CorpsWallSlip is applicable to a variety of retaining walls buttressed at their toe by a structural feature such as a reinforced concrete slab. The presence of the structural feature at the toe of the retaining wall may result in a tendency for the earth retaining structure to rotate rather than slide during earthquake shaking. Other examples of Corps earth retaining structures having this structural feature include

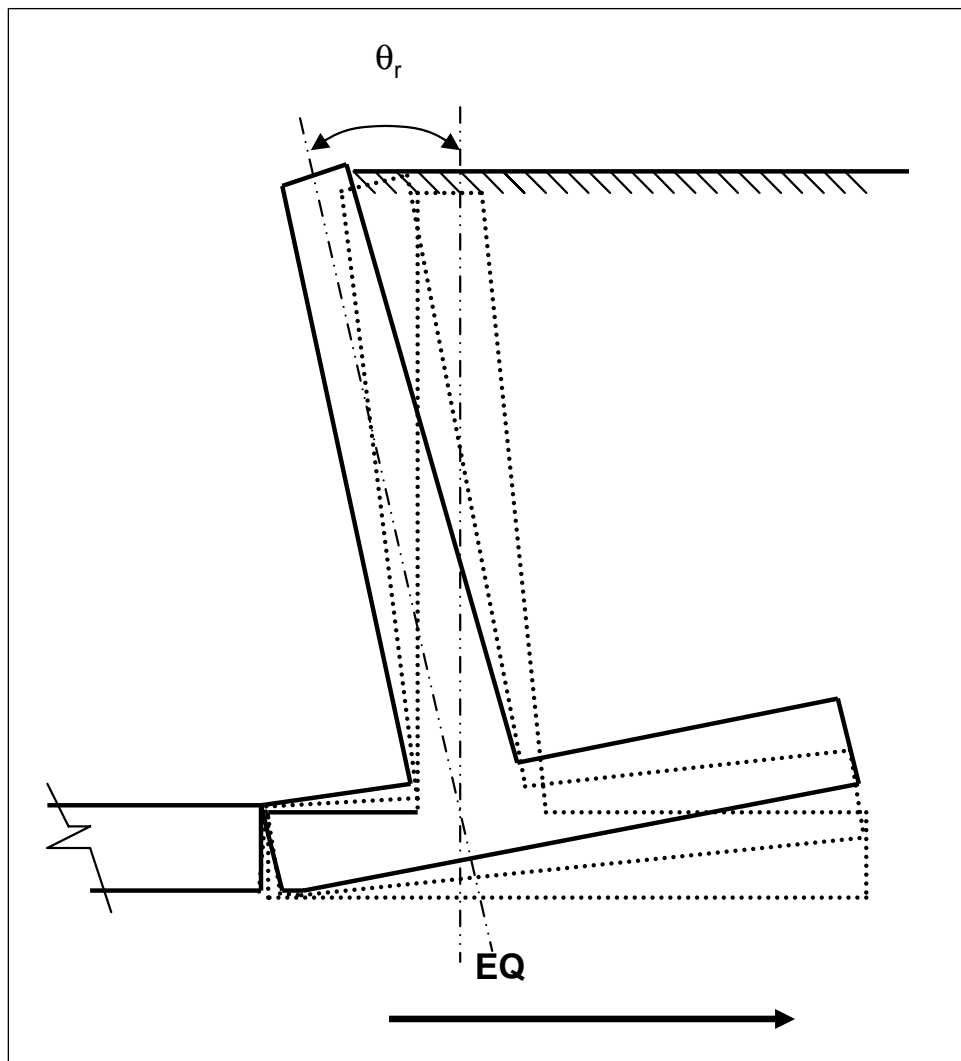


Figure 1.2. Rotational response of a cantilever retaining wall with a permanent earthquake induced rotation,  $\theta_r$ .

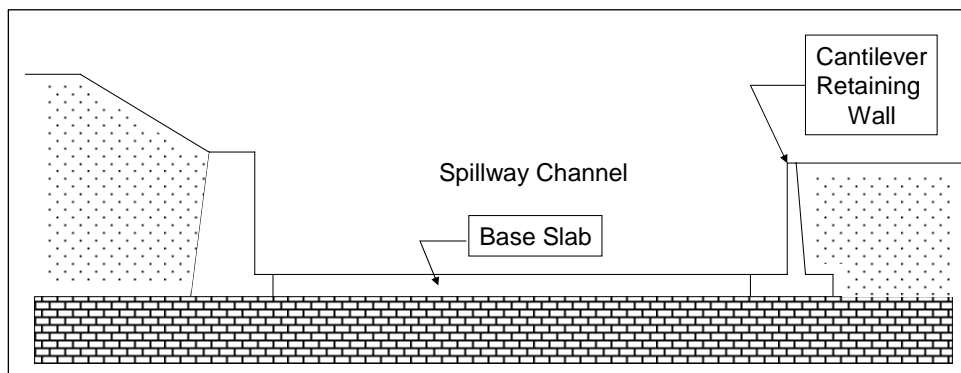


Figure 1.3. Rock-founded cantilever retaining wall bordering a spillway channel.

navigation walls, spillway chute walls, spillway discharge channel walls, approach channel walls to outlet works structures, highway and railway relocation retaining walls, and flood wall channels. CorpsWallSlip may also be used to predict permanent seismically induced translational displacements of retaining walls buttressed at their toe by a reinforced concrete slab, as shown in Figure 1.3.

There are three categories of analytical approaches used to perform a seismic stability analysis. They are listed in order of sophistication and complexity:

- Pseudo-static methods with a preselected seismic coefficient
- Sliding block methods
- Stress-deformation methods

Each category will be subsequently discussed. Because sliding block methods are the focus of this report, they will be discussed last.

#### **1.1.1 Pseudo-static methods with a preselected seismic coefficient**

Pseudo-static methods with a preselected seismic coefficient in the horizontal and in the vertical direction often require bold assumptions about the manner in which the earthquake shaking is represented and the simplifications made for their use in stability computations. Essentially, pseudo-static methods are force-equilibrium methods of analysis expressing the safety and stability of an earth retaining structure to dynamic earth forces in terms of (1) the factor of safety against sliding along the base of the wall, (2) the ability of the wall to resist the earth forces acting to overturn the wall, and (3) the factor of safety against a bearing capacity failure or crushing of the concrete or rock at the toe in the case of a rock foundation. An example using 1992 Corps criteria (now outdated) is discussed in Section 6.2 of Chapter 6 in Ebeling and Morrison (1992). Pseudo-static methods with horizontal and vertical preselected seismic coefficients represent earthquake loading as static forces. In these types of computations, the earthquake “demand” is represented by (1) a horizontal seismic coefficient and (2) a vertical seismic coefficient (sometimes specified as zero) acting at mass centers. Values for these coefficients (typical symbols are  $k_h$  and  $k_v$ ) are dimensionless numbers that, when multiplied times the weight of some body, give a pseudo-static inertia force for use in analysis or design. The horizontal and vertical inertia forces are applied to the mass center of the body as shown in Figure 1.4. The coefficients  $k_h$  and  $k_v$  are,

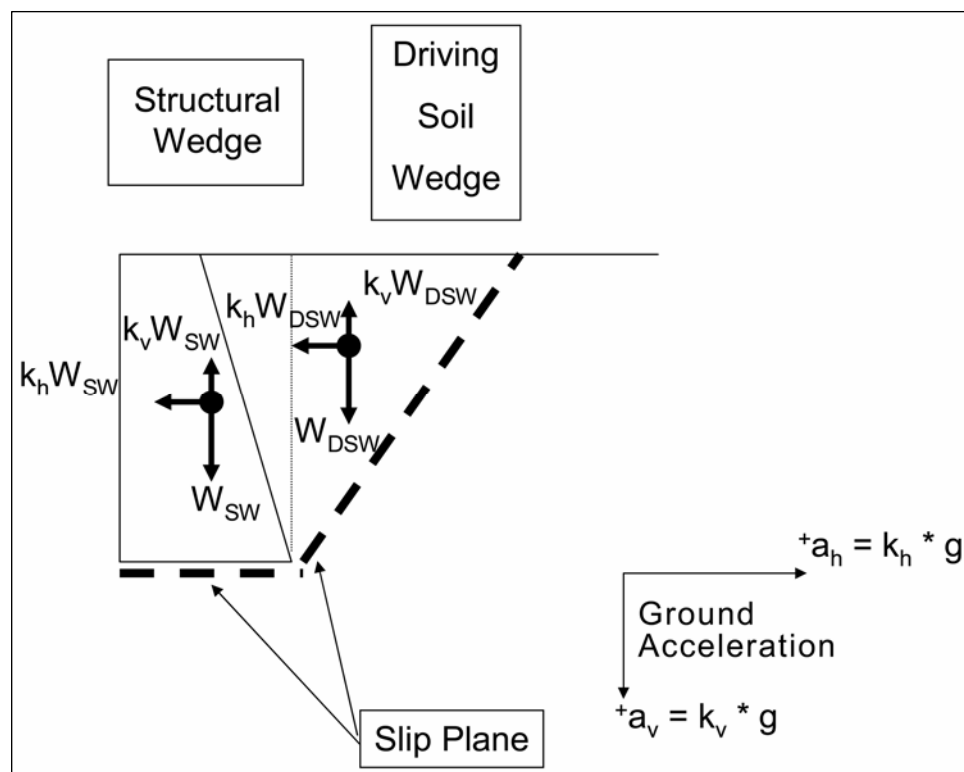


Figure 1.4. Gravity retaining wall and driving soil wedge treated as a rigid body.

in effect, decimal fractions of the acceleration of gravity ( $g$ ). For some analyses, it is appropriate to use acceleration values of  $k_h g$  and  $k_v g$  smaller than the horizontal and vertical peak accelerations, respectively, anticipated during the design earthquake event. It is important to recognize that this category of method of analysis does not provide quantitative information regarding seismically induced displacements.

For retaining walls in which the permanent relative motion of the retaining structure and retained soil (i.e., the backfill) are sufficient to fully mobilize the shear strength in the soil, soil wedge solutions in which a wedge of soil bounded by the structural wedge and by an assumed failure plane within the retained soil are considered to move as a rigid body and with the same horizontal acceleration (Figure 1.4). Table 1.1 lists the approximate magnitudes of movements required to reach minimum active earth pressure conditions. Although the guidance in Clough and Duncan (1991) is for static loading, after careful evaluation Ebeling and Morrison (1992, in Section 2.2.2) concluded that the Table 1.1 values may also be used as rough guidance for minimum retained soil seismic displacement to fully mobilize a soil's shear resistance, resulting in dynamic active earth pressures.

Table 1.1. Approximate magnitudes of movements required to reach minimum active earth pressure conditions (after Clough and Duncan (1991)).

Type of Retained Soil	Values of $Y/H^a$
	Active
Dense Sand	0.001
Medium-Loose Sand	0.002
Loose Sand	0.004

<sup>a</sup>  $Y$  = movement of top of wall required to reach minimum active pressure, by tilting or lateral translation.

$H$  = height of wall.

A commonly cited expression for the forces the driving soil wedge exerts on the structural wedge was first proposed by Okabe (1924, 1926) and Mononobe and Matsuo (1929). A form of their expression for  $P_{AE}$  in use today (see Chapter 4 in Ebeling and Morrison (1992)) is given in Figure 1.5. Their formulation is referred to as Mononobe-Okabe with  $P_{AE}$  expressed in terms of an active earth pressure coefficient,  $K_{AE}$ , with the subscript A designating active and the subscript E designating earthquake. The Mononobe-Okabe formulation is an extension of Coulomb's theory of static active earth pressures with a horizontal seismic coefficient and a vertical seismic coefficient acting at the center of a Coulomb's "driving" soil wedge mass of a moist retained soil (i.e., with no water table), as shown in this figure. Equation 36 in Chapter 4 of Ebeling and Morrison (1992) gives the Mononobe-Okabe relationship for  $K_{AE}$ . The general wedge solution resulting in this same value for  $P_{AE}$  as can be calculated by the Mononobe-Okabe relationship is given in Appendix A of Ebeling and Morrison (1992). For retaining wall problems analyzed using the simplified wedge method, EM 1110-2-2100 in Section 5-5, part (3)b provides guidance on assumptions regarding the magnitude of the seismic coefficient  $k_h$  that may be used as a fraction of peak ground acceleration. Guidance is also given regarding the magnitude of the seismic coefficient  $k_v$ , expressed as a fraction of the value for  $k_h$ . *Minimum*  $k_h$  values are cited in Table G-1, Section G-4 of Appendix G, part (a) in EM 1110-2-2100 according to the seismic zone in which the project resides.

Because seismically induced deformations are not an explicit part of this computational process and given that pseudo-static methods represent earthquake loads by static forces, the results are difficult to interpret. This is because displacement is more closely related to assessment of the *seismic performance* for a retaining structure than are factors of safety.

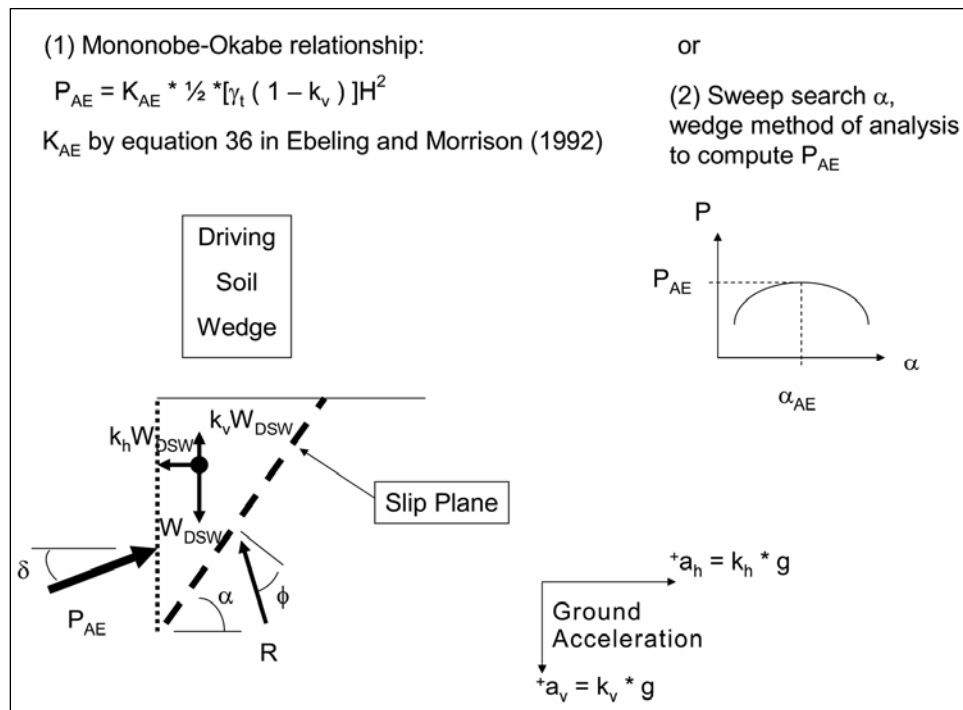


Figure 1.5. Simplified driving wedge method of analysis and the Mononobe-Okabe active earth pressure force relationship.

### 1.1.2 Stress-deformation methods

Stress-deformation methods are specialized applications of finite element or finite difference programs for the dynamic analysis of earth retaining structures to seismic loading using numerical techniques to account for the nonlinear engineering properties of soils. The problem being analyzed is often referred to as a soil-structure interaction (SSI) problem. Acceleration time-histories are typically used to represent the earthquake ground motions in this type of formulation. The general procedure of stress-deformation dynamic analysis is straightforward and follows the usual engineering approach: (1) define the problem, (2) idealize the physical system, (3) set up the equations of motion for the dynamic problem, (4) characterize the dynamic engineering properties of the (structure, soil, and/or rock) materials as per the constitutive material model(s) being used, (5) solve the equations of motion, and (6) evaluate the results. Steps (1), (2), (4), and (6) are handled by the engineer while steps (3) and (5) are dealt with by the engineering software. A partial listing of computer-based codes for dynamic analysis of soil systems is given in Appendix D of Ebeling and Morrison (1992). Use of this type of advanced engineering software requires specialized knowledge in the fields of geotechnical and structural engineering dynamics as well as in numerical

methods. Two computer programs, FLUSH and FLAC, will briefly be discussed to give the reader a sense of what is involved with the application of computationally complex numerical codes in a complete soil-structure interaction dynamic analysis and the numerous input and modeling considerations required.

#### *1.1.2.1 FLUSH*

The ASCE Standard 4-86 (1986) states that SSI denotes the phenomenon of coupling between a structure and its supporting soil or rock medium during earthquake shaking. The resulting dynamic soil pressures are a result of the degree of interactions that occur between the structure and the soil. This response is dependent on (1) the characteristics of the ground motion, (2) the retained and foundation soils (or rock), and (3) the structure itself. One method of analysis for SSI is referred to as the direct method and treats the structure and the surrounding retained soil and foundation medium in a single analysis step. FLUSH is a classic example of this category of software which uses the finite element method in this dynamic analysis (Lysmer, Udaka, Tsai, and Seed 1975).

Two-dimensional (2-D) cross sections of the retaining structure and portions of the retained soil and foundation are typically modeled in the FLUSH analysis. Nonlinear soil behavior is treated through equivalent linearization of the shear stiffness of each soil element with the effective shear strains that develop during earthquake shaking for the user-specified earthquake acceleration time-history. Material damping is assigned to each soil (and/or rock) element and to each structural element comprising the mesh. Material damping is strain-compatible for each soil, rock, and structural material type. FLUSH solves the equation of motion in the frequency domain. The acceleration time-history is introduced through the base nodes of the mesh; fictitious (artificial) boundary conditions that allow for the introduction of vertically propagating shear waves resulting in horizontal motion of the nodes of the mesh during earthquake shaking and for vertically propagating compression waves that allow for the vertical motion of the nodes. Lateral boundaries, referred to as transmitting boundaries, are imposed on the 2-D mesh to allow for energy absorbing boundary conditions to be specified. Because it is essentially a wave propagation problem being solved, great care is exercised by the seismic engineer to size the mesh so that moderate to high wave frequencies are not artificially excluded in the dynamic numerical analysis. Sizing of the 2-D mesh as it pertains to the height of the elements and with regard to

the maximum shear wave frequency vertically transmitted by the elements first involves the analysis of representative 1-D soil columns.

To assess the maximum frequency that may be transmitted by a user-proposed 2-D finite element mesh in a FLUSH analysis, representative imaginary sections within the 2-D model problem are first analyzed by the vertical shear wave propagation program SHAKE (Schnabel, Lysmer, and Seed 1972) and by a 1-D finite element column using FLUSH. Strain-compatible shear stiffness results from the SHAKE analyses are used to determine the maximum height of the soil elements for the maximum frequency of the vertically propagating shear wave needed to be transmitted in the FLUSH (2-D) analysis. A 1-D soil column is then constructed using finite elements and analyzed using FLUSH to verify that the required vertically propagating shear wave frequencies are being transmitted by the FLUSH mesh. The wavelength associated with the highest frequency transmitted by the mesh is related to the heights of the elements and to the strain-compatible shear wave velocities via the strain-compatible shear stiffness of each of the elements. Recall that FLUSH accounts for nonlinear response of soils during earthquake shaking through adjustments of the soil shear stiffness and material damping parameters as a function of shear strain that develop in each element of the finite element mesh. Note that the results of this assessment are dependent on the characteristics of the acceleration time-history used in the analysis.

FLUSH output obtained via the extraction mode includes time-histories of the dynamic stresses within each element and dynamic displacements at each node in the finite element model. Time-histories of nodal point forces may also be obtained using specialized software. The computed dynamic stresses are then superimposed on the static stresses so as to attain the total stresses. Static stresses are typically obtained from a SOILSTRUCT finite element analysis (Ebeling, Peters, and Clough 1992).

In a static analysis using SOILSTRUCT, the nonlinear stress-strain behavior of soils are accounted for in an incremental, equivalent linear method of analysis in which the sequential excavation (if any), followed by sequential construction of the structure and incremental placement of retained soil, is made. Examples of this application to Corps structures for static loading(s) are given in Clough and Duncan (1969), Ebeling et al. (1993), Ebeling and Mosher (1996), Ebeling, Peters, and Mosher (1997),



Ebeling and Wahl (1997), and Ebeling, Pace, and Morrison (1997). The mesh used in the FLUSH dynamic analysis will be the basis for the mesh used in the SOILSTRUCT static analysis, for the convenience of combining results.

#### 1.1.2.2 *FLAC*

The Corps recently completed its first research application of FLAC to the seismic analysis of a cantilever retaining wall (Green and Ebeling 2002). FLAC is a commercially available, 2-D, explicit finite difference program written primarily for geotechnical applications. The basic formulation of FLAC is plane-strain. Dynamic analyses can be performed with FLAC using the optional dynamic calculation module, wherein user-specified acceleration, velocity, or stress time-histories can be input as an exterior boundary condition or as an interior excitation. FLAC allows for energy absorbing boundary conditions to be specified, which limits the numerical reflection of seismic waves at the model perimeter. The nonlinear constitutive models (10 are built-in), in conjunction with the explicit solution scheme, in FLAC give stable solutions to unstable physical processes, such as sliding or overturning of a retaining wall. FLAC solves the full dynamic equations of motion, even for essentially static systems, which enables accurate modeling of unstable processes, e.g., retaining wall failures.

FLAC, like FLUSH, has restrictions associated with the wavelength associated with the highest frequency transmitted within the grid. A procedure similar to that used to design the FLUSH mesh and involving 1-D soil column analyses, via SHAKE, is used to layout the FLAC grid for the dynamic retaining wall problem analyzed and for the specified acceleration time-history. Section 3.3.4 of Green and Ebeling (2002) discusses the dimensions of the finite difference grid and the maximum frequency that can pass through without numerical distortion.

A disadvantage of FLAC is the long computational times, particularly when modeling stiff materials, which have large physical wave speeds. The size of the time-step depends on the dimension of the elements, the wave speed of the material, and the type of damping specified (i.e., mass proportional or stiffness proportional), where stiffness proportional to include Rayleigh damping, requires a much smaller time-step. The critical time-step for numerical stability and accuracy considerations is automatically computed by FLAC, based on these factors listed. For those readers unfamiliar with the concept of critical time-step for numerical stability and

accuracy considerations in a seismic time-history engineering analysis procedure, please refer to Ebeling (1992, Part V), or to Ebeling, Green, and French (1997). The Lagrangian formulation in FLAC updates the grid coordinates each time-step, thus allowing large cumulative deformations to be modeled. This is in contrast to Eulerian formulation in which the material moves and deforms relative to a fixed grid, and is therefore limited to small deformation analyses.

#### 1.1.2.3 FLUSH versus FLAC

The advantages of FLUSH are that it has considerably faster run times than FLAC and has been applied to a number of dynamic SSI problems. FLUSH is now freely downloadable from the Internet. The major disadvantage of FLUSH is that it does not allow for *permanent* displacement of the wall (although strain softening associated with earthquake-induced soil or rock deformations is accounted for in the analysis). A disadvantage of FLAC is that the earthquake engineering community and the Corps are just now developing modeling procedures for the application of FLAC to dynamic SSI problems, learning how to perform the analyses and interpret the computed results.

#### 1.1.3 Sliding block methods

Sliding block methods of analysis of earth retaining structures can be viewed as a compromise between the simplistic pseudo-static methods with a preselected seismic coefficient and the computationally complex stress-deformation methods of analysis (e.g., via FLUSH, FLAC, etc.). Sliding block methods of analysis calculate a permanent deformation of a retaining structural system due to a user-specified design earthquake event.

The numerous variations of rigid sliding block methods of seismic analysis as applied to slopes, earthen dams, retaining wall systems, and foundations have their roots in the methodology outlined in Newmark (1965) and

what has come to be known as the Newmark sliding block model.<sup>1</sup> This problem was first studied in detail by Newmark (1965) using the sliding block on a sloping plane analogy. Procedural refinements were contributed by Franklin and Chang (1977), Wong (1982), Whitman and Liao (1985), Ambraseys and Menu (1988), and others. Makdisi and Seed (1978) and Idriss (1985, Figure 47), proposed relationships based on a modification to the Newmark permanent displacement procedure to allow for the dynamic response of embankments.

#### *1.1.3.1 Concepts of Newmark's sliding (rigid) block method of analysis*

Franklin and Chang (1977) and Hynes-Griffin and Franklin (1984) illustrate key concepts of a Newmark sliding block analysis using a potential sliding mass within an embankment under earthquake loading. The problem engineering idealization is shown in Figure 1.6. The Figure 1.6.a potential sliding mass is in a condition of incipient sliding with full mobilization of the shear resistance for the soil along the slip plane shown in this figure. The corresponding sliding factor of safety is equal to unity. This condition results from the acceleration of the earthen mass into the embankment (i.e., to the left) and away from the cut.  $W$  is the weight of the sliding mass. The force  $N$  times  $W$  in this figure is the inertia force required to reduce the sliding factor of safety to unity. By D'Alembert's principle, the inertia force,  $N$  times  $W$ , is applied pseudo-statically to the soil mass in a direction opposite to acceleration of the mass,  $N$  times  $g$ , with  $N$  being a decimal fraction of the acceleration of gravity,  $g$  (the universal gravitational constant). The acceleration of the soil mass contained within the slip plane shown in Figure 1.6.a is limited to an acceleration value of  $N$  times  $g$  because the shear stress required for equilibrium along the slip plane can never be less than the shear strength of the soil. To state this in another way, the sliding factor of safety can never be less than 1.0.

---

<sup>1</sup> An interesting footnote in seismic engineering history is given in Whitman (2000): Dr. Robert Whitman, Professor Emeritus of MIT, in 1953 performed a calculation of the permanent displacement of a slope as a result of earthquake-induced ground motions using a sliding block concept for a consulting job that Professor Donald Taylor (of MIT) had with the U.S. Army Corps of Engineers. Professor Newmark was part of the same consulting panel and sent word back to Dr. Whitman that he found this approach to be interesting, and that if he (Whitman) did not pursue it, he (Newmark) would. Dr. Whitman did not, and Professor Newmark did. Professor Newmark's research culminated in his now classic 1965 *Geotechnique* paper on this topic, the fifth Rankine lecture.

So if the earthquake-induced ground acceleration should increase to a value greater than the value  $N$  times  $g$ , the Figure 1.6.a mass above this slip plane would move downhill relative to the embankment. During this permanent slope displacement, the “sliding” mass would only feel the acceleration value  $N$  times  $g$  and not the ground acceleration values.

Figure 1.6.b shows the force polygon for the “sliding” soil mass. The angle inclination  $\theta$  of the inertia force may be found as the angle that is most critical, that is, the angle that minimizes  $N$ . Franklin and Chang (1977) and Hynes and Franklin (1984) state that the angle  $\theta$  is typically set equal to zero in seismic slope stability analyses. The angle  $\beta$  is the direction of the resultant force,  $S$ , of the distributed shear stresses along the interface and is determined during the course of the slope stability analyses to determine the value of  $N$  that results in a sliding factor of safety of 1.0 for the slope’s sliding mass. The force  $P$  is the resultant of the normal forces. The Figure 1.6.b force polygon for the slope mass is applied to an “idealized” sliding rigid block model on a plane inclined at an angle  $\beta$  to horizontal in Figure 1.6.c. This idealization is the basis for the designation as the Newmark’s sliding (rigid) block method of analysis, representing the sliding mass of the embankment.

Figure 1.6.d is an idealization of the limiting force versus displacement relationships applied to this problem. The resistance to sliding is assumed to be rigid-plastic, as shown in this figure. This resistance to sliding is unsymmetrical because the block can slide downhill more easily than uphill. It is the usual practice to assume that uphill sliding never occurs, i.e., a worst-case assumption, and results in the greatest permanent displacement (downhill).

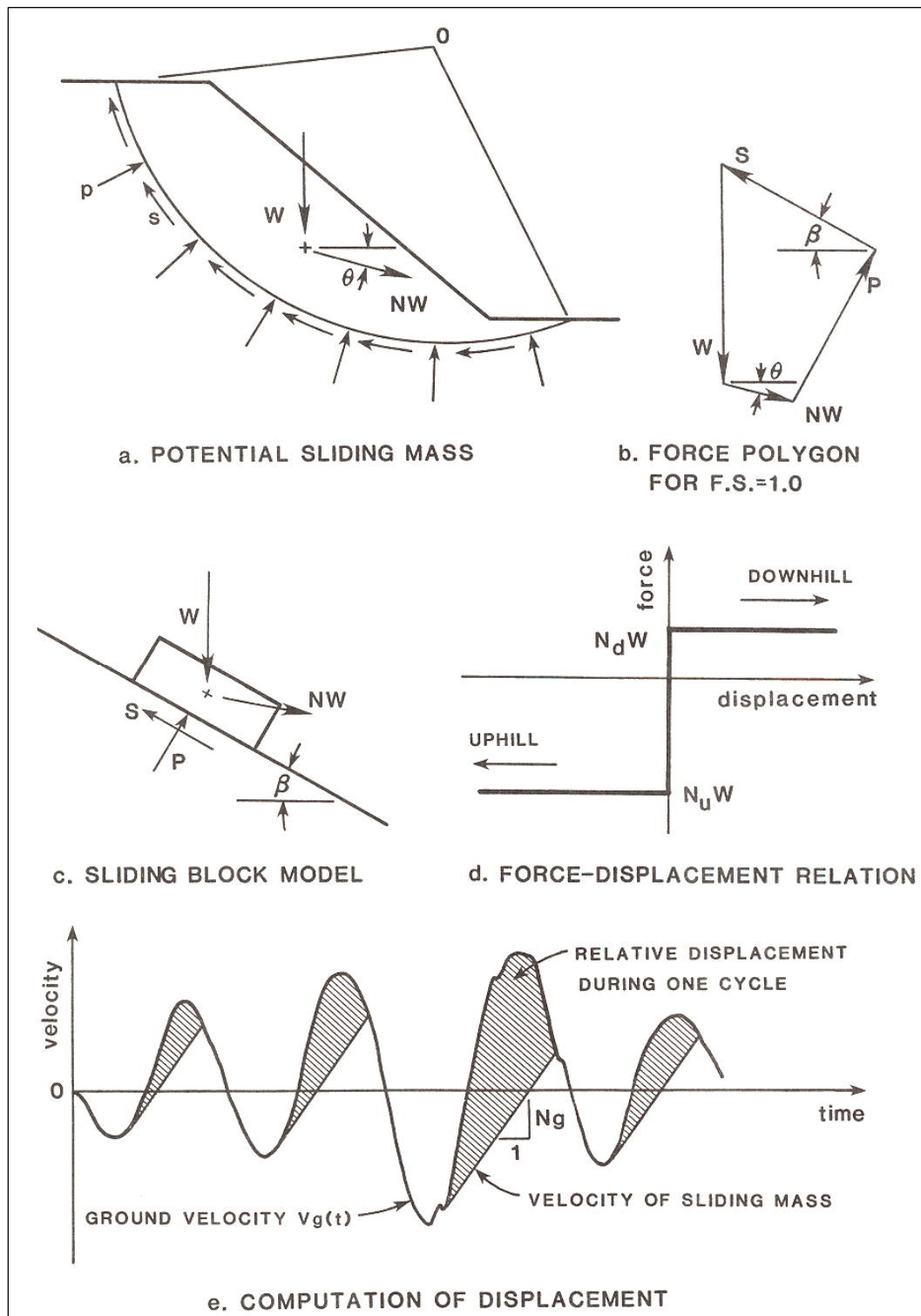


Figure 1.6. Elements of the Newmark (rigid) sliding block method of analysis (from Hynes-Griffin and Franklin 1984).

Figure 1.6.e shows a time-history plot of the velocity of the embankment during earthquake shaking. Not shown is the corresponding (ground/embankment) acceleration time-history for this particular earthquake event. (Earthquake shaking is usually represented by an acceleration time-history. Since the ground acceleration varies with time, let ground acceleration be represented by variable fraction  $A$  times the constant acceleration of gravity,  $g$ . Recall that the integral of the acceleration time-history is equal to the Figure 1.6.e velocity time-history.) For an embankment that suffers a slope failure from seismic ground motions, the total permanent displacement of a sliding mass relative to the base is the sum of the increments of displacement occurring during a number of individual pulses of ground motion. These incremental relative displacements are determined as follows. For each time the acceleration of the embankment, equal to  $A$  times  $g$ , is greater than the constant  $N$  times  $g$ , relative displacements (between the slope mass and the embankment) will *initiate*. There are four of these incremental, permanent displacement pulses occurring in Figure 1.6.e. During slope displacements, the sliding mass will move at a slower velocity than will the embankment (designated the ground velocity in this figure). The integral of the difference in velocities between the sliding mass and the embankment velocity is equal to the incremental, relative displacement of the sliding mass. The total permanent downhill displacement is the sum of the four incremental displacement cycles depicted in this figure. Note that incremental sliding of the slope terminates when the velocities of the embankment and of the sliding mass converge to the same value.

**Summary:** The idealized engineering problem depicted in Figure 1.6 describes the essential features of the Newmark sliding (rigid) block method of analysis as first applied to slopes: (1) There is a level of earthquake shaking as characterized in terms of a value of acceleration designated  $N$  times  $g$ , which fully mobilizes the shear resistance along a sliding plane of a potential sliding mass, corresponding to a factor of safety against sliding of 1.0 for that mass. (2) For a given embankment (or equivalently, ground) acceleration time-history in which accelerations exceed the value of  $N$  times  $g$ , incremental permanent displacements will occur. (3) The magnitude of the incremental displacements may be numerically quantified using the procedure outlined in Figure 1.6.e. (4) Total permanent displacement is equal to the sum of the incremental displacement pulses. Although this procedure has been applied to other types of structures, the essential features of the Newmark (rigid) sliding block method of analysis remain the same.

### 1.1.3.2 Sliding block method of analysis applied to retaining structures

A variation proposed on the Newmark sliding block method of analysis for earth retaining structures is the displacement controlled approach (Section 6.3 in Ebeling and Morrison (1992)). It incorporates retaining wall movements explicitly in the stability analysis of earth retaining structures. This methodology is applied as either (1) the displacement controlled *design* of a new retaining wall or as (2) an *analysis* of earthquake-induced displacements of an existing retaining wall.

**The displacement controlled *design* of retaining wall:** In this approach the retaining wall geometry is the primary variable. It is, in effect, a procedure for choosing a seismic coefficient based upon explicit choice of an allowable permanent displacement. Once the seismic coefficient is selected, the usual stability analysis against sliding is performed, including the use of the Mononobe-Okabe equations (or, alternatively, a sweep-search, soil wedge solution). The wall is proportioned to resist the applied earth and inertial force loadings. No safety factor is required to be applied to the required weight of wall evaluated by this approach; the appropriate level of safety is incorporated into the step used to calculate the horizontal seismic coefficient. This procedure of analysis represents an improved alternative to the conventional equilibrium method of analysis that expresses the stability of a rigid wall (of prescribed geometry and material properties) in terms of a pseudo-static method with a preselected seismic coefficient and preselected factor of safety against sliding along its base, discussed in Section 1.1.1. Section 6.3.1 in Ebeling and Morrison (1992) outlines the computational steps in the (seismic) displacement controlled design of a retaining wall.

**The *analysis* of earthquake-induced displacements of a retaining wall:** The retaining wall geometry and material properties are typically first established for the usual, unusual, and extreme load cases with nonseismic loadings. In the subsequent seismic analysis of the retaining wall using the earthquake-induced displacement approach, the primary variable is the permanent displacement. The seismic inertia coefficient  $N^*$  that reduces the sliding factor of safety for the driving soil wedge and the structural wedge to unity is first determined. (Ebeling and Morrison (1992) designated the value for a retaining wall's maximum transmissible acceleration as  $N^*g$ .) Figure 1.7 shows the driving soil wedge and structural wedge treated as a single rigid block in this approach. The resulting permanent seismic displacement of the retaining wall is subsequently

determined for the earthquake specified by the design engineer. Section 6.3.2 in Ebeling and Morrison (1992) outlines the computational steps in the analysis of earthquake-induced displacements of a retaining wall (with specified geometry and material properties).

The analytical procedure that was developed by Richards and Elms (1979) recognizes that for some limiting value of horizontal acceleration, identified as  $N^*g$  in Figure 1.7, the horizontal inertia force acting on a retaining wall with no toe fill will nominally exceed the shear resistance provided by the foundation along the interface between the base of the wall and the foundation. This implies that although the soil base (i.e., the foundation to the wall) may be accelerating horizontally at values greater than  $N^*g$ , the wall will be sliding along the base under the action of the horizontal inertial force that corresponds to the horizontal acceleration,  $N^*g$ . This results in movement of the soil base relative to the movement of the wall and vice versa. The relative movement *commences* at the point in time designated as point a in the first time-history shown in Figure 1.8 and continues until the (absolute) velocity of the base is equal to the (absolute) velocity of the wall, designated as time point b in the second time-history of this same figure. The (absolute) velocity of the soil base is equal to the integral over time of the soil acceleration, and the (absolute) velocity of the wall between time points a and b is equal to the integral of the wall acceleration, which is a constant  $N^*g$ . The *relative* velocity of the wall,  $v_r$ , shown in the third time-history is equal to the integral of the difference between the base acceleration and the constant wall acceleration,  $N^*g$ , between time points a and b, as shown in Figure 1.8. The relative displacement of the wall is the fourth time-history and equal to the integral of the relative velocity of the wall, which occurs between the two points in time labeled a and b in Figure 1.8. Note that at time point b when the wall is stopping its first increment of relative movement, the acceleration is less than  $N^*g$  as shown in the first time-history. This observation demonstrates that the relative velocity of the wall (shown in the third time-history) controls the *cessation* of the seismically induced incremental wall movement. Additional incremental relative displacements occur for the wall between the two latter points in time labeled c and d in Figure 1.8 with the residual relative wall displacements,  $d_r$ , equal to the cumulative relative displacements computed during the entire time of earthquake shaking (labeled as point d in the fourth time-history). Lastly,  $N^*g$  is referred to as either the maximum transmissible acceleration or the yield acceleration.



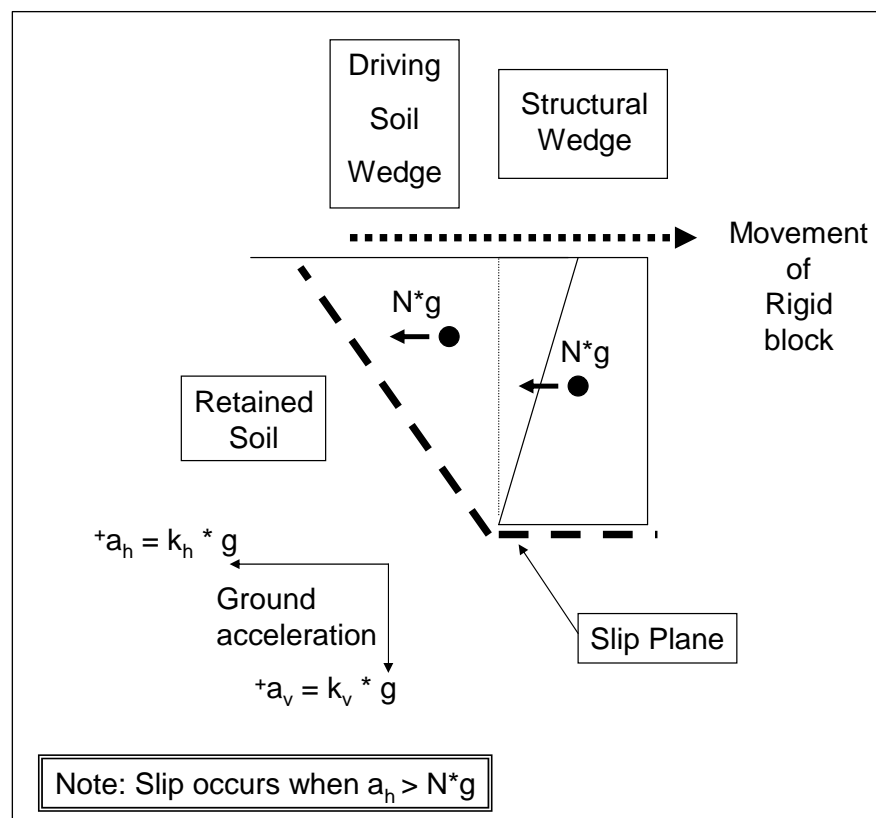


Figure 1.7. Gravity retaining wall and failure wedge treated as a sliding block (after Whitman 1990).

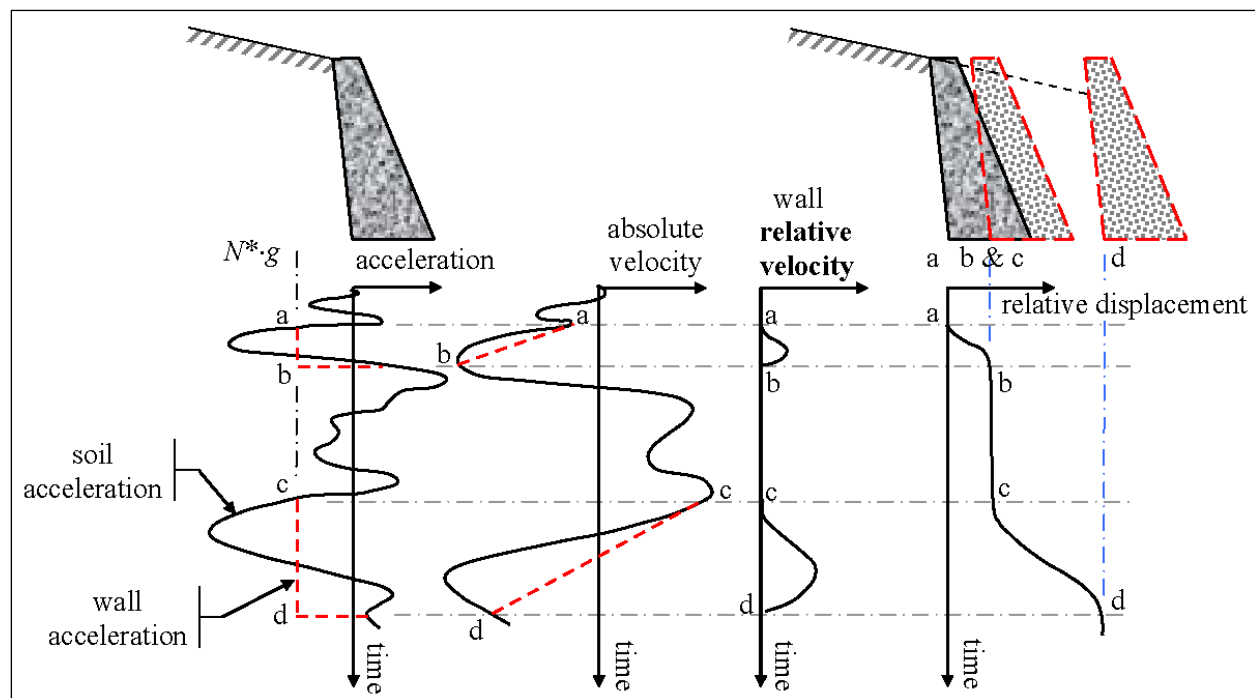


Figure 1.8. Incremental failure by base sliding (adapted from Richards and Elms 1979).

Ebeling and Morrison (1992) observe that the approach has been reasonably well validated for the case of walls retaining granular, moist backfills (i.e., no water table). A key item is the selection of suitable shear strength parameters. In an effective stress analysis, the issue of the suitable friction angle is particularly troublesome when the peak friction angle is significantly greater than the residual friction angle. In the displacement controlled approach examples given in Section 6.2 of Ebeling and Morrison (1992), effective stress based shear strength parameters (i.e., effective cohesion  $c'$  and effective angle of internal friction  $\phi'$ ) were used to define the shear strength of the dilative granular backfills, with  $c'$  set equal to zero in all cases because of the level of deformations anticipated in a sliding block analysis during seismic shaking. In 1992 Ebeling and Morrison concluded that it is conservative to use the residual friction angle in a sliding block analysis, and this should be the usual practice for displacement-based analysis of granular retained soils. For this report the primary author would broaden the concept to the assignment of effective (or total) shear strength parameters for the retained soil be consistent with the level of shearing-induced deformations encountered for each design earthquake in a sliding block analysis and note that active earth pressures are used to define the loading imposed on the structural wedge by the driving soil wedge. (Refer to Table 1.1 for guidance regarding wall movements required to fully mobilize the shear resistance within the retained soil during earthquake shaking.)

CorpsWallSlip has the ability to perform a sliding analysis of a user-specified retaining wall section such as the rock-founded retaining wall shown in Figure 1.9. This retaining wall is an idealization of the Figure 1.3 cantilever retaining wall problem. Besides the overall wall and retained soil geometry and material properties, the engineer provides as input a characterization of the earthquake ground motion. CorpsWallSlip has two options; input may be either (1) ground motion parameters of peak ground acceleration and velocity and earthquake magnitude values are specified in the simplified sliding block formulation or (2) baseline-corrected, horizontal and vertical acceleration time-histories that are used to represent the earthquake ground motions in the complete time-history formulation. CorpsWallSlip represents the effect of the invert spillway slab on the toe of the cantilever wall through a user-specified, limiting resisting force,  $P_{\text{resist}}$ . The magnitude of the  $P_{\text{resist}}$  may be estimated using the simplified procedure developed by Strom and Ebeling (2004). Details regarding the sliding block

method of analysis formulated in CorpsWallSlip are given in Chapter 2 of this report.

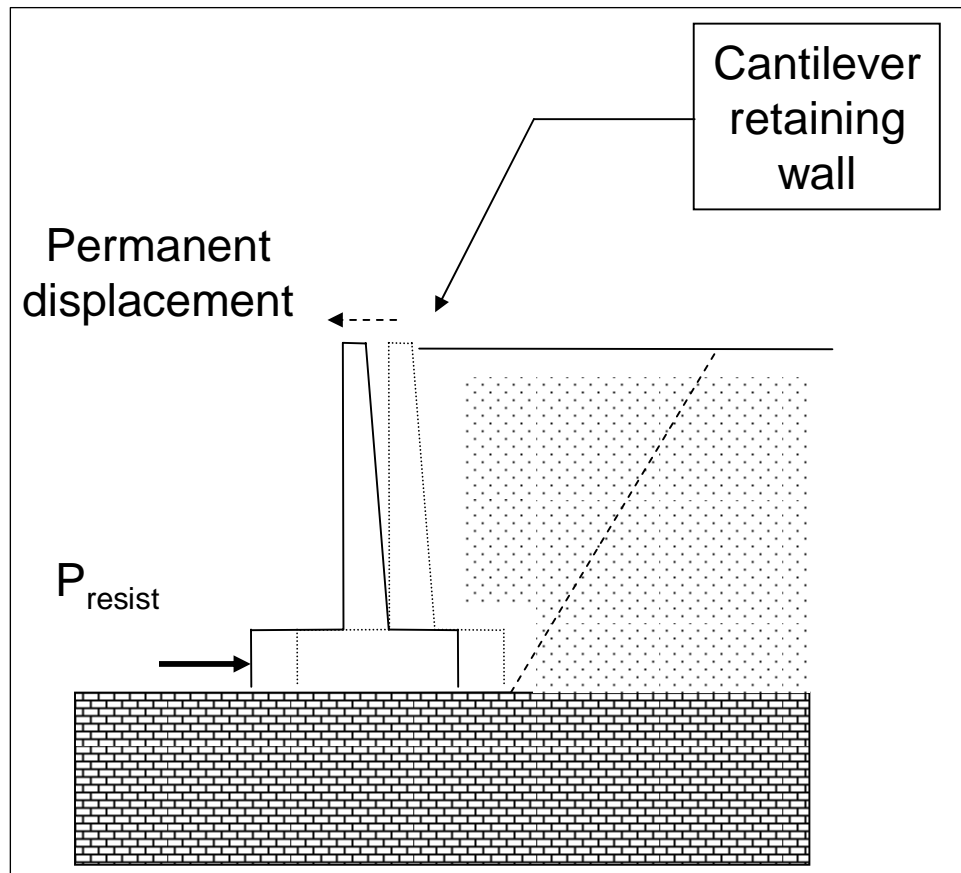


Figure 1.9. Permanent, seismically induced displacement of a rock-founded cantilever wall retaining moist backfill and with toe restraint, computed using CorpsWallSlip.

In most sliding block formulations, including that used in CorpsWallSlip, an active earth pressure force is applied to the structural wedge in the permanent displacement analysis. Table 1.1 lists the approximate magnitudes of movements required to reach minimum active earth pressure conditions. Although the guidance in Clough and Duncan (1991) is for static loading, after careful evaluation Ebeling and Morrison (1992, in Section 2.2.2) concluded that the Table 1.1 values may also be used as rough guidance for minimum retained soil seismic displacement to fully mobilize a soil's shear resistance, resulting in dynamic active earth pressures. That is, the permanent displacements computed using CorpsWallSlip must equal or exceed the Table 1.1 values (given as displacement-normalized wall heights in this table). If not, then the dynamic earth pressures are underestimated in the analysis.

## 1.2 New rotational analysis model based on a rigid block problem formulation

The permanent displacement of retaining structures is not restricted to walls that slide along their base as a result of inertial forces imparted during earthquake shaking. For some retaining wall system configurations and material properties, permanent displacements may instead result from the rotation of a retaining wall about a point along its wall-to-foundation interface.

The idealized permanent displacement due to rigid body noncentroidal rotation of a retaining wall about its toe during earthquake shaking and with toe restraint is shown in Figure 1.10. The buttressing effect of a reinforced concrete slab is represented in this simplified dynamic model by the user-specified force,  $P_{\text{resist}}$ , acting on a vertical section extending upwards from the toe of the wall as per, for example, Strom and Ebeling (2004).

The Figure 1.10 cantilever retaining wall that is buttressed by an invert spillway slab (which is a reinforced concrete slab) exemplifies a category of Corps retaining walls that may be susceptible to earthquake-induced rotation. The primary author of this report is of the opinion that the assignment of the point of rotation to the toe of the wall becomes a reasonable simplifying assumption because of the constraint provided by the Figure 1.10 invert spillway slab to lateral translations, combined with the effects of the stiff, competent rock foundation. A key result of a CorpsWallRotate analysis idealized in Figure 1.10 is the permanent, earthquake-induced displacement of a retaining wall caused by rotation about the toe of the wall.

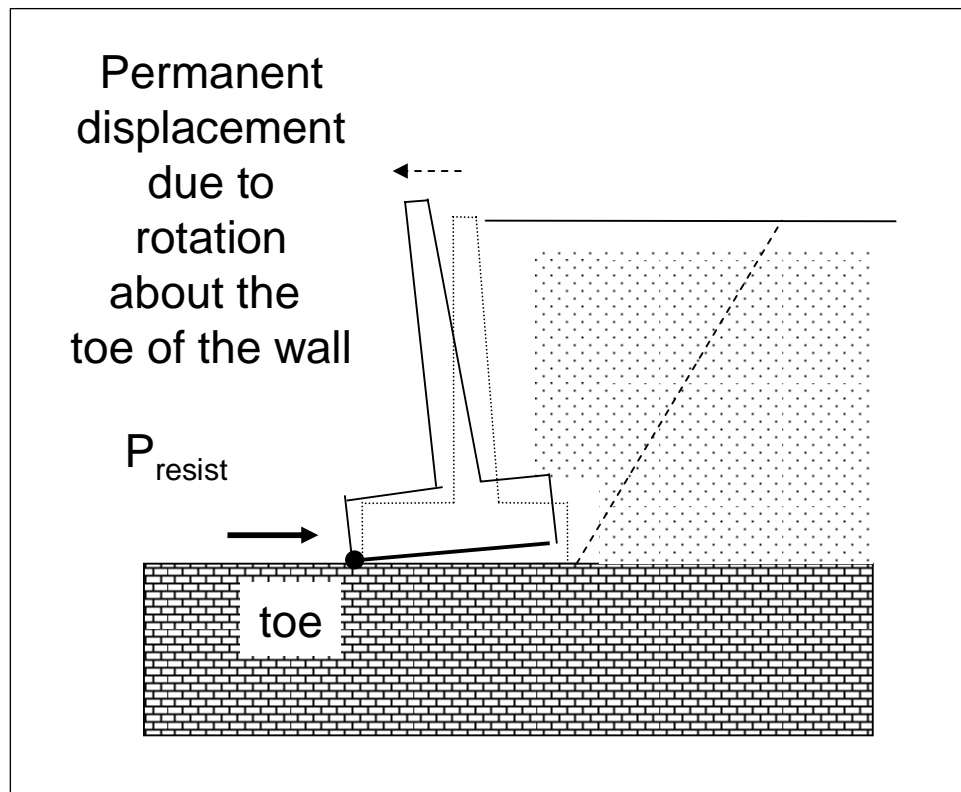


Figure 1.10. Idealized permanent, seismically induced displacement due to the rotation about the toe of a rock-founded wall retaining moist backfill, with toe restraint, computed using CorpsWallRotate.

As in Zeng and Steedman (2000) rigid gravity wall formulation, discussed in Ebeling and White (2006), rotation of a rigid block model of the structural retaining wall system in this new formulation is assumed to occur about the toe of the wall (i.e., the rigid block is “pinned” to the rigid base at its toe). This new Ebeling and White procedure differs from the Steedman and Zeng formulation by (1) formal consideration of a toe-restraint in the analysis (due to the presence of a reinforced concrete slab against the toe of the wall); (2) the ability of the user to assign a vertical acceleration time-history in addition to a horizontal acceleration time-history; (3) consideration of a pool of water in front of the wall, a submerged foundation and a partially submerged retained soil (Figure 1.11); and (4) the implementation of this formulation within corresponding PC software CorpsWallRotate using a graphical user interface (GUI) for input of geometry, input of material properties, input/verification of earthquake time-history files, and visualization of results. In addition, (5) a sweep-search wedge formulation within the retained soil is used to determine the value of  $P_{\text{AE}}$  rather than relying on the Mononobe-Okabe relationship (cited in the Steedman and Zeng

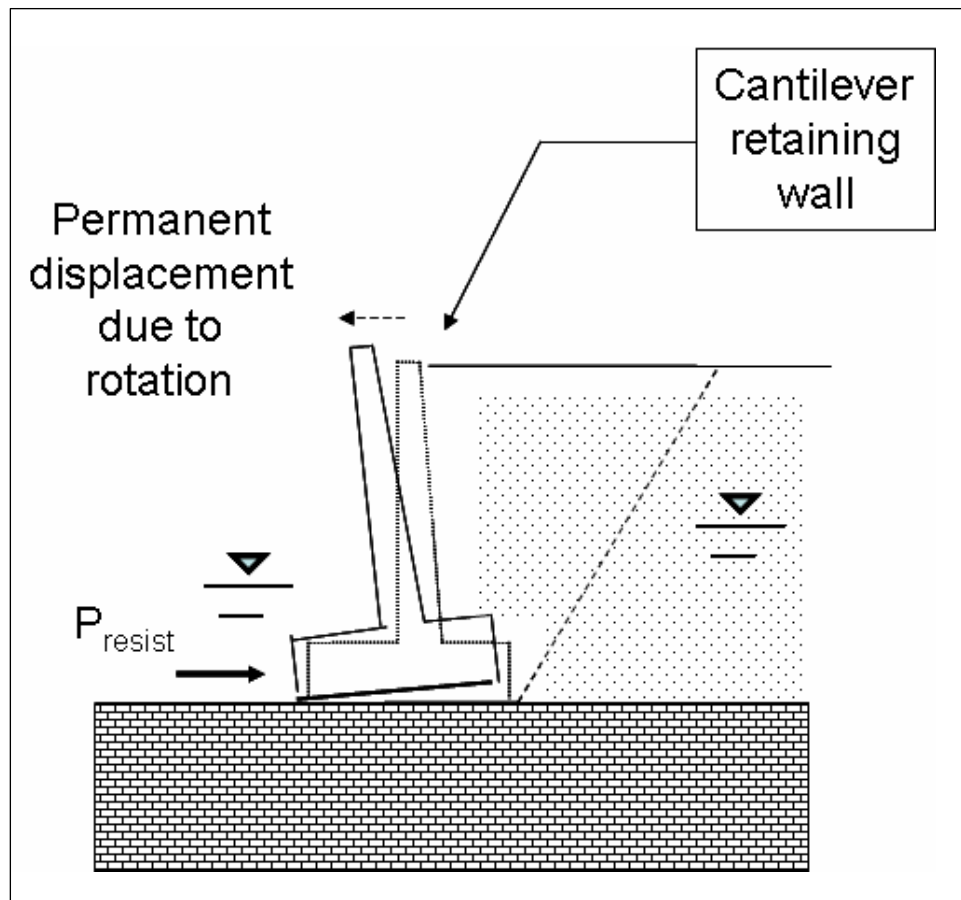


Figure 1.11. Permanent, seismically induced displacement due to the rotation about the toe of a rock-founded, partially submerged cantilever retaining wall and with toe restraint, computed using CorpsWallRotate.

(1996) formulation). Recall that the Mononobe-Okabe relationship is valid for a retained soil with a constant surface slope and whose strength is characterized by the Mohr-Coulomb shear strength parameter  $\phi$  (e.g., refer to Equations 33 through 35 in Ebeling and Morrison (1992)). The advantage of the sweep-search method as formulated and implemented in CorpsWallRotate and in CorpsWallSlip is that it allows for (a) the analysis of bilinear ground surfaces (Figure 1.12) and/or (b) the analysis of cohesive ( $S_u$ ) soils.<sup>1</sup>

<sup>1</sup> In the formulation described in this report, a cohesive soil refers to a total stress analysis in which the shear strength of the soil is characterized in terms of its undrained shear strength,  $S_u$ . Note that minimum wall movements needed to fully mobilize the shear resistance of the soil, on the order of those listed in Table 1.1, will impact the characterization of the retained soil shear strength parameters used in the permanent displacement analysis.

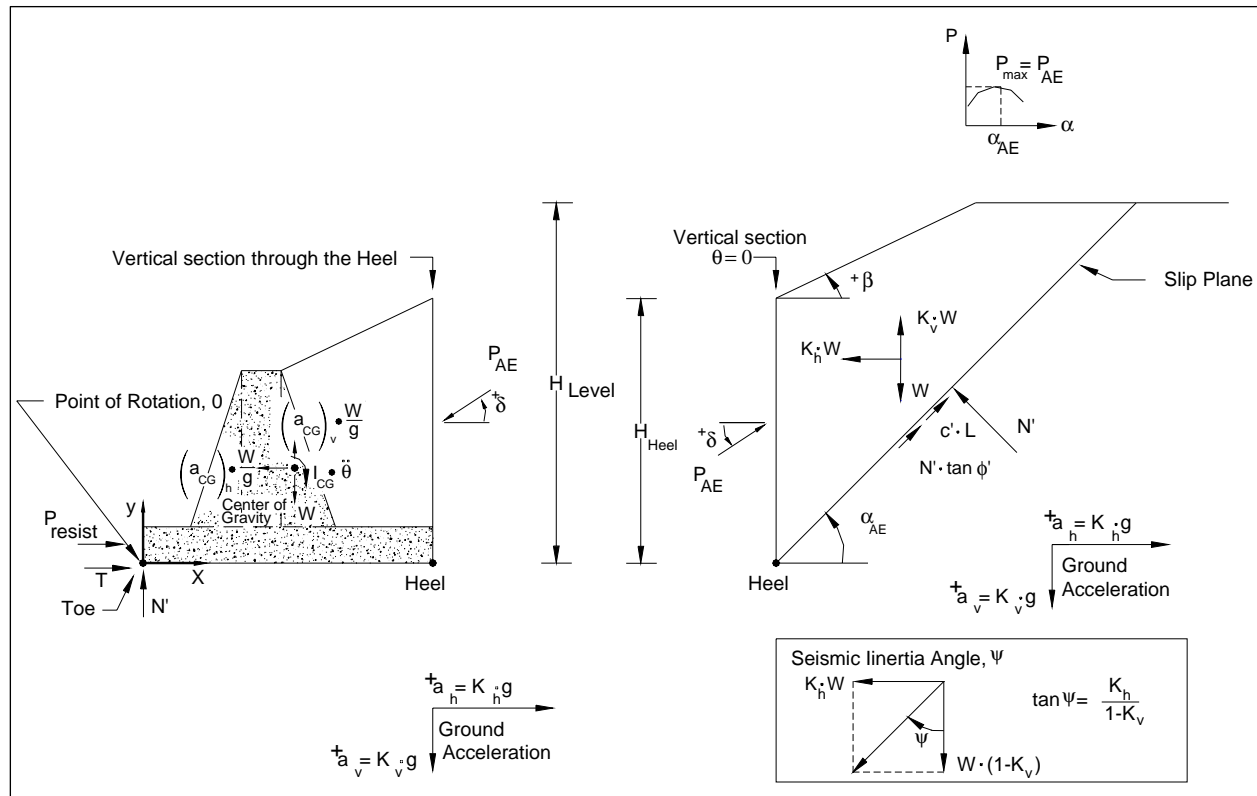


Figure 1.12. Structural wedge with toe resistance retaining a driving soil wedge with a bilinear moist slope (i.e., no water table) analyzed by effective stress analysis with full mobilization of  $(c', \phi')$  shear resistance within the backfill.

### 1.3 Tendency of a retaining wall to slide or to rotate during earthquake shaking

An important difference between the Newmark sliding block method of analysis for earth retaining structures (i.e., the displacement controlled approach that is discussed in Section 1.1.3) and the rotational analysis of a retaining structure modeled as a rigid block is the acceleration imparted to the rigid block. When a rigid block undergoes permanent *sliding* displacement during earthquake shaking, the largest magnitude horizontal acceleration felt by the rigid block (and the retaining structure contained within the rigid block) is  $N^*g$ , which is less than the peak value for ground acceleration. The maximum transmissible acceleration,  $N^*g$ , is sometimes referred to as the yield acceleration; it is not the user-defined, horizontal ground (or, equivalently, the rigid base) acceleration. For a rigid block that undergoes *rotation* during earthquake shaking, the accelerations felt by this rigid block during shaking are those of the ground acceleration time-history. This is because continuous contact between the rigid block

undergoing rotation and the ground is maintained at the point of rotation, i.e., the toe in Figure 1.10, during the entire earthquake shaking process.

Thus for a rigid block that undergoes *rotation* during earthquake shaking, the horizontal acceleration of (rigid) mass center is a function not only of the horizontal ground acceleration but it is also a function of the angular acceleration and the angular velocity during rotation (see Ebeling and White (2006)). This differs from the situation of a rigid block that undergoes permanent *sliding* displacement during earthquake shaking; the largest magnitude horizontal acceleration felt by this rigid block is  $N \cdot g$ . Unlike the sliding (rigid) block model, which effectively isolates the sliding block from the shaking base below, the rotating rigid block model continues to transmit horizontal acceleration through the “pin,” located at the toe of the wall, into the wall.

A key step in the evaluation process of the idealized rigid block formulations of this report and of Ebeling and White (2006) for translation and for rotation is the computation of the maximum transmissible acceleration and the computation of the threshold value of acceleration corresponding to lift-off of the base of the wall in rotation. Comparison of these values determines if the wall will tend to slide before it will rotate or vice versa. The lower of the two values dictates the kinematic mechanism for the retaining wall system model. Both of these computational steps are discussed in this report and incorporated in both CorpsWallSlip and CorpsWallRotate.

## 1.4 Seismic design criteria for Corps retaining structures

Current Corps engineering methodology is to evaluate retaining walls for usual, unusual, and extreme loadings. Consideration of earthquake loadings is part of the design process for Corps earth retaining structures. Engineering Regulation (ER) 1110-2-1806 provides requirements governing the seismic design and evaluation of structures located at Corps projects. The engineering procedures outlined in this Corps document are applicable to the analysis of existing, or the design of new earth retaining structures. The Corps regulation for earthquake loadings, ER 1110-2-1806, specifies two *project specific* earthquakes, the Operational Basis Earthquake (OBE) and the Maximum Design Earthquake (MDE).

The OBE is an earthquake that can reasonably be expected to occur within the service life of the project, that is, with a 50-percent probability of



exceedance during the service life. (This corresponds to a return period of 144 years for a project with a service life of 100 years.) The associated performance requirement is that the project functions with little or no damage, and without interruption of function. The purpose of the OBE is to protect against economic losses from damage or loss of service, and therefore alternative choices of return period for the OBE may be based on economic considerations. The OBE is determined by a Probabilistic Seismic Hazard Analysis (PSHA). The OBE is classified as an unusual event. Retaining walls are expected to remain serviceable and operable immediately following an OBE event, or immediately following any earthquake that can reasonably be expected to occur within the service life of the project.

The MDE is the maximum level of ground motion for which a structure is designed or evaluated. The associated performance requirement is that the project performs without catastrophic failure, such as an uncontrolled release of a reservoir, although severe damage or economic loss may be tolerated. For *critical features*, the MDE is the same as the Maximum Credible Earthquake (MCE). [Section 5(a) and Table B-1 in ER 1110-2-1806 outlines the assessment of the hazard potential classification of Civil Works projects and is related to the consequences of project failure. *Critical features* are the engineering structures, natural site conditions, or operating equipment and utilities at high hazard projects whose failure during earthquake could result, in loss of life.] For all other features, the MDE shall be selected as a lesser earthquake than the MCE which provides economical designs meeting appropriate safety standards. The MDE is the maximum level of ground motion for which a structure is designed or evaluated. Although not formally stated in the ER, recent (limited) application to select, normal Corps (non-critical) structures is to assume the MDE is an earthquake that has a 10 percent chance of being exceeded in a 100-year period (or a 950-year return period). The MDE for normal structures is determined by PSHA. For critical structures the MDE is the Maximum Credible Earthquake (MCE), which is determined by a deterministic seismic hazard assessment (DSHA). The MCE is defined as the greatest earthquake that can reasonably be expected to be generated on a specific source, on the basis of seismological and geological evidence. Significant damage resulting from an MDE event can be considered as acceptable provided the damaged structure can be repaired and put back in service without risk to life.

Factors of safety and safety requirements for retaining walls subject to seismic loading conditions are provided in EM 1110-2-2100. This supersedes the stability guidance for retaining walls contained in EM 1110-2-2502 (but *not* the engineering procedures, which are based on the simplified pseudo-static procedure of analysis).

Factors of safety for sliding and flotation, and the safety provisions related to resultant location and allowable bearing capacity contained in EM 1110-2-2100 are dependent on:

- Load condition category (usual, unusual, or extreme),
- Site information knowledge (well-defined, ordinary, or limited), and
- Structure importance (normal, or critical)

EM 1110-2-2100 associates each of the three load condition categories to a range in annual probability (or, equivalently, a range in return period). Additional “structure specific” information related to load condition categories and probabilities is contained in Appendix B of EM 1110-2-2100.

## 1.5 Axial load capacity of spillway invert slabs

Reinforced concrete slabs provide an important contribution to the overall seismic stability of retaining walls. Figure 1.3 shows, for example, an invert spillway buttressing a cantilever retaining wall that borders a spillway channel. Key to the seismic performance of this spillway retaining wall is the stabilizing force that the channel invert slab exerts at the toe of this wall. The magnitude of this stabilizing force will depend on the limit state axial load capacity of this invert slab.

Invert slabs can be founded on earth or rock. Types of construction used by the Corps include an “independent block plan” and a “continuous reinforcing plan.” Invert slabs when loaded axially can exhibit either short column or long column behavior with the later referring to slabs whose axial capacity is reduced by second-order deformations (i.e.,  $P \bullet \Delta$  effects).

Slab capacity in terms of axial load versus moment interaction is determined based on ultimate strength design principles, which can be applied to both unreinforced (plain concrete) and reinforced concrete invert slab sections. Influences from the subgrade reaction, slab dead load, and axial load eccentricity when considered in a second-order analysis suggest the

axial load capacity can be based on a short column design with second-order displacements due to  $P \cdot \Delta$  effects having little if any effect on column axial load capacity, according to Strom and Ebeling (2004).

The axial load resistance  $P_{\text{resist}}$  provided by the Figure 1.3 invert slab is illustrated in Figure 1.10. Limited investigations, by Strom and Ebeling (2004), based on the Corps minimum thickness for invert slabs constructed on rock and earth, and for both continuous reinforcing plans and independent block plans, indicate the limit state axial load capacity or ultimate axial load resistance of the slab ( $P_{\text{resist}}$ ) may be on the order of:

- 120 kips per foot width of slab for a 1.0-foot-thick invert slab on rock
- 240 kips per foot width of slab for a 2.0-foot-thick invert slab on soil

The above values are valid for both anchored and unanchored invert slabs, and for the minimum contraction joint spacings typically found on Corps projects. However, a site-specific evaluation of the limiting axial resisting force due to the buttressing effect of the any type of slab on the toe of a retaining wall is required. Refer to Strom and Ebeling (2004) for a simplified engineering methodology for the assessment of  $P_{\text{resist}}$  for all types of slabs buttressing all types of retaining structures, including the Figure 1.3 invert spillway slab.

## 1.6 Background and research objective

Engineer Manual 1110-2-2502 Retaining and Flood Walls gives engineering procedures that are currently being used by District engineers in their *initial* assessment of seismic wall performance of existing earth retaining structures and the (preliminary) sizing of new retaining structures. The engineering procedures given in EM 1110-2-2502 for retaining walls make extensive use of the simplified pseudo-static procedure of analysis of earth retaining structures and expresses wall performance criteria in terms of computed factors of safety against sliding and bearing failure, and base area in compression. The simplified pseudo-static procedure of analysis makes it difficult to interpret the actual wall performance for Corps projects subjected to “strong” design ground motions because of simplifications made in the procedure of analysis. In a pseudo-static analysis an over-simplification occurs when the engineer is forced to render the complex, horizontal and vertical earthquake acceleration time-history events to constant values of accelerations and assume a constant direction for each. These constant values are denoted as the pseudo-static

acceleration coefficients in the horizontal and vertical directions (refer to Section 1.1.1 of this report). The engineer is also required to assume a constant direction for each of these components. An acceleration time-history, in actuality, varies both in magnitude and in direction with time.

The simplified pseudo-static procedure does not allow for interpretation of *actual* wall performance by District engineers. Intense shaking imparted by the OBE and MCE design events makes the interpretation of the simplified procedure of analysis even more difficult. The more important questions for the wall are whether the wall slides into the spillway basin, or rotates into the spillway basin, or even tips over onto its side during the earthquake event. The simplified pseudo-static procedure of analysis is not capable of answering these questions. The answers depend on the magnitude of the pseudo-static coefficient used in the calculations compared to the magnitude of the peak values for the acceleration pulses as well as the number and duration of these strong shaking acceleration pulses in the design earthquake event time-history. When considering both horizontal and vertical accelerations, the resulting wall response is further complicated by the time-history of phasing between the pulses of horizontal and vertical accelerations. Only the permanent wall sliding displacement/wall rotation method of time-history analysis can answer these questions. Again, wall displacements will influence the seismic earth pressure forces imparted on the wall by the retained soil.

Formal consideration of the permanent seismic wall displacement in the seismic design process for Corps-type retaining structures is given in Ebeling and Morrison (1992). The key aspect of the engineering approach presented in this Corps document is that simplified procedures for computing the seismically induced earth loads on retaining structures are also dependent upon the amount of permanent wall displacement that is expected to occur for each specified design earthquake. The Ebeling and Morrison simplified engineering procedures for Corps retaining structures are geared towards hand calculations. The engineering formulation and corresponding PC software CorpsWallSlip discussed in this report extend these simplified procedures to walls that slide during earthquake shaking and make possible the use of acceleration time-histories in the Corps design/analysis process when time-histories are made available on Corps projects. CorpsWallSlip may be used to predict permanent seismically induced translational displacements of walls retaining backfill, with or without a toe restraint. It is particularly applicable to rock-founded L-walls

and T-walls (i.e., cantilever retaining walls) which border spillway channels (Figure 1.3).

The engineering methods contained in this report and implemented within CorpsWallSlip allow the engineer to determine if a given retaining wall has a tendency to slide or to rotate for a specified seismic event. This is a new PC software capability for the seismic design/evaluation process for Corps retaining structures.

## 1.7 Organization of report

Chapter 2 describes a new translational (i.e., sliding) block analysis model of a retaining structure buttressed by a reinforced concrete slab. It is a special variation of the engineering formulation for the seismic analysis of the permanent displacement of a retaining structure modeled as a rigid sliding block but with a toe restraint. The formulation used to compute the permanent sliding displacement response of a retaining wall to either (1) an earthquake acceleration time-history via a complete time-history analysis or (2) to user-specified peak ground earthquake response values via a simplified sliding block analysis is given. The numerical method used to compute the sliding displacement time-history via the complete time-history analysis of the rigid block model is presented.

Chapter 3 describes the computation of the threshold value of acceleration corresponding to lift-off of the base of the wall in rotation. Key aspects of the new Ebeling and White (2006) engineering formulation for the seismic analysis of the permanent rotation of a retaining structure modeled as a rigid block *with toe restraint* are summarized.

Chapter 4 describes key aspects of the visual modeler and visual post-processor CorpsWallSlip. Specifically, a description of the GUI for input of geometry, input of material properties, input/verification of earthquake time-history files, and for visualization of results is presented to make the user familiar with its operation.

Chapter 5 presents a summary, conclusions, and recommendations for additional research.

Appendix A presents a derivation of the dynamic active earth pressure force using the sweep-search wedge method which is implemented in CorpsWallSlip to calculate  $P_{AE}$ .

Appendix B describes an approach for computing the point of application,  $h_{PAE}$ , of the dynamic active earth pressure force,  $P_{AE}$ , for moist retained soil.

Appendix C describes an approach for computing the dynamic active earth pressure distribution for a partially submerged, retained soil.

Appendix D describes the procedures for computing the water pressures acting on the structural wedge, including the computation of hydrodynamic water pressures due to earthquake shaking of a pool (when present) in front of the retaining wall. With most Corps hydraulic structures that act as earth retaining structures possessing a vertical face in contact with the pool (when present), hydrodynamic water pressures are approximated in the CorpsWallSlip using the Westergaard procedure.

Appendix E outlines the mass moment of inertia computation made by CorpsWallSlip for the structural wedge.

Appendix F lists and describes the contents of the ASCII input data file to the FORTRAN engineering computer program portion of CorpsWallSlip. This data file, always designated as CWROTATE.IN, is created by the GUI, the visual modeler portion of CorpsWallSlip. Both formulations share many engineering computations. So in order to facilitate the maintenance of both engineering formulations and corresponding software, the same FORTRAN code is used with the two visual modelers and post-processors. The first line of input is used to designate a CorpsWallSlip analysis. Other key codes are used in the input data to further distinguish between the two engineering formulations.

Appendix G lists the CorpsWallSlip ASCII output files.

Appendix H discusses two example computations of static, active earth pressure distributions and depth of cracking in cohesive soils.

## **2 New Translational Block Analysis Model of a Retaining Structure Buttressed by a Reinforced Concrete Slab**

### **2.1 Introduction**

This chapter describes a new engineering formulation developed for computing the permanent translational response of rock-founded retaining walls buttressed at their toe by a reinforced concrete slab to earthquake ground motions. The resulting engineering formulation is implemented within corresponding PC software CorpsWallSlip using a GUI for input of geometry, input of material properties, input/verification of earthquake time-history files, and visualization of results. The PC software CorpsWallSlip (sometimes referred to as CWSlip) was developed to perform an analysis of the permanent sliding displacement response for each proposed retaining wall section to either (1) a user-specified earthquake acceleration time-history via a complete time-history analysis or (2) user-specified peak ground earthquake response values via a simplified sliding block analysis. The complete time-history method of analysis is discussed first in this chapter, followed by a discussion of the simplified sliding block analysis. (Key aspects of the visual modeler and visual post-processor CorpsWallSlip are described in Chapter 4.)

A key result from the translational (i.e., sliding) block method of analysis is the computation of the permanent deformation of a retaining structural system from either (1) a user-specified design earthquake event or (2) simplified permanent displacement relationships with the ground motion characterized by peak acceleration and peak velocity and earthquake magnitude values. For a complete time-history analysis, this design earthquake event is represented by an acceleration time-history specified within the rock-foundation base. Chapter 1 discussed the numerous variations of rigid sliding block methods of seismic analysis as applied to slopes, earthen dams, retaining wall systems, and foundations. They all have their roots in the methodology outlined in Newmark (1965) and what has come to be known as the Newmark sliding block model (Section 1.1.3). This chapter discusses the formulation of the translational (rigid) block analysis of the Figure 2.1 cantilever retaining structure buttressed by, e.g., a concrete slab at its toe, as implemented in CorpsWallSlip for Corps retaining

walls. The effect of this reinforced concrete slab is represented by the user-specified force  $P_{\text{resist}}$  acting on a vertical section extending upwards from the toe of the wall. Strom and Ebeling (2004) present a simplified engineering procedure to estimate the magnitude of  $P_{\text{resist}}$ .

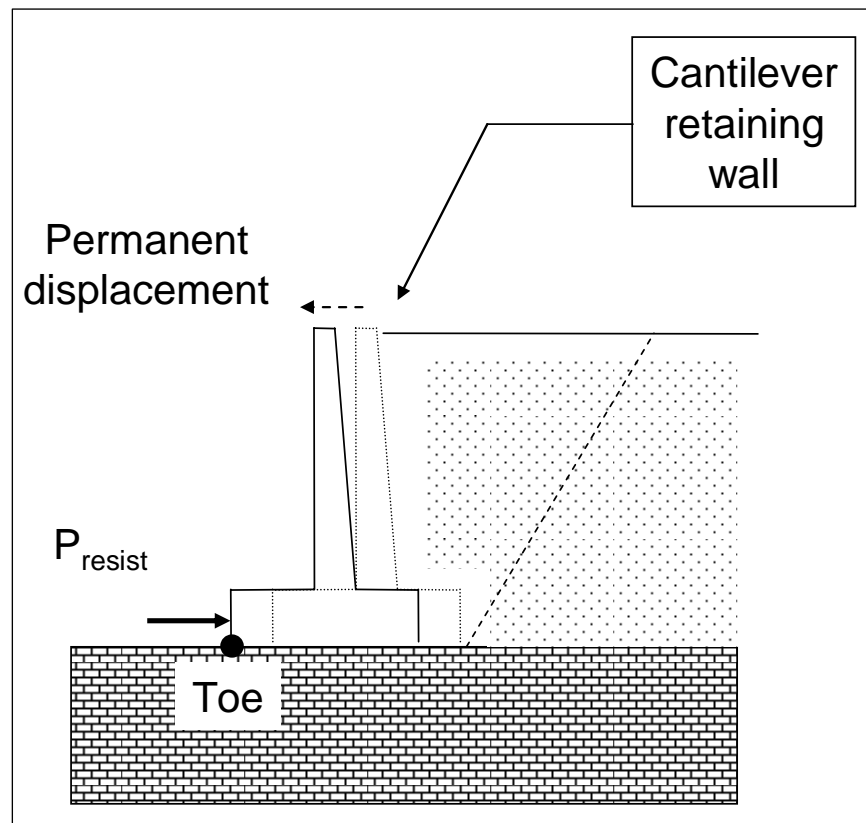


Figure 2.1. Permanent, seismically induced displacement of a rock-founded cantilever wall retaining moist backfill and with toe restraint, computed using CorpsWallSlip.

## 2.2 Contrasting a translational with the rotational analysis of a rigid block

A complete rotational time-history analysis of permanent deformation of a retaining wall during earthquake shaking is discussed in Ebeling and White (2006). An important difference between the translational (i.e., Newmark sliding) block method of analysis for earth retaining structures and the rotational analysis of a retaining structure modeled as a rigid block is *the acceleration imparted to the rigid block*. When a rigid block undergoes permanent *sliding* displacement during earthquake shaking, the largest magnitude horizontal acceleration felt by the rigid block (and the retaining structure contained within the rigid block model) is *less* than the peak value for ground acceleration, as depicted in Figure 1.8. Ebeling and



Morrison (1992) designated the value for a retaining wall's maximum transmissible acceleration as  $N^*g$ . The maximum transmissible acceleration,  $N^*g$ , is sometimes referred to as the yield acceleration; it is not the user-defined, horizontal ground (or, equivalently, the rigid base) acceleration. Contrast this to the response of a rigid block that undergoes *rotation* during earthquake shaking; the accelerations felt by this rigid block during shaking are those of the ground acceleration time-history. This is because continuous contact between the rigid block undergoing rotation and the ground (modeled as a rigid base) is maintained at the point of rotation (e.g., the toe of the Figure 1.10 retaining wall) during the entire earthquake shaking process. The acceleration imparted to the center of mass of a rotating rigid block is discussed in Sections 1.2 and 3.2 of Ebeling and White (2006).

***Does a wall slide or does it rotate during earthquake shaking?***

The first step in determining if the retaining wall will rotate prior to sliding during earthquake shaking, or vice versa, is to compute (1) the value of acceleration that is needed for lift-off of the wall from its base in rotation about the toe of the wall using the Ebeling and White (2006) procedure summarized in Chapter 3 of this report; and (2) the limiting acceleration required to reduce the factor of safety against sliding to a limiting value of 1.0 (commonly referred to as the maximum transmissible acceleration using the procedure outlined in this chapter). These two computations are accomplished by the PC-based software CorpsWallSlip. The second step is to compare these limiting acceleration values. For the simplified decoupled analyses outlined in this report, the mode of deformation is dictated by the smaller of the two acceleration values.

## **2.3 Maximum transmissible acceleration**

In the earthquake-induced translational displacement analysis of a retaining wall, the primary variable is the permanent displacement. In a complete time-history analysis, a user-defined (ground) acceleration time-history is applied to the Figure 2.2 rigid base on which the retaining wall is founded in the idealized model. The seismic inertia coefficient ( $N^*$  in Ebeling and Morrison (1992) terminology) that reduces the sliding factor of safety for the driving soil wedge and the structural wedge to unity is first determined. The value for the maximum transmissible acceleration (i.e.,  $N^*g$ ; the yield acceleration in Ebeling and Morrison (1992) terminology) is the horizontal acceleration imparted to the retaining wall system, consisting of the driving wedge and structural wedge (see Figure 1.7), that will

nominally exceed the shear resistance provided by the foundation along (or immediately below) the interface between the base of the retaining structure and the foundation. The driving soil wedge (Figure A.1) is represented by the dynamic force  $P_{AE}$  in the Figure 2.2 free-body diagram of the structural wedge figure showing the dynamic forces acting on a rigid block model of the structural wedge with sliding along its base during shaking of the rigid base.<sup>1</sup> This cantilever wall, which retains moist backfill, is subjected to the five external forces of the weight of the structural wedge  $W$ , the dynamic active earth pressure force  $P_{AE}$ , the resisting force  $P_{resist}$  provided by the reinforced concrete slab at the toe of the wall, and the rigid base-to-wall reaction shear and normal forces  $T$  and  $N'$ , respectively. The procedures outlined in Appendix A and Appendix B are used to compute the value of  $P_{AE}$  at each acceleration time-history time-step. The structural wedge and driving soil wedges are assumed to act as a single rigid body, as shown in Figure 1.7. Thus, inertial forces due to the acceleration values applied at a given time-step to the structural and driving wedges impact the magnitude of  $P_{AE}$ , as outlined in the sweep-search soil wedge solution procedure summarized in Appendix A. Consequently, when the value for acceleration of the rigid block changes with time-steps, the value of  $P_{AE}$  changes as well.

At the onset of sliding of the Figure 2.2 retaining wall, the horizontal driving force equals the stabilizing (i.e., restoring) force. The summation of the Figure 2.2 horizontal forces acting on the rigid body results in

$$\frac{W}{g} \cdot (a_{CG})_h + P_{AE} \cdot \cos(\delta) = P_{resist} + T \cdot \cos(\varepsilon) + N' \cdot \sin(\varepsilon) \quad (2.1)$$

$T$  is the shear force required for equilibrium of forces acting on the structural wedge. At incipient sliding, the shear strength along the base to foundation interface becomes fully mobilized (i.e.,  $FS_{slide} = 1.0$ ). Assuming a full mobilization of shear resistance along the base (of length  $L_{base}$ ), the shear force may be computed utilizing the Mohr-Coulomb failure criteria, in an effective stress analysis, as

<sup>1</sup> The inertial forces are applied according to D'Alembert's principle. The advantage of the inertia-force method based on D'Alembert's principle is that it converts a dynamics problem into an equivalent problem in equilibrium.

$$T = c'_{base} \bullet L_{base} + N' \bullet \tan(\delta'_{base}) \quad (2.2)$$

Introducing Equation 2.2, Equation 2.1 becomes

$$\frac{W}{g} \bullet (a_{CG})_h + P_{AE} \bullet \cos(\delta) = \quad (2.3)$$

$$P_{resist} + [c'_{base} \bullet L_{base} + N' \bullet \tan(\delta'_{base})] \bullet \cos(\varepsilon) + N' \bullet \sin(\varepsilon)$$

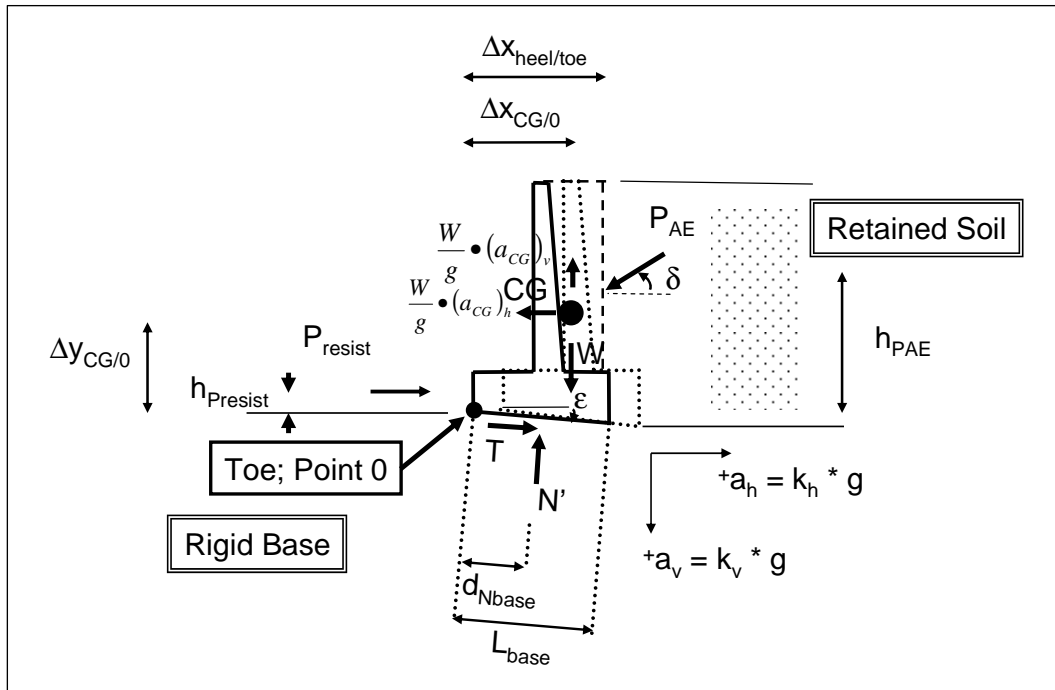


Figure 2.2. Inertia forces and resultant force vectors acting on a rigid block model of a cantilever wall retaining moist backfill with sliding along its base during horizontal and vertical shaking of the inclined rigid base.

Simplifying, Equation 2.3 becomes

$$\frac{W}{g} \bullet (a_{CG})_h + P_{AE} \bullet \cos(\delta) = \quad (2.3)$$

$$P_{resist} + c'_{base} \bullet L_{base} \bullet \cos(\varepsilon) + N' \bullet [\tan(\delta'_{base}) \bullet \cos(\varepsilon) + \sin(\varepsilon)]$$

The summation of the Figure 2.2 vertical forces acting on the rigid body results in

$$0 = N' \bullet \cos(\varepsilon) - T \bullet \sin(\varepsilon) - W + \frac{W}{g} \bullet (a_{CG})_v - P_{AE} \bullet \sin(\delta) \quad (2.4)$$

Introducing Equation 2.2, Equation 2.4 becomes

$$0 = N' \bullet \cos(\varepsilon) - [c'_{base} \bullet L_{base} + N' \bullet \tan(\delta'_{base})] \bullet \sin(\varepsilon) \quad (2.5)$$

$$-W + \frac{W}{g} \bullet (a_{CG})_v - P_{AE} \bullet \sin(\delta)$$

Simplifying, Equation 2.5 becomes

$$N' = \frac{c'_{base} \bullet L_{base} \bullet \sin(\varepsilon) + W - \frac{W}{g} \bullet (a_{CG})_v + P_{AE} \bullet \sin(\delta)}{\cos(\varepsilon) - \tan(\delta'_{base}) \bullet \sin(\varepsilon)} \quad (2.6)$$

Introducing Equation 2.6, Equation 2.3 becomes

$$\begin{aligned} & \frac{W}{g} \bullet (a_{CG})_h + P_{AE} \bullet \cos(\delta) = \\ & P_{resist} + c'_{base} \bullet L_{base} \bullet \cos(\varepsilon) + \\ & \left[ \frac{c'_{base} \bullet L_{base} \bullet \sin(\varepsilon) + W - \frac{W}{g} \bullet (a_{CG})_v + P_{AE} \bullet \sin(\delta)}{\cos(\varepsilon) - \tan(\delta'_{base}) \bullet \sin(\varepsilon)} \right] \\ & \bullet [\tan(\delta'_{base}) \bullet \cos(\varepsilon) + \sin(\varepsilon)] \end{aligned} \quad (2.7)$$

Equation 2.7 represents the equilibrium relationship for the (rigid) structural wedge when the earthquake accelerations are such that the factor of safety against sliding along its base is equal to 1.0. For a factor of safety > 1.0 against sliding, the retaining wall does not slide. The rigid body CG accelerations are the same as the rigid base accelerations (i.e., within the rock foundation). However, the accelerations felt by the rigid body (i.e., at its center of gravity, CG) will differ from the rigid base accelerations for user-defined rigid base acceleration (time-history) values that exceed the

value for acceleration that results in a factor of safety against sliding equal to 1.0. During sliding, the acceleration felt by the rigid body at its center of gravity, CG, is of constant magnitude.

The component of the threshold acceleration occurring at translation (i.e., sliding) along the base is designated as

$$(a_{CG})_{\text{threshold-sliding-h}} = (k_{CG})_{\text{threshold-sliding-h}} \bullet g \quad (2.8)$$

where  $(k_{CG})_{\text{threshold-sliding-h}}$  is a value of horizontal ground acceleration, expressed in decimal fraction. In Ebeling and Morrison (1992), the acceleration  $(a_{CG})_{\text{threshold-sliding-h}}$  is referred to as the maximum transmissible acceleration,  $(N \bullet g)$ , or as the yield acceleration. Note that the horizontal acceleration value  $[(k_{CG})_{\text{threshold-sliding-h}} \text{ times } g]$  is not a user-specified constant. Since the horizontal limiting acceleration is of interest, one option is to set the vertical component of acceleration occurring at sliding equal to zero, as done by Richards and Elms (1979) and others.<sup>1</sup> By making this assumption and introducing Equation 2.8, Equation 2.7 becomes

$$(k_{CG})_{\text{threshold-sliding-h}} = \frac{\left\langle \frac{P_{\text{resist}} + c'_{\text{base}} \bullet L_{\text{base}} \bullet \cos(\varepsilon) - P_{\text{AE}} \bullet \cos(\delta) + \left[ \frac{c'_{\text{base}} \bullet L_{\text{base}} \bullet \sin(\varepsilon) + W + P_{\text{AE}} \bullet \sin(\delta)}{\cos(\varepsilon) - \tan(\delta'_{\text{base}}) \bullet \sin(\varepsilon)} \right] \bullet [\tan(\delta'_{\text{base}}) \bullet \cos(\varepsilon) + \sin(\varepsilon)]}{W} \right\rangle}{W} \quad (2.9)$$

Because of the inclusion of acceleration in  $P_{\text{AE}}$  formulation (refer to Appendix A) in this equation, CorpsWallSlip solves Equation 2.9 using a trial-and-error numerical approach. Note that no safety factor need be applied to the weight of the wall/structural wedge nor to its shear strength in this calculation.

The summation of overturning and resisting moments about the toe (i.e., point O) of the Figure 2.2 forces acting on the rigid body results in

<sup>1</sup> Another option, implemented in CorpsWallSlip, is to assign a constant value to the vertical acceleration component. A procedure for determining the value for this constant is discussed in Sections 2.5 and 2.6.

$$\begin{aligned}
& \frac{W}{g} \cdot (a_{CG})_h \cdot \Delta y_{CG/0} + \frac{W}{g} \cdot (a_{CG})_v \cdot \Delta x_{CG/0} \\
& + P_{AE} \cdot \cos(\delta) \cdot [(y_{heel} + h_{PAE}) - y_{toe}] + N' \cdot d_{Nbase} = \\
& P_{resist} \cdot h_{Presist} + W \cdot \Delta x_{CG/0} + P_{AE} \cdot \sin(\delta) \cdot \Delta x_{heel/toe}
\end{aligned} \tag{2.10}$$

Recall the computation of  $h_{PAE}$  as well as the distribution of earth pressure forces corresponding to  $P_{AE}$  are discussed in Appendix B and Appendix C. Solving for the location of the result effective force normal to the base,  $d_{Nbase}$ , Equation 2.10 becomes

$$d_{Nbase} = \frac{\left[ -\frac{W}{g} \cdot (a_{CG})_h \cdot \Delta y_{CG/0} - \frac{W}{g} \cdot (a_{CG})_v \cdot \Delta x_{CG/0} - P_{AE} \cdot \cos(\delta) \cdot [(y_{heel} + h_{PAE}) - y_{toe}] + P_{resist} \cdot h_{Presist} + W \cdot \Delta x_{CG/0} + P_{AE} \cdot \sin(\delta) \cdot \Delta x_{heel/toe} \right]}{N'} \tag{2.11}$$

Because of the inclusion of acceleration in  $P_{AE}$  formulation (refer to Appendix A) in this equation, CorpsW<sub>allSlip</sub> solves Equation 2.11 using a trial-and-error numerical approach. Introducing the horizontal limiting acceleration (i.e., Equation 2.8) in the case of a wall sliding along its base and setting the vertical component of acceleration occurring at sliding equal to zero, Equation 2.11 simplifies to

$$d_{Nbase} = \frac{\left[ -W \cdot (k_{CG})_{threshold-sliding-h} \cdot \Delta y_{CG/0} - P_{AE} \cdot \cos(\delta) \cdot [(y_{heel} + h_{PAE}) - y_{toe}] + P_{resist} \cdot h_{Presist} + W \cdot \Delta x_{CG/0} + P_{AE} \cdot \sin(\delta) \cdot \Delta x_{heel/toe} \right]}{N'} \tag{2.12}$$

During sliding, the value of  $P_{AE}$  is computed using the horizontal acceleration value  $[(k_{CG})_{threshold-sliding-h} \text{ times } g]$ , the maximum transmissible acceleration ( $N \cdot g$  in Ebeling and Morrison (1992) notation). Recall that full contact is maintained between the base of the wall and its foundation during sliding in this formulation.

## 2.4 Time-history of permanent wall displacement

Earthquake shaking of the rock foundation is represented by time-histories of acceleration in the translational block formulation implemented in CorpsWallSlip for the complete time-history analysis option.<sup>1</sup> Since the ground acceleration varies with time, let the horizontal ground acceleration be represented by variable fraction  $A$  times the constant acceleration of gravity,  $g$ , in Figure 1.8. Recall that the integral of the acceleration time-history is equal to the velocity time-history and the integral of velocity is displacement (i.e., the permanent wall displacement in this case). For a “rigid block” (i.e., retaining wall structural wedge and driving wedge) subjected to an acceleration of value larger than the Figure 1.8 maximum transmissible acceleration, labeled  $N^*g$  in this figure, the rigid block will displace. When this occurs over several time-steps, the total permanent displacement of a sliding structural wedge relative to the base (i.e., the rock foundation) is the sum of the increments of displacement occurring during a number of individual pulses of ground motion as shown in this figure. These incremental relative displacements are determined as follows: For each time the acceleration of the ground, equal to  $A$  times  $g$ , is greater than the constant  $N^*$  times  $g$  shown in this figure, relative displacements (between the retaining wall mass and the foundation) will *initiate*. The integral of the difference in velocities between the sliding structural wedge and the rock foundation velocity is equal to the incremental, relative displacement of the sliding structural wedge.

This section describes the numerical method implemented within CorpsWallSlip to compute the translational time-history of a rigid block retaining structure during earthquake shaking for the complete time-history analysis option. It mirrors the numerical procedure used to compute the rotational time-history of a rigid block rotating about its toe, discussed in Section 3.8 of Ebeling and White (2006).

### 2.4.1 Introduction to a step-by-step solution scheme

Earthquake acceleration time-histories are used to represent the earthquake demand in this formulation. They are specified within the rigid base of Figure 2.2. It is the experience of the primary author of this report that

---

<sup>1</sup> Baseline-corrected, horizontal and vertical acceleration time-histories are to be used to represent the earthquake ground motions in CorpsWallSlip.

the duration of ground acceleration time-histories used on Corps projects is on the order of tens of seconds, and up to about one minute of earthquake shaking. The number of time increments (i.e., discrete acceleration point values) contained in the acceleration time-history corresponds to the number of solutions made in the translational wall analysis by CorpsWallSlip. The number of time increments is defined by the duration of earthquake shaking and the time increment  $DT$  used in digitization of the acceleration time-history.<sup>1</sup> There is no standard time increment  $DT$  for the digitization and subsequent processing of acceleration time-histories for Corps projects. However, Ebeling, Green, and French (1997) observe that a  $DT$  equal to 0.02, 0.01, or 0.005 sec is the most common. For example, an earthquake acceleration time-history with 40 sec of shaking and a time-step of 0.02 sec will contain 2,000 discretized acceleration points. If the acceleration time-history was processed with a  $DT$  equal to 0.01 or 0.005 sec, then the discretized acceleration time-histories would contain 4,000 and 8,000 acceleration points, respectively.

A step-by-step solution scheme is followed in order to obtain the wall's permanent translational relative velocity,  $relV$ , and displacement,  $relD$ , in the time domain by CorpsWallSlip. An overview of the characteristics of this numerical formulation is depicted in Figure 2.3. A key feature of the numerical formulation used is the assumption of a *linear* variation in relative acceleration  $relA$  over time-step  $DT$ , from time  $t_i$  to time  $t_{i+1}$ . Values of the user-provided ground acceleration (specified within the rigid base model) are compared against the maximum transmissible acceleration value  $[(k_{CG})_{\text{threshold-sliding-h}} \text{ times } g]$  at each time-step. (Recall the value for maximum transmissible acceleration value  $[(k_{CG})_{\text{threshold-sliding-h}} \text{ times } g]$  is a constant.) This idealized figure assumes that the wall is undergoing positive relative acceleration (i.e., value for acceleration of the ground is greater than the value of  $[(k_{CG})_{\text{threshold-sliding-h}} \text{ times } g]$ ), positive relative velocity, and positive (permanent) displacement at time  $t_i$ , which continues through time  $t_{i+1}$ . The relative acceleration values  $relA0$  and  $relA1$  are equal to the difference between the horizontal ground acceleration value minus the constant value of  $[(k_{CG})_{\text{threshold-sliding-h}} \text{ times } g]$  at times  $t_i$  and  $t_{i+1}$ , respectively, and assumed positive at both time-steps. (Other cases will be considered later.) The idealized figure also assumes that the

---

<sup>1</sup> Note that CorpsWallSlip requires the time-step  $DT$  for the horizontal and vertical acceleration time-histories used in the same analysis be the same value.



relative acceleration increases in magnitude over this time-step  $\Delta T$ , as depicted in this figure. The relative velocity is computed by integrating the relative acceleration during each segment of wall translation.

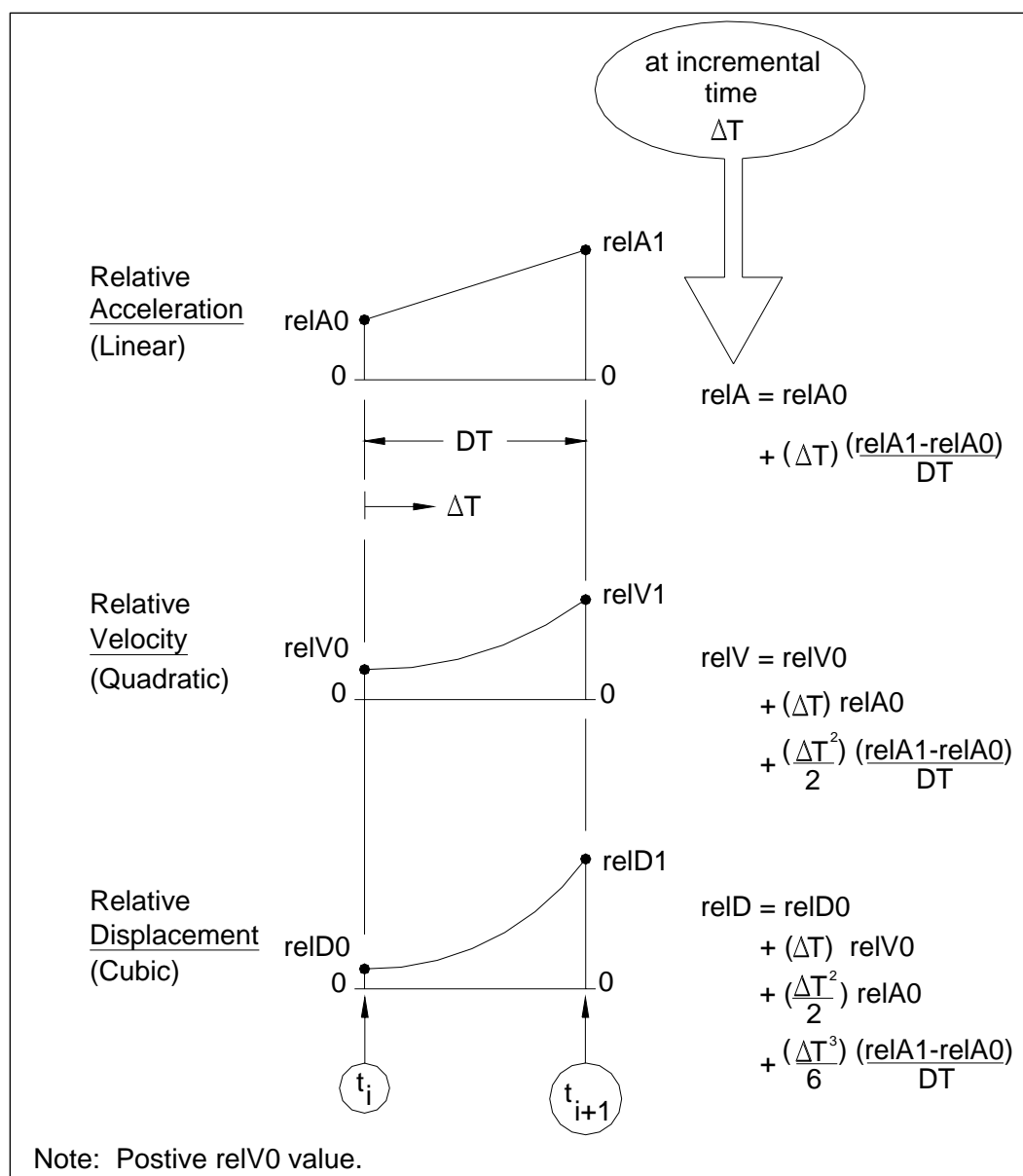


Figure 2.3. Complete equations for relative motions over time increment  $\Delta T$  based on linearly varying acceleration.

$$relV = \int_0^t relA \, dt \quad \text{when } relV > 0 \quad (2.13)$$

or

$$relV = 0 \quad \text{when Equation 2.13 gives } relV \text{ less than } 0 \quad (2.14)$$

So for a linear variation in relative acceleration over time-step  $DT$ , the relative velocity,  $relV$ , is a quadratic relationship. Note that  $C_{orps}W_{allSlip}$  assumes that the wall cannot slide back into the retained soil, which is expressed by Equation 2.14. Similarly, with the permanent relative displacement of the wall being the integration of the relative velocity, the relative displacement of the wall is a cubic relationship listed in Figure 2.3. The permanent relative displacement of the wall is the integration of the relative velocity

$$relD = \int_0^t relV \, dt \quad (2.15)$$

This series of computations using relative accelerations and Equations 2.13 through 2.15 are repeated for each sequence of wall translations that occurs for the duration of earthquake shaking. The experience of the primary author of this report is that when the acceleration time-histories used as input to  $C_{orps}W_{allSlip}$  are based on previously recorded earthquake events (a typical scenario), the permanent displacement occurs during several, separate pulses occurring throughout the duration of shaking.

In Figure 2.3, the value for relative acceleration  $relA$ , relative velocity  $relV$ , and (permanent wall) relative displacement  $relD$  at any point in time  $\Delta t$  after  $t_i$  and before time  $t_{i+1}$  are given by the linear, quadratic and cubic relationships contained on the right-hand side of these three figures (with  $\Delta t$  less than or equal to  $DT$ ).

Recall that during sliding the acceleration felt by the wall equals the maximum transmissible acceleration. Thus, the sliding (rigid) block model effectively isolates the sliding block from the shaking (rigid) base below.

### 2.4.2 Positive relative accelerations $relA0$ and $relA1$ at times $t_i$ and $t_{i+1}$

Expanding on the details of the computations for the numerical formulation depicted in Figure 2.3, the computation of the relative acceleration,  $relA$ , relative velocity,  $relV$ , and relative displacement,  $relD$ , at time  $t_{i+1}$  are made as follows: Values for  $relA$ ,  $relV$ ,  $relD$ , at time  $t_i$  are known from the previous computation step in the step-by-step solution scheme. The value for  $relA$  at time  $t_{i+1}$  (designated  $relA1$  in the figure) is computed as the difference between horizontal ground acceleration minus the constant value of  $[(k_{CG})_{\text{threshold-sliding-h}} \text{ times } g]$ . Referring to Figure 2.4, the relative velocity at time  $t_{i+1}$  (designated  $relV1$ ) is computed from the value for relative velocity at time  $t_i$  (designated  $relV0$ ) plus the positive area under the linear relative acceleration relationship over the time-step  $DT$ , designated  $Area_a$  in this figure. By the trapezoidal rule,  $relV1$  at time  $t_{i+1}$  is

$$relV1 = relV0 + \frac{DT}{2} \bullet (relA0 + relA1) \quad (2.16)$$

with the values for  $relV0$  and  $relA0$  now known values that were computed in the previous solution step. Note the wall is in motion at time  $t_i$ , as reflected by a positive value for relative velocity (designated  $relV0$  in Figure 2.4). Similarly, the permanent relative wall displacement at time  $t_{i+1}$  (designated  $relD1$ ) is computed from the value for relative displacement at time  $t_i$  (designated  $relD0$ ) plus the positive area under the quadratic relative velocity relationship over the time-step  $DT$ , designated  $Area_v$  in this figure. For this linear acceleration method,  $relD1$  at time  $t_{i+1}$  is

$$relD1 = relD0 + DT \bullet relV0 + \frac{DT^2}{6} \bullet (2 \bullet relA0 + relA1) \quad (2.17)$$

with the value for  $relD0$  being a known value that was computed in the previous solution step. The value for relative velocity  $relV$  and (permanent wall) displacement  $relD$  at time  $t_{i+1}$  are also described in terms of the area relationships contained in Figure 2.4. In this manner a step-by-step solution scheme is followed throughout the entire time-history of earthquake shaking in order to obtain the wall velocity,  $relV$ , and relative displacement,  $relD$ , at each increment in time in the Figure 2.4 case of positive values for  $relA$  at times  $t_i$  and  $t_{i+1}$ .

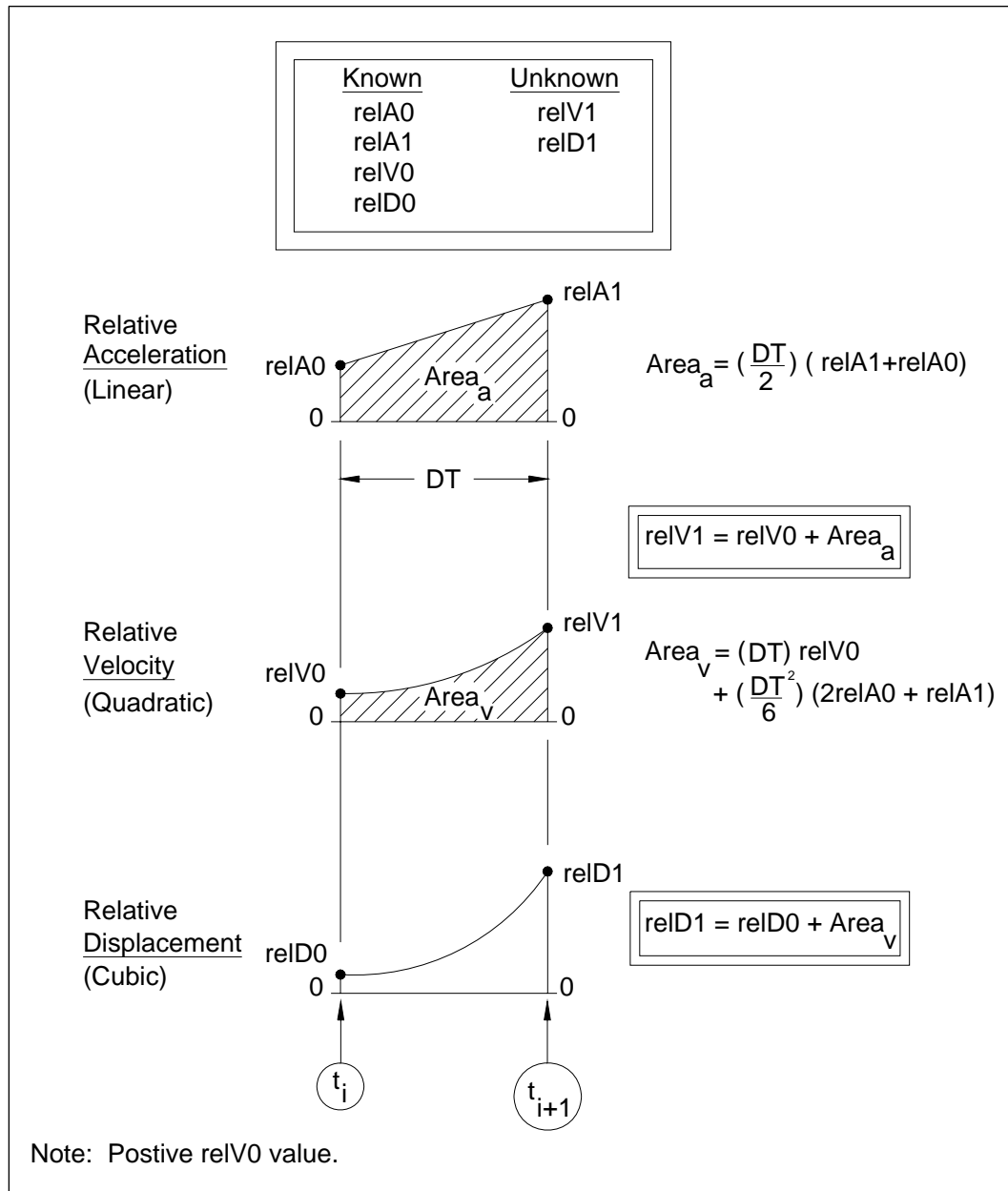


Figure 2.4. Relative velocity and displacements at the end of time increment DT based on linearly varying relative acceleration.

In summary, Figure 2.4 outlines a numerical procedure to obtain values for relative velocity and for relative displacement at time  $t_{i+1}$  in situations for which values of relative acceleration relA at times  $t_i$  and  $t_{i+1}$  are both positive. However, there are three other situations that can arise during the step-by-step solution: (a) the case of a negative value for relA at time  $t_i$  and a positive value for relA at time  $t_{i+1}$ ; (b) the case of wall decelerating over the entire time-step DT for which the values of relA are negative at both times  $t_i$  and  $t_{i+1}$ ; and (c) the case of a positive value for relA at time  $t_i$

and a negative value for  $relA$  at time  $t_{i+1}$ . In all four cases, the assumption of **linear relative acceleration** over time-step  $DT$  is made and the basic concept of **integrating** positive areas above and/or negative areas below the time line of relative acceleration,  $relA$ , to obtain the *change* in relative velocity,  $relV$ , and then, in turn, the integration of positive and/or negative areas above and/or below the time line of  $relV$  to obtain the *change* in relative displacement,  $relD$ , is used to determine the values for  $relV$  and  $relD$ , respectively, at time  $t_{i+1}$ . These three additional step-by-step solutions will be discussed next. Note the frequent use of the trapezoidal rule for  $relV$  and the linear acceleration method for  $relD$  in the solution processes to be described.

#### 2.4.3 Positive relative acceleration $relA0$ at time $t_i$ and negative relative acceleration $relA1$ at $t_{i+1}$

Next consider a wall in motion (i.e., with a positive value for  $relV$ ) at time  $t_i$  but with the Figure 2.5 case of a negative value for  $relA0$  computed at time-step  $t_i$  and positive value for  $relA1$  computed at the next time-step of  $t_{i+1}$ .<sup>1</sup> The first step is to determine the time instant [ $t_i$  plus  $lhsDT$ ] at which the relative acceleration  $relA$  is equal to zero, as labeled in the figure. By linear interpolation, this time increment  $lhsDT$  is

$$lhsDT = \left| relA0 \bullet \left( \frac{DT}{relA1 - relA0} \right) \right| \quad (2.18)$$

The negative area between the negative portion of the linear acceleration line and the time line over the Figure 2.5 time increment  $lhsDT$  is

$$NegativeArea_{-A+} = \frac{1}{2} \bullet lhsDT \bullet (relA0 + 0) \quad (2.19)$$

---

<sup>1</sup> Note the assumption of a linear variation in relative acceleration over the time-step  $DT$  in Figure 2.5.

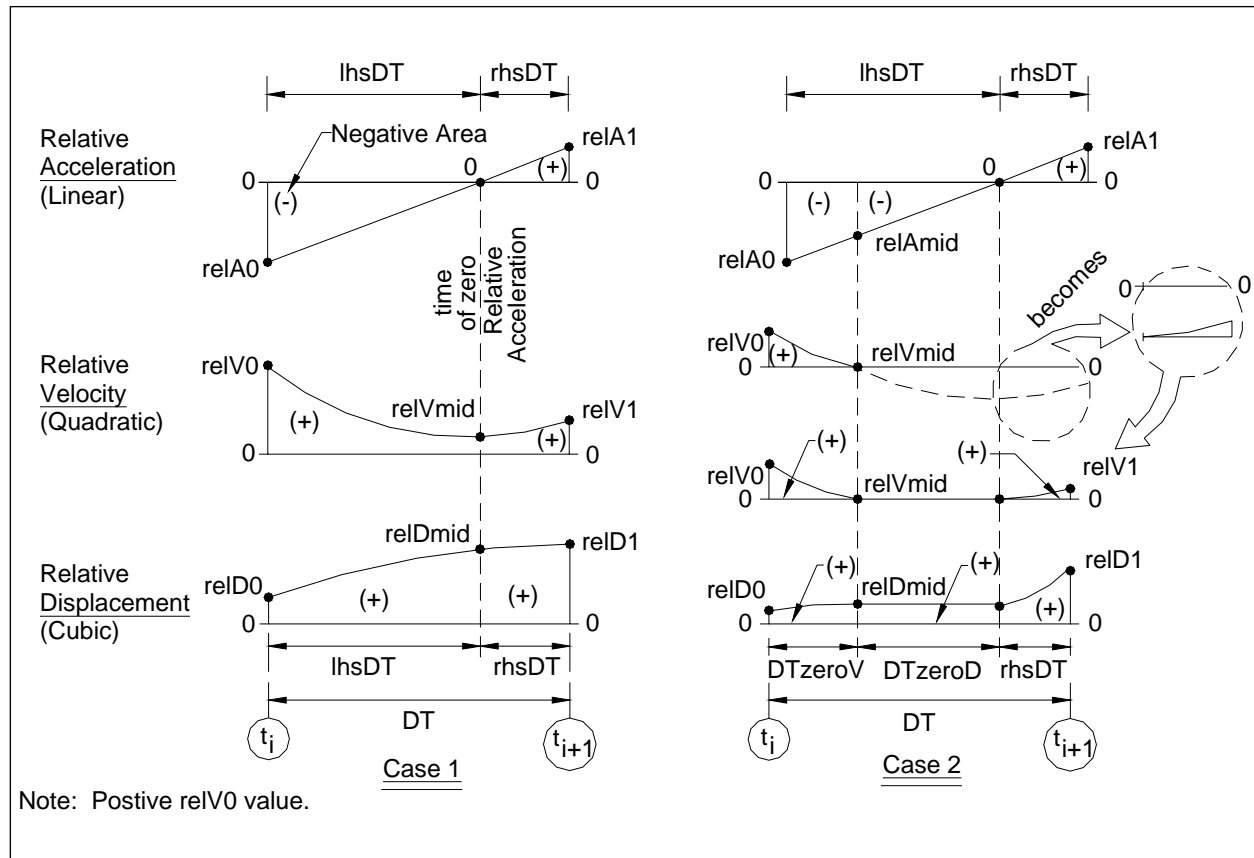


Figure 2.5. Two possible outcomes for the case of a negative relative acceleration at time  $t_i$  and a positive relative acceleration at time  $t_{i+1}$ .

Recall that the wall is in motion at time  $t_i$  when relative velocity (designated  $relV0$  in the figure) is positive. There are two possible outcomes for the Figure 2.5 step-by-step numerical solutions for values of  $relV$  and of  $relD$  at time  $t_{i+1}$ , depending upon the magnitude of  $relV0$  relative to the magnitude of  $NegativeArea_{-A+}$ . These possible scenarios are depicted by two columns of figures in Figure 2.5, labeled as the Case 1 and Case 2 figure groups.

**Case 1:** This case results when the positive value for  $relV$  at time  $t_i$  is greater than the magnitude of  $NegativeArea_{-A+}$  (i.e., the negative area between the negative portion of the linear acceleration line and the time line over the portion of the Figure 2.5 time increment labeled  $lhsDT$ ). The three left-hand side figures in Figure 2.5 are used to describe the Case 1 step-by-step solution scheme: The top figure describes the relative acceleration,  $relA$ , the middle figure describes the relative velocity,  $relV$ , and the lower figure describes the (permanent) relative wall displacement  $relD$ .

The top Case 1 figure depicts the case of a (labeled) negative triangular area between the linear relative deceleration  $relA$  line and the time line (i.e.,  $NegativeArea_{-A+}$  by Equation 2.19), being of less magnitude than the positive value for relative velocity at time  $t_i$  (designated  $relV0$ ). Consequently, the wall will remain in displacement (i.e., sliding) during the entire time-step  $DT$ . At the increment in time  $lhsDT$  after time  $t_i$ , a portion of the negative deceleration area reduces the value of relative velocity from the positive value of magnitude  $relV0$  at time  $t_i$  to a smaller magnitude value at time  $[t_i \text{ plus } lhsDT]$ , as shown in this figure. The relative velocity at time  $[t_i \text{ plus } lhsDT]$  is

$$relVmid = relV0 + \frac{1}{2} \bullet lhsDT \bullet (relA0 + 0) \quad (2.20)$$

The *change* in relative displacement from time  $t_i$  to time  $[t_i \text{ plus } lhsDT]$  is equal to the labeled positive area between the quadratic relative velocity curve and the time line. At time  $[t_i \text{ plus } lhsDT]$  the relative wall displacement increases in magnitude from  $relD0$  to  $relDmid$ .

$$relDmid = relD0 + lhsDT \bullet relV0 + \frac{(lhsDT)^2}{6} \bullet (2 \bullet relA0 + 0) \quad (2.21)$$

The wall continues in motion, with positive relative velocity and with additional permanent deformation after time  $[t_i \text{ plus } lhsDT]$  when the relative acceleration of the wall is positive. At time  $[t_i \text{ plus } lhsDT]$  the magnitude of the wall's relative velocity begins to increase in magnitude as a result of the positive relative acceleration of the wall. The positive (labeled) triangular area between the time line and the linear acceleration line, shown in the top Case 1 figure, equals the *change* in relative velocity and for the wall, consequently, the value for relative velocity at time  $t_{i+1}$  (labeled  $relV1$  in the Case 1 middle figure) is

$$relV1 = relVmid + \frac{1}{2} \bullet rhsDT \bullet (0 + relA1) \quad (2.22)$$

The *change* in wall displacement from time  $[t_i \text{ plus } lhsDT]$  to time  $t_{i+1}$  is equal to the integral of the positive relative velocity of the middle  $relV$  figure. The permanent wall displacement increases in value from  $relDmid$  to  $relD1$ , as depicted in the bottom figure.

$$relD1 = relDmid + rhsDT \bullet relVmid + \frac{(rhsDT)^2}{6} \bullet (2 \bullet 0 + relA1) \quad (2.23)$$

**Case 2:** This case results when the positive value for relative velocity at time  $t_i$  is less than the magnitude of NegativeArea<sub>-A+</sub> (i.e., the negative area between the negative portion of the linear acceleration line and the time line over the portion of the Figure 2.5 time increment labeled lhsDT). The four right-hand side figures in Figure 2.5 are used to describe the Case 2 step-by-step solution scheme. From the top to bottom, one figure describes the relative acceleration, two figures describe the relative velocity, and one figure describes the permanent relative wall displacement.

The top, right-hand side, Case 2 figure depicts the case of a (labeled) negative triangular area between the linear relative deceleration line and the time line, being of greater magnitude than the positive value for relative velocity at time  $t_i$  (designated relV0). Consequently, the wall will come to rest before time  $t_{i+1}$  is achieved. At an increment in time DTzeroV after time  $t_i$ , a portion of the negative deceleration area reduces the value of relative velocity from the positive value of magnitude relV0 at time  $t_i$  to a value of 0 at time  $[t_i \text{ plus } DTzeroV]$ , as shown in this figure. At time  $[t_i \text{ plus } DTzeroV]$  the relative acceleration is

$$relA_{mid} = DT_{zeroD} \bullet \left( \frac{relA0}{lhsDT} \right) \quad (2.24)$$

where DTzeroD is the time increment shown in Figure 2.5. The Figure 2.5 negative (relative) deceleration area below time increment DTzeroV is

$$AreaTrapezoid_{-A+} = \frac{1}{2} \bullet DT_{zeroV} \bullet (relA0 + relA_{mid}) \quad (2.25)$$

The Figure 2.5 negative relative deceleration area below time increment DTzeroD is

$$AreaTriangle_{-A+} = \frac{1}{2} \bullet DT_{zeroD} \bullet (relA_{mid} + 0) \quad (2.26)$$

Thus, the total Figure 2.5 negative relative deceleration area below time increment lhsDT is



$$NegativeArea_{-A+} = AreaTrapezoid_{-A+} + AreaTriangle_{-A+} \quad (2.27)$$

The relative velocity at time [t<sub>i</sub> plus DTzeroV] is

$$relVmid = relV0 + AreaTrapezoid_{-A+} \quad (2.28)$$

With a value for relVmid equal to zero, Equation 2.28 becomes

$$0 = relV0 + AreaTrapezoid_{-A+} \quad (2.29)$$

Expanding by adding the term AreaTriangle<sub>-A+</sub> to both sides, Equation 2.29 becomes

$$AreaTriangle_{-A+} = relV0 + AreaTrapezoid_{-A+} + AreaTriangle_{-A+} \quad (2.30)$$

Which by introducing Equation 2.27, becomes

$$AreaTriangle_{-A+} = relV0 + NegativeArea_{-A+} \quad (2.31)$$

Introducing Equations 2.26 and 2.24 and solving for DTzeroD, Equation 2.31 becomes

$$DTzeroD = \sqrt{2 \bullet \left( \frac{lhsDT}{relAO} \right) \bullet (relV0 + NegativeArea_{-A+})} \quad (2.32)$$

Recognizing the time increment lhsDT is equivalent to

$$lhsDT = DTzeroV + DTzeroD \quad (2.33)$$

and by introducing Equation 2.33 and 2.25 into Equation 2.32 and solving for DTzeroV,

$$DTzeroV = lhsDT - \sqrt{2 \bullet \left( \frac{lhsDT}{relAO} \right) \bullet (relV0 + NegativeArea_{-A+})} \quad (2.34)$$

The *change* in relative displacement from time t<sub>i</sub> to time [t<sub>i</sub> plus DTzeroV] is equal to the labeled positive area between the quadratic relative velocity curve and the time line. At time [t<sub>i</sub> plus DTzeroV] the wall displacement increases in magnitude from relD0 to relDmid. The relative velocity at time [t<sub>i</sub> plus DTzeroV], expressed in terms of DTzeroV, is

$$relV_{mid} = relV_0 + \frac{1}{2} \bullet DT_{zeroV} \bullet (relA_0 + relA_{mid}) \quad (2.35)$$

with the relative acceleration at time  $[t_i \text{ plus } DT_{zeroV}]$  equal to

$$relA_{mid} = relA_0 + \left( \frac{relA_1 - relA_0}{DT} \right) \bullet DT_{zeroV} \quad (2.36)$$

The *change* in relative displacement from time  $t_i$  to time  $[t_i \text{ plus } DT_{zeroV}]$  is equal to the labeled positive area between the quadratic relative velocity curve and the time line. At time  $[t_i \text{ plus } DT_{zeroV}]$  the wall displacement increases in magnitude from  $relD_0$  to  $relD_{mid}$ .

$$relD_{mid} = relD_0 + DT_{zeroV} \bullet relV_0 \quad (2.37)$$

$$+ \frac{(DT_{zeroV})^2}{6} \bullet (2 \bullet relA_0 + relA_{mid})$$

The wall remains at rest with zero relative velocity and with no additional permanent relative displacement from time  $[t_i \text{ plus } DT_{zeroV}]$  until time  $[t_i \text{ plus } lhsDT]$  when the relative acceleration of the wall begins (again). At time  $[t_i \text{ plus } lhsDT]$  the wall begins to develop further permanent displacement as a result of the positive relative reacceleration of the wall. The positive (labeled) triangular area between the time line and the linear relative acceleration line, shown in the right-hand side of the top figure, equals the *change* in relative velocity and with the wall at rest, consequently, the value for relative velocity at time  $t_{i+1}$  (labeled  $relV_1$  in the lower relative velocity figure) is

$$relV_1 = \frac{1}{2} \bullet rhsDT \bullet (0 + relA_1) \quad (2.38)$$

The *change* in wall displacement from time  $[t_i \text{ plus } lhsDT]$  to time  $t_{i+1}$  is equal to the integral of the positive relative velocity, as depicted in the middle two, right-hand side  $relV$  figures. The top  $relV$  figure being a computational figure, and the bottom  $relV$  figure being the  $relV$  curve-shift figure that properly accounts for zero wall relative velocity over time increment  $DT_{zeroD}$ , with an insert detailed, curve-shift figure for  $relV$  shown of this computational  $relV$  figure in Figure 2.5. The permanent relative wall

displacement increases in value from  $relD_{mid}$  to  $relD1$ , as depicted in the bottom figure.

$$relD1 = relD_{mid} + rhsDT \bullet 0 + \frac{(rhsDT)^2}{6} \bullet (2 \bullet 0 + relA1) \quad (2.39)$$

#### 2.4.4 Negative relative accelerations $relA0$ and $relA1$ at times $t_i$ and $t_{i+1}$

Next consider a wall in motion (i.e., with a positive value for relative velocity) at time  $t_i$  but with the Figure 2.6 case of a negative values for relative acceleration computed at time-steps  $t_i$  and  $t_{i+1}$ .<sup>1</sup> The first step is to determine if the wall, which is in motion at time  $t_i$ , comes to rest during the time-step  $DT$ .

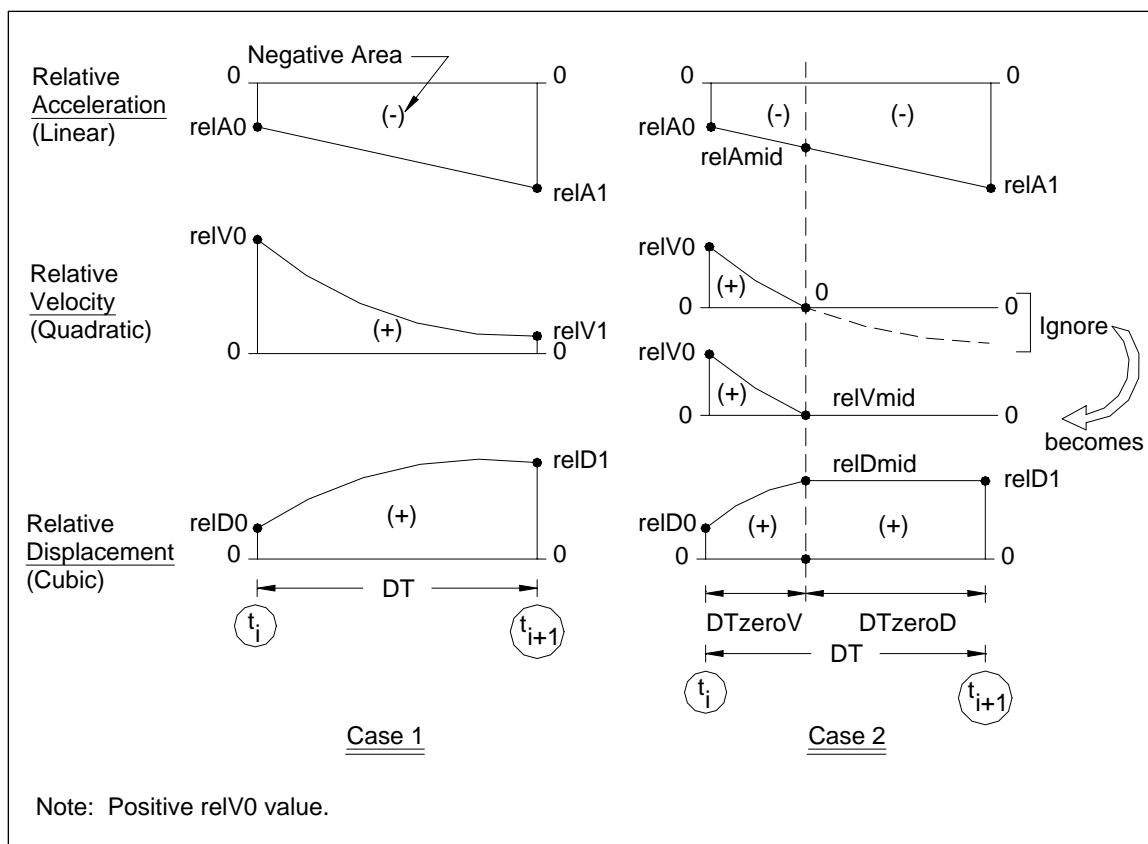


Figure 2.6. Two possible outcomes for the case of negative relative accelerations at times  $t_i$  and  $t_{i+1}$ .

<sup>1</sup> Again, note the assumption of a linear variation in relative acceleration over the time-step  $DT$  shown in Figure 2.6.

The negative area between the negative portion of the linear acceleration line and the time line over the Figure 2.6 time increment DT is

$$\text{NegativeArea}_{-A-} = \frac{1}{2} \bullet DT \bullet (\text{rel}A0 + \text{rel}A1) \quad (2.40)$$

There are two possible outcomes for the Figure 2.6 step-by-step numerical solution for relative velocity and relative displacement at time  $t_{i+1}$ , depending upon the magnitude of  $\text{rel}V0$  relative to the magnitude of Equation 2.40  $\text{NegativeArea}_{-A-}$ . These possible scenarios are depicted by two columns of figures in Figure 2.6, labeled as Case 1 and Case 2 figure groups.

**Case 1:** This case results when the positive value for relative velocity at time  $t_i$  is greater than the magnitude of  $\text{NegativeArea}_{-A-}$  (i.e., the negative area between the negative portion of the linear acceleration line and the time line over the Figure 2.6 time-step DT). The three left-hand side figures in Figure 2.6 are used to describe the Case 1 step-by-step solution scheme: The top figure describes the relative acceleration, the middle figure describes the relative velocity, and the lower figure describes the permanent relative wall displacement.

The top Case 1 figure depicts the case of a (labeled) negative area between the linear relative deceleration line and the time line (i.e.,  $\text{NegativeArea}_{-A-}$  by Equation 2.40), being of less magnitude than the positive value for relative velocity at time  $t_i$  (designated  $\text{rel}V0$ ). Consequently, the wall will remain in motion during the entire time-step DT. At the time-step DT after time  $t_i$ , the negative deceleration area reduces the value of relative velocity from the positive value of magnitude  $\text{rel}V0$  at time  $t_i$  to a smaller magnitude value at time  $[t_i \text{ plus } DT]$ , as shown in this figure. The relative velocity at time  $[t_i \text{ plus } DT]$  is

$$\text{rel}V1 = \text{rel}V0 + \frac{1}{2} \bullet DT \bullet (\text{rel}A0 + \text{rel}V1) \quad (2.41)$$

The *change* in relative displacement from time  $t_i$  to time  $[t_i \text{ plus } DT]$  is equal to the labeled positive area between the quadratic relative velocity curve and the time line. At time  $[t_i \text{ plus } DT]$  the wall displacement increases in magnitude from  $\text{rel}D0$  to  $\text{rel}D1$ .

$$relD1 = relD0 + DT \bullet relV0 + \frac{(DT)^2}{6} \bullet (2 \bullet relA0 + relA1) \quad (2.42)$$

**Case 2:** This case results when the positive value for relative velocity at time  $t_i$  is less than the magnitude of NegativeArea<sub>-A-</sub> (i.e., the negative area between the negative portion of the linear acceleration line and the time line over the portion of the Figure 2.6 time increment labeled lhsDT). The four right-hand side figures in Figure 2.6 are used to describe the Case 2 step-by-step solution scheme. From the top to bottom, one figure describes the relative acceleration, two figures describe the relative velocity, and one figure describes the permanent relative wall displacement.

The top, right-hand side, Case 2 figure depicts the case of a (labeled) negative area between the linear relative deceleration line and the time line (i.e., NegativeArea<sub>-A-</sub> by Equation 2.40), being of greater magnitude than the positive value for relative velocity at time  $t_i$  (designated relV0). Consequently, the wall will come to rest before time  $t_{i+1}$  is achieved. At an increment in time DTzeroV after time  $t_i$ , a portion of the negative deceleration area reduces the value of relative velocity from the positive value of magnitude relV0 at time  $t_i$  to a value of 0 at time  $[t_i \text{ plus } DTzeroV]$ , as shown in this figure. At time  $[t_i \text{ plus } DTzeroV]$  the relative acceleration is

$$relA_{mid} = relA0 + DTzeroV \bullet \left( \frac{relA1 - relA0}{DT} \right) \quad (2.43)$$

where DTzeroV is the time increment shown in Figure 2.6. The Figure 2.6 negative relative deceleration area below time increment DTzeroV is

$$AreaTrapezoid_{-A-} = \frac{1}{2} \bullet DTzeroV \bullet (relA0 + relA_{mid}) \quad (2.44)$$

Introducing Equations 2.43, Equation 2.44 becomes

$$AreaTrapezoid_{-A-} = \left\{ \frac{1}{2} \bullet DTzeroV \bullet relA0 + \frac{DTzeroV}{2} \bullet \left[ relA0 + DTzeroV \bullet \left( \frac{relA1 - relA0}{DT} \right) \right] \right\} \quad (2.45)$$

This simplifies to

$$AreaTrapezoid_{-A-} = DTzeroV \bullet relAO + \frac{(DTzeroV)^2}{2} \bullet \left( \frac{relA1 - relAO}{DT} \right) \quad (2.46)$$

The *change* in rotation from time  $t_i$  to time [  $t_i$  plus  $DTzeroV$  ] is equal to the labeled positive area between the quadratic relative velocity curve and the time line. At time [  $t_i$  plus  $DTzeroV$  ] the wall displacement increases in magnitude from  $relDO$  to  $relDmid$ . The relative velocity at time [  $t_i$  plus  $DTzeroV$  ] is

$$relVmid = relVO + AreaTrapezoid_{-A-} \quad (2.47)$$

With a value for  $relVmid$  equal to zero, Equation 2.47 becomes

$$0 = \left[ \frac{1}{2} \bullet \left( \frac{relA1 - relAO}{DT} \right) \right] \bullet (DTzeroV)^2 + relAO \bullet DTzeroV + relVO \quad (2.48)$$

This quadratic equation has a general solution of

$$DTzeroV = \frac{-relAO \pm \sqrt{(relAO)^2 - 4 \bullet \left[ \frac{1}{2} \bullet \left( \frac{relA1 - relAO}{DT} \right) \right] \bullet relVO}}{2 \bullet \left[ \frac{1}{2} \bullet \left( \frac{relA1 - relAO}{DT} \right) \right]} \quad (2.49)$$

Even though this solution provides for two possible values for  $DTzeroV$ , only the positive value is assigned to  $DTzeroV$  in  $C_{orps}W_{allSlip}$ .

The *change* in displacement from time  $t_i$  to time [  $t_i$  plus  $DTzeroV$  ] is equal to the labeled positive area between the quadratic relative velocity curve and the time line. At time [  $t_i$  plus  $DTzeroV$  ] the relative wall displacement increases in magnitude from  $relDO$  to  $relDTmid$ .

$$relDmid = relDO + DTzeroV \bullet relVO \quad (bis 2.37)$$

$$+ \frac{(DTzeroV)^2}{6} \bullet (2 \bullet relAO + relA_{mid})$$

The wall remains at rest with zero relative velocity and with no additional permanent displacement from time [  $t_i$  plus  $DTzeroV$  ] until time [  $t_i$  plus

DT]. Consequently, at time  $t_{i+1}$  the permanent relative wall displacement is constant, as depicted in the bottom figure.

$$relD1 = relDmid \quad (2.50)$$

with the value for  $relDmid$  given by Equation 2.37.

#### 2.4.5 Positive relative acceleration $relA0$ at time $t_i$ and negative relative acceleration $relA1$ at $t_{i+1}$

Next consider a wall in motion (i.e., with a positive value for relative velocity) at time  $t_i$  but with the Figure 2.7 case of a positive value for relative acceleration at time-step  $t_i$  and negative value for relative acceleration at the next time-step of  $t_{i+1}$ .<sup>1</sup> The first step is to determine the time instant [ $t_i$  plus  $lhsDT$ ] at which the relative acceleration is equal to zero, as labeled in the figure. By linear interpolation, this time increment  $lhsDT$  is

$$lhsDT = \left| relA0 \cdot \left( \frac{DT}{relA1 - relA0} \right) \right| \quad (\text{bis 2.18})$$

The positive area between the positive portion of the linear acceleration line and the time line over the Figure 2.7 time increment  $lhsDT$  is

$$PositiveArea_{+A-} = \frac{1}{2} \cdot lhsDT \cdot (relA0 + 0) \quad (2.51)$$

The Figure 2.7 time increment  $rhsDT$  is given by

$$rhsDT = DT - lhsDT \quad (2.52)$$

The negative area between the negative portion of the linear acceleration line and the time line over the Figure 2.7 time increment  $rhsDT$  is

$$NegativeArea_{+A-} = \frac{1}{2} \cdot rhsDT \cdot (0 + relA1) \quad (2.53)$$

---

<sup>1</sup> Again, observe the assumption of a linear variation in relative acceleration over the time-step  $DT$  shown in Figure 2.7.

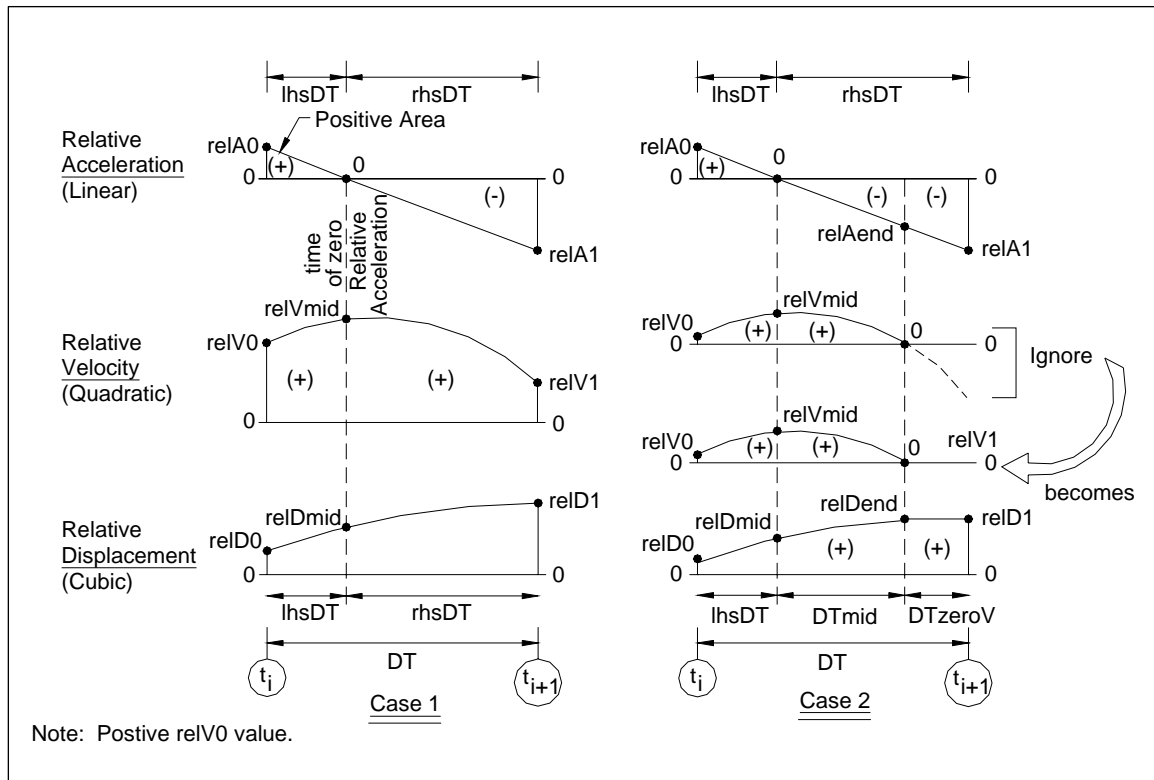


Figure 2.7. Two possible outcomes for the case of a positive relative acceleration at time  $t_i$  and a negative relative acceleration at time  $t_{i+1}$ .

There are two possible outcomes for the Figure 2.7 step-by-step numerical solution for relative velocity and relative displacement at time  $t_{i+1}$ , depending upon the magnitude of  $relV0$  relative to the magnitude of the sum of the  $PositiveArea_{+A-}$  plus the  $NegativeArea_{+A-}$ . These possible scenarios are depicted by two columns of figures in Figure 2.7, labeled as Case 1 and Case 2 figure groups.

**Case 1:** This case results if (a) the  $NegativeArea_{+A-}$  exceeds  $PositiveArea_{+A-}$  but the positive value for relative velocity at time  $t_i$  is greater than the magnitude of the negative sum of  $PositiveArea_{+A-}$  plus  $NegativeArea_{+A-}$ , or (b) the  $NegativeArea_{+A-}$  is less than  $PositiveArea_{+A-}$ , consequently the positive value for  $relV0$  at time  $t_i$  will increase to a larger value of  $relV1$  at time  $t_{i+1}$  (with an increase equal to the positive sum of  $PositiveArea_{+A-}$  plus  $NegativeArea_{+A-}$ ). The three left-hand side figures in Figure 2.7 are used to describe the Case 1 step-by-step solution scheme: The top figure describes the relative acceleration, the middle figure describes the relative velocity, and the lower figure describes the permanent relative wall displacement.



The top Case 1 figure depicts the case of a wall sliding during the entire time-step DT because either (a) the  $NegativeArea_{+A-}$  exceeds  $PositiveArea_{+A-}$  but the positive value for relative velocity at time  $t_i$  is greater than the magnitude of the sum of  $PositiveArea_{+A-}$  plus  $NegativeArea_{+A-}$ , or because (b) the  $NegativeArea_{+A-}$  is less than  $PositiveArea_{+A-}$ . At the increment in time  $lhsDT$  after time  $t_i$ , the positive acceleration area increases the value of relative velocity from the positive value of magnitude  $relV0$  at time  $t_i$  to a larger magnitude value at time  $[t_i \text{ plus } lhsDT]$ , as shown in this figure. The relative velocity at time  $[t_i \text{ plus } lhsDT]$  is

$$relVmid = relV0 + \frac{1}{2} \bullet lhsDT \bullet (relA0 + 0) \quad (\text{bis 2.20})$$

The *change* in displacement from time  $t_i$  to time  $[t_i \text{ plus } lhsDT]$  is equal to the labeled positive area between the quadratic relative velocity curve and the time line. At time  $[t_i \text{ plus } lhsDT]$  the wall displacement increases in magnitude from  $relD0$  to  $relDmid$ .

$$relDmid = relD0 + lhsDT \bullet relV0 + \frac{(lhsDT)^2}{6} \bullet (2 \bullet relA0 + 0) \quad (\text{bis 2.21})$$

The wall continues in motion, with positive relative velocity and with additional permanent relative displacement after time  $[t_i \text{ plus } lhsDT]$  when the relative acceleration of the wall is positive. At time  $[t_i \text{ plus } lhsDT]$  the magnitude of wall relative velocity begins to decrease in magnitude as a result of the relative deceleration of the wall. The negative (labeled) triangular area between the time line and the linear relative deceleration line, shown in the top Case 1 figure, equals the *change* in relative velocity and for the wall. Consequently, the value for relative velocity at time  $t_{i+1}$  (labeled  $relV1$  in the Case 1 middle figure) is

$$relV1 = relVmid + \frac{1}{2} \bullet rhsDT \bullet (0 + relA1) \quad (\text{bis 2.22})$$

The *change* in wall displacement from time  $[t_i \text{ plus } lhsDT]$  to time  $t_{i+1}$  is equal to the integral of the positive relative velocity of the middle  $relV$ -figure. The permanent relative wall displacement increases in value from  $relDmid$  to  $relD1$ , as depicted in the bottom figure.

$$relD1 = relDmid + rhsDT \bullet relVmid + \frac{(rhsDT)^2}{6} \bullet (2 \bullet 0 + relA1) \quad (\text{bis 2.23})$$

**Case 2:** This case results when the  $NegativeArea_{+A-}$  exceeds  $PositiveArea_{+A-}$  and the positive value for relative velocity at time  $t_i$  is less than the magnitude of the sum of  $PositiveArea_{+A-}$  plus  $NegativeArea_{+A-}$ . The four right-hand side figures in Figure 2.7 are used to describe the Case 2 step-by-step solution scheme. From the top to bottom, one figure describes the relative acceleration, two figures describe the relative velocity, and one figure describes the permanent relative wall displacement.

The top, right-hand side, Case 2 figure depicts the case of the sum of a (labeled) positive triangular area between the linear relative deceleration line and the time line (i.e.,  $PositiveArea_{+A-}$  by Equation 2.51) plus a (labeled) negative triangular area between the linear relative deceleration line and the time line (i.e.,  $NegativeArea_{+A-}$  by Equation 2.53), being negative and of greater magnitude than the positive value for relative velocity at time  $t_i$  (designated  $relV0$ ). Consequently, the wall will come to rest before time  $t_{i+1}$  is achieved.

At time  $[t_i \text{ plus } lhsDT]$  the wall's relative velocity increases in magnitude from  $relV0$  to  $relVmid$ . The relative velocity at time  $[t_i \text{ plus } lhsDT]$  is

$$relVmid = relV0 + \frac{1}{2} \bullet lhsDT \bullet (relA0 + 0) \quad (\text{bis 2.20})$$

with the relative acceleration at time  $[t_i \text{ plus } lhsDT]$  equal to zero.

The *change* in displacement from time  $t_i$  to time  $[t_i \text{ plus } lhsDT]$  is equal to the labeled positive area between the quadratic relative velocity curve and the time line. At time  $[t_i \text{ plus } lhsDT]$  the wall displacement increases in magnitude from  $relD0$  to  $relDmid$ .

$$relDmid = relD0 + lhsDT \bullet relV0 + \frac{(lhsDT)^2}{6} \bullet (2 \bullet relA0 + 0) \quad (2.54)$$

At an increment in time  $[lhsDT + DTmid]$  after time  $t_i$ , a portion of the negative deceleration area reduces the value of relative velocity from the positive value of magnitude  $relVmid$  at time  $[t_i \text{ plus } lhsDT]$  to a value of 0

at time  $[t_i \text{ plus } (lhsDT+DTmid)]$ , as shown in this figure. At time  $[t_i \text{ plus } (lhsDT+DTmid)]$  the relative acceleration is

$$relAend = DTmid \bullet \left( \frac{relA1}{rhsDT} \right) \quad (2.55)$$

where  $DTmid$  is the time increment shown in Figure 2.7. The Figure 2.7 negative relative acceleration area below time increment  $DTmid$  is

$$AreaTriangle_{+A-} = \frac{1}{2} \bullet DTmid \bullet (0 + relAend) \quad (2.56)$$

The Figure 2.7 negative relative acceleration area below time increment  $DTzeroV$  is

$$AreaTrapezoid_{+A-} = \frac{1}{2} \bullet DTzeroV \bullet (relAend + relA1) \quad (2.57)$$

Thus, the total Figure 2.7 negative relative acceleration area below time increment  $rhsDT$  is

$$NegativeArea_{+A-} = AreaTrapezoid_{+A-} + AreaTriangle_{+A-} \quad (2.58)$$

With the relative velocity at time  $[t_i \text{ plus } (lhsDT+DTmid)]$  equal to zero,

$$0 = relVmid + AreaTriangle_{+A-} \quad (2.59)$$

By introducing Equations 2.20, 2.51, 2.55, and 2.56, and solving for  $DTmid$ , Equation 2.59 becomes

$$DTmid = \sqrt{-2 \bullet \left( \frac{rhsDT}{relA1} \right) \bullet (relV0 + PositiveArea_{+A-})} \quad (2.60)$$

At time  $[t_i \text{ plus } (lhsDT+DTmid)]$  the relative wall displacement comes to rest with

$$\begin{aligned} relDend &= relDmid + DTmid \bullet relVmid \\ &+ \frac{(DTmid)^2}{6} \bullet (2 \bullet 0 + relAend) \end{aligned} \quad (2.61)$$

The wall remains at rest with zero relative velocity and with no additional permanent relative displacement from time  $[t_i \text{ plus } (l_{hs}DT + DT_{mid})]$  until time  $t_{i+1}$ . The permanent relative wall displacement at this time  $t_{i+1}$  is

$$relD1 = relDend \quad (2.62)$$

#### 2.4.6 Starting the $C_{orps}W_{all}Slip$ analysis and the initiation of wall translation during a DT time-step

**Start of the step-by-step time-history analysis:** The numerical formulation used in the step-by-step time-history analysis by  $C_{orps}W_{all}Slip$  assumes that the wall is at rest at the start of the analysis (i.e., at time  $t_i$  equal to 0 and with  $i = 1$ ). Consequently, relative acceleration, relative velocity, and relative displacement are equal to zero as an initial boundary condition at the first time-step (i.e., with  $i = 1$ ). Recall the relative acceleration at time  $t_i$  is equal to the difference between the horizontal ground acceleration value at time  $t_i$  minus the constant value of  $[(k_{CG})_{threshold-sliding-h} \text{ times } g]$ .

**Initiation of wall displacement during the first DT time-step:** At the end of the first DT time-step, at time increment  $t_2$  (i.e.,  $t_{i+1}$  and with  $i = 1$  so the subscript  $i + 1$  becomes 2), a relative acceleration value is computed by  $C_{orps}W_{all}Slip$ . If a positive value for relative acceleration is computed at time increment  $t_2$  then the system is in motion (i.e., sliding) during this first time-step DT.

However, if a negative value for relative acceleration is computed and the system has been at rest and with zero relative acceleration at time  $t_1 = 0$  (i.e.,  $t_i$  and for  $i = 1$ ) then the system is at rest at time  $t_2$ . This means that the correct value for relative acceleration is zero at time  $t_2$ .

**Initiation of wall displacement during a DT time-step:** A wall is at rest at the beginning of any DT time-step (designated time  $t_i$  in Figures 2.3 through 2.7) when relative velocity and relative displacement are equal to zero. At all DT time-steps other than the first time-step, the values at time  $t_i$  for relative acceleration, relative velocity, and relative displacement were computed during the previous time-step and then assigned as known values for this next time-step. The step-by-step numerical procedure implemented in  $C_{orps}W_{all}Slip$  allows for wall displacement to initiate during any DT time-step during earthquake shaking. This will occur for a wall at rest at time  $t_i$ , i.e., the start of the time-step, when a positive value

is computed for relative acceleration at time  $t_{i+1}$ . The numerical procedure outlined in Figure 2.4 allows for the computation of relative velocity and relative displacement at time  $t_{i+1}$  for this case.

#### 2.4.7 Cessation of wall translation

A wall is in motion at the start of any DT time-step (designated time  $t_i$  in Figures 2.3 through 2.7) when relative velocity (i.e.,  $relV$ ) is nonzero. The step-by-step numerical procedure implemented in  $C_{orps}W_{all}Slip$  allows for wall translation (i.e., sliding) to terminate during any DT time-step during earthquake shaking. This occurs when the deceleration of the wall is sufficiently large during time-step DT. The applicable numerical procedures are labeled as Case 2 in Figures 2.6 and 2.7.

In the case of wall translation decelerating and with negative values for relative acceleration at times  $t_i$  and  $t_{i+1}$  during time-step DT, the relative velocity at time  $t_{i+1}$  (designated  $relV1$ ) and the relative wall displacement at time  $t_{i+1}$  (designated  $relD1$ ) are made using the Case 2 approach outlined in Figure 2.6. Note the relative velocity reduces to zero at a time increment  $DT_{zeroV}$  after time  $t_i$ . The wall remains at rest and with zero relative velocity over time increment  $DT_{zeroD}$ , as shown in this figure.

In the case of wall translation decelerating and with a positive value for relative acceleration at time  $t_i$  and a negative value for relative acceleration at time  $t_{i+1}$  during time-step DT, the relative velocity at time  $t_{i+1}$  (designated  $relV1$ ) and the relative wall displacement at time  $t_{i+1}$  (designated  $relD1$ ) are made using the Case 2 approach outlined in Figure 2.7. Note the relative velocity reduces to zero at a time increment  $[lhsDT + DT_{mid}]$  after time  $t_i$ . The wall remains at rest and with zero relative velocity over time increment  $DT_{zeroV}$ , as shown in this figure.

Note that wall translation can begin again at a later point in time, as described in the Subsection 2.4.6 paragraph entitled “initiation of wall rotation during a DT time-step.”

## 2.5 New translational analysis model of a wall retaining a partially submerged backfill and buttressed by a reinforced concrete slab

### 2.5.1 Introduction

The formulation for a rock-founded wall retaining a partially submerged backfill and for the case of a pool in front of the retaining wall is summarized in this subsection. The formulation presented is an extension of the moist backfill formulation discussed in the previous sections of this chapter. Water pressures are assumed to act along three faces of the structural wedge denoted as the toe, base, and the heel regions of Figure 2.8. Forces acting on the toe are due to the presence of a pool of water in front of the wall. A leaking vertical joint is assumed between the base slab and the structural wedge with water pressures above the toe controlled by the presence of the pool. The computation of water pressures acting on this partially submerged structural wedge is discussed in detail in Appendix D.<sup>1</sup> The Figure 2.8 distributions of water pressures are converted into equivalent resultant forces, expressed in global x- and y-coordinates, and their points of application along each of the three regions. These resultant water pressure forces are used in an effective stress based stability analysis of the structural wedge. Dynamic considerations for the pool during earthquake shaking are accounted for in the analysis using hydrodynamic water pressures computed using the Westergaard (1931) procedure of analysis (see Appendix D). The hydrodynamic water pressure resultant force  $P_{wd}$  (Equation D.5) is shown acting on the structural wedge in this figure (and shown acting in a direction consistent with the direction of positive horizontal acceleration,  $+a_h$ ).

---

<sup>1</sup> In the initial CorpsWallSlip version, no excess pore water pressures due to earthquake-induced shear strains within the soil regions are included in the current CorpsWallSlip formulation (i.e., the excess pore water pressure ratio  $r_u$  is equal to zero). Refer to Ebeling and Morrison (1992) for a complete description and discussion of  $r_u$ .

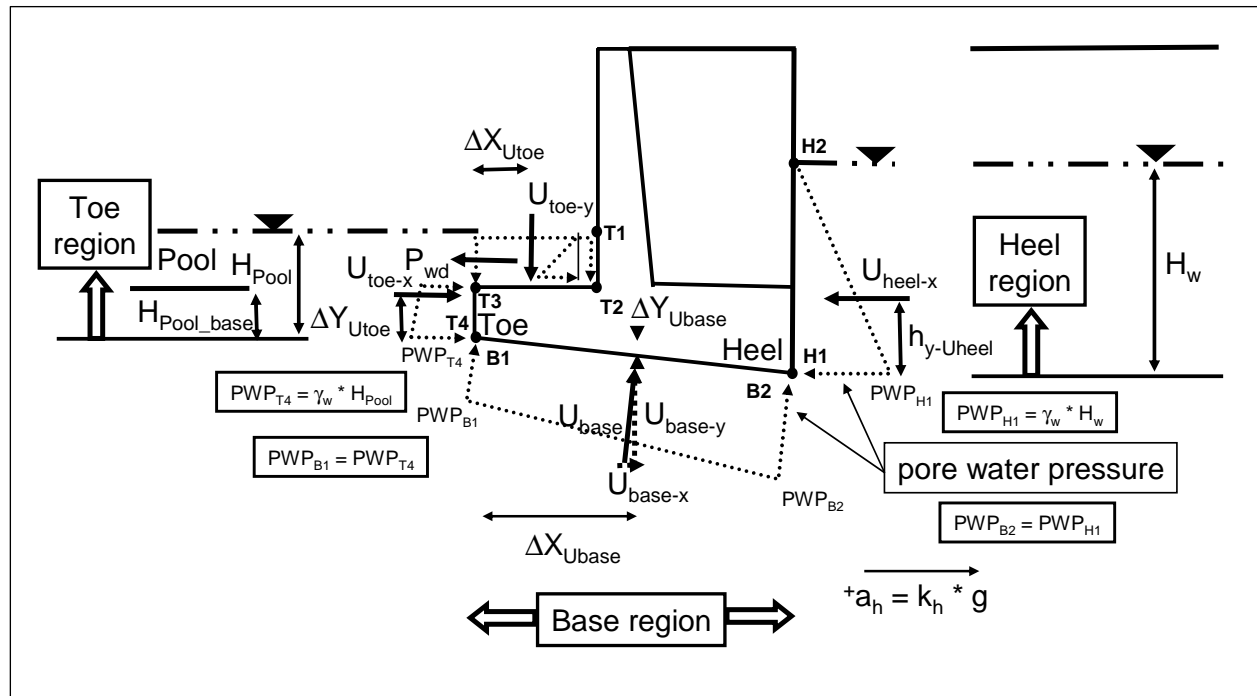


Figure 2.8. Control points, water pressures, and corresponding resultant forces acting normal to faces of the three regions of a structural wedge sliding along its base – effective stress analysis.

In the case of a wall sliding along its base, contact between the base of the structural wedge and the foundation is maintained during earthquake shaking. Recall that a simplistic rigid base assumption is made in this formulation for rock-founded earth retaining structures. There is no formation of a gap sometime during earthquake shaking. Note that the Figure 2.8 water pressure distribution is the steady-state pore water pressures resulting from a structural wedge in full contact with the rock foundation, shown in Figure D.1.

The resultant water pressure forces  $U_{toe}$ ,  $U_{base}$ ,  $U_{heel}$ , and  $P_{wd}$  shown in Figure 2.8 are superimposed on the free-body diagram of forces acting on the Figure 2.2 structural wedge, resulting in the Figure 2.9 free-body diagram. Recall  $P_{resist}$  is the force provided by the reinforced concrete (toe) slab.

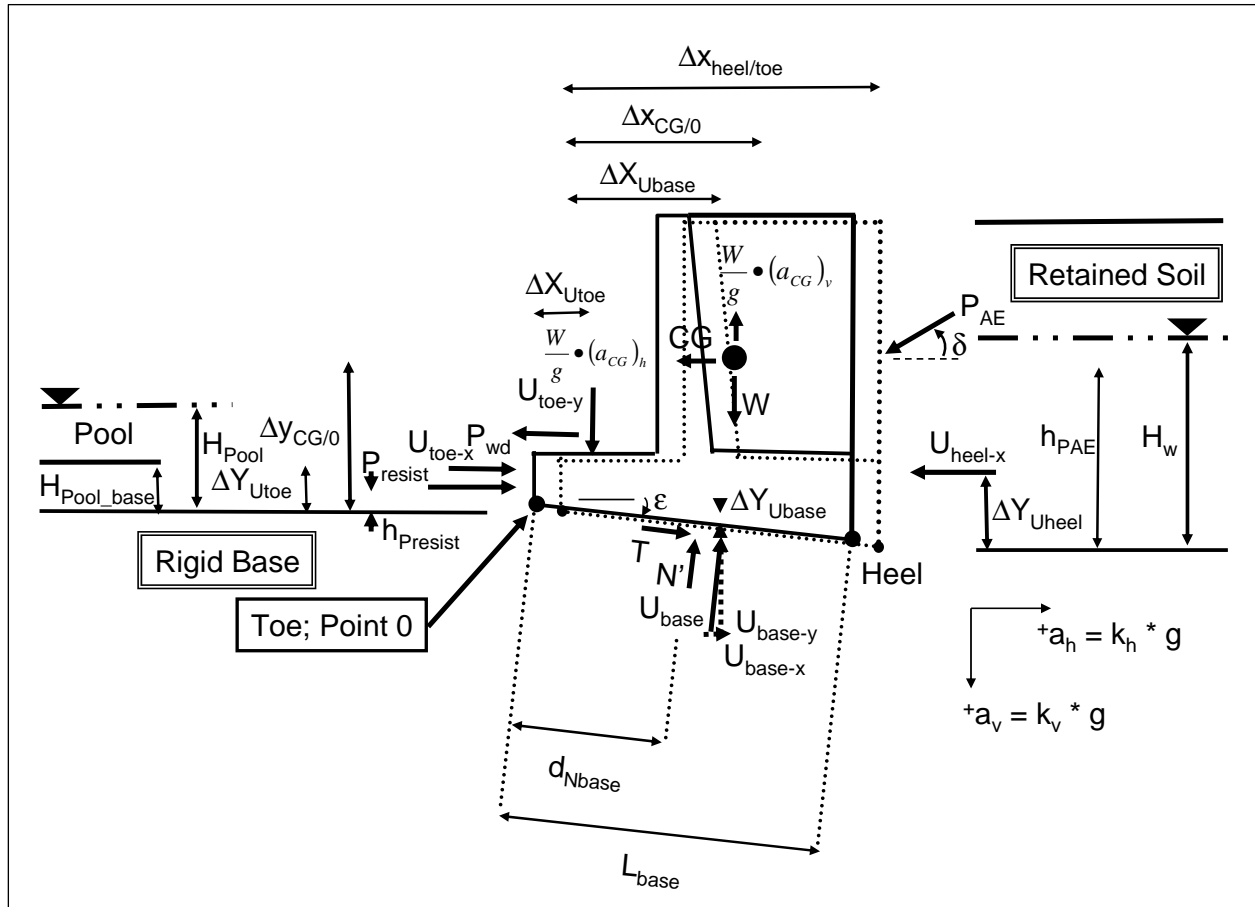


Figure 2.9. Inertia forces and resultant force vectors acting on a rigid block model of a (inclined base) cantilever wall retaining a partially submerged backfill with sliding along the base of the wall during earthquake shaking of the inclined rigid base – effective stress analysis.

### 2.5.2 Threshold value of acceleration corresponding to incipient lateral translation of the retaining wall – partially submerged backfill

At the onset of sliding of the Figure 2.9 retaining wall, the horizontal driving force equals the stabilizing (i.e., restoring) force. The summation of the Figure 2.9 horizontal forces acting on the rigid body results in

$$\begin{aligned} \frac{W}{g} \cdot (a_{CG})_h + P_{AE} \cdot \cos(\delta) + U_{heel-x} + P_{wd} = \\ P_{resist} + T \cdot \cos(\epsilon) + N' \cdot \sin(\epsilon) + U_{base-x} + U_{toe-x} \end{aligned} \quad (2.63)$$

$T$  is the shear force required for equilibrium of forces acting on the structural wedge (i.e.,  $FS_{slide} = 1.0$ ). At incipient sliding, the shear strength along the base to foundation interface becomes fully mobilized. Assuming



a full mobilization of shear resistance along the base (of length  $L_{base}$ ), the shear force may be computed utilizing the Mohr-Coulomb failure criteria, in an effective stress analysis, as

$$T = c'_{base} \bullet L_{base} + N' \bullet \tan(\delta'_{base}) \quad (\text{bis 2.2})$$

The summation of the Figure 2.9 vertical forces acting on the rigid body results in

$$\begin{aligned} 0 = N' \bullet \cos(\varepsilon) - T \bullet \sin(\varepsilon) - W \\ + \frac{W}{g} \bullet (a_{CG})_v - P_{AE} \bullet \sin(\delta) + U_{base-y} - U_{toe-y} \end{aligned} \quad (2.64)$$

Introducing Equation 2.2 for T, Equation 2.64 becomes

$$N' = \frac{c'_{base} \bullet L_{base} \bullet \sin(\varepsilon) + W - \frac{W}{g} \bullet (a_{CG})_v + P_{AE} \bullet \sin(\delta) - U_{base-y} + U_{toe-y}}{\cos(\varepsilon) - \tan(\delta'_{base}) \bullet \sin(\varepsilon)} \quad (2.65)$$

Introducing Equations 2.2 and 2.65 and collecting variables, Equation 2.63 becomes

$$\begin{aligned} \frac{W}{g} \bullet (a_{CG})_h + P_{AE} \bullet \cos(\delta) + U_{heel-x} + P_{wd} = \\ P_{resist} + c'_{base} \bullet L_{base} \bullet \cos(\varepsilon) + U_{toe-x} + U_{base-x} + \\ \left[ \frac{c'_{base} \bullet L_{base} \bullet \sin(\varepsilon) + W - \frac{W}{g} \bullet (a_{CG})_v + P_{AE} \bullet \sin(\delta) - U_{base-y} + U_{toe-y}}{\cos(\varepsilon) - \tan(\delta'_{base}) \bullet \sin(\varepsilon)} \right] \\ \bullet [\tan(\delta'_{base}) \bullet \cos(\varepsilon) + \sin(\varepsilon)] \end{aligned} \quad (2.66)$$

Equation 2.66 represents the equilibrium relationship for the (rigid) structural wedge when the earthquake accelerations are such that the factor of safety against sliding along its base is equal to 1.0. For a factor of safety

> 1.0 against sliding, the retaining wall does not slide. The rigid body CG accelerations are the same as the rigid base accelerations (i.e., within the rock foundation). However, the accelerations felt by the rigid body (i.e., at its center of gravity, CG) will differ from the rigid base accelerations for user-defined rigid base acceleration (time-history) values that exceed the value for acceleration that results in a factor of safety against sliding equal to 1.0. During sliding, the acceleration felt by the rigid body at its center of gravity, CG, is of constant magnitude.

The component of the threshold acceleration occurring at translation (i.e., sliding) along the base is designated as

$$(a_{CG})_{\text{threshold-sliding-h}} = (k_{CG})_{\text{threshold-sliding-h}} \bullet g \quad (\text{bis 2.8})$$

where  $(k_{CG})_{\text{threshold-sliding-h}}$  is a value of horizontal ground acceleration, expressed in decimal fraction. In Ebeling and Morrison (1992), the acceleration  $(a_{CG})_{\text{threshold-sliding-h}}$  is referred to as the maximum transmissible acceleration ( $N \cdot g$ ) or as the yield acceleration. Note that the horizontal acceleration value  $[(k_{CG})_{\text{threshold-sliding-h}} \text{ times } g]$  is not a user-specified constant.

For a user-specified constant<sup>1</sup> for vertical acceleration [i.e.,  $(a_{CG})_v = \text{constant}$ ], CorpsWallSlip solves Equation 2.66 by introducing  $(a_{CG})_{\text{threshold-sliding-h}}$  and  $(k_{CG})_{\text{threshold-sliding-h}}$  for  $(a_{CG})_h$  and  $(k_{CG})_h$ . Because of the inclusion of acceleration in  $P_{AE}$  formulation (refer to Appendix A) in this equation, CorpsWallSlip solves Equation 2.66 using a trial-and-error numerical approach. Note that no safety factor need be applied to the weight of the wall/structural wedge nor to its shear strength in this calculation. The value of maximum transmissible (horizontal) acceleration at incipient sliding is reported in the WORKslide.TMP output file generated in each CorpsWallSlip analysis. This file may be viewed using the visual modeler boxes labeled **Show Sliding Evaluation** on the **Analysis** tab.

In CorpsWallSlip output data files the Equation 2.66 horizontal forces acting on the structural wedge are grouped into driving forces and resisting forces, which are defined as

<sup>1</sup> A procedure for determining the value for this constant (for vertical acceleration) is discussed in Section 2.6.

$$Driving\ Forces = \frac{W}{g} \bullet (a_{CG})_h + P_{AE} \bullet \cos(\delta) + U_{heel-x} + P_{wd} \quad (2.67)$$

and

$$\begin{aligned} \text{Resisting Forces} = & P_{resist} + c'_{base} \bullet L_{base} \bullet \cos(\varepsilon) + U_{toe-x} + U_{base-x} + \\ & \left\{ \frac{c'_{base} \bullet L_{base} \bullet \sin(\varepsilon) + W - \frac{W}{g} \bullet (a_{CG})_v + P_{AE} \bullet \sin(\delta) - U_{base-y} + U_{toe-y}}{\cos(\varepsilon) - \tan(\delta'_{base}) \bullet \sin(\varepsilon)} \right\} \quad (2.68) \\ & \bullet [\tan(\delta'_{base}) \bullet \cos(\varepsilon) + \sin(\varepsilon)] \end{aligned}$$

Introducing Equation 2.65, the resisting forces is also expressed as

$$\begin{aligned} \text{Resisting Forces} = & P_{resist} + c'_{base} \bullet L_{base} \bullet \cos(\varepsilon) + U_{toe-x} + U_{base-x} + \quad (2.69) \\ & \{N'\} \bullet [\tan(\delta'_{base}) \bullet \cos(\varepsilon) + \sin(\varepsilon)] \end{aligned}$$

In a total stress analysis the internal pore water pressure force terms  $U_{base}$  and  $U_{heel}$  are excluded from Equations 2.66 through 2.69 and  $c'$  is set equal to  $S_u$  with  $\phi'$  set equal to zero. Additionally,  $N'$  is set equal to  $N$  in Equations 2.63 through 2.69.

Since the horizontal limiting acceleration is of interest, another option is a simplified form of Equation 2.66 that may be derived by setting the vertical component of acceleration occurring at sliding equal to zero, as done by Richards and Elms (1979) and others. By making this assumption and introducing Equation 2.8, Equation 2.66 becomes

$$(k_{CG})_{\text{threshold-sliding-h}} = \frac{\left\langle \begin{aligned} &P_{\text{resist}} + c'_{\text{base}} \bullet L_{\text{base}} \bullet \cos(\varepsilon) + U_{\text{toe-x}} + U_{\text{base-x}} - P_{\text{AE}} \bullet \cos(\delta) - U_{\text{heel-x}} - P_{\text{wd}} + \\ &\left\{ \frac{c'_{\text{base}} \bullet L_{\text{base}} \bullet \sin(\varepsilon) + W + P_{\text{AE}} \bullet \sin(\delta) - U_{\text{base-y}} + U_{\text{toe-y}}}{\cos(\varepsilon) - \tan(\delta'_{\text{base}}) \bullet \sin(\varepsilon)} \right\} \\ &\bullet [\tan(\delta'_{\text{base}}) \bullet \cos(\varepsilon) + \sin(\varepsilon)] \end{aligned} \right\rangle}{W} \quad (2.70)$$

Because of the inclusion of acceleration in  $P_{\text{AE}}$  formulation (refer to Appendix A) in this equation,  $C_{\text{orps}}W_{\text{allSlip}}$  solves Equation 2.70 using a trial-and-error numerical approach.

In a total stress analysis the internal pore water pressure force terms  $U_{\text{base}}$  and  $U_{\text{heel}}$  are excluded from Equations 2.63 through 2.70.

The summation of overturning and resisting moments about the toe (i.e., point 0) of the Figure 2.9 forces acting on the rigid body results in

$$\begin{aligned} &\frac{W}{g} \bullet (a_{CG})_h \bullet \Delta y_{CG/0} + \frac{W}{g} \bullet (a_{CG})_v \bullet \Delta x_{CG/0} \\ &+ P_{\text{AE}} \bullet \cos(\delta) \bullet [(y_{\text{heel}} + h_{\text{PAE}}) - y_{\text{toe}}] + N' \bullet d_{\text{Nbase}} \\ &+ U_{\text{heel-x}} \bullet [(y_{\text{heel}} + \Delta Y_{U_{\text{heel}}}) - y_{\text{toe}}] \\ &+ U_{\text{base-y}} \bullet \Delta X_{U_{\text{base}}} + U_{\text{base-x}} \bullet \Delta Y_{U_{\text{base}}} \\ &+ P_{\text{wd}} \bullet [H_{\text{Pool\_base}} + 0.4 \bullet (H_{\text{Pool}} - H_{\text{Pool\_base}})] \\ &= P_{\text{resist}} \bullet h_{\text{Presist}} + W \bullet \Delta x_{CG/0} + P_{\text{AE}} \bullet \sin(\delta) \bullet \Delta x_{\text{heel/toe}} \\ &+ U_{\text{toe-x}} \bullet \Delta Y_{U_{\text{toe}}} + U_{\text{toe-y}} \bullet \Delta X_{U_{\text{toe}}} \end{aligned} \quad (2.71)$$

Solving for the location of the result effective force normal to the base,  $d_{\text{Nbase}}$ , Equation 2.10 becomes

$$d_{Nbase} = \frac{\left[ \begin{aligned} & -\frac{W}{g} \cdot (a_{CG})_h \cdot \Delta y_{CG/0} - \frac{W}{g} \cdot (a_{CG})_v \cdot \Delta x_{CG/0} \\ & -P_{AE} \cdot \cos(\delta) \cdot [(y_{heel} + h_{PAE}) - y_{toe}] \\ & -U_{heel-x} \cdot [(y_{heel} + \Delta Y_{Uheel}) - y_{toe}] \\ & -U_{base-y} \cdot \Delta X_{Ubase} - U_{base-x} \cdot \Delta Y_{Ubase} \\ & -P_{wd} \cdot [H_{Pool\_base} + 0.4 \cdot (H_{Pool} - H_{Pool\_base})] \\ & + P_{resist} \cdot h_{Presist} + W \cdot \Delta x_{CG/0} + P_{AE} \cdot \sin(\delta) \cdot \Delta x_{heel/toe} \\ & + U_{toe-x} \cdot \Delta Y_{Utoe} + U_{toe-y} \cdot \Delta X_{Utoe} \end{aligned} \right]}{N'} \quad (2.72)$$

Because of the inclusion of acceleration in  $P_{AE}$  formulation (refer to Appendix A) in this equation, CorpsWallSlip solves Equation 2.72 using a trial-and-error numerical approach. Introducing the horizontal limiting acceleration (i.e., Equation 2.8) in the case of a wall sliding along its base and setting the vertical component of acceleration occurring at sliding equal to zero, Equation 2.72 can be simplified to

$$d_{Nbase} = \frac{\left[ \begin{aligned} & -\frac{W}{g} \cdot (k_{CG})_{threshold-sliding-h} \cdot \Delta y_{CG/0} \\ & -P_{AE} \cdot \cos(\delta) \cdot [(y_{heel} + h_{PAE}) - y_{toe}] \\ & -U_{heel-x} \cdot [(y_{heel} + \Delta Y_{Uheel}) - y_{toe}] \\ & -U_{base-y} \cdot \Delta X_{Ubase} - U_{base-x} \cdot \Delta Y_{Ubase} \\ & -P_{wd} \cdot [H_{Pool\_base} + 0.4 \cdot (H_{Pool} - H_{Pool\_base})] \\ & + P_{resist} \cdot h_{Presist} + W \cdot \Delta x_{CG/0} + P_{AE} \cdot \sin(\delta) \cdot \Delta x_{heel/toe} \\ & + U_{toe-x} \cdot \Delta Y_{Utoe} + U_{toe-y} \cdot \Delta X_{Utoe} \end{aligned} \right]}{N'} \quad (2.73)$$

During sliding, the value of  $P_{AE}$  is computed using the horizontal acceleration value  $[(k_{CG})_{threshold-sliding-h} \text{ times } g]$ , the maximum transmissible acceleration ( $N \cdot g$  in Ebeling and Morrison (1992) notation). Recall that full contact is maintained between the base of the wall and its foundation during sliding in this formulation.

In a total stress analysis, the internal pore water pressure force terms  $U_{base}$  and  $U_{heel}$  are excluded from Equations 2.71 through 2.73.

### **2.5.3 Numerical method for computing the translational time-history of a rigid block retaining structure**

Earthquake acceleration time-histories are used to represent the earthquake demand in a displacement analysis of rigid body structural wedge (permanent) translation for the complete time-history analysis option. A step-by-step solution scheme is followed in order to obtain the wall's relative velocity and relative displacement in the time domain by CorpsWallSlip. An overview of the characteristics of this numerical formulation is given in Section 2.4.

### **2.6 Vertical acceleration in the new translational analysis model of a wall retaining a partially submerged backfill and buttressed by a reinforced concrete slab**

Vertical accelerations can be included in the Newmark (1965) sliding block analysis of earth retaining structures. However, several sliding block formulations, e.g., Richards and Elms (1979) and others, set the vertical component of acceleration occurring at sliding equal to zero in their formulations. Whitman and Liao (1985a, pages 30 and 74) observe that the vertical earthquake ground motion component is generally not considered to be of as much significance as the horizontal component and has generally been ignored in sliding block analyses. From their study of the effect of vertical accelerations using 14 earthquake records on wall displacements (summarized in Section 6.5 of their report), they conclude that incorporating vertical ground accelerations causes greater residual displacement.

Current Corps projects often involve the development of horizontal and vertical acceleration time-histories for use in the design of various project features. One of the Corps projects leading to the development of CorpsWallSlip is sited in a high seismic region on the West coast and situated in close proximity to an active fault that dominates the ground motion hazard. Initial assessments of the Maximum Credible Earthquake design events led to the development of horizontal and vertical acceleration time-histories with positive/negative peak values of 1.2g/-1.02g and 0.83g/-1.2g, respectively. Normally the polarity of ground motions is not retained in their development so that in a sliding block analysis four combinations of horizontal and vertical ground motions are investigated, with two due to the reverse in sign for the horizontal and two due to the reverse in sign for the vertical acceleration time-histories. This can easily be

accomplished by selecting the option to invert a time-history in the CorpsWallSlip Visual Modeler in the horizontal and/or vertical earthquake time-history tabs. For the case of a “dry” site (i.e., no pool nor water table within the retained soil), with cohesionless soils, interface friction  $\delta$  between the driving and structural wedges equal to zero, the computed value for the effective normal force acting along the base of a structural wedge would be less than or equal to zero according to Equation 2.6 or Equation 2.65. The shear force resistance along the base of the structural wedge would be less than or equal to zero by Equation 2.2, resulting in infinite relative displacements. Consequently, a vertical acceleration time-history with magnitudes (at time-steps) approaching or exceeding 1 g cannot be used in the current formulation.

In an attempt to answer questions regarding the impact of a vertical acceleration time-history of significant amplitude on seismic response, as is the case for the Corps project discussed in the previous paragraph, an alternative method to incorporate the effects of vertical accelerations in a Newmark sliding block analysis is proposed. This new approach is incorporated in CorpsWallSlip PC-based program.

In a Newmark sliding block complete time-history analysis of a retaining structure, CorpsWallSlip allows the user to specify a constant value for vertical acceleration to be used (a) in the equilibrium Equation 2.7 or 2.66 when computing (in a trial-and-error numerical procedure) the value of maximum horizontal transmissible acceleration,  $(a_{CG})_{\text{threshold-sliding-h}}$ , and (b) during the entire horizontal sliding block time-history analysis. This software implements the following two new for determining an approximate, constant, effective value for vertical acceleration:

**Method 1 - average vertical acceleration value:** Using the user-specified horizontal acceleration time-history and the user-provided constant value for vertical acceleration, the value for maximum horizontal transmissible acceleration,  $(a_{CG})_{\text{threshold-sliding-h}}$ , is computed and a sliding block time-history analysis is performed. The software then identifies at which  $i$  time increments that *incremental* sliding  $(d_r)_i$  takes place and the total number of incremental time-step increments  $i$  during which sliding occurs, designated  $n_{\text{slide}}$ . The average vertical acceleration value for the user-specified vertical acceleration time-history is computed for all these  $i$  time increments using the relationship

$$(a_{CG})_{v-ave} = \frac{\sum_i^{n_{slide}} (a_v)_i}{n_{slide}} \quad (2.74)$$

The sign for the average vertical acceleration  $(a_v)_i$  during each select time increment  $i$  for which incremental sliding occurs is maintained in this calculation.

A trial-and-error procedure is used to determine the appropriate value for the constant vertical acceleration value. The primary author of this report usually starts with a constant vertical (Y) acceleration value set equal to zero. A Newmark sliding block analysis is made, including a computation made by CorpsW<sub>all</sub>Slip using Equation 2.74 to determine a value for  $(a_{CG})_{v-ave}$ . Then a second Newmark sliding block analysis is made in which the constant vertical acceleration value is set equal to the previously computed value for  $(a_{CG})_{v-ave}$  by the user. This second computation results in an updated value for  $(a_{CG})_{v-ave}$ . The iterative process is repeated until the difference between old and new values is minor, usually within four computations.

**Method 2 - weighted vertical acceleration value:** This approach is a variation of Method 1. Using the user-specified horizontal acceleration time-history and the user-provided constant value for vertical (Y) acceleration, the value for maximum horizontal transmissible acceleration,  $(a_{CG})_{threshold-sliding-h}$ , is computed and a sliding block time-history analysis is performed. The software then identifies at which  $i$  time increments during which incremental sliding  $(d_r)_i$  takes place and the total number of time increments  $i$  during which sliding occurs is designated  $n_{slide}$ . The total horizontal displacement is

$$d_r = \sum_i^{n_{slide}} (d_r)_i \quad (2.75)$$

A weighted vertical acceleration value is computed for the user-specified vertical acceleration time-history with average vertical acceleration value,  $(a_v)_i$ , computed for each time increment  $i$  of incremental displacements using the following relationship



$$(a_{CG})_{v\text{-weighted}} = \sum_i^{n_{\text{slide}}} \left\{ (a_v)_i \bullet \left[ \frac{(d_r)_i}{d_r} \right] \right\} \quad (2.76)$$

Again, the sign for the average vertical acceleration,  $(a_v)_i$ , during each select time increment  $i$  of incremental displacements is maintained in this calculation.

A trial-and-error procedure is used to determine the appropriate value for the constant vertical acceleration value. The primary author of this report usually starts with a constant vertical (Y) acceleration value set equal to zero. A Newmark sliding block analysis is made, including a computation made by CorpsWallSlip using Equations 2.75 and 2.76 to determine a value for  $(a_{CG})_{v\text{-weighted}}$ . Then a second Newmark sliding block analysis is made in which the constant vertical (Y) acceleration value is set equal to the previously computed value for  $(a_{CG})_{v\text{-weighted}}$  by the user. This second computation results in an updated value for  $(a_{CG})_{v\text{-weighted}}$ . The process is repeated until the difference between old and new values is minor, usually within four computations.

Method 2 differs from Method 1 in that the weighting factor applied to each of the average vertical acceleration,  $(a_v)_i$ , values at the  $i$  time increments of incremental sliding is assigned according to the relative magnitude of incremental displacements occurring at each time increment. Method 1 applies a uniform weighting factor.

## 2.7 Simplified Newmark sliding block permanent displacement analysis

CorpsWallSlip provides for the computation of seismically induced permanent wall displacement using a simplified Newmark sliding block analysis. The advantage of this method of analysis is that only user-specified peak ground response values are required for the design earthquake, compared with the user-specified acceleration time-history for the complete time-history analysis.

The simplified sliding block analysis consists of a three-step process:

1. The maximum transmissible acceleration,  $(a_{CG})_{\text{threshold-sliding-h}} = [(k_{CG})_{\text{threshold-sliding-h}} \text{ times } g]$ , is computed using Equation 2.66 (or Equation 2.70 in the case of the vertical component of acceleration set

- equal to zero) for the structural wedge. This iterative computation is made internally with the results reported in WORKslide.TMP output file generated in each CorpsWallSlip analysis. This file may be viewed using the visual modeler box labeled **Show Sliding Evaluation** on the **Analysis** tab.
2. Ground motion parameters such as peak ground acceleration and velocity and earthquake magnitude values are determined by the project seismic design team and are user input to CorpsWallSlip.
  3. Using the parameters from steps (1) and (2), the value (or range in values) of the seismically induced permanent translation is computed using each one of the simplified sliding block relationships discussed in this section and selected by the user. These computations are made internally with the permanent displacement results reported in WORKslide.TMP output file generated in each CorpsWallSlip analysis. This file may be viewed using the visual modeler box labeled **Show Sliding Evaluation** on the **Analysis** tab.

The simplified sliding block relationships of Ambraseys and Menu (1988), Cai and Bathurst (1996), Whitman and Liao (1985a, 1985b) Richards and Elms (1979), and Makdisi and Seed (1978) are incorporated in CorpsWallSlip. Their relationships are summarized in the following subsections. These relationships were derived using acceleration time-histories from soil sites.

### 2.7.1 Ambraseys and Menu (1988) mean and 95% confidence relationships

Ambraseys and Menu (1988) report the permanent displacement,  $d_r$ , as

$$\log(d_r) = 0.9 + \log \left[ \left( 1 - \frac{(k_{CG})_{\text{threshold-sliding-h}}}{A} \right)^{2.53} \bullet \left( \frac{(k_{CG})_{\text{threshold-sliding-h}}}{A} \right)^{-1.09} \right] + 0.3 \bullet t \quad (2.77)$$

$(k_{CG})_{\text{threshold-sliding-h}}$  and  $A$  are in decimal fraction of  $g$  and  $d_r$  is in units of cm.

This relationship is developed for unsymmetrical (one-way) displacements occurring in the direction of maximum acceleration, and allows for varying probabilities of exceedance through the  $t$  variable term. It is computed for

near field conditions, for earthquake surface wave magnitude  $M_s = 6.9$  ( $\pm 0.3$ ), and computed ignoring the vertical component of ground acceleration. Ambraseys and Menu proved for a mean estimate, a 50 percent confidence that the computed displacement will not be exceeded, by setting the value for  $t$  equal to 0 in their relationship. Ambraseys and Menu also proved for a mean estimate, a 95 percent confidence that the computed displacement will not be exceeded, by setting the value for  $t$  equal to 1.96 in their relationship. Duration was found to be of little significance to displacement calculation, within the range of magnitudes considered. Velocity is not required for input; however, other deformation estimation techniques do incorporate peak recorded velocity, thus care should be taken to compare results among relationships with similar velocity constraints.

### 2.7.2 Cai and Bathurst (1996) mean upper bound relationship for the Franklin and Chang (1977) data

Cai and Bathurst (1996) proposed the following mean upper bound permanent displacement,  $d_r$ , relationship for the Franklin and Chang (1977) data as

$$d_r = 35 \cdot \frac{V^2}{A \cdot g} \cdot \left\{ e^{\left[ -6.91 \cdot \frac{(k_{CG})_{\text{threshold-sliding-h}}}{A} \right]} \right\} \cdot \left[ \frac{(k_{CG})_{\text{threshold-sliding-h}}}{A} \right]^{-0.38} \quad (2.78)$$

with  $A \cdot g$  and  $V$  equal to the peak ground acceleration and velocity of the design ground motion, respectively. Ground acceleration  $A \cdot g$  is in units of  $\text{in}/\text{sec}^2$ ,  $V$  is in units of  $\text{in}/\text{sec}$ , and  $d_r$  is in units of inches.  $(k_{CG})_{\text{threshold-sliding-h}}$  and  $A$  are in decimal fraction of  $g$ . A regression was made on the data of Franklin and Chang (1977), which in turn were integrations of 169 strong motion records from 27 earthquakes and 10 synthetic accelerograms. Owing to wide scatter in these permanent displacement data, upper bound values constrained the relationships. Cai and Bathurst consider their relationship gives a reasonable estimate of the upper bound displacement over the entire range of the ratio of the yield acceleration divided by peak acceleration (i.e., between zero and 1) and is less conservative than the relationship proposed by Richards and Elms (1979), especially when this ratio is small (e.g., ratio  $< 0.3$ ). Velocity is a required input.

### 2.7.3 Cai and Bathurst (1996) mean upper bound relationship for the Newmark (1965) data

Cai and Bathurst (1996) performed a regression analysis on the entire range of Newmark (1965) permanent displacement data and proposed the following  $d_r$  relationship

$$d_r = 9.2 \cdot \frac{V^2}{A \cdot g} \cdot e^{\left[ -5.87 \cdot \frac{(k_{CG})_{\text{threshold-sliding-h}}}{A} \right]} \cdot \left[ \frac{(k_{CG})_{\text{threshold-sliding-h}}}{A} \right]^{-0.49} \quad (2.79)$$

with  $A \cdot g$  and  $V$  equal to the peak ground acceleration and velocity of the design ground motion, respectively. Ground acceleration  $A \cdot g$  is in units of  $\text{in}/\text{sec}^2$ ,  $V$  is in units of  $\text{in}/\text{sec}$ , and  $d_r$  is in units of inches.  $(k_{CG})_{\text{threshold-sliding-h}}$  and  $A$  are in decimal fraction of  $g$ . The Newmark (1965) data were based on integrations of four strong motion records from four west coast earthquakes (Ferndale, 21 Dec. 1954; Eureka, 21 Dec. 1954; Olympia, 13 April 1949; and El Centro, 18 May 1940). Recorded peak ground accelerations for all four acceleration time-histories were above 0.15  $g$ . Cai and Bathurst proved for a mean estimate, a 50 percent confidence that the computed displacement will not be exceeded. Velocity is a required input.

### 2.7.4 Whitman and Liao (1985a and 1985b) mean and 95 percent confidence relationships

Whitman and Liao (1985b) report the mean value for the permanent displacement,  $d_r$ , computed ignoring the vertical component of ground acceleration, as given by the relationship

$$d_r = 37 \cdot \frac{V^2}{A \cdot g} \cdot e^{\left( -9.4 \left( \frac{(k_{CG})_{\text{threshold-sliding-h}}}{A} \right) \right)} \quad (2.80)$$

with  $A \cdot g$  and  $V$  equal to the peak ground acceleration and velocity of the design ground motion, respectively. Ground acceleration  $A \cdot g$  is in units of  $\text{in}/\text{sec}^2$ ,  $V$  is in units of  $\text{in}/\text{sec}$ , and  $d_r$  is in units of inches.  $(k_{CG})_{\text{threshold-sliding-h}}$  and  $A$  are in decimal fraction of  $g$ . Whitman and Liao (1985a) provide a second relationship for the permanent displacement seismically induced,  $d_r$ ,

$$d_r = 495 \bullet \frac{V^2}{A \bullet g} \bullet e^{-9.4 \left( \frac{(k_{CG})_{\text{threshold-sliding-h}}}{A} \right)} \quad (2.81)$$

According to Whitman and Liao, this relationship for  $d_r$  ensures that there will be a 95 percent confidence that the computed value for  $d_r$  will not be exceeded during an earthquake for the assigned  $A$  and  $V$  values.

Both Whitman and Liao equations were based on a statistical analysis of a suite of 14 earthquake records, each with two components of motion. All peak accelerations were greater than 0.15  $g$  to avoid scaling problems. All but two of the records considered were in the magnitude range from 6.3 to 6.7; two records were from larger earthquakes ( $M = 7.1$  from Western Washington Earthquake of 30 Dec 1934, Olympia, Washington, Highway Test Lab;  $M = 7.7$  from Kern County, California Earthquake of 21 July 1952, Taft Lincoln School).

#### **2.7.5 Richards and Elms (1979) upper bound relationship for the Franklin and Chang (1977) data**

Richards and Elms (1979) proposed the following upper bound permanent displacement,  $d_r$ , relationship for the Franklin and Chang (1977) data as

$$d_r = 0.087 \bullet \frac{V^2}{A \bullet g} \bullet \left[ \frac{(k_{CG})_{\text{threshold-sliding-h}}}{A} \right]^{-4} \quad (2.82)$$

With ground velocity  $V$  in units of in/sec, ground acceleration  $A \bullet g$  in units of in/sec<sup>2</sup> and  $d_r$  in units of inches.  $(k_{CG})_{\text{threshold-sliding-h}}$  and  $A$  are in decimal fraction of  $g$ . This relationship is based on a straight line (full logarithmic) fit to Franklin and Chang's (1977) upper bound data and was proposed specifically to estimate upper bound displacement of a gravity retaining wall. They note that the maximum transmissible acceleration of the sliding structural wedge is dependent on dynamic lateral earth pressure acting at the back of the wall. Cai and Bathurst observe that the Richards and Elms relationship is considered conservative, especially for ratios of maximum transmissible acceleration divided by peak ground acceleration values less than about 0.3.

### **2.7.6 Makdisi and Seed (1978) range in displacements for (Richter) magnitude 6.5, 7.5, and 8.25 events**

The Makdisi and Seed relationships implemented within CorpsWallSlip were developed from the Makdisi and Seed (1977) figures (not shown). The upper and lower range in  $d_r$  values is reported. This range in  $d_r$  data corresponds to earthquakes with specific magnitudes of 6.5, 7.5, and 8.25. Local (Richter) earthquake magnitude is a required input, but velocity is not; however, other deformation estimation techniques do incorporate peak recorded velocity, thus care should be taken to compare results among relationships with similar velocity constraints.

### 3 Threshold Value of Acceleration Corresponding to Incipient Lift-Off of the Base of the Wall in Rotation

#### 3.1 Introduction

The permanent displacement of retaining structures is not restricted to walls that slide along their base as a result of inertial forces imparted during earthquake shaking. For some retaining wall system configurations and material properties, permanent displacements may instead result from the rotation of a retaining wall about a point along its wall-to-foundation interface. Two key steps in the evaluation process of the idealized rigid block structural wedge formulation are (1) the computation of the maximum transmissible acceleration (discussed in Chapter 2) and (2) the computation of threshold value of acceleration corresponding to lift-off of the base of the wall in rotation. Comparison of these values determines if the wall will tend to slide before it will rotate or vice versa. The lower of the two values dictates the kinematic mechanism for the retaining wall system model. This chapter summarizes the Ebeling and White (2006) CorpsWallRotate formulation and computation of threshold value of acceleration corresponding to lift-off of the base of the wall in rotation about its toe, which is also implemented within CorpsWallSlip.

The idealized permanent displacement due to rigid body noncentroidal rotation of a retaining wall about its toe during earthquake shaking and with toe restraint is shown in Figure 3.1.<sup>1</sup> The buttressing effect of a reinforced concrete slab is represented in this simplified dynamic model

---

<sup>1</sup> Chapter 2 of Ebeling and White (2006) reviewed key aspects of four existing, simplified engineering formulations (Nadim and Whitman (1984), Siddharthan et al. (1992), Fishman and Richards (1997, 1998), Steedman and Zeng (1996), and Zeng and Steedman (2000)) used to analyze seismically induced permanent displacement due to rotation of a rigid block retaining wall about a point along its base. These four formulations involve retaining walls *without toe restraint*. Section 1.2 of this report summarizes five new features contained within the Ebeling and White (2006) formulation, implemented in CorpsWallRotate, that are of importance to the seismic rotational analysis of Corps earth retaining structures with a reinforced concrete slab buttressing the toe of the wall. Recall the Figure 1.3 cantilever retaining wall is buttressed by an invert spillway slab (which is a reinforced concrete slab). The primary author of this report is of the opinion that the assignment of the point of rotation to the toe of the wall becomes a reasonable simplifying assumption because of the constraint provided by the Figure 1.3 invert spillway slab to lateral translations, combined with the effects of the stiff, competent rock foundation.

by the user-specified force  $P_{\text{resist}}$  acting on a vertical section extending upwards from the toe of the wall as per Strom and Ebeling (2004).

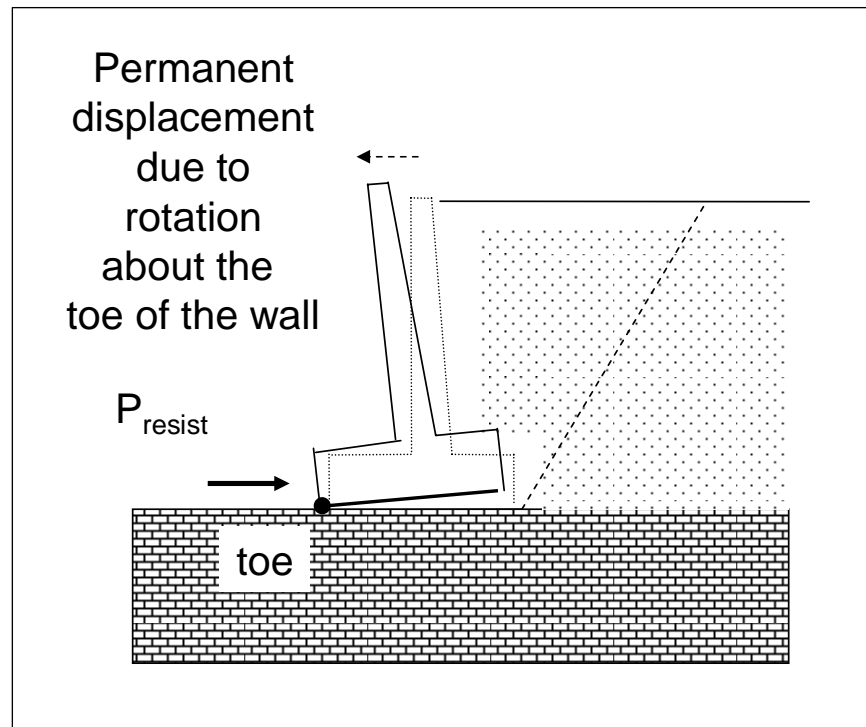


Figure 3.1. Idealized permanent, seismically induced displacement due to the rotation about the toe of a rock-founded wall retaining moist backfill, with toe restraint, computed using CorpsWallRotate.

### 3.2 Threshold value of acceleration corresponding to incipient lift-off of the base of a wall, retaining moist backfill, in rotation

During ground shaking, inertial forces are induced on the retaining wall system. The time-varying inertial forces lead to elastic deformations which can ultimately result in permanent rotation of the wall or sliding of the wall. In the case of permanent rotation of a rigid block model of the retaining wall system, (1) inertial forces vary in magnitude and direction with time, and (2) their magnitudes are proportional to the value of acceleration at any given instant in time but acting in the direction opposite to acceleration. Additionally, a rotational acceleration about the point of rotation (e.g., refer to Figure 3.1) develops once the threshold acceleration for lift-off of the base of the wall in rotation is exceeded, which leads to permanent rotation of the wall relative to the top-of-foundation. When the ground acceleration (in a time-history analysis) drops below this threshold acceleration value, restoring forces and moments will act to slow the speed of rotation, reducing the rate of



increase of the angle of wall rotation. An increment of permanent wall rotation occurs during this interval in time. Additional permanent rotation will be induced during further cycles of ground acceleration if the threshold acceleration for lift-off of the base of the wall in rotation is again exceeded. The angle of permanent wall rotation accumulates with each of these excursion cycles in a manner similar to the accumulation of permanent sliding displacement in Newmark's sliding block method, discussed in the previous chapter. The primary author of this report observes that for a retaining wall system of specified geometry and material properties (i.e., unit weights and shear strength parameters, etc.) the threshold values of acceleration corresponding to incipient lift-off of the base of the wall in rotation and for incipient sliding of the wall are not the same.

So the first step in determining if the retaining wall will rotate prior to sliding during earthquake shaking, or vice versa, is to compute (1) the value of acceleration at the center of gravity of the structural wedge that is needed for lift-off of the wall from its base in rotation about the toe of the wall (to be discussed in this chapter); and (2) the limiting acceleration required to reduce the factor of safety against sliding to a limiting value of 1.0 (commonly referred to as the maximum transmissible acceleration,  $N^*g$ , sometimes referred to as the yield acceleration and discussed in Chapter 2). The second step is to compare these limiting acceleration values. For the simplified decoupled analyses outlined in this report, the mode of deformation is dictated by the smaller of the two acceleration values. These two steps are incorporated within  $\text{CorpsWallSlip}$ .

Relative-motion analysis of the rigid body model of the Figure 3.2 wall retaining moist backfill is used to establish the acceleration of (rigid) mass center point  $CG^1$  by establishing the relationship between the acceleration of point  $CG$  and the acceleration of point  $O$ . In the rotational  $\text{CorpsWallRotate}$  time-history formulation, the acceleration of point  $O$  at the toe of the retaining wall is set equal to acceleration of the ground,  $a_{\text{ground}}$ , and is a known, user-specified quantity. The horizontal and vertical components of the ground acceleration,  $a_{\text{ground}}$ , are designated as  $a_h$  and  $a_v$  in

---

<sup>1</sup> Computation of the center of mass as well as mass moment of inertia  $I_O$  about point  $O$  and  $I_{CG}$  about the center of gravity point  $CG$  of the structural wedge by  $\text{CorpsWallSlip}$  and  $\text{CorpsWallRotate}$  is outlined in Appendix E.

this figure, with subscript “h” or “v” meaning “horizontal” or “vertical.”<sup>1</sup> In this figure  $\theta$  and  $\ddot{\theta}$  designate the rotation and angular acceleration, respectively, at the particular time-step.

The free-body and kinetic diagrams of a rigid block structural wedge model in rotation about its toe are summarized in Figure 3.2, and they are combined in Figure 3.3 into a single figure showing the dynamic forces acting on a rigid block model of the structural wedge with rotation about the toe of the wall during horizontal and vertical shaking of the rigid base.<sup>2</sup> This cantilever wall retaining moist backfill is subjected to the five external forces of the weight of the structural wedge,  $W$ , the dynamic active earth pressure force,  $P_{AE}$ , the resisting force,  $P_{resist}$ , provided by the reinforced concrete slab at the toe of the wall, and the horizontal and vertical components of the rigid base-to-wall reaction forces  $T$  and  $N'$ , respectively, acting through the toe of the wall.

At the onset of lift-off of the base of the Figure 3.3 retaining wall (with level base) subject to pure rotation about its toe, the rotating (i.e., overturning) moment equals the stabilizing (i.e., restoring) moment. The summation of moments about point 0 of the Figure 3.3 forces acting on the rigid body results in

$$\begin{aligned} \frac{W}{g} \cdot (a_{CG})_h \cdot \Delta y_{CG/O} + \frac{W}{g} \cdot (a_{CG})_v \cdot \Delta x_{CG/O} + P_{AE} \cdot \cos(\delta) \cdot h_{PAE} = \\ P_{resist} \cdot h_{Presist} + W \cdot \Delta x_{CG/O} + P_{AE} \cdot \sin(\delta) \cdot \Delta x_{heel/toe} \end{aligned} \quad (3.1)$$

Note that  $\ddot{\theta}$  is a very small number at the *onset* of lift-off and is set equal to zero as its limiting value when deriving this relationship. The component of the threshold acceleration occurring at lift-off of the base is designated as

<sup>1</sup> Note that values of  $a_h$  and  $a_v$  are established by a pair of user-defined horizontal and vertical acceleration time-histories in CorpsWallRotate, each of which changes in magnitude and possibly direction at each increment in time during earthquake shaking.

<sup>2</sup> The inertial forces are applied according to D'Alembert's principle. The advantage of the inertia-force method based on D'Alembert's principle is that it converts a dynamics problem into an equivalent problem in equilibrium.

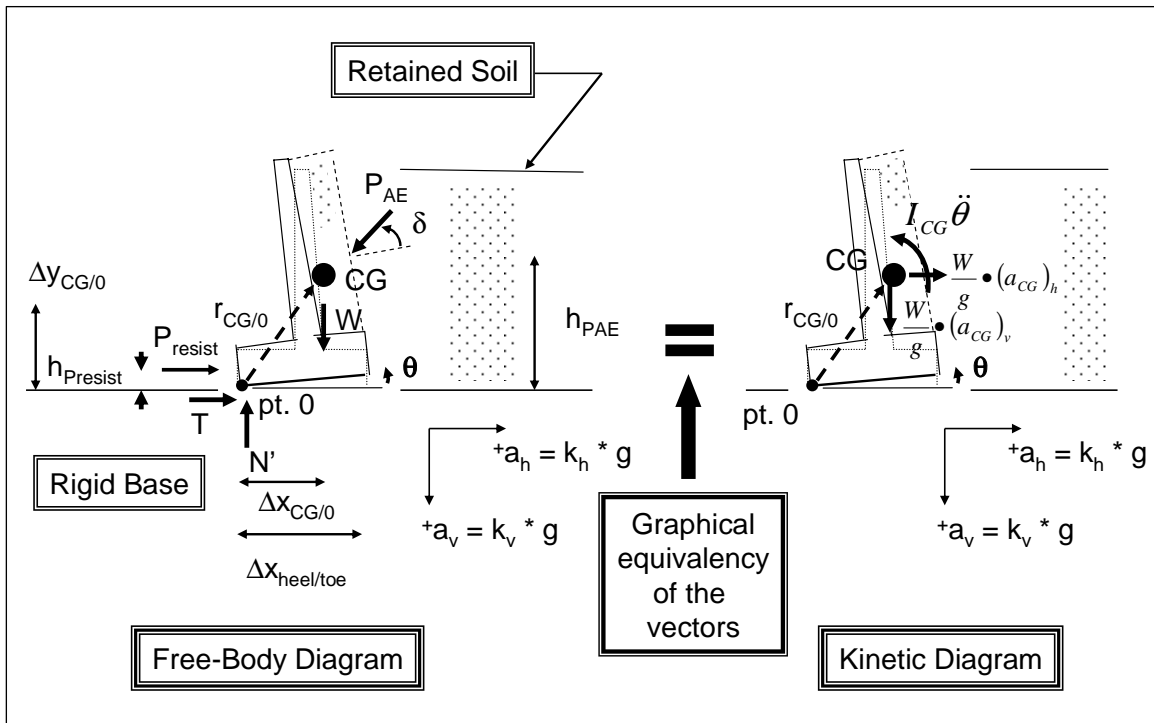


Figure 3.2. Free-body and kinetic diagrams of a rigid block model of a cantilever wall retaining moist backfill with rotation about the toe of the wall during horizontal and vertical shaking of the rigid level base.

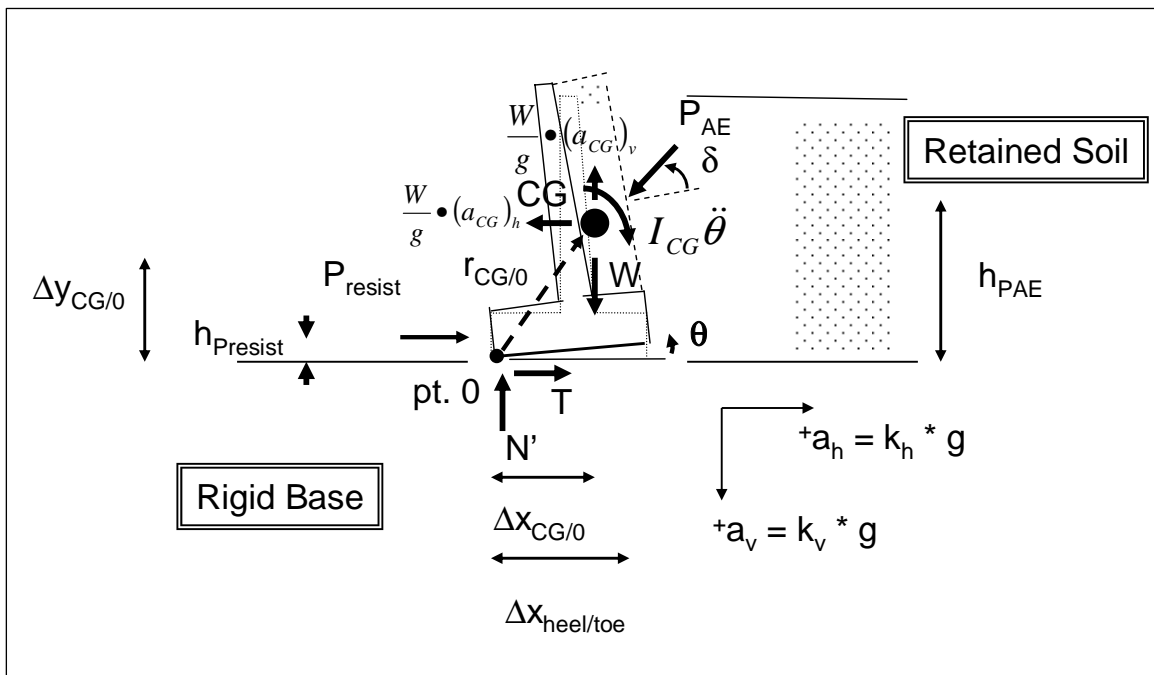


Figure 3.3. Inertia forces and resultant force vectors acting on a rigid block model of a cantilever wall retaining moist backfill with rotation about the toe of the wall during horizontal and vertical shaking of the rigid level base.

$$(a_{CG})_{\text{threshold-rotation-h}} = (k_{CG})_{\text{threshold-rotation-h}} \bullet g \quad (3.2)$$

where  $(k_{CG})_{\text{threshold-rotation-h}}$  is a value of horizontal ground acceleration, expressed in decimal fraction. Note that the horizontal acceleration value  $[(k_{CG})_{\text{threshold-rotation-h}} \text{ times } g]$  is not a user-specified constant. Since the horizontal limiting acceleration is of interest, one option is to set the vertical component of acceleration occurring at lift-off in rotation equal to zero, as done by Nadim and Whitman (1984).<sup>1</sup> By making this assumption and introducing Equation 3.2, Equation 3.1 becomes

$$(k_{CG})_{\text{threshold-rotation-h}} = \frac{P_{\text{resist}} \bullet h_{\text{Presist}} + W \bullet \Delta x_{CG/0} + P_{AE} \bullet \sin(\delta) \bullet \Delta x_{\text{heel/toe}} - P_{AE} \bullet \cos(\delta) \bullet h_{PAE}}{W \bullet \Delta y_{CG/0}} \quad (3.3)$$

Because of the inclusion of acceleration in  $P_{AE}$  formulation (refer to Appendix A),  $C_{\text{orps}}W_{\text{all}}\text{Rotate}$  solves Equation 3.3 using a trial-and-error numerical approach. This same iterative procedure is implemented in  $C_{\text{orps}}W_{\text{all}}\text{Slip}$ . The value for  $h_{PAE}$  is determined using the procedure outlined in Appendix B for walls retaining moist backfill and the procedures outlined in Appendix C for all other cases.

### 3.3 Threshold value of acceleration corresponding to incipient lift-off of the base of a wall, retaining a partially submerged backfill, in rotation

The formulation to compute the threshold value of acceleration corresponding to incipient lift-off of the base of a wall for a rock-founded wall retaining a partially submerged backfill and for the case of a pool in front of the retaining wall is summarized in this subsection. The Ebeling and White (2006) formulation presented is an extension of the moist backfill formulation discussed in the previous section.

<sup>1</sup> Another option, implemented in  $C_{\text{orps}}W_{\text{all}}\text{Slip}$  and  $C_{\text{orps}}W_{\text{all}}\text{Rotate}$ , is to assign a constant value to the vertical acceleration component. A procedure for determining the values for this constant is discussed in Sections 3.9 and 3.10 of Ebeling and White (2006).

### 3.3.1 Water pressures acting on the structural wedge

Water pressures are assumed to act along three faces of the structural wedge denoted as the toe, base, and the heel regions of Figure 3.4. Forces acting on the toe are due to the presence of a pool of water in front of the wall. A leaking vertical joint is assumed between the (buttressing) base slab and the structural wedge with water pressures above the toe controlled by the presence of the pool. The computation of water pressures acting on this partially submerged structural wedge is discussed in detail in Appendix D.<sup>1</sup> The Figure 3.4 distributions of water pressures are converted into equivalent resultant forces, expressed in global x- and y-coordinates, and their points of application along each of the three regions. These resultant water pressure forces are used in an effective stress based stability analysis of the structural wedge. Dynamic considerations for the pool during earthquake shaking are accounted for in the analysis using hydrodynamic water pressures computed using the Westergaard (1931) procedure of analysis (see Appendix D). The hydrodynamic water pressure resultant force,  $P_{wd}$  (Equation D.5), is shown acting on the structural wedge in this figure (and shown acting in a direction consistent with the direction of positive horizontal acceleration,  $+a_h$ ).

---

<sup>1</sup> In the initial CorpsWallSlip and CorpsWallRotate versions, no excess pore water pressures due to earthquake-induced shear strains within the soil regions are included (i.e., the excess pore water pressure ratio,  $r_u$ , is equal to zero). Refer to Ebeling and Morrison (1992) for a complete description and discussion of  $r_u$ .

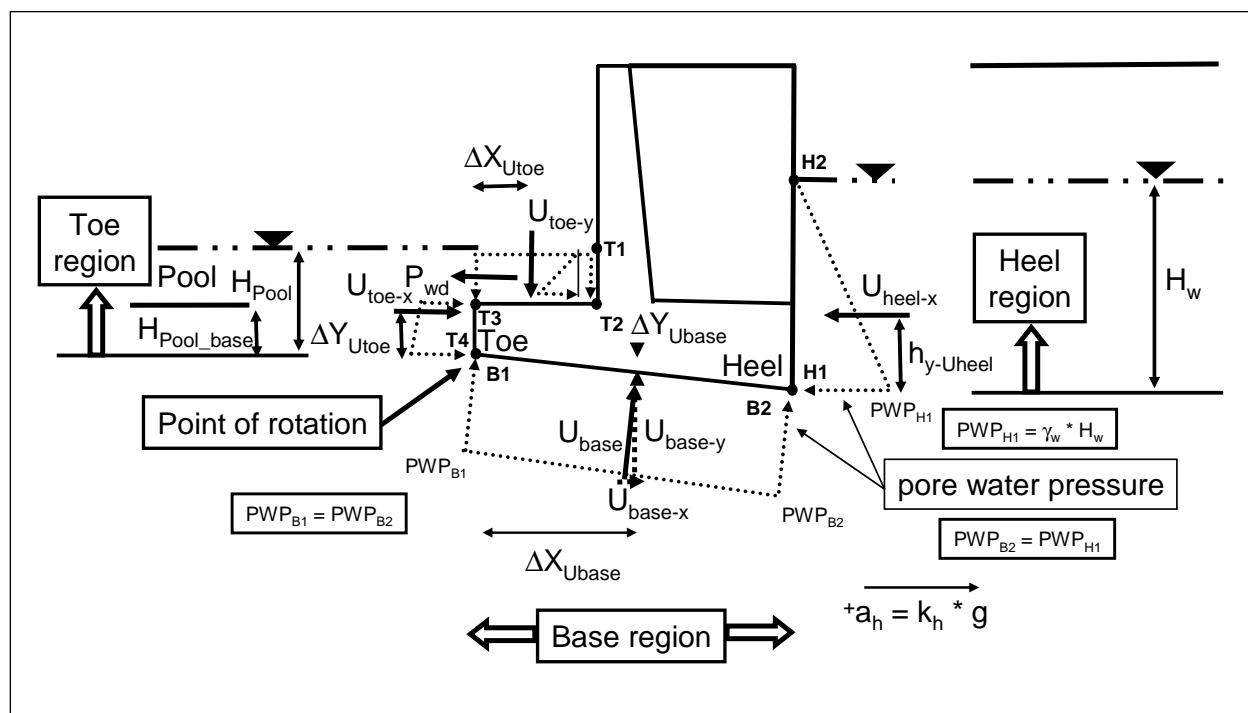


Figure 3.4. Control points, water pressures, and corresponding resultant forces acting normal to faces of the three regions of a structural wedge rotating about its toe – effective stress analysis.

In the case of rotation about the toe, contact between the base of the structural wedge and the foundation is lost sometime during earthquake shaking. Recall that a simplistic rigid base assumption is made in this formulation for rock-founded earth retaining structures. Due to the possible formation of a gap sometime during earthquake shaking, the Figure 3.4 pore water pressure distribution is used along the base. Note that this distribution differs from the steady-state pore water pressures resulting from a structural wedge in full contact with the rock foundation, shown in Figure D.1. The exact pore water distribution within the structure-to-foundation gap is a complex problem and a subject for state-of-the-art research. In CorpsWallRotate, it is recognized that the Figure 3.4 (or, equivalently, Figure D.4) pore water pressure distribution along the base of the structural wedge makes the simplistic assumption that the hydrostatic pore water pressure at the heel of the wall extends along the entire base of the structural wedge. It is based on the assumption that a gap opens early on during earthquake shaking during rotation about the toe of the retaining wall. This same formulation is implemented within CorpsWallSlip in the computation of the threshold value of acceleration corresponding to incipient lift-off of the base of a wall.

The resultant water pressure forces  $U_{toe}$ ,  $U_{base}$ ,  $U_{heel}$ , and  $P_{wd}$  shown in Figure 3.4 are superimposed on the free-body diagram of forces acting on the Figure 3.5 structural wedge, resulting in the Figure 3.5 free-body diagram. Recall  $P_{resist}$  is the force provided by the reinforced concrete, buttressing (toe) slab.

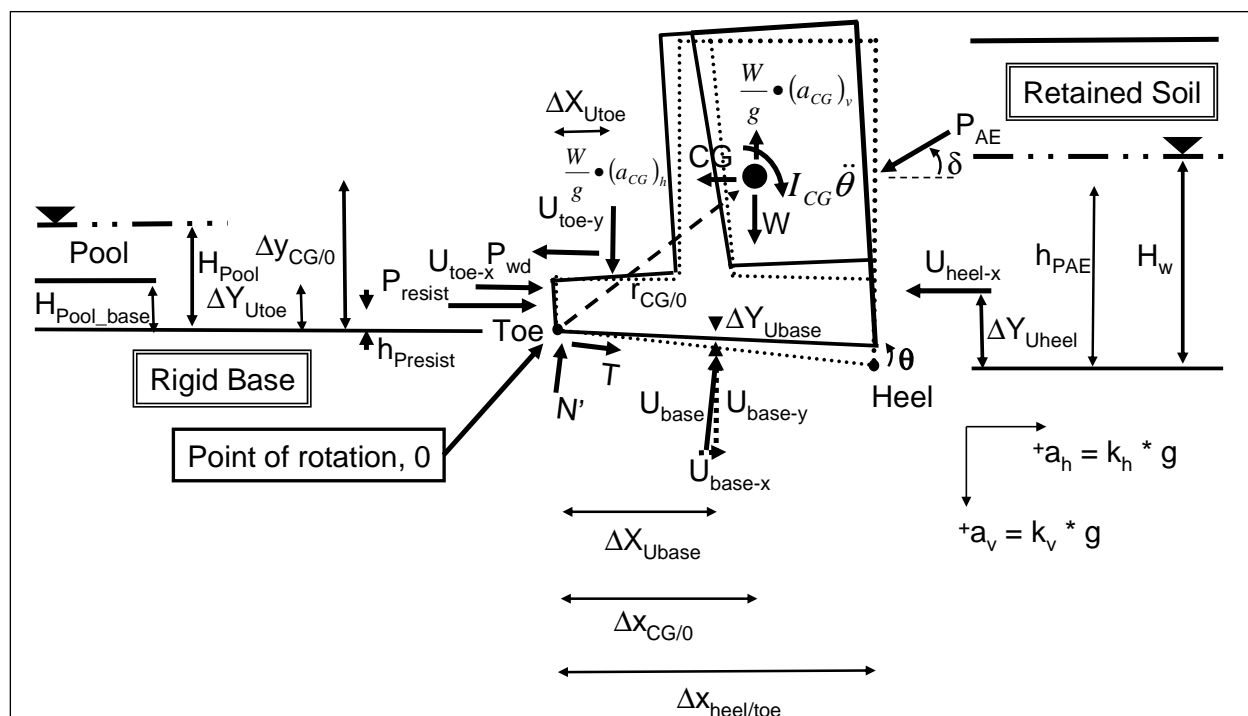


Figure 3.5. Inertia forces and resultant force vectors acting on a rigid block model of a (inclined base) cantilever wall retaining a partially submerged backfill with rotation about the toe of the wall during horizontal and vertical shaking of the inclined rigid base – effective stress analysis.

### 3.3.2 Threshold value of acceleration corresponding to incipient lift-off of the base of the wall in rotation – partially submerged backfill

At the onset of lift-off of the (inclined) base of the Figure 3.5 retaining wall subject to pure rotation about its toe, the rotating (i.e., overturning) moment equals the stabilizing (i.e., restoring) moment. The summation of moments about point 0 of the Figure 3.5 forces acting on a rigid body results in the following modified form of Equation 3.1,

$$\begin{aligned}
& \frac{W}{g} \cdot (a_{CG})_h \cdot \Delta y_{CG/0} + \frac{W}{g} \cdot (a_{CG})_v \cdot \Delta x_{CG/0} + P_{AE} \cdot \cos(\delta) \cdot [(y_{heel} + h_{PAE}) - y_{toe}] \\
& + U_{heel-x} \cdot [(y_{heel} + \Delta Y_{Uheel}) - y_{toe}] + U_{base-y} \cdot \Delta x_{Ubase} + U_{base-x} \cdot \Delta Y_{Ubase} \\
& + P_{wd} \cdot [H_{Pool\_base} + 0.4 \cdot (H_{Pool} - H_{Pool\_base})] \tag{3.4} \\
& = P_{resist} \cdot h_{Presist} + W \cdot \Delta x_{CG/0} + P_{AE} \cdot \sin(\delta) \cdot \Delta x_{heel/toe} \\
& + U_{toe-x} \cdot \Delta Y_{Utoe} + U_{toe-y} \cdot \Delta x_{Utoe}
\end{aligned}$$

Note that  $\ddot{\theta}$  is a very small number at the *onset* of lift-off and is set equal to zero as its limiting value when deriving this relationship. The component of the threshold acceleration occurring at lift-off of the base is designated as

$$(a_{CG})_{threshold-rotation-h} = (k_{CG})_{threshold-rotation-h} \cdot g \tag{bis 3.2}$$

where  $(k_{CG})_{threshold-rotation-h}$  is a value of horizontal ground acceleration, expressed in decimal fraction. Note that the horizontal acceleration value  $[(k_{CG})_{threshold-rotation-h} \text{ times } g]$  is a not a user-specified constant.

For a user-specified constant<sup>1</sup> for vertical acceleration [i.e.,  $(a_{CG})_v = \text{constant}$ ], CorpsWallRotate and CorpsWallSlip solve Equation 3.4 by introducing  $(a_{CG})_{threshold-rotation-h}$  and  $(k_{CG})_{threshold-rotation-h}$  for  $(a_{CG})_h$  and  $(k_{CG})_h$ . Because of the inclusion of acceleration in  $P_{AE}$  formulation (refer to Appendix A), CorpsWallRotate and CorpsWallSlip solve Equation 3.4 using a trial-and-error numerical approach. The value of horizontal acceleration at incipient lift-off in rotation is reported in the WORKrotate.TMP output file generated in each CorpsWallRotate and CorpsWallSlip analysis. This file may be viewed using the visual modeler boxes labeled **Show Lift-Off Evaluation** on the **Analysis** tab.

<sup>1</sup> A procedure for determining the value for this constant (for vertical acceleration) is discussed in Section 4.10 of Ebeling and White (2006).



In a total stress analysis, the internal pore water pressure force terms  $U_{base}$  and  $U_{heel}$  are excluded from Equation 3.4.

Since the horizontal limiting acceleration is of interest, another simplified form of Equation 3.4 may be derived by setting the vertical component of acceleration in the incipient lift-off in rotation equal to zero, as done by Nadim and Whitman (1984). By making this assumption and introducing Equation 3.2, Equation 3.4 becomes

$$(k_{CG})_{threshold-rotation-h} = \frac{\left[ \begin{aligned} &P_{resist} \bullet h_{Presist} + W \bullet \Delta x_{CG/0} + P_{AE} \bullet \sin(\delta) \bullet \Delta x_{heel/toe} + \\ &U_{toe-x} \bullet \Delta Y_{Utoe} + U_{toe-y} \bullet \Delta X_{Utoe} - P_{AE} \bullet \cos(\delta) \bullet [(y_{heel} + h_{PAE}) - y_{toe}] - \\ &U_{heel-x} \bullet [(y_{heel} + \Delta Y_{Uheel}) - y_{toe}] - U_{base-y} \bullet \Delta X_{Ubase} - U_{base-x} \bullet \Delta Y_{Ubase} - \\ &P_{wd} \bullet [H_{Pool\_base} + 0.4 \bullet (H_{Pool} - H_{Pool\_base})] \end{aligned} \right]}{W \bullet \Delta y_{CG/0}} \quad (3.5)$$

Because of the inclusion of acceleration in  $P_{AE}$  formulation (refer to Appendix A), CorpsWallRotate and CorpsWallSlip solve Equation 3.5 using a trial-and-error numerical approach.

In a total stress analysis, the internal pore water pressure force terms  $U_{base}$  and  $U_{heel}$  are excluded from Equation 3.5.

CorpsWallSlip does not perform a rotational time-history analysis. If the seismically induced, permanent rotational wall movements are of interest, CorpsWallRotate will perform the computations.

## **4 The Visual Modeler and Visual Post-Processor – CorpsWallSlip**

### **4.1 Introduction**

This chapter discusses the Visual Modeler, how to perform a CorpsWallSlip analysis, and how to interpret the results using the Visual Post-Processor. It also provides guidance for using the CorpsWallSlip software package. The software package is referred to by its abbreviated name, CWSlip, throughout this chapter.

### **4.2 Visual modeler and visual post-processor**

#### **4.2.1 Introduction to the visual modeling environment**

CWSlip is a program for performing a Newmark rigid sliding block analysis of seismically induced permanent displacement of a variety of wall structures during earthquake loading. The user has the option of performing one of two different types of translational analyses, either (1) a complete time-history analysis, or (2) a simplified sliding block analysis. This chapter is intended to give the user an understanding of how the CWSlip program is to be used to its greatest potential. To that end it also tries to imbue the user with an understanding of the work in creating and executing a CWSlip analysis.

Input data for the CWSlip program fall into six different groups for the complete time-history analysis type, and the user-interface reflects those groupings using tabs. The input groupings are:

- Horizontal earthquake time-history data
- Vertical earthquake time-history data
- Structural geometry
- Structural wedge information
- Driving wedge information
- Analysis specific data

Input data for the CWSlip program fall into five different groups for the simplified sliding block analysis, and the user-interface reflects those groupings using tabs. The input groupings are:

- Simplified analysis using peak ground motion parameter(s) data
- Structural geometry
- Structural wedge information
- Driving wedge information
- Analysis specific data

There is one other tab, a “splash” tab that shows a typical example of the type of problem handled by the CWSlip program; this tab is labeled as the **Introduction** tab. Above the **Introduction** tab shown in Figure 4.1 is a drop down menu entitled “File.” Activating this menu allows the user to open an existing, user-created, **\*\*\*.CWS** file that replenishes the contents of all tabs. Also on the **Analysis** tab are the controls to run an analysis and post-processing options.

**Introduction Tab:** The first tab, labeled Introduction, shows the structural wedge, idealized as a rigid body, and the forces acting on it (Figure 4.1) for the complete time-history analysis. The rock-founded cantilever retaining wall is buttressed at its toe by, e.g., an invert spillway slab (not shown). The translation of the structural wedge is assumed to occur during earthquake shaking. A drop down box entitled **Analysis Type** is activated and the complete time-history analysis is selected, rather than the simplified sliding block analysis option.

**Forces Shown on the Introduction Tab:**  $P_{AE}$  is the dynamic active earth pressure force due to the driving, moist soil wedge (not shown) or the partially submerged soil wedge (when a water table is present in the retained soil). Inertial effects due to earthquake shaking are incorporated in  $P_{AE}$ .  $W$  is the weight of the structural wedge, including both the weight of the (cantilever) retaining wall as well as the weight of the soil contained with this idealized structural wedge.  $W$  times  $k_h$  and  $W$  times  $k_v$  are the horizontal and vertical inertial forces, respectively, acting on the structural wedge during earthquake shaking. The reactions of the rock foundation on the structural wedge are represented through the horizontal and vertical forces  $T$  and  $N'$ , respectively.  $P_{resist}$  is the force provided to the toe of the (cantilever) retaining wall by the invert spillway slab (not shown) during earthquake shaking.

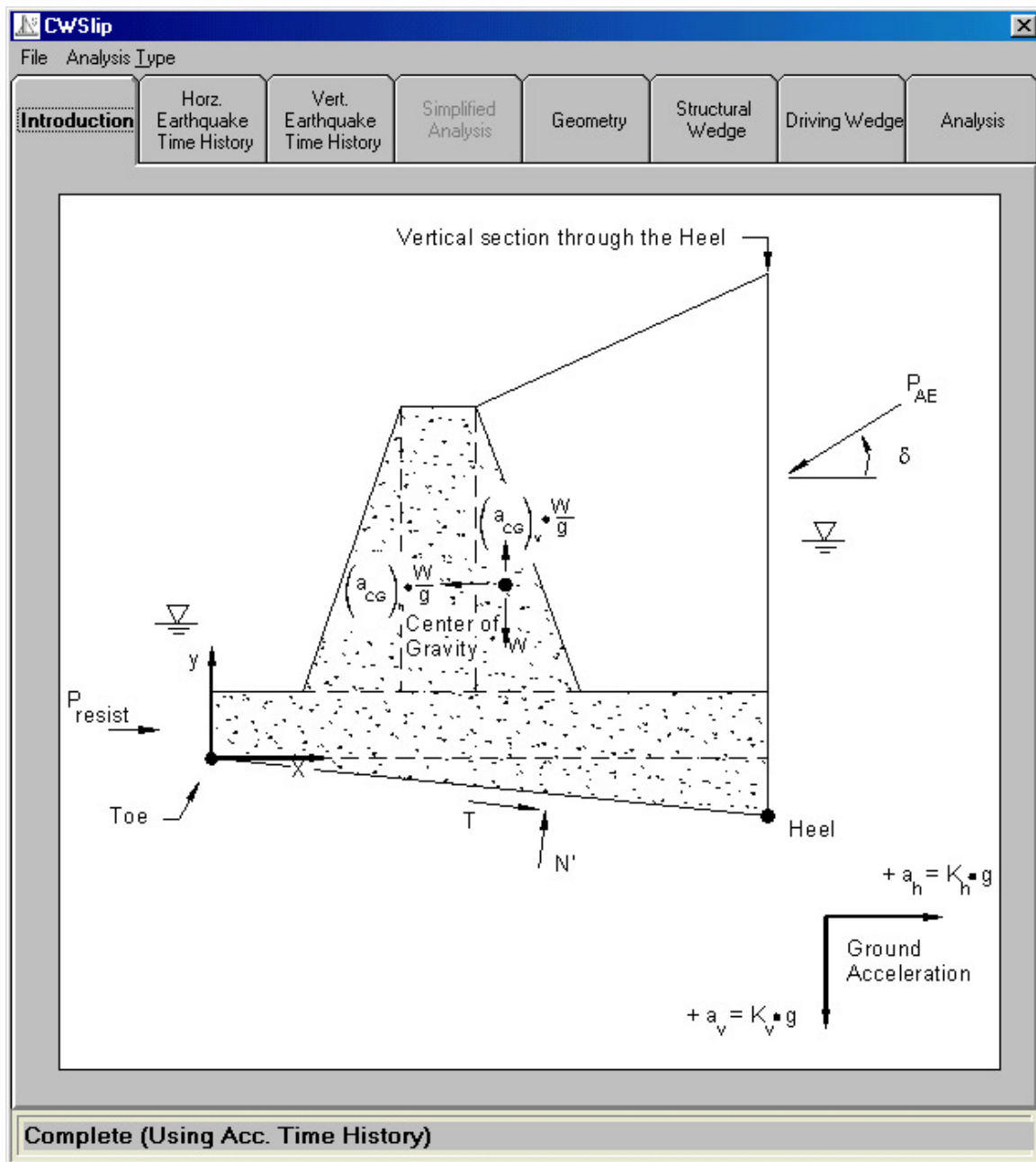


Figure 4.1. The **Introduction** tab features and idealized structural wedge diagram – complete time-history analysis.

#### 4.2.2 Earthquake time-history input

Both horizontal and vertical time-history input follow the same input pattern. First an appropriate, baseline corrected acceleration time-history data file is selected for the Corps project by the user. Given the non-standardized nature of earthquake time-history data files, certain attributes need to be specified to correctly read the input (ASCII) data file.

These attributes are entered in the Format section of the **Earthquake Time-History** (EQTH) tabs – Horizontal and Vertical. This is an exceptionally powerful tool for handling any format EQTH files. Figure 4.2 show the **Horizontal Earthquake Time-History** tab.

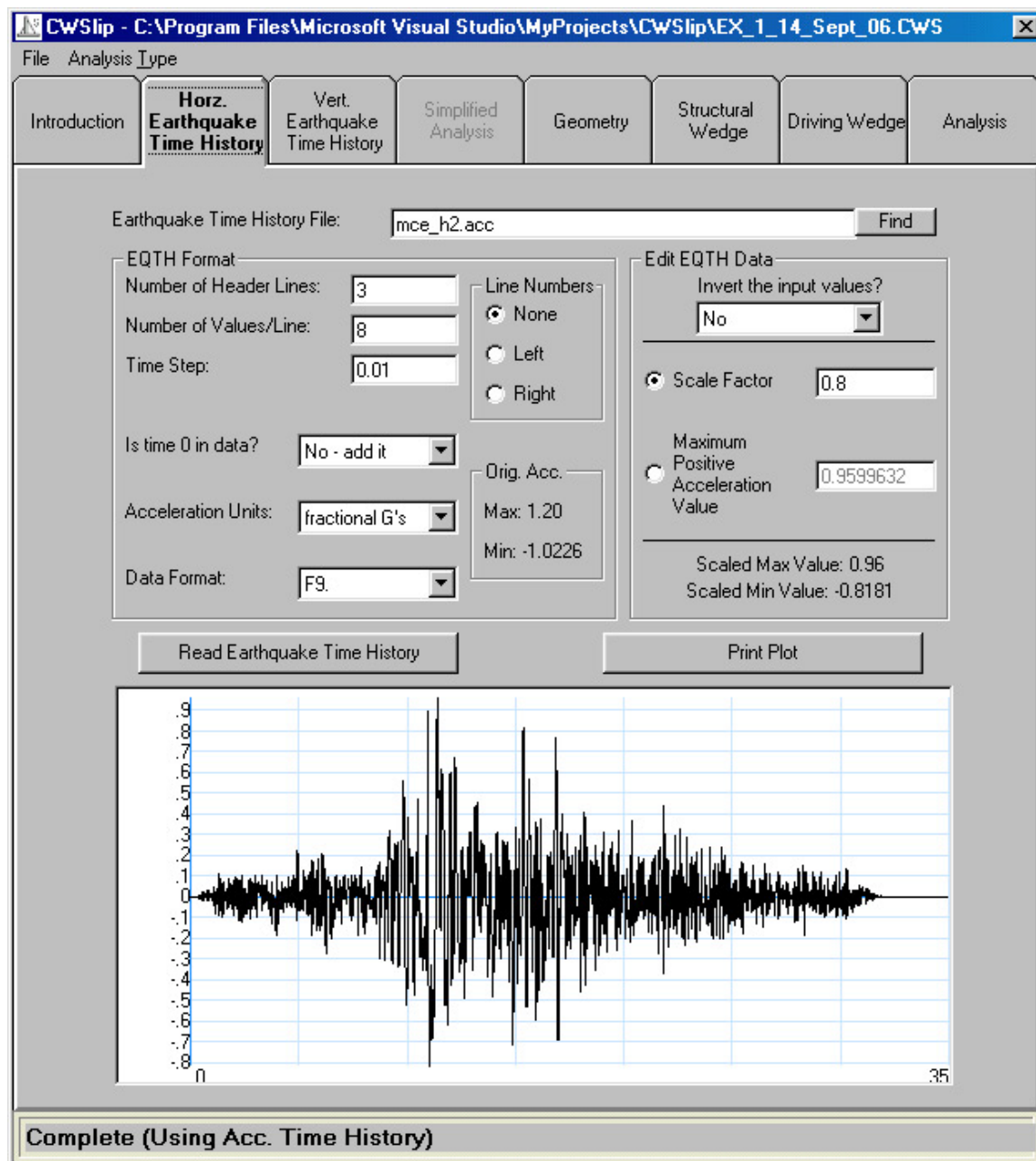


Figure 4.2. A strong earthquake time-history ground motion shown in the **Earthquake** tab.

To read in an appropriate EQTH data file, the user must first specify a file to be read in. The user can type a specific filename or select a file using the **Find** button that exists on the **Earthquake Time-History** tabs.

When a file has been selected, a format must be built. All specifications for reading a file are grouped in a frame labeled **EQTH Format**. To know what information to enter for reading the file, it will be beneficial to be able to peruse the file to find each section of data.

The first data in each EQTH file are a number of header lines. These are of no concern to the CWSlip program, so entering how many header lines there are allows the program to skip those lines. Also of no concern to the program CWSlip are line numbers in the input. In order to ignore them, the user must specify whether these line numbers exists, and if they do, which side of the data are they on.

It is more important to know how many data samples are on each line. Entering the **Number of Values/Line** keeps the program from entering blank samples or ignoring samples. The value entered for **Time-Step** should be the amount of time that occurs between samples, establishing the sampling frequency and the total time for the earthquake data.

Since CWSlip works from the beginning of an earthquake, it is to be assumed that the first sample, time step 0, will be of value 0.0 in whatever units are to be chosen. If the EQTH file does not have this zero point, it will have to be added. This can be done using the combo box provided.

In the same manner, the units that the data were recorded in can be specified. NOTE: The vertical EQTH file uses the same units as the Horizontal EQTH file. EQTH units must be consistent.

Finally, there is a combo box that shows several options for a data format. These formats are displayed as if they were in a FORTRAN FORMAT statement. These are especially important in areas where data text may run together.

After an EQTH format has been built for a particular file, the user can read in the **Earthquake Time-History**. When the button has been pressed, the actual values of the maximum and minimum values for that file are displayed in the **Data Limits** sub-frame of the **EQTH Format** frame.

A plot of the input data also is displayed at the bottom of the tab. The **Edit EQTH Data** frame is also enabled.

The **Edit EQTH Data** frame is a tool that allows the user to scale the EQTH data to values more appropriate for modeling the problem at hand. There is a combo box that allows the user to invert the user-specified earthquake acceleration time-history values, which is valuable for determining how the direction of peak values influences the computed results.

There are also two possible ways of scaling the input data, either by setting an absolute scale value to multiply the samples by or by setting an absolute maximum value for the positive peak value and scaling the other samples to match. To choose the scale method, click the radio button beside that option. Then type in the value desired.

When this is done the inactive choice will be updated with the related value. Also, the scaled minimum and maximum values will be displayed, and the data plot at the bottom of the form will reflect the changes.

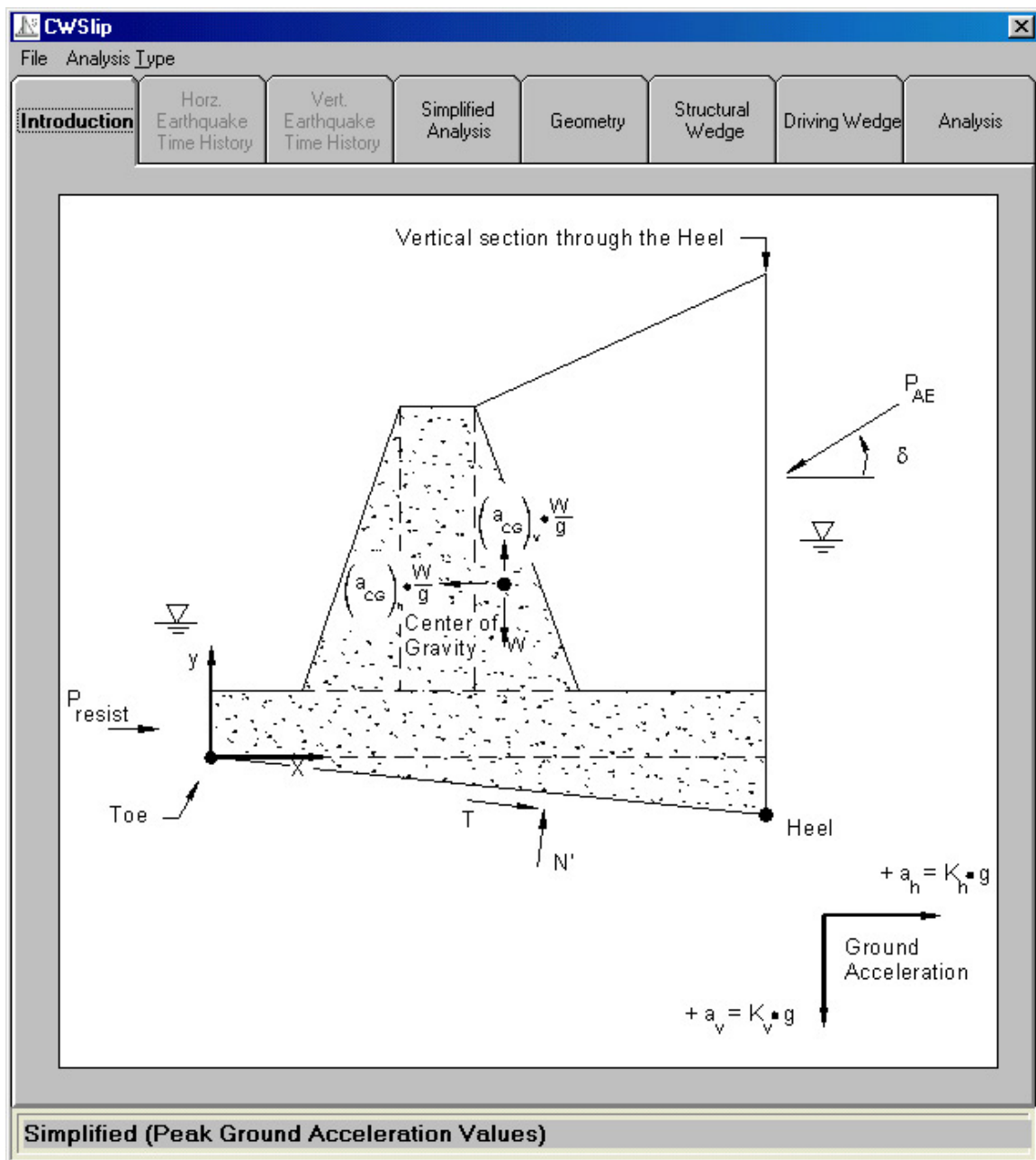
If the user desires a hardcopy of the scaled data in the same format as at the bottom of the tab, there is a button labeled **Print Plot**.

Vertical acceleration time-histories are handled in a similar fashion as the horizontal acceleration time-histories.

#### **4.2.3 Selection of the simplified sliding block methods of analysis and peak ground motion parameter input data**

Information for the simplified sliding block methods of analysis falls into two categories, (1) selection of the simplified sliding block methods of analysis and (2) specification of the peak ground motion parameter(s).

**Introduction Tab:** The first tab, labeled Introduction, shows the structural wedge, idealized as a rigid body, and the forces acting on it (Figure 4.3) for the simplified sliding block analysis. The rock-founded cantilever retaining wall is buttressed at its toe by, e.g., an invert spillway slab (not shown). The translation of the structural wedge is assumed to occur during earthquake shaking. A drop down box entitled **Analysis Type** is activated by selecting the simplified sliding block method of analysis rather than the complete time-history analysis. The forces shown on the **Introduction** tab are the same as described in Section 4.2.1.



The **Simplified Analysis** tab shown in Figure 4.4 lists eight simplified sliding block methods of analysis available for use in the CWSlip analysis of seismically induced permanent displacement of the user-specified retaining wall system. The user selects which of the eight methods of simplified sliding block methods of analysis will be used in the permanent displacement calculation step. More than one may be selected.



CWSlip - C:\Program Files\Microsoft Visual Studio\MyProjects\CWSlip\EX\_1\_14\_Sept\_06.CWS

File Analysis Type

Introduction Horz. Earthquake Time History Vert. Earthquake Time History **Simplified Analysis** Geometry Structural Wedge Driving Wedge Analysis

Choose Method(s) for Simplified Displacement Analysis

Publication	Description	
<input type="checkbox"/> Ambraseys & Menu (1988)	Mean relationship	Limitations
<input type="checkbox"/> Ambraseys & Menu (1988)	95% confidence that computed displacement will not be exceeded	Limitations
<input type="checkbox"/> Cai & Bathurst (1996)	Mean upper bound relationship for Franklin and Chang (1977) data	Limitations
<input type="checkbox"/> Cai & Bathurst (1996)	Mean relationship for Newark (1965) data	Limitations
<input type="checkbox"/> Whitman & Liao (1985)	Mean relationship	Limitations
<input type="checkbox"/> Whitman & Liao (1985)	95% confidence that computed displacement will not be exceeded	Limitations
<input type="checkbox"/> Richards & Elms (1979)	Upper bound relationship to the Franklin and Chang (1977) data	Limitations
<input type="checkbox"/> Makdisi & Seed (1978)	Range in values	Limitations

Data Required for Simplified Method(s) Analysis

Peak Acceleration Units Peak Velocity Units Magnitude

0 fractional G's 0 ft/sec 6.50

Simplified (Peak Ground Acceleration Values)

Figure 4.4. Simplified sliding block method of **Analysis** tab.

The second step in the simplified sliding block analysis is to provide the peak ground motion values to be used in the analysis (or analyses). The value for peak horizontal ground acceleration is required by each of the eight methods of analysis. The five simplified sliding block analyses typed in green font in Figure 4.4 also require peak horizontal ground velocity. The Makdisi and Seed (1978) simplified sliding block analysis, listed in red font, in Figure 4.4 also requires a selection of a Richter (Local) earthquake magnitude of 6.5, 7.5, or 8.25.

#### 4.2.4 Structural geometry input

For simplification of the geometric modeling and engineering analysis required to configure the structural wedge for analysis, it is assumed that the structural geometry of any structure designed by this program will be described in axis-aligned right-triangular and rectangular regions. Using this idea, a structural region template was created (see the lower image in Figure 4.5) that allows the user to specify regions as widths and heights for an accurate representation of the wall. There are a total of ten different regions that may be used. Each region is placed in relation to the other regions, and most regions can be represented as zero width and/or height, effectively removing it from the structure. The result of this modeling technique is the possibility to model almost any standard Corps retaining wall cross section.

The following diagrams, Figures 4.6 and 4.7, illustrate how the sections can be used to create different wall cross sections. Figure 4.6 displays each of the ten sections as well as their widths and heights. Each section is either rectangular or right triangular, and can therefore be defined by specifying the width and height of each of the sections that, when assembled together, form the structural wedge. Three material regions of concrete, moist soil, and saturated soil are allowed. The concrete material regions are assigned to material region numbers 1, 2, 6, 7, and 10. Moist soil material regions are assigned numbers 4, 5, and 9, while saturated soil material regions are assigned numbers 3 and 8. Values for the three material unit weights are specified by the user as part of the input data.

Figure 4.7 shows examples of how different walls may be configured using the ten sections. By entering a width or height of zero, sections may be entirely ignored for a structural wedge. For example, in the first diagram, region 6 is not used and therefore its width (or height) is set to zero as user input.

When region 10 is specified, as in the case of some Figure 4.7 hypothetical wall geometries, the user is allowed to input the height of the region but not its width. The width of region 10 is dictated by the geometry (specifically, the width) of region 1, as shown in these figures. When this region is present, the user specifies its height.

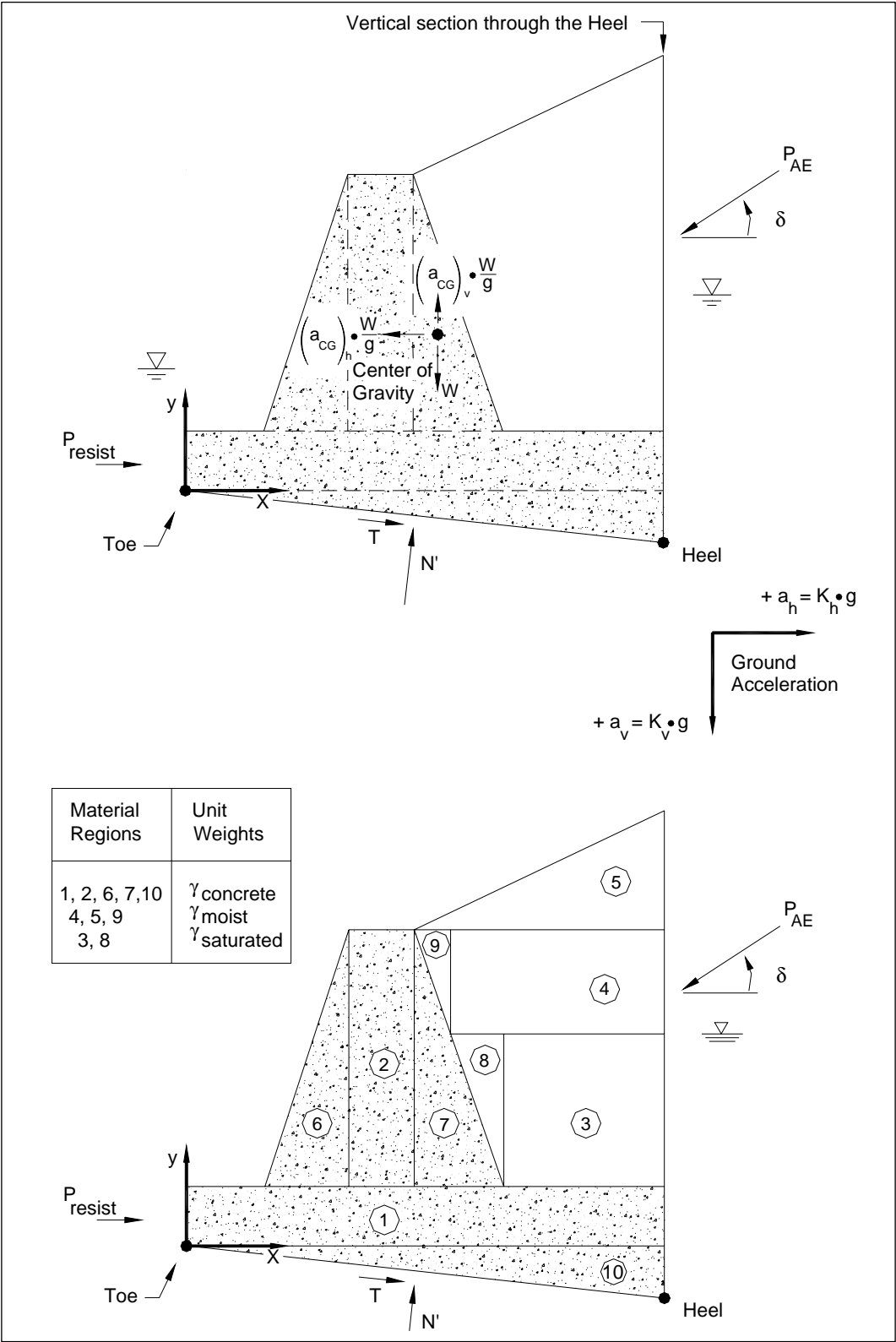


Figure 4.5. Dynamic forces acting on the free-body section of the structural wedge and its material regions.

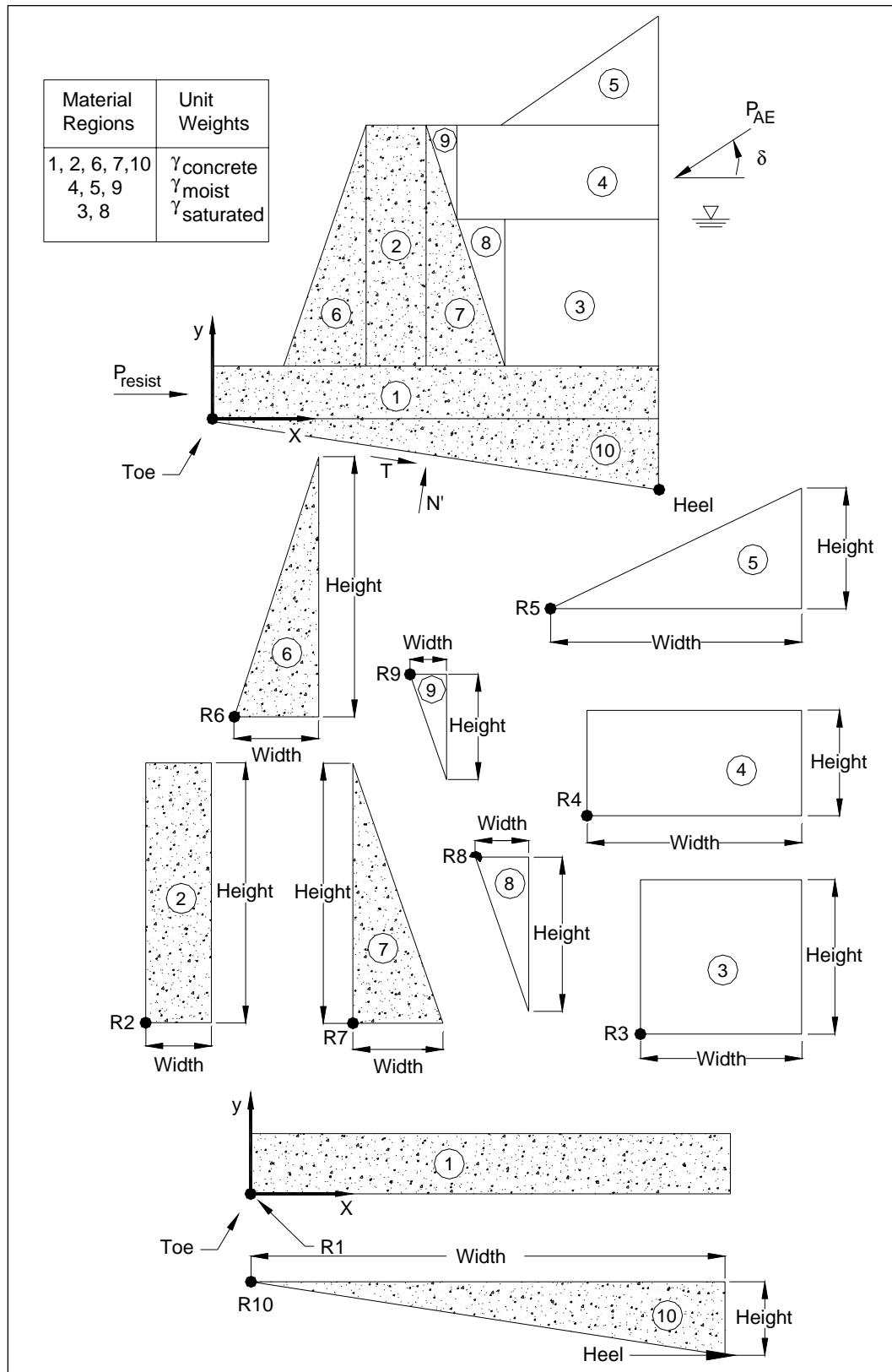
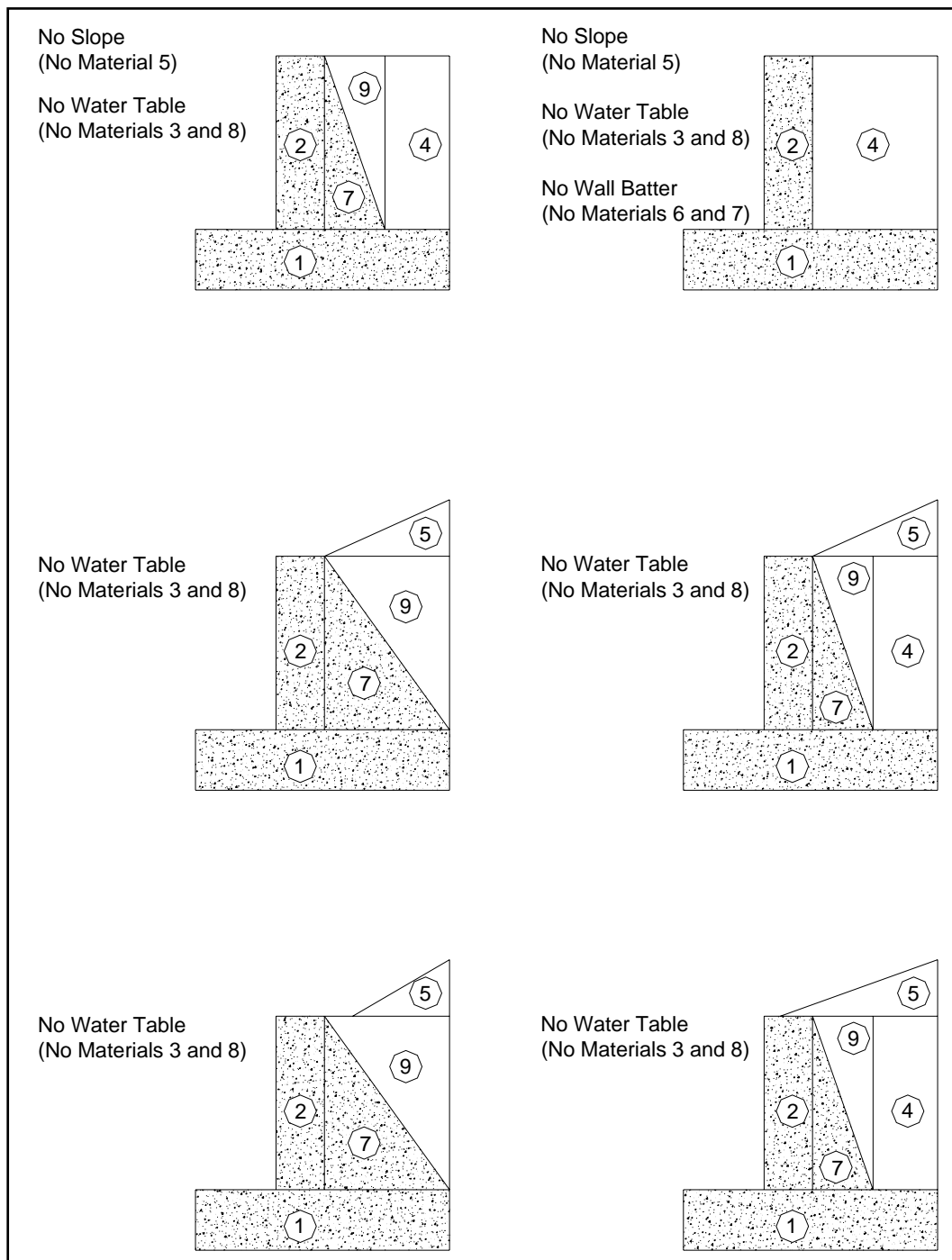
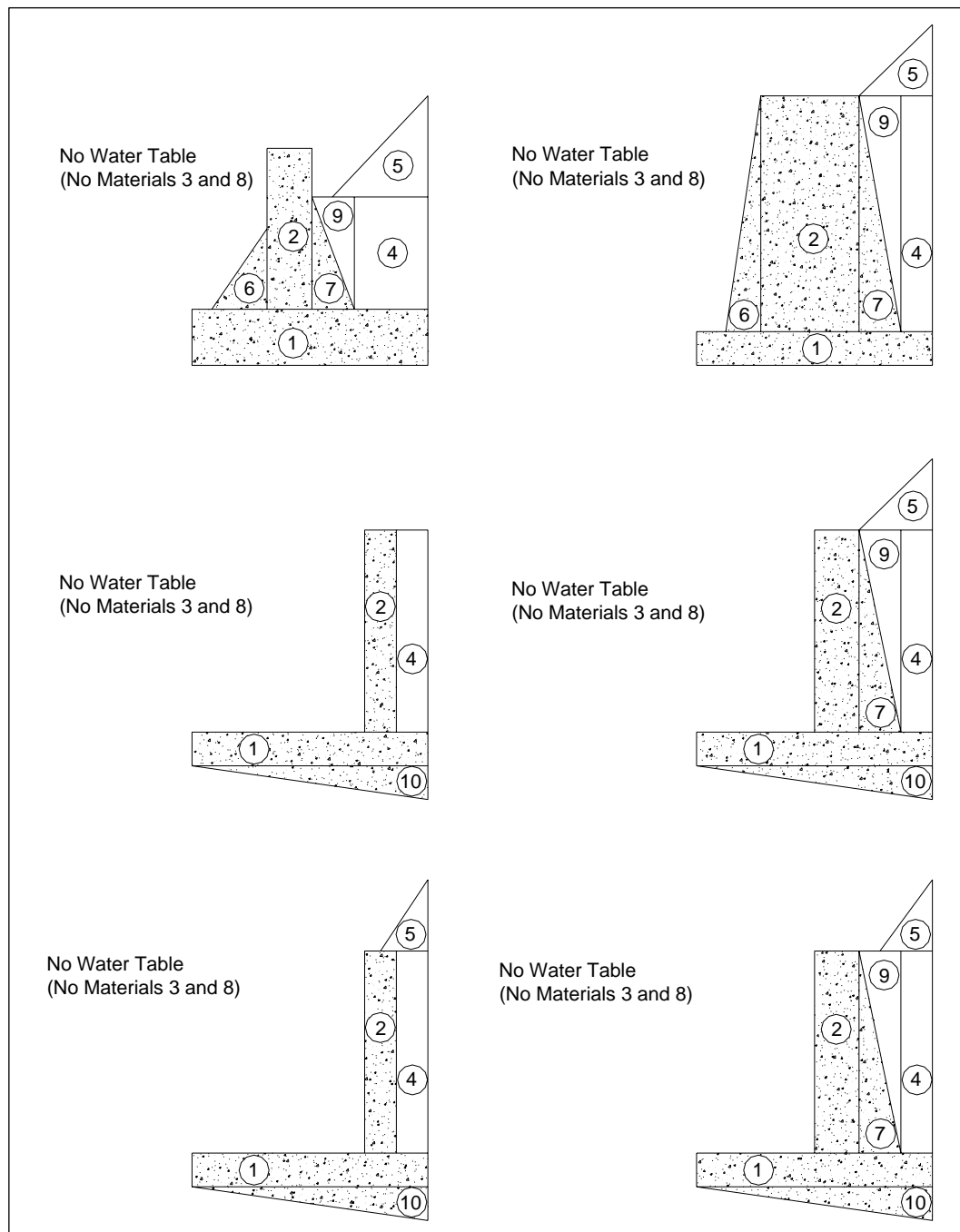


Figure 4.6. Examples of width and height definition for each of the ten structural wedge material regions.

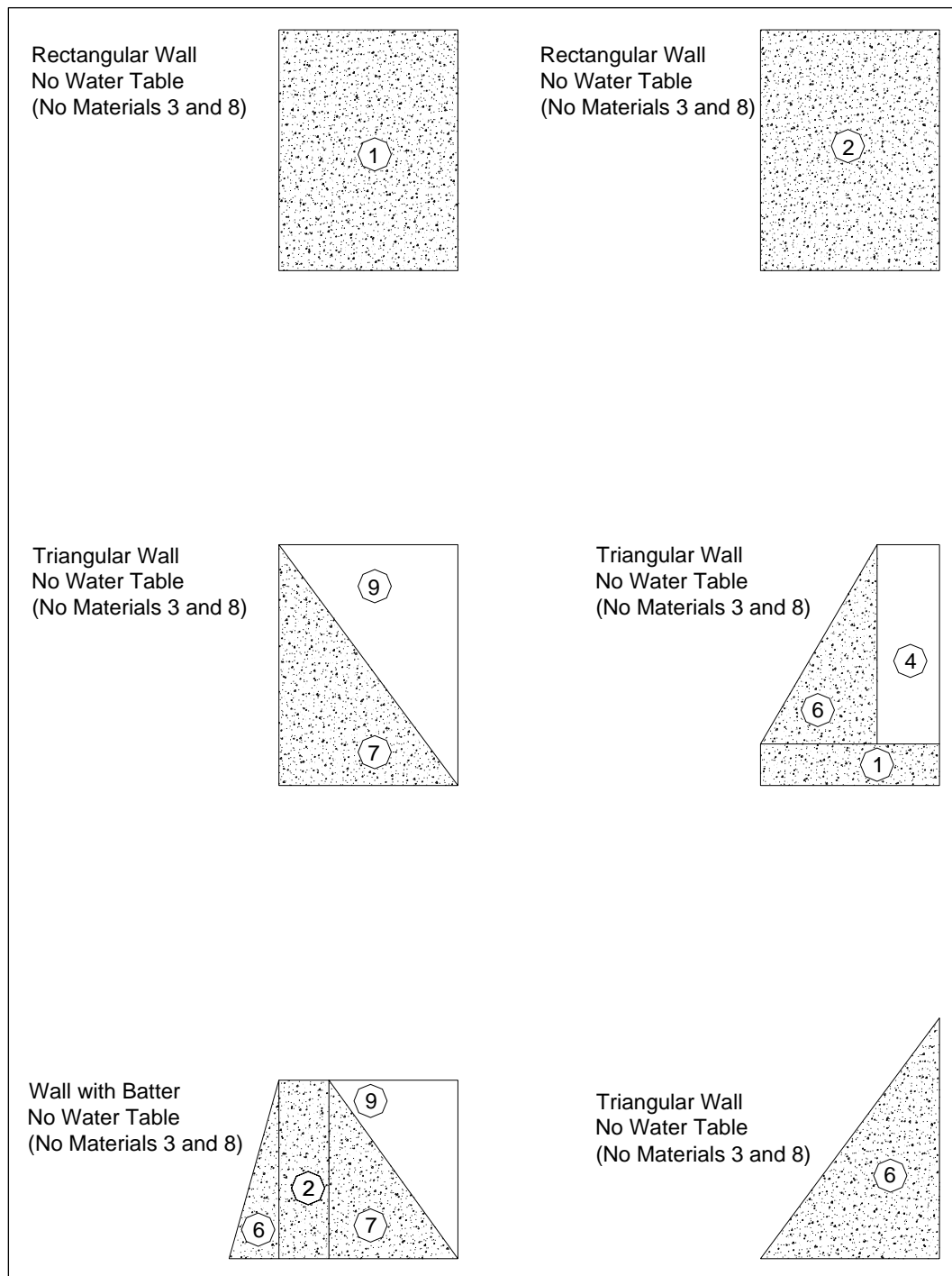


a. Moist backfill (Continued)

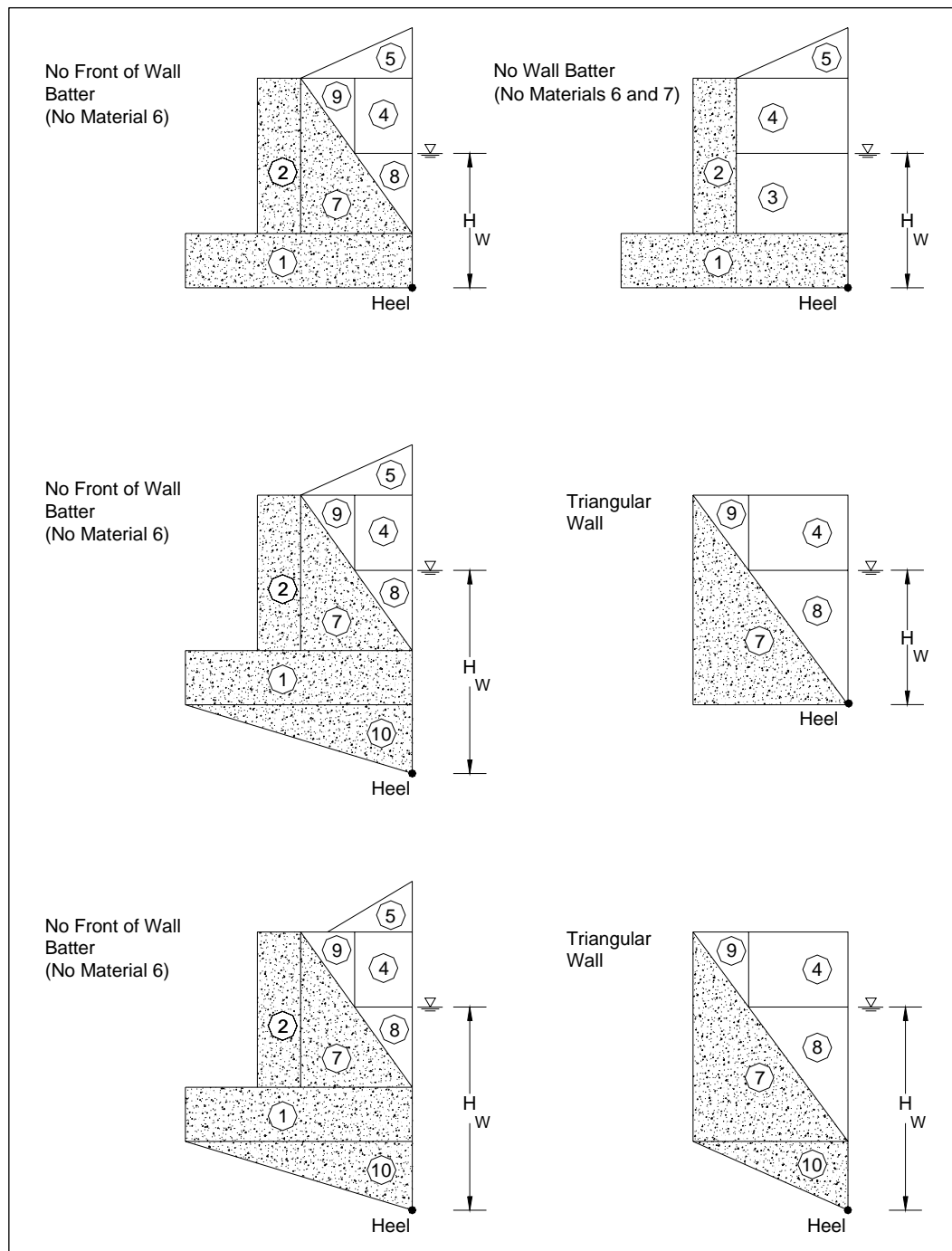
Figure 4.7. Examples of structural wedge material regions (Sheet 1 of 4).



a. Moist backfill (Continued)  
Figure 4.7. (Sheet 2 of 4).



a. Moist backfill (Concluded)  
Figure 4.7.(Sheet 3 of 4).



b. Partially submerged backfill.  
Figure 4.7. (Sheet 4 of 4).

Figure 4.7b shows the configurations possible if a water table is specified in the retained soil. Regions 3 and 8 are created when a table within the retained soil is higher than the concrete structure above the heel point.



The Figure 4.8 **Geometry** input tab is designed around this template scheme and provides a visual confirmation for the user. At the upper left of the tab, there is a region template that shows all of the regions that can possibly be used in CWSlip. Each region is color-coded to show which of the three materials it belongs to. The currently selected region (chosen in the **Region Information** box) is highlighted to show the user which geometry is being changed.

At the upper right of the tab is a drawing of the geometry as created by the user. Three data points are also displayed for the structure (*although overlapping points may hide others*). The toe point is the lower leftmost point of the wall and it is displayed in purple. All geometry is placed relative to this toe location. Its coordinate is entered in the **Toe Position** box, using the units specified in the **Units of Length** combo box. Since all data are relative to this point, changing the toe position will not change the input geometry plot.

Another point displayed on the input geometry plot is the rotation point for the threshold value of acceleration corresponding to incipient lift-off of the base of the wall in rotation computation, discussed in Chapter 3. In this initial version of CorpsWallSlip, the rotation point will be specified by default to be the same as the toe point and will hide the toe point dot in the input geometry plot. The rotation point, displayed in red, is the point at the base, coincident with the toe of the wall. It is the point about which the structural wedge will rotate. Note that the rotation point is restricted to the toe point in the **Rotation Point** data box display. *The boxes for the coordinate entries are gray, signifying a fixed value that the user may not change.*

The last point that is displayed on the input geometry plot is the center of gravity for the structural wedge, displayed in light green. The center of gravity is computed for the user, based on the geometry for the model and the material unit weights for each region of the geometry. The actual absolute coordinates of the center of gravity are displayed in the **Center of Gravity** box. *Because it is a computed value, its (coordinate) entry boxes are gray to designate that the user need not perform this tedious calculation.*

CWSlip - C:\Program Files\Microsoft Visual Studio\MyProjects\CWSlip\EX\_1\_14\_Sept\_06.CWS

File Analysis Type

Introduction Horz. Earthquake Time History Vert. Earthquake Time History Simplified Analysis **Geometry** Structural Wedge Driving Wedge Analysis

Order of Input

- 1) Concrete Regions
- 2) Water Table
- 3) Backfill

**Toe Position**

X:

Y:

**Pool (height above Toe)**

Surface:

Base:

**Backfill Water Table**

Height (above Heel):

**Region Information**

Current Region:

Width:

Height:

**Unit Weights - lb/ft<sup>3</sup>**

Concrete:

Moist:

Saturated:

Water:

**Rotation Point**

X:

Y:

**Center Of Gravity**

X:

Y:

**Resisting Force - lbs**

Height:

Force:

**Complete (Using Acc. Time History)**

Figure 4.8. The input **Geometry** tab in action.

There are four unit weights for the model. These unit weights are for concrete, moist soil, saturated soil, and water. They are user-specified input in the **Unit Weights** data box, using the units displayed in the title for the box.

The input geometry is input using the **Region Information** box. The user can select a region to edit, which will be highlighted in the region template plot, and then specify a width and height for that region. Any

other affected regions are adjusted to fit the new region and the results are displayed in the input geometry window.

Another way to change the geometry of the model is to specify the **Back-fill Water Table Height**. The water table height specifies the separation point between moist and saturated soil, in the input geometry (and in the driving wedge, discussed later). The water table height is specified relative to the heel of the model, defined as the lower rightmost point, possibly below the toe.

On the pool side, the water must be taken into account for rotation or sliding, too. The **Pool Base** height is set by the top of the buttressing, reinforced concrete toe slab, and is measured (vertically) from the toe. The **Pool Height** is also measured relative to the toe. These two heights define the total height of the pool for hydrodynamic water pressure calculations (see Appendix D).

The last bit of input data to be entered on the input **Geometry** tab is a force representing the buttressing action of the reinforced concrete slab acting on the vertical face extending upwards from the toe of the wall. This is a user-specified force, which acts horizontally at a user-specified height above the toe of the retaining wall. (Refer to Strom and Ebeling (2004) for a method to determine the magnitude of this force.) The relative height and magnitude are specified in the **Resisting Force** box, using the units in the title of the box. Its height is measured relative to the toe.

From the **Geometry** tab, a button click can let the user view the water pressures for the structural geometry, relative to the water heights (Figure 4.9). (Refer to Appendix D for a complete description of the assumptions made for water pressures in this initial version.) Another tab shows the computed data for the structural wedge (Figure 4.10). Tables showing the current input and computed values (center of gravity, moment about the rotation point, etc.) can be viewed, saved to a file, or printed. It is also possible to print a plot of the input data from this window.

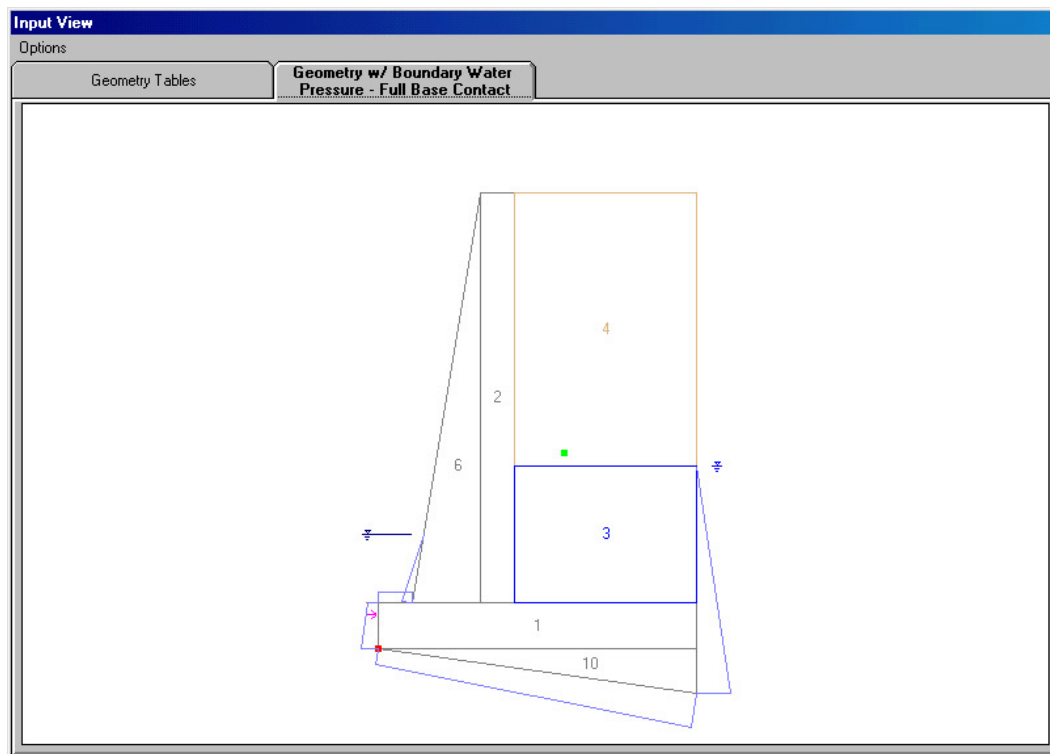


Figure 4.9. Boundary water pressure diagram – full contact along the base of the retaining wall with its foundation in a sliding block analysis.

Input View

Options

Geometry Tables

Geometry w/ Boundary Water Pressure - Full Base Contact

\*\*\*\*\* Region Information \*\*\*\*\*

#	Width	Height	Unit Weight	Area	Unit Mass	Total Mass
1	14.00	2.00	150.00	28.00	4.662	130.540
2	1.50	18.00	150.00	27.00	4.662	125.878
3	8.00	6.00	130.00	48.00	4.041	193.945
4	8.00	12.00	125.00	96.00	3.885	372.972
5	0.00	0.00	125.00	0.00	3.885	0.000
6	3.00	18.00	150.00	27.00	4.662	125.878
7	0.00	0.00	150.00	0.00	4.662	0.000
8	0.00	0.00	130.00	0.00	4.041	0.000
9	0.00	0.00	125.00	0.00	3.885	0.000
10	14.00	2.00	150.00	14.00	4.662	65.270

Distance from Center of Gravity to

#	Center of Gravity X	Center of Gravity Y	Rotation Point	Total Weight	Reference Point X	Reference Point Y
1	7.00	1.00	7.07	4200.00	0.00	0.00
2	5.25	11.00	12.19	4050.00	4.50	2.00
3	10.00	5.00	11.18	6240.00	6.00	2.00
4	10.00	14.00	17.20	12000.00	6.00	8.00
5	14.00	20.00	24.41	0.00	14.00	20.00
6	3.50	8.00	8.73	4050.00	1.50	2.00
7	6.00	2.00	6.32	0.00	6.00	2.00
8	6.00	2.00	6.32	0.00	6.00	2.00
9	6.00	2.00	6.32	0.00	6.00	2.00

Figure 4.10. Summary of the user-defined geometry and computed weight, mass, and moments of inertia for the structural wedge as defined in the **Geometry** tab.

#### 4.2.5 Structural wedge data

To simplify the computation of forces upon a wall, the model of the retaining system was split into two wedges: The structural wedge contains the retaining wall geometry, and the driving wedge to the right of the structure that “pushes” against the structural wedge.

From the **Structural Wedge** data tab, it is possible to enter the engineering material properties for the structural wedge. Soil strength can be entered using parameters associated with either the **Effective Stress** or **Total Stress** method of analysis, with either choice determining what is input. Consideration of seismically induced permanent deformations are part of the material property specification process. These data input tabs for the structural wedge are shown in Figures 4.11 and 4.12, respectively.

If **Effective Stress** method of analysis is chosen then the effective angle of internal friction and the effective cohesion need to be entered for both the foundation soil and the soil-to-concrete interface at the base of the retaining wall.

If **Total Stress** is chosen then the undrained shear strength is required for both foundation soil and the soil-to-concrete interface. The tab changes reflect the different input. Note that in a total stress analysis the friction angle (PHI) box does not accept user input and its value is internally set equal to zero by CWSlip.

The screenshot shows the CWSlip software window with the title bar "CWSlip - C:\Program Files\Microsoft Visual Studio\MyProjects\CWSlip\EX\_1\_14\_Sept\_06.CWS". The menu bar includes "File" and "Analysis Type". The main window has a tabbed interface with the following tabs: "Introduction", "Horz. Earthquake Time History", "Vert. Earthquake Time History", "Simplified Analysis", "Geometry", "Structural Wedge" (which is the active tab), "Driving Wedge", and "Analysis".

Inside the "Structural Wedge" tab, there are three main sections:

- Soil Strength:** Contains two radio buttons: "Effective Stress" (which is selected) and "Total Stress".
- Interface:** Contains two input fields:
  - "Effective PHI" with a value of "34.0" and the unit "degrees".
  - "Effective Cohesion C" with a value of "0.0" and the unit "lb/ft^2".
- Foundation:** Contains two input fields:
  - "Effective PHI" with a value of "32.0" and the unit "degrees".
  - "Effective Cohesion C" with a value of "2400.0" and the unit "lb/ft^2".

At the bottom of the window, there is a status bar that reads "Complete (Using Acc. Time History)".

Figure 4.11. Defining the material properties of the **Structural Wedge** tab for an effective stress analysis.

The screenshot shows the CWSlip software window with the title bar "CWSlip - C:\Program Files\Microsoft Visual Studio\MyProjects\CWSlip\EX\_1\_14\_Sept\_06.CWS". The menu bar includes "File", "Analysis", and "Type". The main window has a tabbed interface with the following tabs: "Introduction", "Horz. Earthquake Time History", "Vert. Earthquake Time History", "Simplified Analysis", "Geometry", "Structural Wedge" (which is the active tab), "Driving Wedge", and "Analysis".

Inside the "Structural Wedge" tab, there are three main sections:

- Soil Strength:** Contains two radio buttons. "Effective Stress" is unselected, and "Total Stress" is selected.
- Interface:** Contains two input fields:
  - "Effective PHI" with a value of "0.0" and the unit "degrees".
  - "Undrained Strength" with a value of "600.0" and the unit "lb/ft^2".
- Foundation:** Contains two input fields:
  - "Effective PHI" with a value of "0.0" and the unit "degrees".
  - "Undrained Strength" with a value of "1800.0" and the unit "lb/ft^2".

At the bottom of the window, there is a status bar that reads "Complete (Using Acc. Time History)".

Figure 4.12. Defining the material properties of the **Structural Wedge** tab for a total stress analysis.

#### 4.2.6 Driving wedge data

Modeled after the input to the PC-based program EQWedge (developed by the primary author of this report), the driving wedge data allow the input of engineering data for determining the force imposed by the driving wedge on the structural wedge. The sweep-search wedge formulation is used to compute this force, as discussed in Appendix A. Some structural wedge geometry data are also displayed on this tab as a reminder for the user.

Once again, the method for determining the soil strength determines the data that are input for the driving wedge soil properties. If **Effective Stress** is chosen then the effective angle of internal friction and the effective cohesion need to be entered for the retained soil of the driving wedge (Figure 4.13). (The effective angle of interface friction is also specified.) Otherwise, if **Total Stress** is chosen then only the undrained shear strength is required for the retained soil of the driving wedge (Figure 4.14). The tab changes to reflect the different input. All other inputs for this tab stay the same.

The value entered for **Delta** is the effective angle of interface friction between the driving wedge and the structural geometry. This interface is the imaginary vertical section that extends upwards from the heel of the wall and delineates the driving wedge from the structural wedge.

The height of the vertical section is determined from the structural wedge geometry. It is provided to give the user knowledge of the length of the vertical interface between the structural wedge geometry and the driving wedge.

The height to level backfill and backfill slope entries define the shape of the driving wedge. It is assumed that the retained soil geometry is as high or higher than the structural wedge geometry, as defined by the height to level backfill. If the retained soil is higher than the structural geometry, then a slope must be specified for the backfill, until it reaches the level backfill limit.

The next three values shown are the moist unit weight, the saturated unit weight, and the hydrostatic water table. These values were all entered in the structural wedge **Geometry** tab, and are provided here as a reminder.



CWSlip - C:\Program Files\Microsoft Visual Studio\MyProjects\CWSlip\EX\_1\_14\_Sept\_06.CWS

File Analysis Type

Introduction Horiz. Earthquake Time History Vert. Earthquake Time History Simplified Analysis Geometry Structural Wedge **Driving Wedge** Analysis

Soil Strength  
☒ Effective Stress  
☐ Total Stress

Input Values

Effective PHI 35.0 degrees

Effective Cohesion C 0.0 lb/ft<sup>2</sup>

Delta 0.0 degrees

Height of Vertical Section 22.0 (from Heel)

Height to Level Backfill 24.0 (from Heel)

Backfill Slope 10.0 degrees

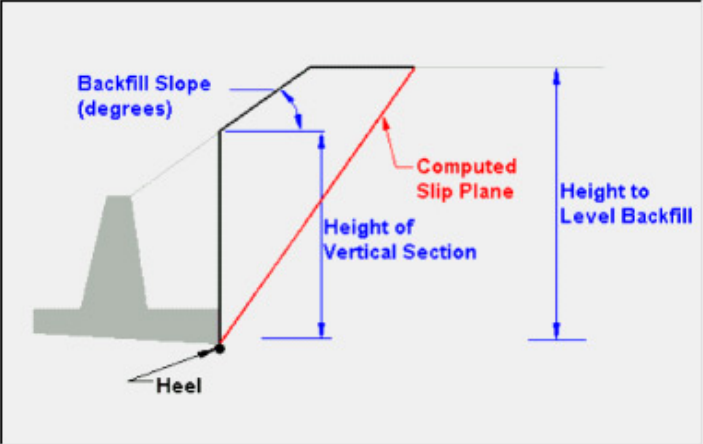
Moist Unit Weight 125.0 lb/ft<sup>3</sup>

Saturated Unit Weight 130.0 lb/ft<sup>3</sup>

Hydrostatic Water Table 10.0 (from Heel)

ru 0.0

Min. angle for slip plane 3.0 degrees (from horizontal)



Backfill Slope (degrees)

Computed Slip Plane

Height of Vertical Section

Height to Level Backfill

Heel

Complete (Using Acc. Time History)

Figure 4.13. Defining the material properties in the **Driving Wedge** tab - effective stress method of analysis.

CWSlip - C:\Program Files\Microsoft Visual Studio\MyProjects\CWSlip\EX\_1\_14\_Sept\_06.CWS

File Analysis Type

Introduction Horz. Earthquake Time History Vert. Earthquake Time History Simplified Analysis Geometry Structural Wedge **Driving Wedge** Analysis

Soil Strength  
☐ Effective Stress  
☒ Total Stress

Input Values

Effective PHI  degrees

Undrained Strength  lb/ft<sup>2</sup>

Delta  degrees

Height of Vertical Section  (from Heel)

Height to Level Backfill  (from Heel)

Backfill Slope  degrees

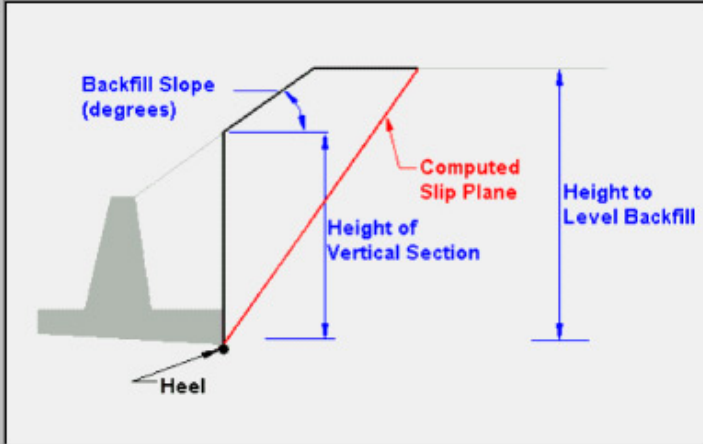
Moist Unit Weight  lb/ft<sup>3</sup>

Saturated Unit Weight  lb/ft<sup>3</sup>

Hydrostatic Water Table  (from Heel)

$r_u$

Min. angle for slip plane  degrees (from horizontal)



Complete (Using Acc. Time History)

Figure 4.14. Defining the material properties in the **Driving Wedge** tab - total stress method of analysis.

The next value,  $r_u$ , is the excess pore water pressure ratio due to earthquake shaking in an effective stress analysis. It is disabled in this program (at this time). However, provisions are made to add this option to CWSlip in the future.

The final value for entry is the minimum angle for the slip plane. Using a sweep-search method of analysis, CWSlip will evaluate all potential slip

planes in 1-degree increments, between the user-provided **Min. angle for slip plane** value (in degrees) and 89 degrees, from horizontal. If a maximum thrust force is not found (refer to insert figure to Figure A.1) then the driving wedge defined by the user-provided minimum angle for slip plane is used to compute the thrust force acting on the structural wedge. A low value for this angle is typically specified by the primary author of this report (e.g., on the order of 5 degrees or so) unless there are geometrical constraints.

#### 4.2.7 Analysis results and visual post-processor

The Figure 4.15 **Analysis** tab is broken into three sections: **Input Parameters**, **Run CWSlip Analyzer**, **View Output**. The Input Parameters section allows the user to enter last-minute analysis options. The Run CWSlip Analyzer section is a button to execute the program. The View Output section contains options for viewing the many outputs of the CWSlip Analysis, including an option to view the total rotation and/or slide of the structure.

Immediately prior to execution of CWSlip it is a good idea to create a restart file containing all the input information. This is accomplished by using the file drop down menu and the save option. The file created has a “CWS” extension. This file may be read in by CWSlip using this same file drop down menu and populate the data contained within all tabs at a later point in time.

After the **Run CWSlip Analyzer** button is activated, a CWRotate.IN ASCII data input file, described in Appendix F, is created by the Visual Modeler and the FORTRAN engineering program is executed.<sup>1</sup> This FORTRAN engineering program creates the output and plot data files that are used in the Figure 4.15 **Visual Output** frame of the **Analysis** tab. Appendix G lists and summarizes the contents of these output and plot data files.

---

<sup>1</sup> The FORTRAN code of CorpsWallSlip evolved from CorpsWallRotate (Ebeling and White (2006)). Both formulations share many engineering computations. In order to facilitate the maintenance of both engineering formulations and corresponding software, the same FORTRAN code is used with the two visual modelers and post-processors.

Figure 4.15. The **Analysis** tab.

In the **Input Parameters** frame allows for the user to select/specify the following four pieces of information:

1. **Vertical Time-History Usage** combo box for the complete time-history analysis:
  - Determine representative constant value
  - Evaluate with representative constant value
  - Evaluate with current time-history

And for the simplified sliding block analysis:

- Evaluate with representative constant value
2. **Constant Y Acceleration** data box.
  3. **Analysis Type** combo box is set to:
    - Sliding Analysis
  4. **Output Units combo** box.

***Complete time-history analysis:*** Input Parameters selection is best described by the following staged seismic evaluation approach: The first step in the process is to determine if the user-specified retaining wall will slide or rotate during shaking when subjected to the Corps Project Design Earthquake:

1. Select **Vertical Time-History Usage: Determine a representative constant value** for the vertical time-history (which will be a trial-and-error, iterative process). In the first iteration specify a **Constant Y Acceleration** set equal to zero. Select **Run CWSlip Analyzer** and view the results to determine the average and the weighted vertical acceleration during sliding (definitions given in Section 2.6), as reported by the **Show Sliding Evaluation** button (or, equivalently, in the WORKslide.TMP ASCII output file). Perform a second CWSlip analysis using an updated **Constant Y Acceleration** value based on this vertical acceleration information. Repeat the analysis until conversion is achieved. Read the updated value for the maximum transmissible acceleration and the updated value for the incipient lift-off in rotation acceleration as reported by the **Show Lift-Off Evaluation** button (or, equivalently, in the WORKrotate.TMP ASCII output file). Note that both analyses are using the same **Constant Y Acceleration** values in their respective computations. The smaller of the two horizontal acceleration constants dictates if the wall will slide or rotate for the given wall geometry, soil shear strengths, and ground motions.
2. If the values for the maximum transmissible acceleration and the value for the incipient lift-off in rotation acceleration are close, it may be worthwhile to perform a second series of rotating block analyses to determine a more accurate value for the **Constant Y Acceleration** that is consistent with the acceleration pulses generating wall rotation for the lift-off evaluation process, rather than using the value determined by using the results based on a sliding block evaluation process. This type of refined rotational

analysis may only be accomplished using the PC-based software CWRotate of Ebeling and White (2006).

If the wall will slide before it will rotate, then for the sliding block analysis using the final **Constant Y Acceleration** value (determined during the sliding pulses<sup>1</sup>), continue viewing the results of the Newmark time-history analysis as reported in the figure(s) activated by the **Plot Sliding Time-History** button. **Show Sliding Evaluation** button (or, equivalently, in the WORKslide.TMP ASCII output file) also reports the value for the cumulative (permanent) horizontal relative wall displacement. Forces acting on the structural wedge are reported in this same data output box and file.

If the wall rotates before it slides, then a second permanent wall rotation analysis using CWRotate is required and the computed CWSlip analysis results of both forces and permanent displacement are not valid.

***Simplified sliding block analysis:*** Input Parameters selection is as follows: The first step in the process is to determine if the user-specified retaining wall will slide or rotate during shaking when subjected to the Corps project design earthquake:

1. Specify a **Constant Y Acceleration**. (In a simplified sliding block analysis, the user will have limited information. The primary author of this report recommends a value that is less than the value for the peak vertical ground acceleration. Select **Run CWSlip Analyzer** and view the results during sliding (definitions given in Section 2.7), as reported by the **Show Sliding Evaluation** button (or, equivalently, in the WORKslide.TMP ASCII output file). Read the value for the maximum transmissible acceleration and the value for the incipient lift-off in rotation acceleration as reported by the **Show Lift-Off Evaluation** button (or, equivalently, in the WORKrotate.TMP ASCII output file). Note that both analyses are using the same **Constant Y Acceleration** values in their respective computations. The smaller of the two horizontal acceleration constants dictates if the wall will slide or rotate for the given wall geometry, soil shear strengths, and ground motions.

---

<sup>1</sup> Based on Input Parameter selection for the **Analysis** tab of a **Sliding Analysis Type** and **Vertical Time History Usage: Determine a representative constant value** or with **Evaluate with representative constant value**.

If the wall will slide before it will rotate, then for the simplified sliding block analysis using the **Constant Y Acceleration** value, continue viewing the results of the simplified (Newmark) sliding block analysis as reported in the figure activated by the **Show Sliding Evaluation** button (or, equivalently, in the WORKslide.TMP ASCII output file) which reports the computed value(s) for the cumulative (permanent) horizontal relative wall displacement for each of the eight user-selected methods of analysis. Forces acting on the structural wedge are reported in this same data output box and file.

If the wall rotates before it slides, then a second permanent wall rotation analysis using CWRotate is required and the computed CWSlip analysis results of both forces and permanent displacement are not valid. Note that an acceleration time-history for the design ground motion is required for a CWRotate analysis.

The three examples discussed in the following two subsections demonstrate this process.

#### **4.2.8 Example 1 – Earth retaining wall at a dry soil site – No reinforced concrete slab buttress at the wall's toe**

In this first example consider the case of the seismic stability evaluation of the Figure 4.16 reinforced concrete earth retaining structure. No buttressing toe slab exists in this evaluation. This 22-ft high earth retaining structure retains moist cohesionless soil, a dense sand, and is founded on rock. During construction, a thin layer of dense sand was used to level the top of rock before pouring the base of the reinforced concrete retaining wall. It is assumed that this Corps project is sited in a high seismic region on the West coast and situated in close proximity to an active fault that dominates the ground motion hazard. The horizontal and vertical strong ground motion component time-histories were taken from a District project and possess scaled horizontal and vertical acceleration time-histories with positive/negative peak values of 0.96g/-0.82g and 0.68g/-0.96g, respectively. Both acceleration time-histories are baseline corrected. The polarity of ground motions was not retained during their development.

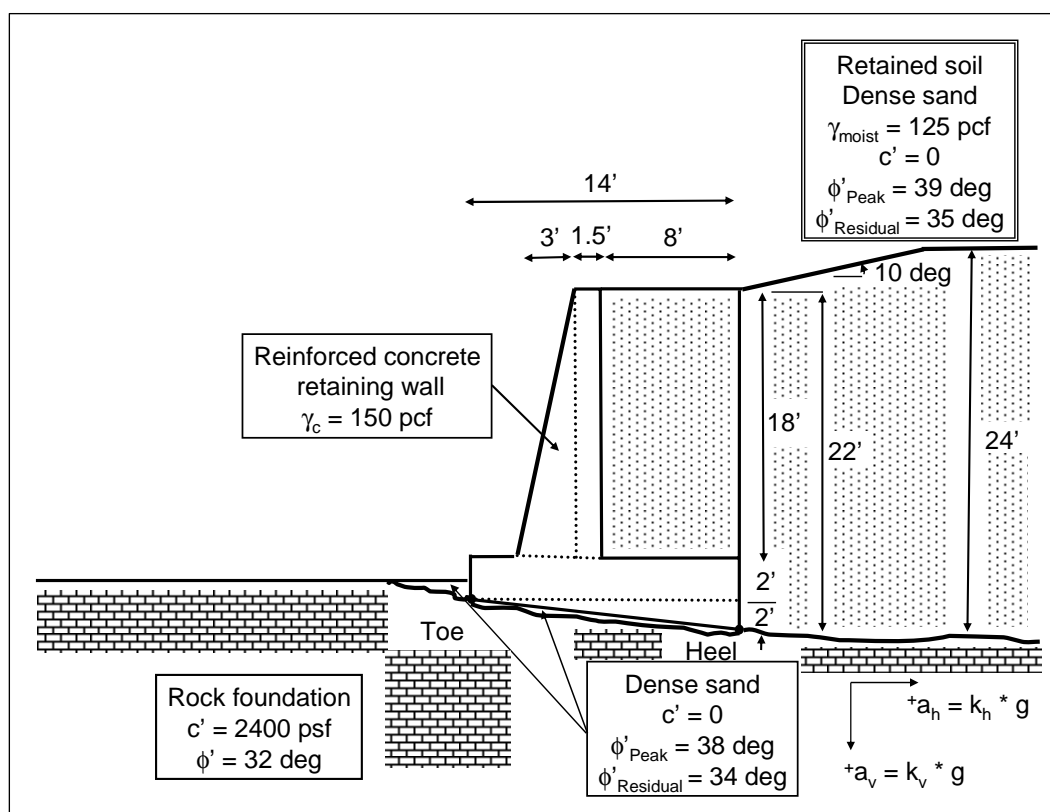


Figure 4.16. Rock-founded earth retaining wall for Example 1.

Figure 4.17 shows the input **Geometry** tab data for this problem. Material region numbers 1, 2, 4, 6, and 10 are used to define the geometry of the structural wedge. Note a resisting force at the toe of the wall is set equal to zero since a reinforced concrete buttress slab is not present.

A minimum angle for slip plane of 3 degrees from horizontal is specified in the **Driving Wedge** tab (not shown). Additionally, residual shear strength parameter values of  $\phi' = 35$  degrees and  $\phi' = 34$  degrees are specified for the retained soil and the cohesionless soil immediately in contact with the base of the structural wedge, respectively.

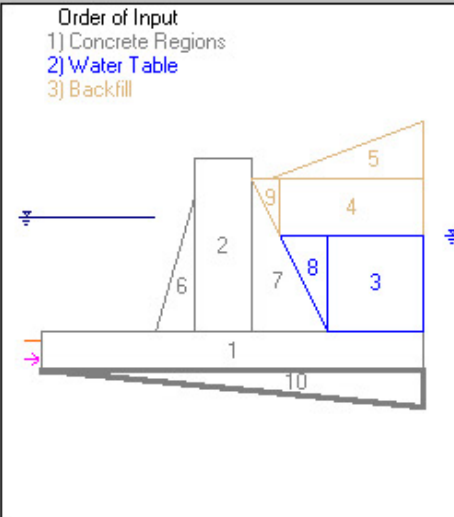
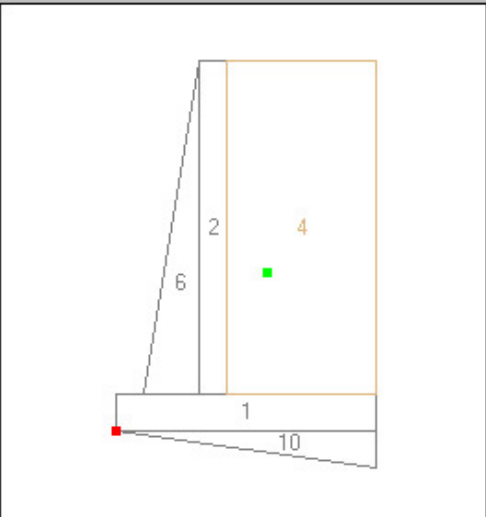


CWSlip - C:\Program Files\Microsoft Visual Studio\MyProjects\CWSlip\EX\_1\_14\_Sept\_06.CWS

File Analysis Type

Introduction Horz. Earthquake Time History Vert. Earthquake Time History Simplified Analysis **Geometry** Structural Wedge Driving Wedge Analysis

Order of Input  
 1) Concrete Regions  
 2) Water Table  
 3) Backfill

Toe Position  
 X: 0  
 Y: 0

Pool (height above Toe)  
 Surface: 0  
 Base: 0

Backfill Water Table  
 Height (above Heel): 0

Region Information  
 Current Region: Region 10  
 Width: 14  
 Height: 2

Unit Weights - lb/ft<sup>3</sup>  
 Concrete: 150  
 Moist: 125  
 Saturated: 130  
 Water: 62.4

View Water Pressures

Rotation Point  
 X: 0  
 Y: 0

Center Of Gravity  
 X: 8.161651234567  
 Y: 8.572530864197

ft

Resisting Force - lbs  
 Height: 0  
 Force: 0

Complete (Using Acc. Time History)

Figure 4.17. Data contained within the input **Geometry** tab for Example 1.

The first step in the CWSlip analysis is to determine if the Figure 4.16 retaining wall will slide or rotate during shaking when subjected to the District's Project Evaluation Earthquake. For a **Sliding Analysis Type** select **Determine a representative constant value** for the **Vertical Time-History Usage** (which will be a trial-and-error, iterative process).

Table 4.1 summarizes the computed results from this two-iteration process. In the first iteration, a **Constant Y Acceleration** is set equal to zero. The program is executed via select **Run CWSlip Analyzer** button and the results used to determine the average and the weighted vertical acceleration during sliding (definitions given in Section 2.6), are viewed by the **Show Sliding Evaluation** button (or, equivalently, in the WORKslide.TMP ASCII output file). Based on the computed average and weighted vertical acceleration values, a second CWSlip **Analysis** is conducted using a **Constant Y Acceleration** set equal to 0.01g. Figure 4.18 shows the **Analysis** tab input and settings for this computation. This second iteration/Newmark sliding block computation is made with **Constant Y Acceleration** set equal to a constant 0.01 g. Conversion is achieved in this computation as demonstrated in the tabulated values. The bottom figure in Figure 4.19 shows the magnitude of vertical acceleration for each time-step during which sliding occurs (specifically, the average acceleration during each time increment of sliding) for this second Newmark sliding block analysis (activated by the **Plot Effective Vertical Acc.** button). The Table 4.1 average and weighted vertical acceleration values are computed using the Section 2.6 Equations 2.74 and 2.76, respectively. Note that even though the peak positive/negative vertical accelerations are 0.68g/-0.96 g, respectively, for the time-history figure second from the top in Figure 4.19, these peak values are not concurrent with the times of sliding. The vertical accelerations that occur during sliding are far lower in magnitude and are labeled effective vertical accelerations (that occur during sliding) in this bottom figure. In this manner, a vertical acceleration time-history possessing peak positive/negative vertical accelerations of 0.68g/-0.96 g, respectively, becomes a **Constant Y Acceleration** of (positive) 0.01 g for the sliding analysis.

Table 4.1. Assessment of **Constant Y Acceleration**, the effective vertical acceleration for Example 1.

Iteration No.	User-Specified Acceleration (kcg) <sub>v</sub> *g	Average Vertical Acceleration (kcg) <sub>v-ave</sub> *g	Weighted Vertical Acceleration (kcg) <sub>v-weighted</sub> *g	Maximum Transmissible Acceleration
1	0	0.0124g	0.0121g	0.35g
2	0.01g	0.0128g	0.0136g	0.34g

Figure 4.18. The final **Analysis** tab for Example 1.

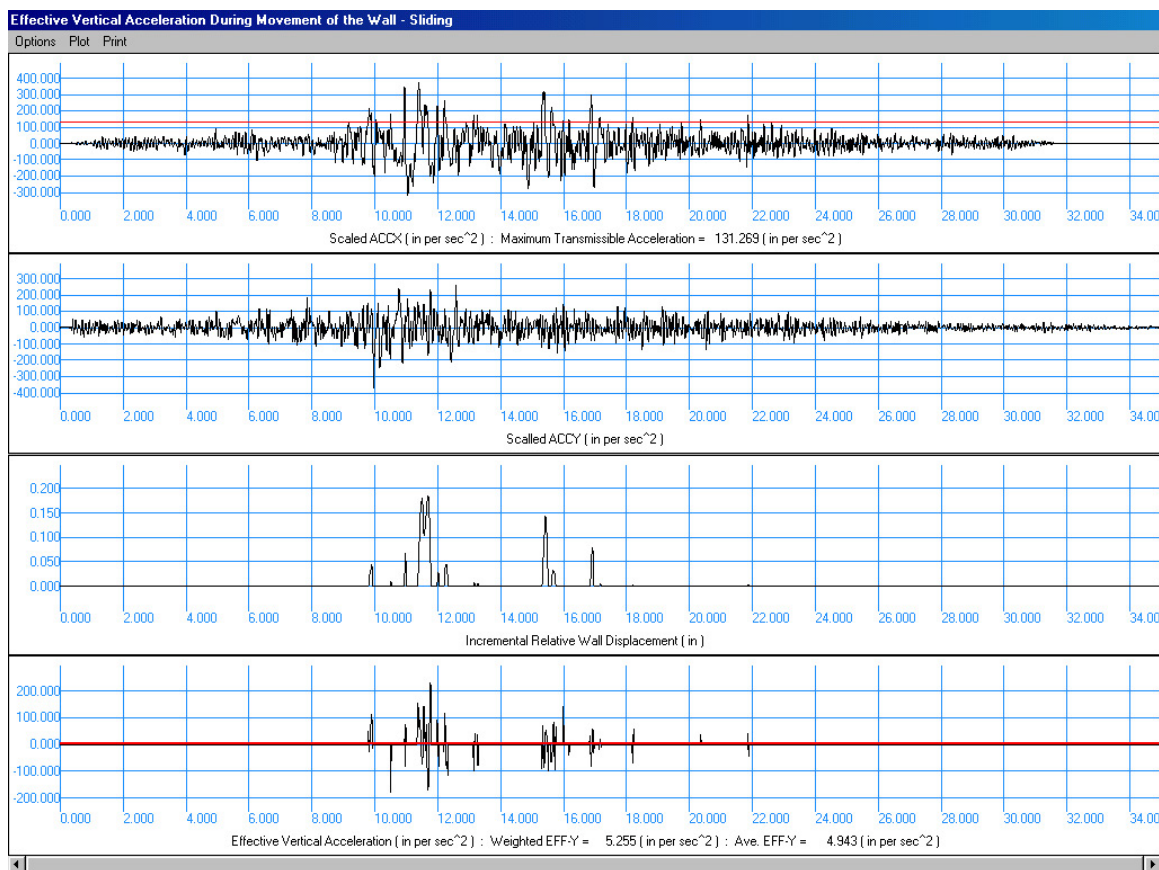


Figure 4.19. Time-history of the evaluation of the effective vertical acceleration.

The computed value for the (horizontal) maximum transmissible acceleration is equal to 0.34 g (reported by the **Show Sliding Evaluation** button or, equivalently, in the WORKslide.TMP ASCII output file). For the incipient lift-off in rotation the computed horizontal acceleration is computed to be 0.37 g (reported by the **Show Lift-Off Evaluation** button or, equivalently, in the WORKrotate.TMP ASCII output file). These computations are also made with a **Constant Y Acceleration** of 0.01 g. (It is reasoned that those horizontal acceleration pulses during which sliding occurs will also dominate the pulses during which rotation will occur.) Since the maximum transmissible acceleration is the smaller of the two horizontal acceleration constants, the wall will slide during earthquake shaking (for

the given wall geometry, soil shear strengths, and ground motions used in this particular analysis).<sup>1</sup>

Since the Figure 4.16 retaining wall will slide before it will rotate, then continue viewing the results for the Newmark time-history permanent deformation analysis results, which for this problem is shown in Figure 4.20. This figure is seen by activating the Plot **Sliding Time History** button on the **Analysis** tab. (Note that the **Show Sliding Evaluation** button (or, equivalently, in the WORKslide.TMP ASCII output file) also reports the value for the cumulative (permanent) horizontal relative wall displacement). The upper figure is a plot of the horizontal acceleration time-history and the red line designates the maximum transmissible acceleration value of 0.34 g. Wall displacements start to occur the first time the acceleration trace plots above this red line. Observe that permanent wall translation starts at about 10 sec after initial shaking and concludes by about 17 sec out of a total of 35 sec of ground shaking. The cumulative permanent displacement is about 9 in., which occurs over about six significant relative (wall) velocity and displacement pulses (refer to the second and third figure down from the top, respectively). During sliding the maximum inertial force imparted to the structural wedge and to the driving soil wedge (and to  $P_{AE}$ ) is due to a horizontal acceleration of 0.34 g, the value for the maximum transmissible acceleration (with a constant vertical acceleration of 0.01 g). Forces acting on the structural wedge are reported by the **Show Sliding Evaluation** button (or, equivalently, in the WORKslide.TMP ASCII output file). By allowing the retaining wall to slide, the retaining wall structural wedge and soil wedge are not subjected to inertia forces due to the higher accelerations values, i.e., up to 0.96 g of horizontal acceleration. Thus, allowing the wall to slide during earthquake shaking provides for lower design forces than would otherwise occur should translational wall movements have been constrained.

---

<sup>1</sup> For completeness, a separate analysis to determine a value for the **Constant Y Acceleration** that is consistent with the acceleration pulses generating wall rotation for the lift-off evaluation process was also conducted using CWRotate and reported in Example 1, Section 5.2.7 of Ebeling and White (2006). After iteration, the CWRotate-computed results were the same as for the sliding block based analyses; a **Constant Y Acceleration** value of 0.01g (after iteration) with the horizontal acceleration for incipient lift-off in rotation computed to be 0.37g. It is reasoned that those horizontal acceleration pulses during which sliding occurs will also dominate the pulses during which rotation will occur.

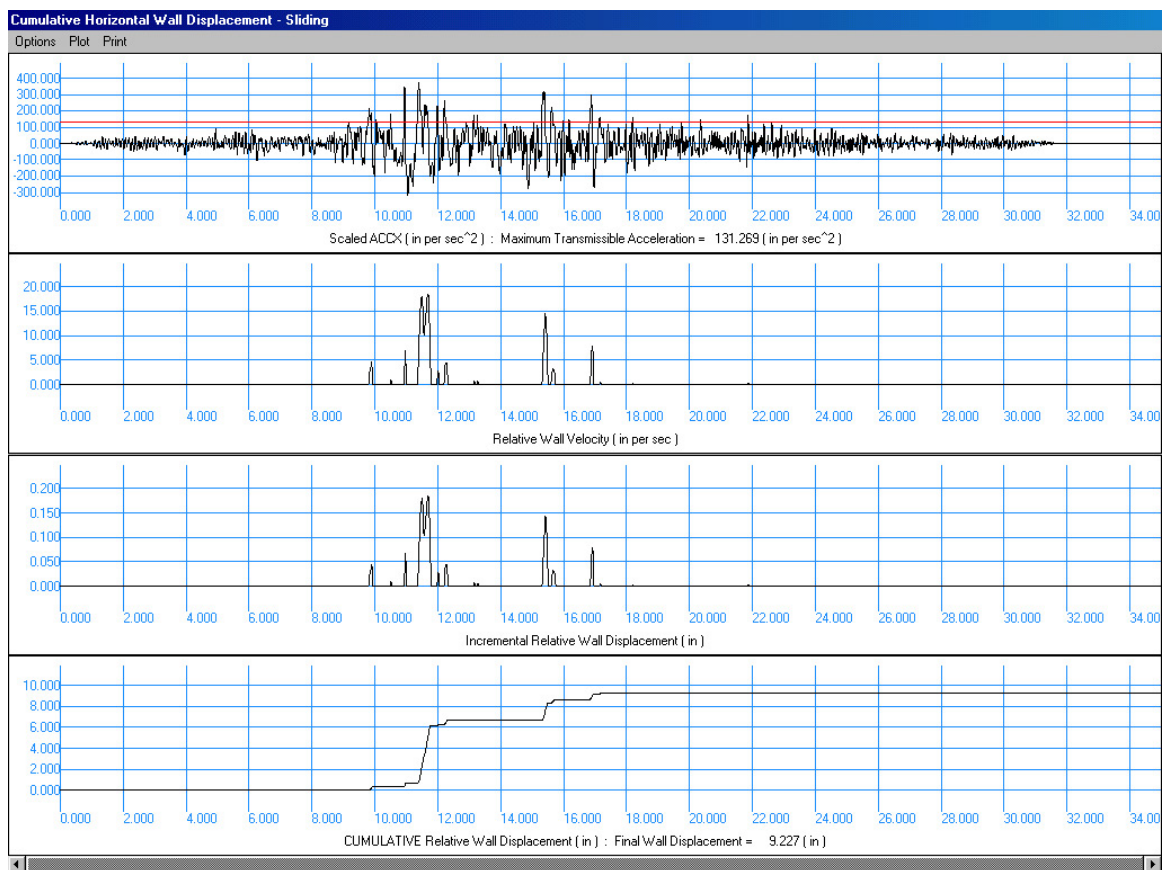


Figure 4.20. Newmark sliding block time-history results for Example 1.

Selected output for the driving soil wedge forces and pressures acting on the structural wedge during sliding are as follows:

```
*****
**** Earth Pressure Forces ****
*****
```

```
PAEqSLIDE =      17817.83 lbs
ALPHAESLIDE = 43.00 degrees
HPAEqSLIDE =   10.23 ft
DCaeSLIDE =    0.00 ft
```

```
=====
Pressure Distributions acting at an angle  0.00 degrees
from normal to the vertical plane through the heel
=====
```

Height above Heel (ft)	Static (lb/ft <sup>2</sup> )	Incremental EQ (lb/ft <sup>2</sup> )	Total EQ (lb/ft <sup>2</sup> )
=====	=====	=====	=====
22.00	0.00	638.30	638.30
3.54	691.52	236.55	928.07
0.00	811.06	159.57	970.64

For a dense sand, the Table 1.1 guidelines indicate that for a 22-ft-high section, active earth pressures may be used in the analysis if wall movements exceed  $\frac{1}{4}$  in. ( $= 0.001$  times 22 ft times 12 in./ft). With predicted wall movements on the order of 9 in., the use of active earth pressures in the dynamic time-history permanent displacement calculations is deemed appropriate.

Since the polarity of ground motions was not retained in their development, this analysis would be repeated three more times with the user reversing the polarity of the horizontal and vertical input ground motions to determine the most critical results.

Using the forces provided in the output file<sup>1</sup>, the user is advised to determine if the bearing capacity of the foundation is adequate.

<sup>1</sup> Appendix G summarizes the contents of the output files.

#### 4.2.9 Example 2 – Earth retaining wall at a dry soil site – 1-foot-thick reinforced concrete slab buttress at the wall's toe

Consider the case of the Figure 4.16 earth retaining structure buttressed by a 1-foot thick reinforced concrete slab as shown in Figure 4.21. As was the case in Example 1, the 22-ft-high earth retaining structure retains moist cohesionless soil, a dense sand, and is founded on rock. During construction, a thin layer of dense sand was used to level the top of rock before pouring the base of the reinforced concrete retaining wall. It is assumed that this Corps project is sited in a high seismic region on the West coast and situated in close proximity to an active fault that dominates the ground motion hazard. The same pair of ground motions are used in both examples: The horizontal and vertical strong ground motion component time-histories were taken from a District project and possess scaled horizontal and vertical acceleration time-histories with positive/negative peak values of 0.96 g/-0.82 g and 0.68 g/-0.96 g, respectively. Both acceleration time-histories are baseline corrected. The polarity of ground motions was not retained during their development.

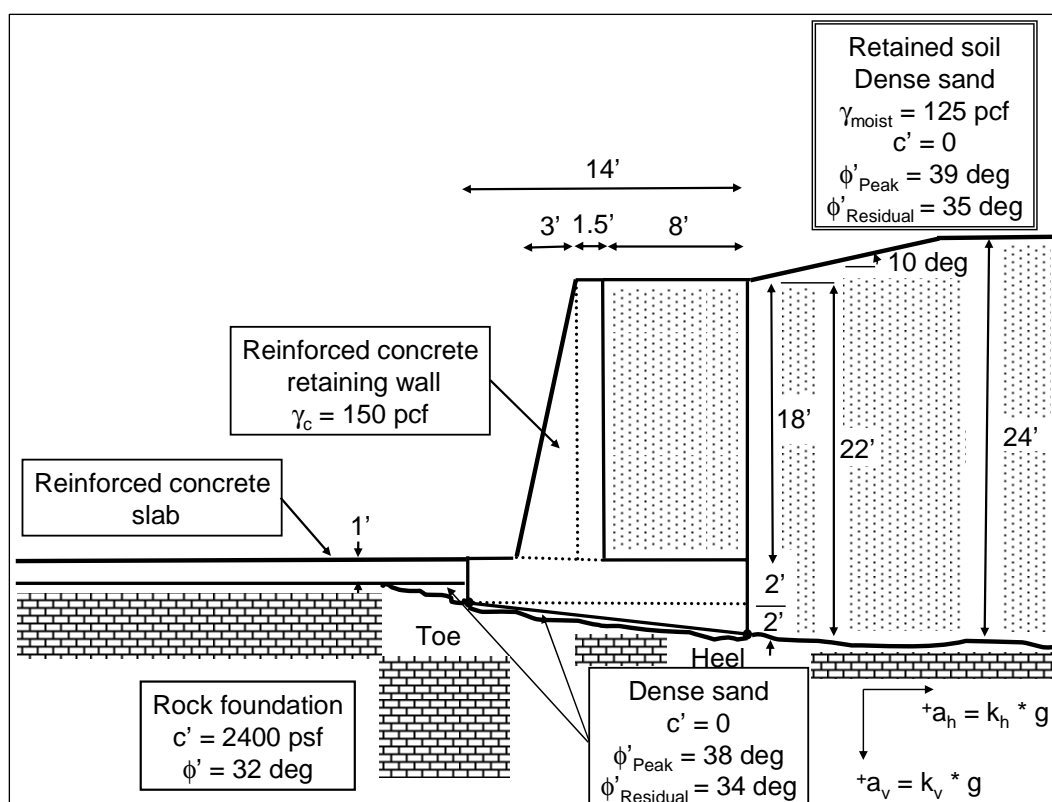


Figure 4.21. Rock-founded earth retaining wall buttressed at the toe of the wall by a 1-ft thick reinforced concrete slab for Example 2.



The input **Geometry** tab data for this simplified peak acceleration values analysis problem is the same as shown in Figure 4.22. Material region numbers 1, 2, 4, 6, and 10 are used to define the geometry of the structural wedge. Note that a 120 kip per ft run of wall resisting force is specified at the toe of the wall and acts at height of 1.5 ft above the toe. Its magnitude is determined using the procedure outlined in Strom and Ebeling (2004).

CWSlip - C:\CWSlip\EX\_1\_14\_Sept\_06.CWS

File Analysis Type

Introduction Horz. Earthquake Time History Vert. Earthquake Time History Simplified Analysis **Geometry** Structural Wedge Driving Wedge Analysis

Order of Input  
1) Concrete Regions  
2) Water Table  
3) Backfill

**Toe Position**  
X: 0  
Y: 0

**Pool (height above Toe)**  
Surface: 0  
Base: 0

**Backfill Water Table**  
Height (above Heel): 0

**Region Information**  
Current Region: Region 4  
Width: 8  
Height: 18

**Unit Weights - lb/ft<sup>3</sup>**  
Concrete: 150  
Moist: 125  
Saturated: 130  
Water: 62.4

**Rotation Point**  
X: 0  
Y: 0

**Center Of Gravity**  
X: 8.1616512345679  
Y: 8.57253086419753

**Resisting Force - lbs**  
Height: 1.5  
Force: 120000

View Water Pressures

Complete (Using Acc. Time History)

Figure 4.22. The input **Geometry** tab for Example 2.

A minimum angle for slip plane of 3 degrees from horizontal is specified in the **Driving Wedge** tab (not shown). Additionally, residual shear strength parameter values of  $\phi' = 35$  degrees and  $\phi' = 34$  degrees are specified for the retained soil and the cohesionless soil immediately in contact with the base of the structural wedge, respectively.

The first step in the CWSlip analysis is to determine if the Figure 4.21 retaining wall will slide or rotate during shaking when subjected to the District's Project Evaluation Earthquake. For a **Sliding Analysis Type** select **Determine a representative constant value** for the **Vertical Time History Usage** (which will be a trial-and-error, iterative process). Table 4.2 summarizes the computed results from this three-iteration process. In the first iteration, the value for **Constant Y Acceleration** is set equal to zero. The program is executed via the **Run CWSlip Analyzer** button and the results are used to determine the average and the weighted vertical acceleration during sliding (definitions given in Section 2.6). These results are observed by activating the **Show Sliding Evaluation** button (or, equivalently, in the WORKslide.TMP ASCII output file). Based on the computed average and weighted vertical acceleration values, a second CWSlip analysis is conducted. This second computation is made using a **Constant Y acceleration** set equal to 0.15 g. The second iteration is followed by a third iteration. Figure 4.23 shows the **Analysis** tab input and settings for this final computation. This third iteration/ Newmark sliding block computation with **Constant Y Acceleration** set equal to a constant 0.13 g provides reasonable convergence, as demonstrated in the tabulated values. Recall the Table 4.2 average and weighted vertical acceleration values are computed using the Section 2.6 Equations 2.74 and 2.76, respectively. Recall the peak positive/negative vertical accelerations are 0.68 g/-0.96 g, respectively, for the vertical acceleration time-history. The vertical accelerations that occur during sliding are far lower in magnitude than the effective vertical accelerations that occur during sliding (figure not shown). In this manner, a vertical acceleration time-history possessing peak positive/negative vertical accelerations of 0.68 g/-0.96 g, respectively, becomes a **Constant Y Acceleration** of (positive) 0.13 g.

Table 4.2. Assessment of **Constant Y Acceleration**, the effective vertical acceleration for Example 2.

Iteration No.	User-Specified (kcg) <sub>v</sub> *g	Average Vertical Acceleration (kcg) <sub>v-ave</sub> *g	Weighted Vertical Acceleration (kcg) <sub>v-weighted</sub> *g	Maximum Transmissible Acceleration
1	0	0.0835 g	0.187 g	0.804 g
2	0.15 g	0.0361 g	0.1097 g	0.71 g
3	0.13 g	0.042 g	0.1216 g	0.72 g

CWSlip - C:\CWSlip\EX\_2\_15\_Jan\_07.CWS

File Analysis Type

Introduction Horz. Earthquake Time History Vert. Earthquake Time History Simplified Analysis Geometry Structural Wedge Driving Wedge **Analysis**

Input Parameters

Vertical Time History Usage: Determine representative constant value

Constant Y Acceleration: 0.13 fractional G's

Analysis Type: Sliding analysis

Output Units: in/sec^2, in/sec, in

**Run CWSlip Analyzer**

View Output

Show Log of CWSlip Execution Show Input Echo of CWSlip Execution

Plot AccX Show AccX File

Plot AccY Show AccY File

Plot AccYX Show AccYX File

Show Sliding Evaluation Show Lift-Off Evaluation

Plot PA File Show PA File

Plot PO File Show PO File

Plot PAE File Show PAE File

Plot Sliding Time History Show Sliding Time History File

Plot Effective Vertical Acc. Show Effective Vertical Acc.

Analysis Type: Complete (Using Acc. Time History)

Figure 4.23. The final **Analysis** tab for Example 2.

The computed value for the (horizontal) maximum transmissible acceleration is equal to 0.72 g (reported by the **Show Sliding Evaluation** button or, equivalently, in the WORKslide.TMP ASCII output file). For the incipient lift-off in rotation the computed horizontal acceleration is computed to be 0.53 g (reported by the **Show Lift-Off Evaluation** button or, equivalently, in the WORKrotate.TMP ASCII output file). These computations are made with a **Constant Y Acceleration** of 0.13 g.<sup>1</sup>

Since the incipient lift-off in rotation acceleration is the smaller of the two horizontal acceleration constants, the wall will rotate during earthquake shaking (for the given wall geometry, soil shear strengths, and ground motions used in this particular analysis).

Since the wall rotates before it slides, a CWRotate analysis is required and the CWSlip analysis is discontinued. Refer to Example 2 in Section 5.2.8 of Ebeling and White (2006) for the compute results of the rotational analysis of this retaining wall problem.

#### **4.2.10 Example 3 – Earth retaining wall at a dry soil site – No reinforced concrete slab buttress at the wall’s toe (no time-histories)**

Consider the case of the seismic stability evaluation of the Figure 4.16 reinforced concrete earth retaining structure (with no buttressing toe slab) of Example 1 but for the case in which project acceleration time-histories are not yet available. (This is often encountered early on in the project history when ground motion assessments are not yet complete.) This 22-ft-high earth retaining structure retains moist cohesionless soil, a dense sand, and is founded on rock. During construction, a thin layer of dense sand was used to level the top of rock before pouring the base of the reinforced concrete retaining wall. For this Corps project only preliminary seismic information is known; (Richter) earthquake magnitude of 6.5, peak horizontal ground acceleration of 0.5 g. A peak value for horizontal

---

<sup>1</sup> For completeness, a separate analysis to determine a value for the **Constant Y Acceleration** that is consistent with the acceleration pulses generating wall rotation for the lift-off evaluation process was also conducted using CWRotate and reported in Example 2, Section 4.2.8 of Ebeling and White (2006). After iteration, the computed results were only slightly different from those obtained for the sliding block based analyses; a **Constant Y Acceleration** value of 0.05g with the horizontal acceleration of incipient lift-off in rotation computed to be 0.52g. The value for incipient lift-off in rotation acceleration is the smaller of the two horizontal acceleration constants.

velocity  $V$  is estimated to be 18 in./sec using the Newmark and Hall (1982) approximation of  $V/A \cdot g = 36$  in./sec/ $g$  of for rock sites.

Figure 4.17 shows the input **Geometry** tab data for this problem. Material region numbers 1, 2, 4, 6, and 10 are used to define the geometry of the structural wedge. Note a resisting force at the toe of the wall is set equal to zero since a reinforced concrete buttress slab is not present.

A minimum angle for slip plane of 3 degrees from horizontal is specified in the **Driving Wedge** tab (not shown). Additionally, residual shear strength parameter values of  $\phi' = 35$  degrees and  $\phi' = 34$  degrees are specified for the retained soil and the cohesionless soil immediately in contact with the base of the structural wedge, respectively.

Figure 4.24 shows the ground motion input data specified in the **Simplified Analysis** tab as well as the eight simplified sliding block procedures selected for this analysis of permanent seismic wall displacement. Recall these relationships were derived using acceleration time-histories from soil sites.

CWSlip - C:\CWSlip\EX\_3\_15\_Jan\_07.CWS

File Analysis Type

Introduction Horz. Earthquake Time History Vert. Earthquake Time History **Simplified Analysis** Geometry Structural Wedge Driving Wedge Analysis

Choose Method(s) for Simplified Displacement Analysis

Publication	Description	
<input checked="" type="checkbox"/> Ambraseys & Menu (1988)	Mean relationship	Limitations
<input checked="" type="checkbox"/> Ambraseys & Menu (1988)	95% confidence that computed displacement will not be exceeded	Limitations
<input checked="" type="checkbox"/> Cai & Bathurst (1996)	Mean upper bound relationship for Franklin and Chang (1977) data	Limitations
<input checked="" type="checkbox"/> Cai & Bathurst (1996)	Mean relationship for Newark (1965) data	Limitations
<input checked="" type="checkbox"/> Whitman & Liao (1985)	Mean relationship	Limitations
<input checked="" type="checkbox"/> Whitman & Liao (1985)	95% confidence that computed displacement will not be exceeded	Limitations
<input checked="" type="checkbox"/> Richards & Elms (1979)	Upper bound relationship to the Franklin and Chang (1977) data	Limitations
<input checked="" type="checkbox"/> Makdisi & Seed (1978)	Range in values	Limitations

Data Required for Simplified Method(s) Analysis

Peak Acceleration	Units	Peak Velocity	Units	Magnitude
0.5	fractional G's	18	in/sec	6.50

Simplified (Peak Ground Acceleration Values)

Figure 4.24. Simplified sliding block method of **Simplified Analysis** tab for Example 3.

The first step in the simplified CWSlip analysis is to determine if the Figure 4.16 retaining wall will slide or rotate during earthquake shaking. For a **Sliding Analysis Type**, the **Constant Y Acceleration** is set equal to zero since no project-specific data are yet available. The program is executed via select **Run CWSlip Analyzer** button as shown in the Figure 4.25 **Analysis** tab.

CWSlip - C:\CWSlip\EX\_3\_15\_Jan\_07.CWS

File Analysis Type

Introduction Horz. Earthquake Time History Vert. Earthquake Time History **Simplified Analysis** Geometry Structural Wedge Driving Wedge Analysis

Input Parameters

Constant Y Acceleration: 0 fractional G's

Analysis Type: Sliding analysis

Output Units: in/sec<sup>2</sup>, in/sec, in

Run CWSlip Analyzer

View Output

Show Log of CWSlip Execution Show Input Echo of CWSlip Execution

Show Sliding Evaluation Show Lift-Off Evaluation

Plot PA File Show PA File

Plot PO File Show PO File

Plot PAE File Show PAE File

Simplified (Peak Ground Acceleration Values)

Figure 4.25. **Analysis** tab for Example 3 simplified sliding block analysis.

The computed value for the (horizontal) maximum transmissible acceleration is equal to 0.35 g (reported by the **Show Sliding Evaluation** button or, equivalently, in the WORKslide.TMP ASCII output file). For the incipient lift-off in rotation the computed horizontal acceleration is computed to be 0.37 g (reported by the **Show Lift-Off Evaluation** button or, equivalently, in the WORKrotate.TMP ASCII output file). Recall these computations are made with a **Constant Y Acceleration** of 0.

Since the Figure 4.16 retaining wall will slide before it will rotate, then continue viewing the results for the simplified sliding block permanent deformation analysis, reported by the **Show Sliding Evaluation** button or, equivalently, in the WORKslide.TMP ASCII output file.

```

.....
STEP 7:          SIMPLIFIED NEWMARK SLIDING BLOCK ANALYSIS RESULTS
.....

*****
* Permanent horizontal displacement computed using *
* Simplified Newmark sliding block relationships *
*          cofkhSLIDE/Amax =      0.700          *
*****

* Permanent      * Units *          Description          *
* Displacement *      *
-----
0.2193          in      Ambraseys and Menu (1988) mean relationship
0.8494          in      Ambraseys and Menu (1988) - 95% confidence
                        that the computed displacement will not be
                        exceeded
0.5335          in      Cai and Bathurst (1996) mean upper bound
                        relationship for the Franklin and Chang
                        (1977) data
0.3020          in      Cai and Bathurst (1996) mean upper bound
                        relationship for the Newmark (1966) data
0.0862          in      Whitman and Laio (1985) mean relationship
1.1530          in      Whitman and Laio (1985) - 95% confidence that
                        the computed displacement will not be
                        exceeded
0.6082          in      Richards and Elms (1979) upper bound
                        relationship for the Franklin and Chang
                        (1977) data
0.1378          in      Makdisi and Seed (1978) lower displacement
                        estimate
1.5669          in      Makdisi and Seed (1978) upper displacement
                        estimate

```

The cumulative permanent displacement is computed to be between less than 2 in. by the eight relationships selected. The range in results among the eight relationships used is attributed to (1) differences in the data base of earthquake ground motions used to develop each of the eight relationships, and (2) some relationships are mean estimates of permanent seismic displacement while others are upper bound estimate. Some upper bound estimates are more conservative than others (Section 2.7).

During sliding the maximum inertial force imparted to the structural wedge and to the driving soil wedge (and to  $P_{AE}$ ) is due to a horizontal acceleration of 0.35 g, the value for the maximum transmissible



acceleration (with a constant vertical acceleration of 0.0). Forces acting on the structural wedge are reported by the **Show Sliding Evaluation** button (or, equivalently, in the WORKslide.TMP ASCII output file). By allowing the retaining wall to slide, the retaining wall structural wedge and soil wedge are not subjected to inertia forces due to the higher accelerations values, i.e., up to 0.5 g of horizontal acceleration. Note  $\text{cofkhSLIDE}/A_{\text{max}} = 0.35 \text{ g}/0.5 \text{ g} = 0.7$ . Thus, allowing the wall to slide during earthquake shaking provides for lower design forces than would otherwise occur should translational wall movements have been constrained.

```
*****
**** Earth Pressure Forces ****
*****
```

```
PAEqSLIDE =      18241.96 lbs
ALPHAPAESLIDE = 43.00 degrees
HPAEqSLIDE =   10.30 ft
DCaeSLIDE =    0.00 ft
Pseudo-Static wedge analysis number IcalEQWedgeSLIDE = 6
Difference in percent between Resisting and Driving Forces =0.94
```

Pae run Numbers identified above are listed in WORKpae.TMP

```
=====
Pressure Distributions acting at an angle  0.00 degrees
from normal to the vertical plane through the heel
=====
```

Height above Heel (ft)	Static (lb/ft <sup>2</sup> )	Incremental EQ (lb/ft <sup>2</sup> )	Total EQ (lb/ft <sup>2</sup> )
22.00	0.00	669.14	669.14
3.54	691.52	247.98	939.50
0.00	811.06	167.29	978.35

```
*****
**** Base Pressure Forces ****
*****
```

```
Shear Force along the base of the structural wedge      = 24429.98 lbs
Force normal to the base of the structural wedge         = 36218.94 lbs
Distance along the base from the TOE to the normal force =    0.44 ft
```

For a dense sand, the Table 1.1 guidelines indicate that for a 22-ft-high section, active earth pressures may be used in the analysis if wall movements exceed  $\frac{1}{4}$  in. ( $= 0.001$  times 22 ft times 12 in./ft). With predicted wall movements on the order of an inch or two, the use of active earth pressures in the dynamic time-history permanent displacement calculations is deemed appropriate.

Using the forces provided in the output file<sup>1</sup>, the user is advised to determine if the bearing capacity of the foundation is adequate.

---

<sup>1</sup> Appendix G summarizes the contents of the output files.

## 5 Summary, Conclusions, and Recommendations

### 5.1 Summary and conclusions

Engineer Manual 1110-2-2502 Retaining and Flood Walls gives engineering procedures that are currently being used by District engineers in their *initial* assessment of seismic wall performance of existing earth retaining structures and the (preliminary) sizing of new retaining structures. The engineering procedures given in EM 1110-2-2502 for retaining walls make extensive use of the simplified pseudo-static procedure of analysis of earth retaining structures and expresses wall performance criteria in terms of computed factors of safety against sliding and bearing failure, and base area in compression. The simplified pseudo-static procedure of analysis makes it difficult to interpret the actual wall performance for Corps projects subjected to “strong” design ground motions because of simplifications made in the procedure of analysis. In a pseudo-static analysis an oversimplification occurs when the engineer is forced to render the complex, horizontal and vertical earthquake acceleration time-history events to constant values of accelerations and assume a constant direction for each. These constant values are denoted as the pseudo-static acceleration coefficients in the horizontal and vertical directions (refer to Section 1.1.1 of this report). The engineer is also required to assume a constant direction for each of these components. An acceleration time-history, in actuality, varies both in magnitude and in direction with time.

The simplified pseudo-static procedure does not allow for interpretation of *actual* wall performance by District engineers. Intense shaking imparted by the OBE and MCE design events makes the interpretation of the simplified procedure of analysis even more difficult. The more important questions for the wall are whether the wall slides into the spillway basin, or rotates into the spillway basin, or even tips over onto its side during the earthquake event. The simplified pseudo-static procedure of analysis is not capable of answering these questions. The answers depend on the magnitude of the pseudo-static coefficient used in the calculations compared to the magnitude of the peak values for the acceleration pulses as well as the number and duration of these strong shaking acceleration pulses in the design earthquake event time-history. When considering both horizontal

and vertical accelerations, the resulting wall response is further complicated by the time-history of phasing between the pulses of horizontal and vertical accelerations. Only the permanent wall sliding displacement/wall rotation method of time-history analysis can answer these questions. Again, wall displacements will influence the seismic earth pressure forces imparted on the wall by the retained soil.

Formal consideration of the permanent seismic wall displacement in the seismic design process for Corps-type retaining structures is given in Ebeling and Morrison (1992). The key aspect of the engineering approach presented in this Corps document is that simplified procedures for computing the seismically induced earth loads on retaining structures are also dependent upon the amount of permanent wall displacement that is expected to occur for each specified design earthquake. The Ebeling and Morrison simplified engineering procedures for Corps retaining structures are geared towards hand calculations. The engineering formulation and corresponding user friendly, PC-based software discussed in this report extend these simplified procedures.

This research report describes the engineering formulation developed for the permanent translational response, including permanent displacement, of rock-founded retaining walls to earthquake ground motions. The corresponding PC software *CorpsWallSlip* developed to perform a sliding block analysis of each user-specified retaining wall section was also discussed. When acceleration time-histories are used as input to the *CorpsWallSlip* complete time-history sliding block analysis to represent the earthquake ground motions, baseline-corrected, horizontal and vertical acceleration time-histories are to be specified as input. A particular formulation of the rotational analysis model for computing the threshold value of acceleration corresponding to lift-off of the base of the wall in rotation (Figure 1.2) was also described. (Note that a more versatile, complete time-history based formulation for computing earthquake-induced, permanent wall rotations using the PC-based software *CorpsWallRotate* has also been developed and is discussed in Ebeling and White (2006).) Additionally, a simplified sliding block formulation that eliminates the need for an acceleration time-history to characterize earthquake shaking was discussed in this report and incorporated within *CorpsWallSlip*. Ground motion parameters such as peak ground acceleration and velocity and earthquake magnitude values are all that are required in this formulation.

The engineering methods contained in this report and implemented within CorpsWallSlip and CorpsWallRotate allow the engineer to determine if a given retaining wall has a tendency to slide or to rotate for a specified seismic event. This is a new capability for the seismic design/evaluation process for Corps retaining structures.

CorpsWallSlip was designed for ease of use in a PC environment and to render the complex problem of seismic evaluation/design of retaining walls that tend to permanently displace during earthquakes to a more straightforward and rapid engineering process. The computed permanent wall translation and other pertinent information allow for a rapid investigation of retaining wall configurations by District engineers.

***Minimum Wall Displacement:*** Recall that CorpsWallSlip applies an active earth pressure force to the structural wedge in the permanent rotation analysis, as is done in most sliding block formulations for retaining walls. Table 1.1 lists the approximate magnitudes of movements required to reach minimum active earth pressure conditions. Although the guidance in Clough and Duncan (1991) is for static loading, after careful evaluation Ebeling and Morrison (1992, in Section 2.2.2) concluded that the Table 1.1 values may also be used as rough guidance for minimum retained soil seismic displacement to fully mobilize a soil shear resistance, resulting in dynamic active earth pressures. That is, the permanent displacements resulting from rotations computed using CorpsWallRotate must equal or exceed the Table 1.1 values (given as displacement-normalized wall heights in this table). If not, then the dynamic earth pressures are underestimated in the analysis.

## 5.2 Recommendations for future research

Engineering formulations and software provisions based on sound seismic engineering principles are needed for a wide variety of the Corps retaining walls that (1) rotate or (2) slide (i.e., translate) during earthquake shaking and (3) for massive concrete retaining walls constrained to rocking. The engineering formulation discussed in this report was developed to address the second of these three different modes of retaining wall responses to earthquake shaking.

The formulation of complete engineering procedures and corresponding software are needed to compute the seismic response of Corps-type earth retaining structures that slide or rock in place during earthquake shaking.

CorpsWallRotate (Ebeling and White 2006) allows for the rapid analysis of rock-founded retaining walls that tend to rotate about their toes during earthquake shaking. A particular formulation of the permanent sliding displacement response of retaining walls for a user-specified earthquake acceleration time-history is incorporated in CorpsWallSlip. It includes a more versatile, simplified sliding block formulation that eliminates the need for an acceleration time-history and uses peak ground acceleration and velocity and earthquake magnitude parameters. An ERDC research effort is needed to develop simplified engineering formulations and corresponding GUI-based PC software for analyzing Corps retaining walls that rock in place during seismic shaking due to their sizeable mass or due to lower levels of ground shaking. Their seismically induced wall movements will not be sufficient to fully mobilize the shear resistance within the retained soils and the resulting (seismic) earth pressures will be larger than the resultant active earth pressure force  $P_{AE}$ , whose formulation is given in Appendix A and implemented within CorpsWallSlip and CorpsWallRotate.

In addition, the engineering methodology and corresponding software CorpsWallSlip and CorpsWallRotate were formulated for rock-founded retaining structures. Research is needed to extend this formulation to soil-founded Corps retaining structures.

For the initial version of CorpsWallSlip (and CorpsWallRotate), a simplified assumption is made that for steady-state conditions, hydrostatic water pressures exist within the heel region of the backfill. This implies that all head loss occurs due to flow within the foundation below the base of the structural wedge as discussed in Appendix D. Future improvements should include the formulation and inclusion of more refined steady-state seepage analyses implemented within CorpsWallSlip (and CorpsWallRotate).

Most Corps hydraulic structures that act as earth retaining structures possess a vertical face in contact with the pool (when present). Consequently, hydrodynamic water pressures acting on this front “wet” face are approximated in the CorpsWallSlip using the Westergaard (1931) procedure (see Appendix D). This procedure needs to be expanded to include consideration of hydrodynamic water pressures acting on inclined “wetted” structural faces during sliding of the structural wedge.

The evaluation of the adequacy of the bearing capacity of the foundation for loadings imposed by wall that rotate needs to be evaluated. This is currently being done using hand computations by engineers using the computed forces provided by CorpsWallSlip and CorpsWallRotate. This evaluation needs to be formulated and then incorporated within CorpsWallSlip (and CorpsWallRotate).

Excess pore water pressures may be generated by earthquake shaking of contractive backfill and foundation soils. The procedures outlined in Ebeling and Morrison (1992) to account for  $r_u > 0$  needs to be incorporated within CorpsWallSlip (and CorpsWallRotate).

The simplified sliding block relationships discussed in Chapter 2 and implemented in CorpsWallSlip were derived using acceleration time-histories from soil sites. Research is needed to develop simplified sliding block relationships for rock sites.

## References

- Ambraseys, N. N., and J. M. Menu. 1988. Earthquake-induced ground displacements. *Earthquake Engineering and Structural Dynamics* 16:985-1006.
- American Society of Civil Engineers (ASCE) Standard. 1986. Seismic analysis of safety-related nuclear structures and commentary on standard for seismic analysis of safety related nuclear structures. ASCE 4-86.
- Bowles, J. N. 1968. *Foundation analysis and design*. New York: McGraw-Hill.
- Cai, Z., and R. J. Bathurst. 1996. Deterministic sliding block methods for estimating seismic displacements of earth structures. *Soil Dynamics and Earthquake Engineering* 15:255-268.
- Chang, C.-J., W. F. Chen, and J. T. P. Yao. 1984. Seismic displacements in slopes by limit analysis. ASCE. *Journal of Geotechnical Engineering* 110(GT7):860-874.
- Chopra, A. K. 1967. Hydrodynamic pressures on dams during earthquakes. ASCE. *Journal of Engineering Mechanics Division* 93(EM6):205-223.
- Clough, G. W., and J. M. Duncan. 1969. *Finite element analyses of Port Allen and Old River Locks*. Contract Report S-69-6. Vicksburg, MS: U.S. Army Engineer Waterways Experiment Station.
- \_\_\_\_\_. 1991. Earth pressures. In *Foundation engineering handbook*, 2nd ed., Chap 6, ed. H. Y. Fang, 223-235. New York: Van Nostrand Reinhold.
- Duncan, J. M., and A. L. Buchignani. 1975. *An engineering manual for slope stability studies*. Berkeley, CA: University of California Department of Civil Engineering, Geotechnical Engineering.
- Ebeling, R. M. 1992. *Introduction to the computation of response spectrum for earthquake engineering*. Technical Report ITL-92-4. Vicksburg, MS: U.S. Army Engineer Waterways Experiment Station.
- Ebeling, R. M., and B. C. White. 2006. *Rotational response of toe-restrained retaining walls to earthquake ground motions*. Technical Report ERDC/ITL TR-06-\_\_\_\_. Vicksburg, MS: U.S. Army Engineer Research and Development Center.
- Ebeling, R. M., R. A. Green, and S. E. French. 1997. *Accuracy of response of single-degree-of-freedom systems to ground motion*. Technical Report ITL-97-7. Vicksburg, MS: U.S. Army Engineer Waterways Experiment Station.
- Ebeling, R. M., and R. L. Mosher. 1996. Red River U-frame Lock No. 1, Backfill-structure-foundation interaction. ASCE. *Journal of Geotechnical Engineering* 122(3): 216-225.



- Ebeling, R. M., R. L. Mosher, K. Abraham, and J. F. Peters. 1993. *Soil-structure interaction study of Red River Lock and Dam No. 1 subjected to sediment loading*. Technical Report ITL-93-3. Vicksburg, MS: U.S. Army Engineer Waterways Experiment Station.
- Ebeling, R. M., J. F. Peters, and R. L. Mosher. 1997. The role of non-linear deformation analyses in the design of a reinforced soil berm at Red River U-frame Lock No. 1. *International Journal for Numerical and Analytical Methods in Geomechanics* 21:753-787.
- Ebeling, R. M., M. E. Pace, and E. E. Morrison. 1997. *Evaluating the stability of existing massive concrete gravity structures founded on rock*. Technical Report REMR-CS-54. Vicksburg, MS: U.S. Army Engineer Waterways Experiment Station.
- Ebeling, R. M., and R. E. Wahl. 1997. *Soil-structure-foundation interaction analysis of new roller-compacted concrete north lock wall at McAlpine Locks*. Technical Report ITL-97-5. Vicksburg, MS: U.S. Army Engineer Waterways Experiment Station.
- Ebeling, R. M., and E. E. Morrison. 1992. *The seismic design of waterfront retaining structures*. Technical Report ITL-92-11. Vicksburg, MS: U.S. Army Engineer Waterways Experiment Station.
- Ebeling, R. M., J. F. Peters, and G. W. Clough. 1992. *Users guide for the incremental construction, soil-structure interaction program SOILSTRUCT*. Technical Report ITL-90-6. Vicksburg, MS: U.S. Army Engineer Waterways Experiment Station.
- Fishman, K. L., and R. Richards, Jr. 1997. *Seismic analysis and design of bridge abutments considering sliding and rotation*. Technical Report NCEER-97-0009. National Center for Earthquake Engineering Research. Buffalo, NY: State University of New York at Buffalo.
- Fishman, K. L., and R. Richards, Jr. 1998. Seismic analysis and model studies of bridge abutments. In *Analysis and Design of Retaining Structures Against Earthquakes*. ASCE Geotechnical Special Publication No. 80, 77-99.
- Franklin, A. G., and F. K. Chang. 1977. *Earthquake resistance of earth and rockfill dams: Report 5: Permanent displacement of earth embankments by Newmark sliding block analysis*. Miscellaneous Paper S-71-17. Vicksburg, MS: U.S. Army Engineer Waterways Experiment Station.
- Green, R. A., and R. M. Ebeling. 2002. *Seismic analysis of cantilever retaining walls, Phase I*. ERDC/ITL TR-02-3. Vicksburg, MS: U.S. Army Engineer Research and Development Center.
- Headquarters, Department of the Army. 1989. *Retaining and flood walls*. Engineer Manual 1110-2-2502. Washington, DC: Headquarters, Department of the Army.
- \_\_\_\_\_. 1990. *Retaining and flood walls*. Engineer Technical Letter 1110-2-322. Washington, DC: Headquarters, Department of the Army.

- Headquarters, Department of the Army. 1995. *Earthquake design and evaluation for Civil Works projects*. Engineer Regulation 1110-2-1806. Washington, DC: Headquarters, Department of the Army.
- \_\_\_\_\_. 2005. *Stability analysis of concrete structures*. Engineer Manual 1110-2-2100. Washington, DC: Headquarters, Department of the Army.
- Hibbler, R. C. 2001. *Engineering mechanics; Statics & dynamics*. 9th ed. Upper Saddle River, NJ: Prentice-Hall.
- Hynes-Griffin, M. E., and A. G. Franklin. 1984. *Rationalizing the seismic coefficient method*. Miscellaneous Paper GL-84-13. Vicksburg, MS: U.S. Army Engineer Waterways Experiment Station.
- Idriss, I. M. 1985. Evaluating seismic risk in engineering practice. In *Proceeding 11th International Conference on Soil Mechanics and Foundation Engineering* 1:255-320.
- Lysmer, J., T. Udaka, C.-F. Tsai, and H. B. Seed. 1975. FLUSH - A computer program for approximate 3-D analysis of soil-structure interaction problems. Report No. EERC 75-30, Earthquake Engineering Research Center. Berkeley: University of California.
- Makdisi, F. I., and H. B. Seed. 1978. Simplified procedure for estimating dam and embankment earthquake-induced deformations. ASCE. *Journal of the Geotechnical Engineering Division* 104(GT7):849-867.
- Mononobe, N., and H. Matsuo. 1929. On the determination of earth pressures during earthquakes. In *Proceedings, World Engineering Congress* 9:177-185.
- Nadim, F. 1980. Tilting and sliding of gravity retaining walls during earthquakes. MS thesis, Department of Civil Engineering, Massachusetts Institute of Technology.
- Nadim, F., and R. V. Whitman. 1984. Coupled sliding and tilting of gravity retaining walls during earthquakes. In *Proceedings of the Eighth World Conference on Earthquake Engineering, San Francisco III*: 477-484.
- Newmark, N. 1965. Effects of earthquakes on dams and embankments. *Geotechnique* 15(2):139-160.
- Newmark, N. N., and W. J. Hall. 1982. *Earthquake spectra and design*. Oakland, CA: Earthquake Engineering Research Institute.
- Okabe, S. 1924. General theory of earth pressures and seismic stability of retaining walls. *Journal Japan Society of Civil Engineering* 10(6).
- \_\_\_\_\_. 1926. General theory of earth pressures. *Journal Japan Society of Civil Engineering* 12(1).
- Richards, R., Jr., and D. Elms. 1979. Seismic behavior of gravity retaining walls. ASCE. *Journal of Geotechnical Engineering Division* 105(GT4):449-464.

- Richards, R., Jr., K. L. Fishman, and R. C. Divito. 1996. Threshold acceleration for rotation and sliding of bridge abutments. ASCE. *Journal of Geotechnical Engineering* 112(9):752-759.
- Schnabel, P. B., J. Lysmer, and H. B. Seed. 1972. SHAKE: A computer program for earthquake response analysis of horizontally layered sites. Report EERC-72-12. Earthquake Engineering Research Center. Berkeley: University of California.
- Seed, H. B., and R. V. Whitman. 1970. *Design of earth retaining structures for dynamic loads*. ASCE Specialty Conference on Lateral Earth Stresses in the Ground and Design of Earth Retaining Structures, 103-147.
- Siddharthan, R., S. Ara, and J. Anderson. 1990. Seismic displacement of rigid retaining walls. In *Proceedings of Fourth U.S. National Conference on Earthquake Engineering*, 673-680.
- Siddharthan, R., S. Ara, and G. M. Norris. 1992. Simple rigid plastic model for seismic tilting of rigid wall. ASCE. *Journal of Structural Engineering* 118(2):469-487.
- Siddharthan, R., P. Gowda, and G. M. Norris. 1991. Displacement based design of retaining walls. In *Proceedings, Second International Conference on Recent Advances in Geotechnical Earthquake Engineering and Soil Dynamics*, 657-661.
- Steedman, R. S., and X. Zeng. 1996. Rotation of large gravity walls on rigid foundations under seismic loading. In *Analysis and design of retaining structures against earthquakes*, Proc. of sessions sponsored by the Soil Dynamics Committee of the Geo-Institute of ASCE, ed. S. Prakash, ASCE Geotechnical Special Publication No. 60, 38-56.
- Strom, R. W., and R. M. Ebeling. 2004. *Simplified methods used to estimate the limit-state axial load capacity of spillway invert slabs*. ERDC/ITL TR-04-3. Vicksburg, MS: U.S. Army Engineer Research and Development Center.
- Westergaard, H. 1931. Water pressures on dams during earthquakes. *Transactions of ASCE*, Paper No. 1835, 418-433.
- Whitman, R. V. 1990. Seismic design behavior of gravity retaining walls. In *Proceedings of ASCE Specialty Conference on Design and Performance of Earth Retaining Structures*, Geotechnical Special Publication No. 25, 817-842.
- \_\_\_\_\_. 1992. Predicting earthquake-induced tilt of gravity retaining walls. In *Retaining Structures, Proceedings of a Conference*, Institution of Civil Engineers, pp. 750-758.
- \_\_\_\_\_. 2000. *Fifty years of soil dynamics*. Fifteenth Nabor Carrillo Lecture. Delivered during the XX National Meeting of Soil Mechanics, Oaxaca, Mexico, November, 88 p.
- Whitman, R. V., and S. Liao. 1985a. *Seismic design of retaining walls*. Miscellaneous Paper GL-85-1. Vicksburg, MS: U.S. Army Engineer Waterways Experiment Station.
- \_\_\_\_\_. 1985b. Seismic design of gravity retaining walls. In *Proceedings of the Eighth World Conference on Earthquake Engineering, San Francisco* 3:533-540.

- Wong, C. 1982. *Seismic analysis and improved seismic design procedure for gravity retaining walls*. Research Report 82-32. Cambridge, MA: Department of Civil Engineering, Massachusetts Institute of Technology.
- Wood, J. 1975. Earthquake induced pressures on rigid wall structure. *Bulletin of New Zealand Society for Earthquake Engineering* 8(3): 175-186.
- Zarrabi, K. 1979. Sliding of gravity retaining wall during earthquakes considering vertical acceleration and changing inclination of failure surface. MS thesis, Department of Civil Engineering, Massachusetts Institute of Technology.
- Zeng, X., and R. S. Steedman. 2000. Rotating block method for seismic displacement of gravity walls. ASCE. *Journal of Geotechnical and Geoenvironmental Engineering* 126(8): 709-717.

# Appendix A: Computation of the Dynamic Active Earth Pressure Forces for a Partially Submerged Retained Soil Using the Sweep-Search Wedge Method

## A.1 Introduction

This appendix describes the derivation of the dynamic active earth pressure force for partially submerged backfills using the sweep-search wedge method. The effect of earthquakes is incorporated through the use of a constant horizontal acceleration,  $a_h = k_h \cdot g$ , and a constant vertical acceleration,  $a_v = k_v \cdot g$ , acting on the soil mass comprising the active wedge within the backfill, as shown in Figure A.1.

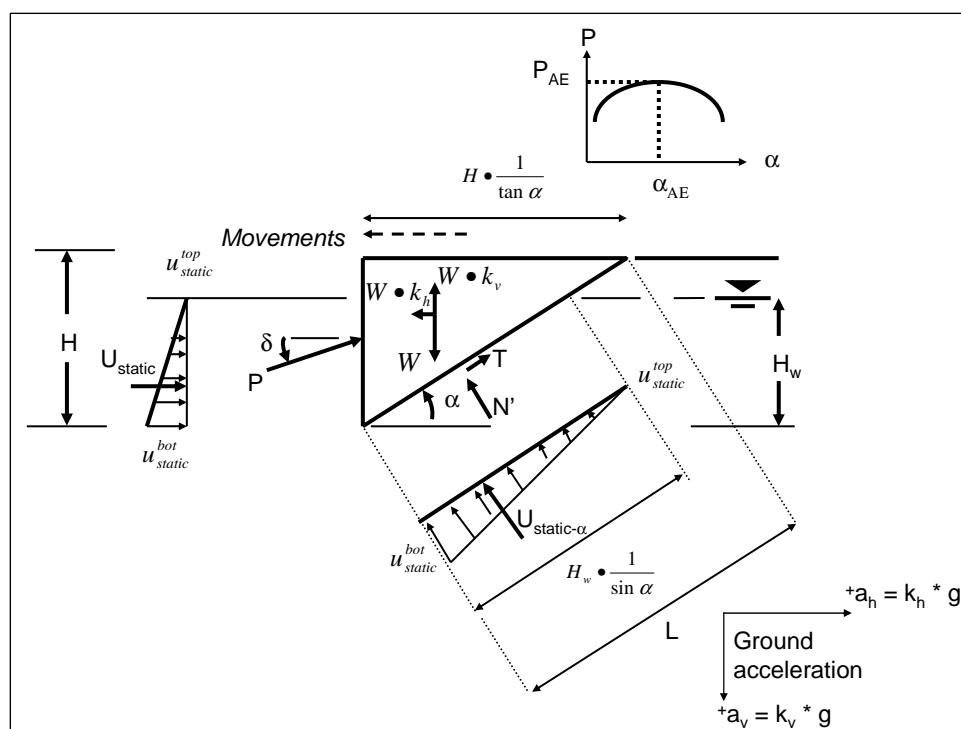


Figure A.1. Dynamic active sweep-search wedge analysis (hydrostatic water table).

The Mohr-Coulomb  $\tau = c + \sigma_n \cdot \tan \phi$  relationship is used to define the shear strength along a potential slip plane in the sweep-search soil wedge formulation derived in this appendix and implemented in CorpsWallSlip (and CorpsWallRotate). For granular soils the cohesion intercept,  $c$ , is

usually set equal (with a non-zero  $\phi$  value) to zero after consideration is given to the anticipated level of permanent deformation associated with anticipated permanent wall movements and the development of the active earth pressure force,  $P_{AE}$ . The purpose for including the cohesion intercept in the shear strength used to define the sliding wedge formulation given in Section A.2 is to derive a set of equations that may be easily adapted to both effective and total stress analyses. In a total stress analysis  $\phi$  is set equal to zero, the cohesion intercept,  $c$ , is set equal to the undrained shear strength,  $S_u$ , and the internal pore water pressures are ignored.

In Section A.2 the relationships used in a sweep-search wedge formulation used to determine the magnitude of the dynamic active earth pressure force,  $P_{AE}$ , is derived for an effective stress analysis using Mohr-Coulomb shear strength parameters  $c'$  and  $\phi'$  for the retained soil.<sup>1,2</sup> The earth and water pressure forces acting on the trial soil wedge are derived for the case

<sup>1</sup> A key item is the selection of suitable shear strength parameters. In an effective stress analysis, the issue of the suitable friction angle is particularly troublesome when the peak friction angle is significantly greater than the residual friction angle. In the displacement controlled approach examples given in Section 6.2 of Ebeling and Morrison (1992), effective stress-based shear strength parameters (i.e., effective cohesion,  $c'$ , and effective angle of internal friction,  $\phi'$ ) were used to define the shear strength of the dilative granular backfills, *with  $c'$  set equal to zero in all cases due to the level of deformations anticipated in a sliding block analysis during seismic shaking*. In 1992 Ebeling and Morrison concluded that it is conservative to use the residual friction angle in a sliding block analysis, and this should be the usual practice for displacement-based analysis of granular retained soils. The primary author of this report would broaden the concept to the assignment of effective (or total) shear strength parameters for the retained soil be consistent with the level of shearing-induced deformations encountered for each design earthquake in a rotational analysis and note that active earth pressures are used to define the loading imposed on the structural wedge by the driving soil wedge. (Refer to Table 1.1 for guidance regarding wall movements required to fully mobilize the shear resistance within the retained soil during earthquake shaking.) Therefore, engineers are cautioned to carefully consider the reasonableness of including a nonzero value for effective cohesion,  $c'$ , in their permanent deformation analyses.

<sup>2</sup> CorpsWallSlip performs a permanent displacement analysis of a retaining wall due to earthquake shaking. Reversal in the direction of the horizontal component of the time-history of earthquake ground shaking occurs many times during the typical tens of seconds of ground motion. Consequently, a reversal in direction of the inertial force imparted to the structural wedge and to the soil driving wedge occurs many times during the course of the analysis using CorpsWallSlip. In a traditional soil wedge formulation for static loading, a crack is typically considered to exist within the upper portion of the soil driving wedge for a cohesive soil (with shear strength,  $S_u$ , specified in a total stress analysis or  $c'$  specified in an effective stress analysis) and the planer wedge slip surface is terminated when it intersects the "zone of cracking" at a depth,  $d_{crack}$ , below the ground surface (e.g., see Appendix H in EM 1110-2-2502). This assumption is not made in the CorpsWallSlip formulation for dynamic loading. Instead, it is assumed that in the dynamic wedge formulation, the crack within the "zone of cracking" at the top of the retained cohesive soil of the driving wedge will not remain open during earthquake shaking *due to the inertial load direction reversals* during this time-history based CorpsWallSlip analysis. So, even for cohesive soils, the Figure A.1 planar slip surface, obtained from the sweep-search method of analysis used by CorpsWallSlip to obtain a value for the earthquake-induced resultant driving force,  $P_{AE}$  (acting on the structural wedge), extends uninterrupted within the driving soil wedge (in the retained soil) to the ground surface and is not terminated by a vertical crack face to the ground surface when it enters the zone of cracking.

of a hydrostatic water table. Any increase in the pore water pressures above their steady state values in response to the shear strains induced within the saturated portion of the backfill during earthquake shaking is typically reflected in a value of excess pore water pressure ratio,  $r_u > 0$ , as discussed in Ebeling and Morrison (1992). No excess pore water pressures are included in the submerged portion of the backfill in this derivation (i.e.,  $r_u$  is equal to zero) although provisions are made to add this option to CorpsWallSlip in the future. Appendix A in Ebeling and Morrison (1992) provides a complete wedge solution derivation that includes excess pore water pressures (using  $r_u$ ).

Section A.3 briefly discusses the computation made by CorpsWallSlip of the static active earth pressure force,  $P_A$ , for partially submerged backfills using the sweep-search wedge method.

Section A.4 summarizes the computations made by CorpsWallSlip of the dynamic active earth pressure force,  $P_{AE}$ , for a total stress analysis in which a value for the shear strength,  $S_u$ , of the retained soil is specified by the user. The dynamic active earth pressure force,  $P_{AE}$ , is again computed using the sweep-search wedge method.

Section A.5 summarizes the computations made by CorpsWallSlip of the static active earth pressure force,  $P_A$ , for a total stress analysis in which a value for the shear strength,  $S_u$ , of the retained soil is specified by the user. The static active earth pressure force,  $P_A$ , is again computed using the sweep-search wedge method.

Section A.6 discusses the computation of the weight of a soil wedge with a bilinear ground surface.

For cohesive soils, including  $c' - \phi'$  soils, no adhesion force is included along the vertical imaginary section extending upwards through the retained soil from the heel of the wall that delineates the Figure A.1 driving soil wedge from the adjacent structural wedge.

## **A.2 Dynamic Active Earth Pressure Force, $P_{AE}$ — Effective Stress Analysis**

Figure A.1 represents a free-body diagram for the derivation, which follows. The base of the wedge is the *trial* planar slip surface representing the active failure plane, which is inclined at angle alpha ( $\alpha$ ) to the

horizontal. The top of the Figure A.1 wedge is bounded by a horizontal ground surface and a vertical face along the interface between the driving soil wedge and the structural wedge.

The weight of the soil wedge acts at the center of mass and is computed as

$$W = \frac{1}{2} \gamma_t \bullet H^2 \bullet \frac{1}{\tan \alpha} \quad (\text{A.1})$$

with  $\gamma_t$  being the total unit weight for the soil wedge.<sup>1,2</sup>

The three forces acting along the planar slip surface are represented by an effective normal force,  $N'$ , a shear force,  $T$ , and the pore water pressure force. Assuming a full mobilization of shear resistance along the slip surface, the shear force may be computed utilizing the Mohr-Coulomb failure criteria as

$$T = N' \tan \phi' + c' \bullet L \quad (\text{A.3})$$

Note that the length of the potential slip plane,  $L$ , relates to the height of the soil wedge,  $H$ , at an angle  $\alpha$  from horizontal by

$$L = H \bullet \left( \frac{1}{\sin \alpha} \right) \quad (\text{A.4})$$

Recall the entire slip plane length,  $L$ , is used in the analysis of the driving soil wedge for cohesive soils to compute  $P_{AE}$  due to the assumption that the “zone of cracking” at the top of the retained cohesive soil of the driving soil wedge will not remain open during earthquake shaking due to load direction reversals during this time-history based CorpsWallSlip analysis.<sup>2</sup>

<sup>1</sup> Using the Figure 4.13 Ebeling and Morrison (1992) relationship,  $\gamma_t$  for the Figure A.1 soil wedge (with a planer slip surface and level backfill) is computed to be

$$\gamma_t = \left( \frac{H_w}{H} \right)^2 \bullet \gamma_{saturated} + \left[ 1 - \left( \frac{H_w}{H} \right)^2 \right] \bullet \gamma_{moist} \quad (\text{A.2})$$

with  $\gamma_{moist}$  the moist unit weight of the soil above the water table and  $\gamma_{saturated}$  the saturated unit weight below the water table. An alternative method for determining the value for  $W$  based on the geometry of the trial soil wedge cross sectional area with regions of moist and saturated unit weights is given in Section A.6.

<sup>2</sup> In the case of a soil wedge defined by the Figure B.1.b bilinear ground surface, the total weight  $W$  is computed using the relationships given in Section A.6.



The total pore water pressures acting along the submerged faces of the soil wedge are described in terms of the steady state pore water pressure.

### A.2.1 Calculation of Water Pressure Forces for a Hydrostatic Water Table

The pore water pressure at the ground water table (Figure A.2) is

$$u_{static}^{top} = 0 \quad (A.5)$$

For a hydrostatic water table, the pore water pressure distribution is linear with depth, and at the bottom of the wedge is computed as

$$u_{static}^{bot} = \gamma_w \cdot H_w \quad (A.6)$$

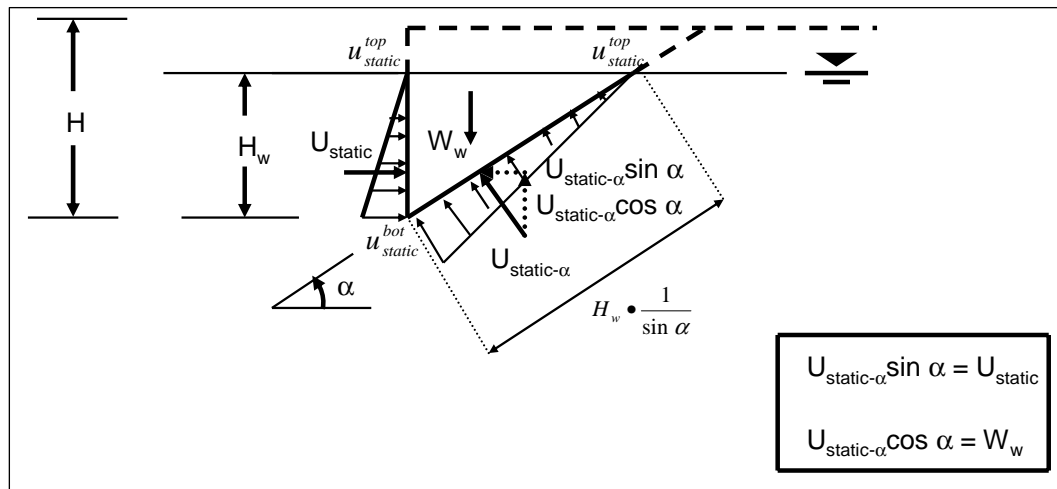


Figure A.2. Equilibrium of horizontal and vertical hydrostatic water pressure forces acting on the retained soil wedge.

### A.2.2 Static Water Pressure Forces Acting on the Wedge

The static pore pressure distribution immediately behind the structural wedge is triangular and the resultant force may be calculated as

$$U_{static} = \frac{1}{2} \gamma_w \cdot H_w^2 \quad (A.7)$$

The static pore pressure force acting normal to the planar slip surface (of angle  $\alpha$  from horizontal) is also triangular and the resultant force may be computed as

$$U_{static-\alpha} = \frac{1}{2} \gamma_w \bullet H_w^2 \bullet \frac{l}{\sin \alpha} \quad (A.8)$$

### A.2.3 Equilibrium of Vertical Forces

Equilibrium of vertical forces acting on the Figure A.1 soil wedge (with a potential slip plane at an angle  $\alpha$  from horizontal) results in the relationship

$$-P \bullet \sin \delta + W(1 - k_v) - [T] \sin \alpha - N' \bullet \cos \alpha - (U_{static-\alpha} + U_{shear-\alpha}) \cos \alpha = 0 \quad (A.9)$$

Introducing Equation A.3 into Equation A.9 results in

$$\begin{aligned} & -P \bullet \sin \delta + W(1 - k_v) - [c' \bullet L + N' \bullet \tan \phi'] \sin \alpha \\ & - N' \bullet \cos \alpha - (U_{static-\alpha} + U_{shear-\alpha}) \cos \alpha = 0 \end{aligned} \quad (A.10)$$

and solving for the normal effective force,  $N'$ , becomes

$$\begin{aligned} N' = & -P \frac{\sin \delta}{\tan \phi' \bullet \sin \alpha + \cos \alpha} + W \frac{(1 - k_v)}{\tan \phi' \bullet \sin \alpha + \cos \alpha} \\ & - (U_{static-\alpha}) \frac{\cos \alpha}{\tan \phi' \bullet \sin \alpha + \cos \alpha} - c' \bullet L \frac{\sin \alpha}{\tan \phi' \bullet \sin \alpha + \cos \alpha} \end{aligned} \quad (A.11)$$

### A.2.4 Equilibrium of Forces in the Horizontal Direction

Equilibrium of horizontal forces acting on the Figure A.1 soil wedge (with a potential slip plane at an angle  $\alpha$  from horizontal) results in the relationship

$$\begin{aligned} & P \bullet \cos \delta - N' \bullet \sin \alpha - (U_{static-\alpha}) \sin \alpha \\ & + [T] \cos \alpha - W \bullet k_h + (U_{static}) = 0 \end{aligned} \quad (A.12)$$

Substituting Equation A.3 into Equation A.12, and with the horizontal components of water pressure forces of equal magnitude and opposite direction (refer to Figure A.2), Equation A.12 simplifies to

$$P \bullet \cos \delta - N' \bullet \sin \alpha + [c' \bullet L + N' \tan \phi'] \cos \alpha - W \bullet k_h = 0 \quad (A.13)$$

Combining the  $N'$  terms results in

$$P \bullet \cos \delta - N'(\sin \alpha - \tan \phi' \bullet \cos \alpha) - W \bullet k_h + c' \bullet L \bullet \cos \alpha = 0 \quad (\text{A.14})$$

Multiplying Equation A.11 (for  $N'$ ) by  $[-(\sin \alpha - \tan \phi' \bullet \cos \alpha)]$  and simplifying<sup>1</sup> becomes

$$\begin{aligned} -N'(-\tan \phi' \bullet \cos \alpha + \sin \alpha) = & +P \sin \delta \bullet \tan(\alpha - \phi') - W(1 - k_v) \tan(\alpha - \phi') \\ & + c' \bullet L \tan(\alpha - \phi') \bullet \sin \alpha + (U_{\text{static}-\alpha}) \cos \alpha \bullet \tan(\alpha - \phi') \end{aligned} \quad (\text{A.16})$$

Substituting Equation A.16 into Equation A.14 gives

$$\begin{aligned} & P \bullet \cos \delta + P \bullet \sin \delta \bullet \tan(\alpha - \phi') \\ & - W(1 - k_v) \tan(\alpha - \phi') + c' \bullet L \bullet \tan(\alpha - \phi') \bullet \sin \alpha \\ & + c' \bullet L \bullet \cos \alpha + (U_{\text{static}-\alpha}) \cos \alpha \bullet \tan(\alpha - \phi') - W \bullet k_h = 0 \end{aligned} \quad (\text{A.17})$$

Combining terms results in

$$\begin{aligned} P[\cos \delta + \sin \delta \bullet \tan(\alpha - \phi')] = & W[(1 - k_v) \tan(\alpha - \phi') + k_h] \\ & - c' \bullet L \bullet \tan(\alpha - \phi') \bullet \sin \alpha - c' \bullet L \bullet \cos \alpha - (U_{\text{static}-\alpha}) \cos \alpha \bullet \tan(\alpha - \phi') \end{aligned} \quad (\text{A.18})$$

Solving for the resultant force,  $P$ , which acts at angle  $\delta$  for the trial soil wedge with a potential slip plane at an angle  $\alpha$  from horizontal,

$$P = \frac{\text{CONSTANT}_{A1} - \text{CONSTANT}_{A2}}{\cos \delta + \sin \delta \bullet \tan(\alpha - \phi')} \quad (\text{A.19})$$

where

$$\text{CONSTANT}_{A1} = W[(1 - k_v) \tan(\alpha - \phi') + k_h] \quad (\text{A.20})$$

and

---

<sup>1</sup> Note:  $\tan(\alpha - \phi) = \frac{\sin \alpha - \tan \phi' \bullet \cos \alpha}{\cos \alpha + \tan \phi' \bullet \sin \alpha} \bullet \frac{\frac{1}{\cos \alpha}}{\frac{1}{\cos \alpha}} = \frac{\tan \alpha - \tan \phi'}{1 + \tan \phi' \bullet \tan \alpha}$  (A.15)

$$\text{CONSTANT}_{A2} = +c' \bullet L \bullet \tan(\alpha - \phi') \bullet \sin \alpha + c' \bullet L \bullet \cos \alpha + (U_{\text{static}-\alpha}) \cos \alpha \bullet \tan(\alpha - \phi') \quad (\text{A.21})$$

The dynamic active earth pressure force,  $P_{AE}$ , is equal to the maximum value of  $P$  for the trial wedges analyzed and  $\alpha_{AE} = \alpha$  for this critical wedge, as shown in Figure A.1.

In order to assign a location to  $P_{AE}$ , the static value for  $P_A$  is needed (refer to Equation 3.24 for the moist backfill, level ground case and to Appendix C for all other cases). CorpsWallSlip proceeds with the computation of  $h_{PAE}$ , the location of the resultant force,  $P_{AE}$ , using the value for  $P_A$  computed by procedure discussed in this next section. The computation of  $h_{PAE}$  by CorpsWallSlip in an effective stress analysis is described in Sections C.1 through C.3 of Appendix C.

### A.3 Static Active Earth Pressure Force, $P_A$ — Effective Stress Analysis

The solution for the static active earth pressure force for an effective stress analysis of a partially submerged backfill is calculated by using a variation of the sweep-search wedge method derived in Section A.2. Hydrostatic water pressures are assumed within the submerged portion of the retained soil, including within the zone of cracking. The relationships needed are developed by setting  $P$  equal to  $P_{\text{Static-effective stress}}$ ,  $k_h$  and  $k_v$  equal to zero, and  $L$  equal to  $L_{\text{net}}$  in Equations A.19 through A.21. The portion of the trial wedge planar slip plane that is below the zone of cracking has the length  $L_{\text{net}}$  as shown in Figure A.3. Mohr-Coulomb shear strength parameters  $c'$  and  $\phi'$  are used to characterize the shear strength of the retained soil. In a traditional soil wedge formulation for static loading, a crack is typically considered to exist within the upper portion of the soil driving wedge for a cohesive soil (with a cohesive shear strength  $c'$  specified in an effective stress analysis) and the planer wedge slip surface is terminated when it intersects the zone of cracking at a depth  $d_{\text{crack}}$  below the ground surface (e.g., see Appendix H in EM 1110-2-2502). This assumption is made in the CorpsWallSlip formulation for static loading (but not when computing  $P_{AE}$

for dynamic loading as discussed previously<sup>1</sup>). A sweep-search wedge method of analysis as idealized in Figure A.3 is used by the  $C_{orps}W_{all}Slip$  to determine the value of the active earth pressure force,  $P_A$ .

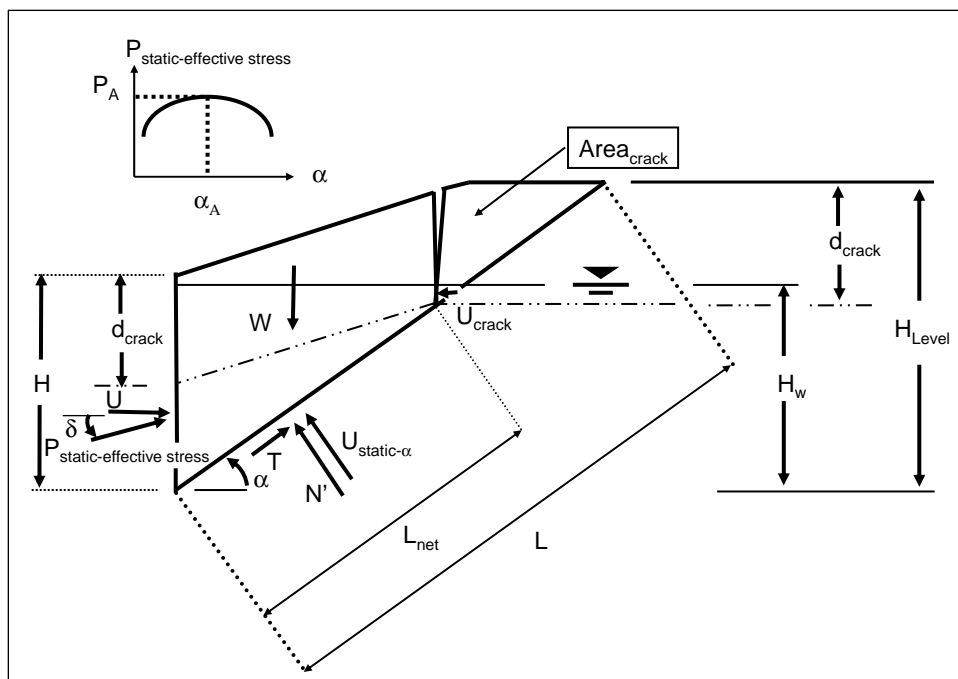


Figure A.3. Static active sweep-search wedge analysis, effective stress analysis with a hydrostatic water table (zone of cracking of depth  $d_{crack}$ ).

For a given trial soil wedge with a potential slip plane at an angle  $\alpha$  from horizontal, the resultant force  $P_{Static-effective stress}$ , which acts at angle  $\delta$  for the trial soil wedge, is given by

<sup>1</sup>  $C_{orps}W_{all}Slip$  performs a permanent displacement analysis of a retaining wall due to earthquake shaking. Reversal in the direction of the horizontal component of the time-history of earthquake ground shaking occurs many times during the typical tens of seconds of ground motion. Consequently, a reversal in direction of the inertial force imparted to the structural wedge and to the soil driving wedge occurs many times during the course of the analysis using  $C_{orps}W_{all}Slip$ . In a traditional soil wedge formulation for static loading, a crack is typically considered to exist within the upper portion of the soil driving wedge for a cohesive soil (with shear strength,  $S_u$ , specified in a total stress analysis or  $c'$  specified in an effective stress analysis) and the planar wedge slip surface is terminated when it intersects the "zone of cracking" at a depth,  $d_{crack}$ , below the ground surface (e.g., see Appendix H in EM 1110-2-2502). This assumption is not made in the  $C_{orps}W_{all}Slip$  formulation for dynamic loading. Instead, it is assumed that in the dynamic wedge formulation, the crack within the "zone of cracking" at the top of the retained cohesive soil of the driving wedge will not remain open during earthquake shaking due to the inertial load direction reversals during this time-history based  $C_{orps}W_{all}Slip$  analysis. So, even for cohesive soils, the Figure A.1 planar slip surface, obtained from the sweep-search method of analysis used by  $C_{orps}W_{all}Slip$  to obtain a value for the earthquake-induced resultant driving force,  $P_{AE}$  (acting on the structural wedge), extends uninterrupted within the driving soil wedge (in the retained soil) to the ground surface and is not terminated by a vertical crack face to the ground surface when it enters the zone of cracking.

$$P_{\text{Static-effective stress}} = \frac{\text{CONSTANT}_{A1-\text{Static}} - \text{CONSTANT}_{A2-\text{Static}}}{\cos \delta + \sin \delta \cdot \tan(\alpha - \phi')} \quad (\text{A.22})$$

where

$$\text{CONSTANT}_{A1-\text{Static}} = W [\tan(\alpha - \phi')] \quad (\text{A.23})$$

and

$$\text{CONSTANT}_{A2-\text{Static}} = +c' \cdot L_{\text{net}} \cdot \tan(\alpha - \phi') \cdot \sin \alpha + c' \cdot L_{\text{net}} \cdot \cos \alpha + (U_{\text{static}-\alpha}) \cos \alpha \cdot \tan(\alpha - \phi') \quad (\text{A.24})$$

The weight,  $W$ , of the soil wedge for the Figure A.3 bilinear soil surface problem (with cracking) is calculated using one of the procedures described in Section A.6. The static active earth pressure force,  $P_A$ , is equal to the maximum value of  $P_{\text{Static-effective stress}}$  for the trial wedges analyzed and  $\alpha_A = \alpha$  for this critical wedge using the (graphical) procedure depicted in Figure A.3.

In preparation for determining the location of resultant for location for  $P_{AE}$  (to be described in Appendix C) Equation A.22 is recast in the following form to distinguish the contribution of the weight and the frictional component of the soil wedge resultant force,  $P_{\text{Static-effective stress}}$ , from the cohesive component:

$$P_{\text{Static-effective stress}} = P_{\text{Static-}\phi\text{-weight}} - P_{\text{Static-C}} \quad (\text{A.25})$$

with

$$P_{\text{Static-}\phi\text{-weight}} = \frac{W [\tan(\alpha - \phi')] - (U_{\text{static}-\alpha}) \cos(\alpha) \cdot \tan(\alpha - \phi')}{\cos \delta + \sin \delta \cdot \tan(\alpha - \phi')} \quad (\text{A.26})$$

and

$$P_{\text{Static-C}} = \frac{c' \cdot L_{\text{net}} \cdot [\tan(\alpha - \phi')] \cdot \sin \alpha + c' \cdot L_{\text{net}} \cdot \cos \alpha}{\cos \delta + \sin \delta \cdot \tan(\alpha - \phi')} \quad (\text{A.27})$$

Note that the frictional/weight component,  $P_{\text{Static-}\phi\text{-weight}}$ , of resultant force  $P_{\text{Static-effective stress}}$  (Equation A.25) is reduced by the cohesion force

component,  $P_{\text{static-C}}$ . The subtraction force  $P_{\text{static-C}}$  in Equation A.25 reflects a resultant force component  $P_{\text{static-C}}$  for a *tensile stress* distribution component, to be discussed in Appendix C.

A depth of cracking is considered in an effective stress analysis of  $P_A$  with the assignment of a nonzero value for cohesion ( $c'$ ). CorpsWallSlip uses a trial-and-error procedure to determine the value for  $d_{\text{crack}}$  when computing  $P_A$ . In this iterative procedure, (1) an initial value for  $d_{\text{crack}}$  is assumed (set equal to zero in the first iteration); (2) the trial wedge procedure of analysis discussed in this section is performed and a corresponding trial value for  $P_A$  is computed, along with values for its frictional/weight force component,  $P_{\text{static-}\phi\text{-weight}}$ , and for cohesion force component,  $P_{\text{static-C}}$ ; (3) a new depth of crack is computed based on values for  $P_{\text{static-}\phi\text{-weight}}$  and  $P_{\text{static-C}}$  and their corresponding earth pressure distributions that are determined using the procedure outlined in Section C.3 for  $P_A$ ; (4) repeat these steps (1) through (3) until convergence in the value for  $d_{\text{crack}}$  is achieved. CorpsWallSlip uses the  $P_A$  value in the computation of  $h_{\text{PAE}}$ , the location of the resultant force  $P_{\text{AE}}$  as discussed in Appendix C, using the last value for  $P_A$  computed by this trial-and-error procedure.

#### A.4 Dynamic Active Earth Pressure Force, $P_{\text{AE}}$ — Total Stress Analysis

In a total stress analysis, the value for the dynamic active earth pressure force,  $P_{\text{AE}}$ , is computed based on a user-specified shear strength,  $S_u$ , for the retained soil. The dynamic active earth pressure force is also computed for this situation using the sweep-search wedge method described in Section A.2 but with the following two changes; (1) cohesion term  $c'$  is set equal to  $S_u$ , with  $\phi'$  and the interface friction angle  $\delta$  set to zero, and (2) the pore water pressures internal to the soil wedge are set equal to zero. The relationships needed are developed from Equations A.19 through A.21. For a given trial soil wedge with a potential slip plane at an angle  $\alpha$  from horizontal, the resultant force  $P_{S_u}$  is given by

$$P_{S_u} = \text{CONSTANT}_{A1-S_u} - \text{CONSTANT}_{A2-S_u} \quad (\text{A.28})$$

where

$$\text{CONSTANT}_{A1-S_u} = W \left[ (1 - k_v) \tan(\alpha) + k_h \right] \quad (\text{A.29})$$

and

$$CONSTANT_{A2-Su} = +S_u \bullet L \bullet \tan(\alpha) \bullet \sin \alpha + S_u \bullet L \bullet \cos \alpha \quad (A.30)$$

The dynamic active earth pressure force,  $P_{AE}$ , is equal to the maximum value of  $P_{Su}$  for the trial wedges analyzed and  $\alpha_{AE} = \alpha$  for this critical wedge, analogous to the (graphical) procedure depicted in Figure A.1 for determining the value of  $P_{AE}$  from all values for  $P$ .

Recall the entire slip plane length,  $L$ , is used in the analysis of the driving soil wedge for cohesive soils to compute  $P_{AE}$  due to the assumption that the zone of cracking at the top of the retained cohesive soil of the driving soil wedge will not remain open during earthquake shaking due to load direction reversals during this time-history based CorpsWallSlip analysis.<sup>1</sup>

In order to assign a location to  $P_{AE}$  the static value for  $P_A$  is needed. CorpsWallSlip proceeds with the computation of  $h_{PAE}$ , the location of the resultant force  $P_{AE}$ , using the value for  $P_A$  computed by procedure discussed in this next section. The computation of  $h_{PAE}$  by CorpsWallSlip in a total stress analysis is described in Section C.4 of Appendix C.

## A.5 Static Active Earth Pressure Force, $P_A$ — Total Stress Analysis

In a traditional soil wedge formulation for static loading, a crack is typically considered to exist within the upper portion of the soil driving wedge for a cohesive soil (with a undrained shear strength,  $S_u$ , specified in a total stress analysis) and the planer wedge slip surface is terminated when it intersects the zone of cracking at a depth,  $d_{crack}$ , below the ground

<sup>1</sup> CorpsWallSlip performs a permanent displacement analysis of a retaining wall due to earthquake shaking. Reversal in the direction of the horizontal component of the time-history of earthquake ground shaking occurs many times during the typical tens of seconds of ground motion. Consequently, a reversal in direction of the inertial force imparted to the structural wedge and to the soil driving wedge occurs many times during the course of the analysis using CorpsWallSlip. In a traditional soil wedge formulation for static loading, a crack is typically considered to exist within the upper portion of the soil driving wedge for a cohesive soil (with shear strength,  $S_u$ , specified in a total stress analysis or  $c'$  specified in an effective stress analysis) and the planer wedge slip surface is terminated when it intersects the "zone of cracking" at a depth,  $d_{crack}$ , below the ground surface (e.g., see Appendix H in EM 1110-2-2502). This assumption is not made in the CorpsWallSlip formulation for dynamic loading. Instead, it is assumed that in the dynamic wedge formulation, the crack within the "zone of cracking" at the top of the retained cohesive soil of the driving wedge will not remain open during earthquake shaking due to the inertial load direction reversals during this time-history based CorpsWallSlip analysis. So, even for cohesive soils, the Figure A.1 planar slip surface, obtained from the sweep-search method of analysis used by CorpsWallSlip to obtain a value for the earthquake-induced resultant driving force,  $P_{AE}$  (acting on the structural wedge), extends uninterrupted within the driving soil wedge (in the retained soil) to the ground surface and is not terminated by a vertical crack face to the ground surface when it enters the zone of cracking.



surface (e.g., see Appendix H in EM 1110-2-2502). This assumption is made in the CorpsWallSlip formulation for static loading (but not when computing  $P_{AE}$  for dynamic loading as discussed previously). A sweep-search wedge method of analysis as idealized in Figure A.4 is used by the CorpsWallSlip to determine the value of the active earth pressure force  $P_A$ . The solution for the static active earth pressure force for a total stress analysis of a partially submerged backfill is calculated by using a variation of the sweep-search wedge method derived in Section A.3. The static active earth pressure force is computed for this situation using the sweep-search wedge method described in Section A.3 but with the following three changes; (1) the term  $P_{\text{Static-effective stress}}$  is set equal to  $P_{\text{Static-total stress}}$ , (2) cohesion term  $c'$  is set equal to  $S_u$ , with  $\phi'$  and the interface friction angle  $\delta$  set to zero, and (3) the pore water pressures internal to the soil wedge are set equal to zero. Hydrostatic water pressures due to the presence of water within the cracks in the zone of cracking are considered.

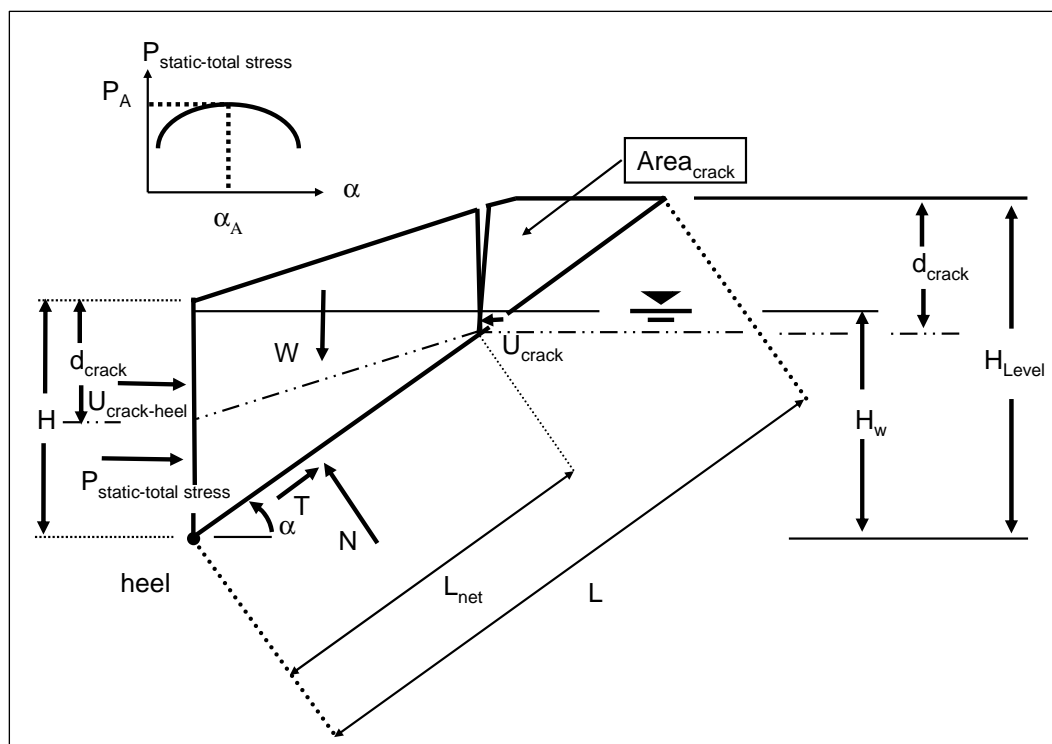


Figure A.4. Static active sweep-search wedge analysis, total stress analysis with a hydrostatic water table (zone of cracking of depth  $d_{\text{crack}}$ ).

The relationships needed are developed from Equations A.22 through A.24. For a given trial soil wedge with a potential slip plane at an angle  $\alpha$  from horizontal, the resultant force  $P_{\text{Static-total stress}}$  is given by

$$P_{\text{static-total stress}} = P_{\text{Static-weight}} - P_{\text{Static-Su}} - \Delta U \quad (\text{A.31})$$

$$P_{\text{Static-weight}} = W \cdot \tan(\alpha) \quad (\text{A.32})$$

$$P_{\text{Static-Su}} = Su \cdot L_{\text{net}} \cdot \tan(\alpha) \cdot \sin(\alpha) + Su \cdot L_{\text{net}} \cdot \cos(\alpha) \quad (\text{A.33})$$

with the difference in water pressure force within the cracks on both sides and acting on the soil driving wedge is given by

$$\Delta U = U_{\text{crack-heel}} - U_{\text{crack}} \quad (\text{A.34})$$

The weight,  $W$ , of the soil wedge for the Figure A.4 bilinear soil surface problem (with cracking) is calculated using one of the procedures described in Section A.6. The static active earth pressure force,  $P_A$ , is equal to the maximum value of  $P_{\text{static-total stress}}$  for the trial wedges analyzed and  $\alpha_A = \alpha$  for this critical wedge, using the (graphical) procedure depicted in Figure A.4.

Equation A.31 distinguishes the contribution of the weight component of the soil wedge to  $P_{\text{static-total stress}}$  from the cohesive component. Note that the weight component,  $P_{\text{static-weight}}$ , of resultant force  $P_{\text{static-total stress}}$  (Equation A.31) is reduced by the cohesion force component,  $P_{\text{static-Su}}$ . The subtraction the force  $P_{\text{static-Su}}$  in Equation A.31 reflects a resultant force component,  $P_{\text{static-Su}}$ , for a *tensile stress* distribution component, to be discussed in Appendix C.

A depth of cracking is considered in a total stress analysis of  $P_A$  with the assignment of a nonzero value for cohesion ( $S_u$ ). CorpsWallSlip uses a trial-and-error procedure to determine the value for  $d_{\text{crack}}$  when computing  $P_A$ . In this iterative procedure, (1) an initial value for  $d_{\text{crack}}$  is assumed (set equal to zero in the first iteration); (2) the trial wedge procedure of analysis discussed in this section is performed and a corresponding trial value for  $P_A$  is computed, along with values for its weight force component,  $P_{\text{static-weight}}$ , and for cohesion force component,  $P_{\text{static-Su}}$ ; (3) a new depth of crack is computed based on values for  $P_{\text{static-weight}}$  and  $P_{\text{static-Su}}$  and their corresponding earth pressure distributions that are determined using the procedure outlined in Section C.4 for  $P_A$ ; (4) repeat these steps (1) through (3) until convergence in the value for  $d_{\text{crack}}$  is achieved. CorpsWallSlip proceeds with the computation of  $h_{\text{PAE}}$ , the location of the

resultant force  $P_{AE}$  as discussed in Appendix C, using the last value for  $P_A$  computed by this trial-and-error procedure.

## A.6 Weight Computation of a Soil Wedge with a Bilinear Ground Surface

$CorpsWallSlip$  computes the value for  $P_{AE}$  and  $P_A$  via Figure B.1 sweep-search method. An advantage of the sweep-search method is that it allows for the analysis of the more practical case of the bilinear ground surface depicted in Figure B.1.b. The computation of the area of soil wedge above and below the water table and total weight,  $W$ , are made as follows:

### A.6.1 $\alpha$ greater than $\alpha_{corner}$

For the case of the soil wedge with a potential slip plane at an angle  $\alpha$  from horizontal being greater than the angle designated  $\alpha_{corner}$ , defining the line between the point corresponding to the heel of the wall and the intersection of the level backfill and the sloping ground surface point 4 in Figure A.5, the total cross-sectional area is

$$Area_{total} = \frac{1}{2} \bullet \{x_1 \bullet [y_2 - y_3] + x_2 \bullet [y_3 - y_1] + x_3 \bullet [y_1 - y_2]\} \quad (A.35)$$

with  $(x_1, y_1)$ ,  $(x_2, y_2)$ , and  $(x_3, y_3)$  being the vertices of the triangle of the trial soil wedge shown in this figure. Point 5 denotes the intersection of the hydrostatic water table with the planar trial wedge that extends from point 1 to point 2. The area of the trial soil wedge below the water table is designated  $AreaW$  in this figure.



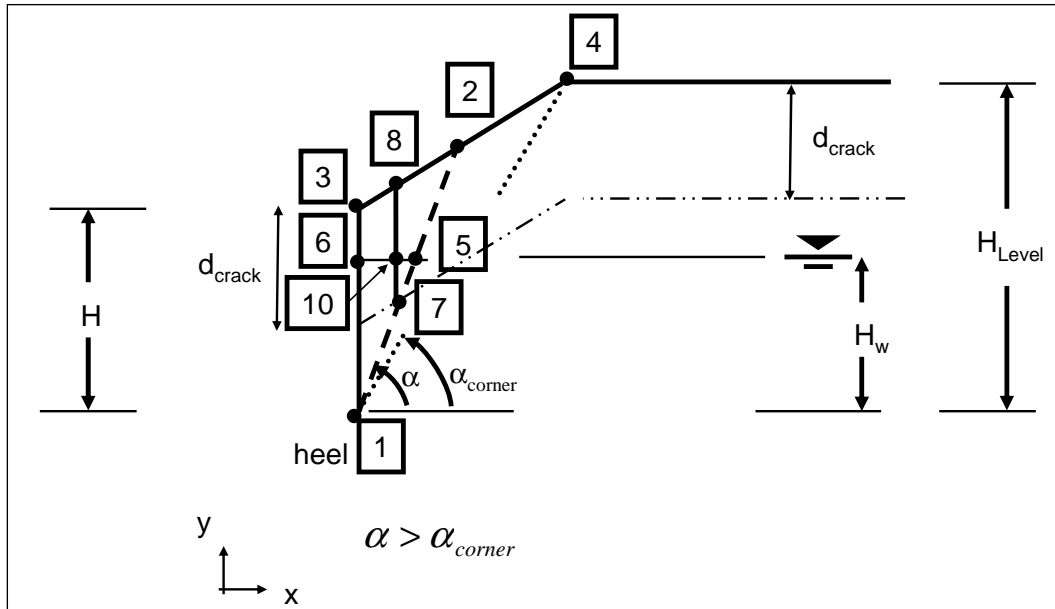


Figure A.6. Soil wedge defined by a bilinear ground surface with  $\alpha$  greater than  $\alpha_{\text{corner}}$  and crack depth  $d_{\text{crack}}$  that extends below the water table.

The portion of the total cross-sectional area (i.e.,  $\text{Area}_{\text{total}}$  by Equation A.35) entirely contained within the depth of cracking zone is given by

$$\text{Area}_{\text{crack}} = \frac{1}{2} \cdot \{x_7 \cdot [y_2 - y_8] + x_2 \cdot [y_8 - y_7] + x_8 \cdot [y_7 - y_2]\} \quad (\text{A.36})$$

with  $(x_7, y_7)$ ,  $(x_2, y_2)$ , and  $(x_8, y_8)$  being the vertices of the triangle of the trial soil wedge identified Figure A.7. Consequently, the total soil wedge area less this triangular zone of cracking ( $\text{Area}_{\text{crack}}$ ) is designated as the  $\text{Area}_{\text{net}}$  and is computed to be

$$\text{Area}_{\text{net}} = \text{Area}_{\text{total}} - \text{Area}_{\text{crack}} \quad (\text{A.37})$$

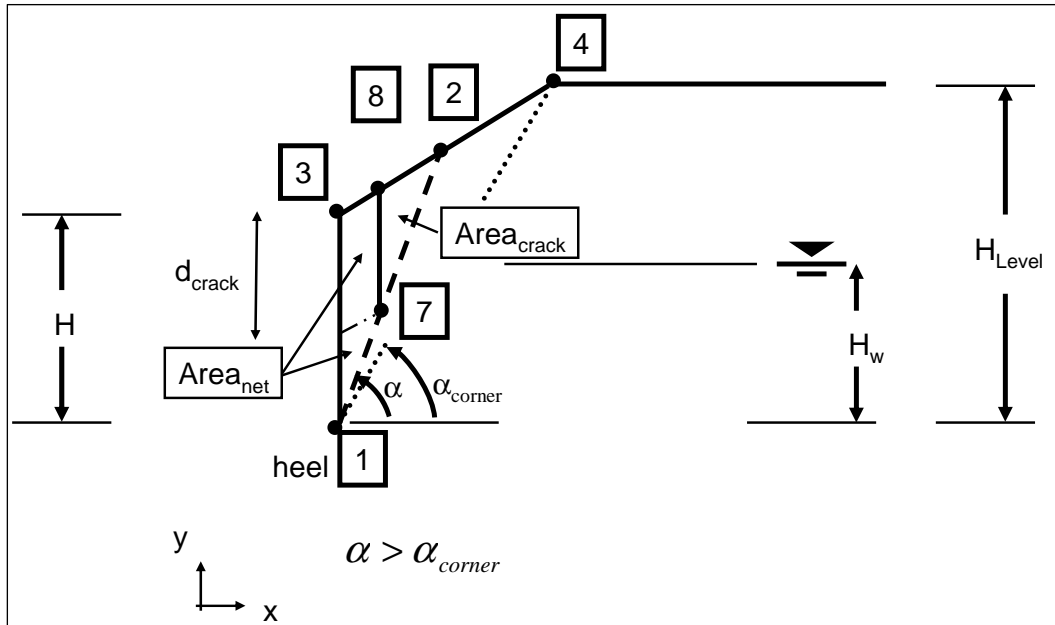


Figure A.7.  $Area_{net}$  and  $Area_{crack}$  within the soil wedge defined by a bilinear ground surface with  $\alpha$  greater than  $\alpha_{corner}$  for a crack depth  $d_{crack}$  that extends below the water table.

The cross-sectional area of the entire submerged portion of the trial soil wedge (with crack) is

$$AreaW = \frac{1}{2} \cdot \{x_1 \cdot [y_5 - y_6] + x_5 \cdot [y_6 - y_1] + x_6 \cdot [y_1 - y_5]\} \quad (A.38)$$

with  $(x_1, y_1)$ ,  $(x_5, y_5)$ , and  $(x_6, y_6)$  being the vertices of the triangle of the submerged portion of the soil wedge, as shown in Figure A.5. The portion of the area given by Equation A.38, i.e., the total submerged cross-sectional area (i.e.,  $AreaW$ ), contained within the depth of cracking is

$$AreaW_{crack} = \frac{1}{2} \cdot \{x_7 \cdot [y_5 - y_{10}] + x_5 \cdot [y_{10} - y_7] + x_{10} \cdot [y_7 - y_5]\} \quad (A.39)$$

with  $(x_7, y_7)$ ,  $(x_5, y_5)$ , and  $(x_{10}, y_{10})$  being the vertices of the triangle of the trial soil wedge identified Figure A.8. The total cross-sectional area of the submerged portion of the trial soil wedge (with crack) less the triangular zone of cracking below the water table is designated in Figure A.8 as  $AreaW_{net}$  and given by

$$AreaW_{net} = AreaW - AreaW_{crack} \quad (A.40)$$

Consequently, the net moist cross-sectional area of the trial soil wedge above the water table is equal to

$$Area_{moist-net} = Area_{net} - AreaW_{net} \quad (A.41)$$

and identified in Figure A.8.

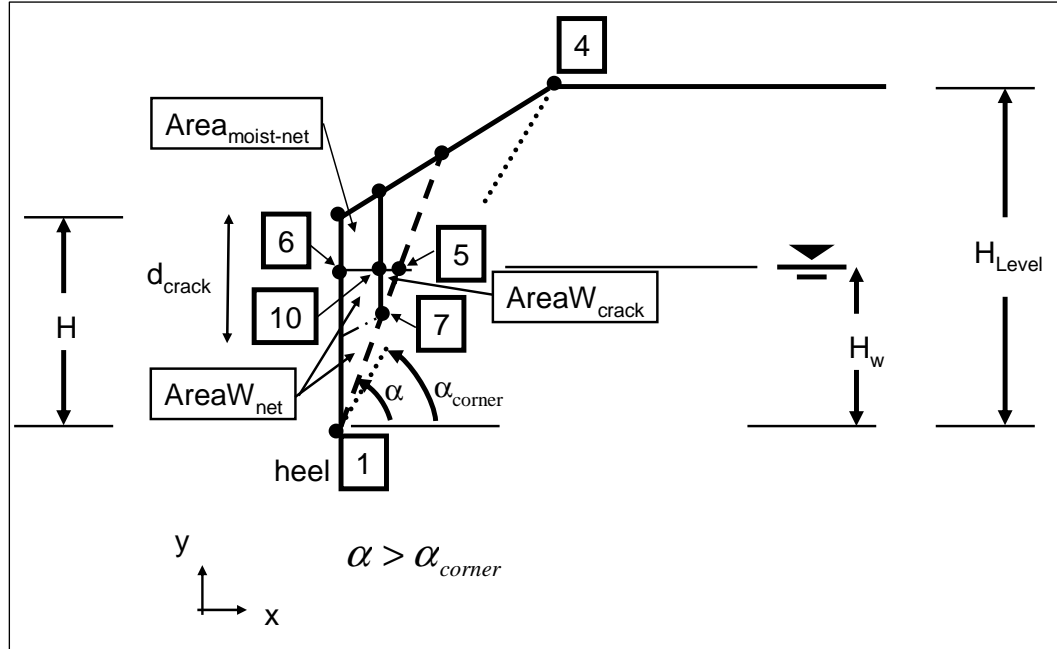


Figure A.8.  $Area_{moist-net}$ ,  $AreaW_{net}$ , and  $AreaW_{crack}$  within the soil wedge defined by a bilinear ground surface with  $\alpha$  greater than  $\alpha_{corner}$  and crack depth  $d_{crack}$  that extends below the water table.

The weight of the net submerged portion of the trial soil wedge,  $W_{saturated}$ , is

$$W_{saturated} = \gamma_{saturated} \bullet AreaW_{net} \quad (A.42)$$

with the weight of the net moist portion of the soil wedge

$$W_{moist} = \gamma_{moist} \bullet Area_{moist-net} \quad (A.43)$$

The total weight for the net trial soil wedge, considering a depth of crack,  $d_{crack}$ , is equal to

$$W = W_{saturated} + W_{moist} \quad (A.44)$$

This and the other relationships given in this subsection are also valid in the case of  $d_{\text{crack}}$  equal to zero, i.e., cohesionless soils.

#### A.6.2 $\alpha_{\text{corner}}$ greater than $\alpha$

For the case in which the angle  $\alpha_{\text{corner}}$  (from horizontal), defining the line between the point corresponding to the heel of the wall and point 4 in Figure A.9 that designates the intersection of the level backfill and the sloping ground surface, is greater than the angle  $\alpha$  of soil wedge for the potential slip plane, the total cross-sectional area is

$$\text{Area}_{\text{total}} = \frac{1}{2} \cdot \left\{ \begin{aligned} &x_1 \cdot [y_2 - y_4] + x_2 \cdot [y_4 - y_1] + x_4 \cdot [y_1 - y_2] + \\ &x_1 \cdot [y_4 - y_3] + x_4 \cdot [y_3 - y_1] + x_3 \cdot [y_1 - y_4] \end{aligned} \right\} \quad (\text{A.45})$$

with  $(x_1, y_1)$ ,  $(x_2, y_2)$ , and  $(x_4, y_4)$ , and with  $(x_1, y_1)$ ,  $(x_4, y_4)$ , and  $(x_3, y_3)$  being the vertices of the two triangles that form the soil wedge shown in this figure. The area of the trial soil wedge below the water table is designated AreaW in this figure and is defined by the vertices  $(x_1, y_1)$ ,  $(x_5, y_5)$ , and  $(x_6, y_6)$ .

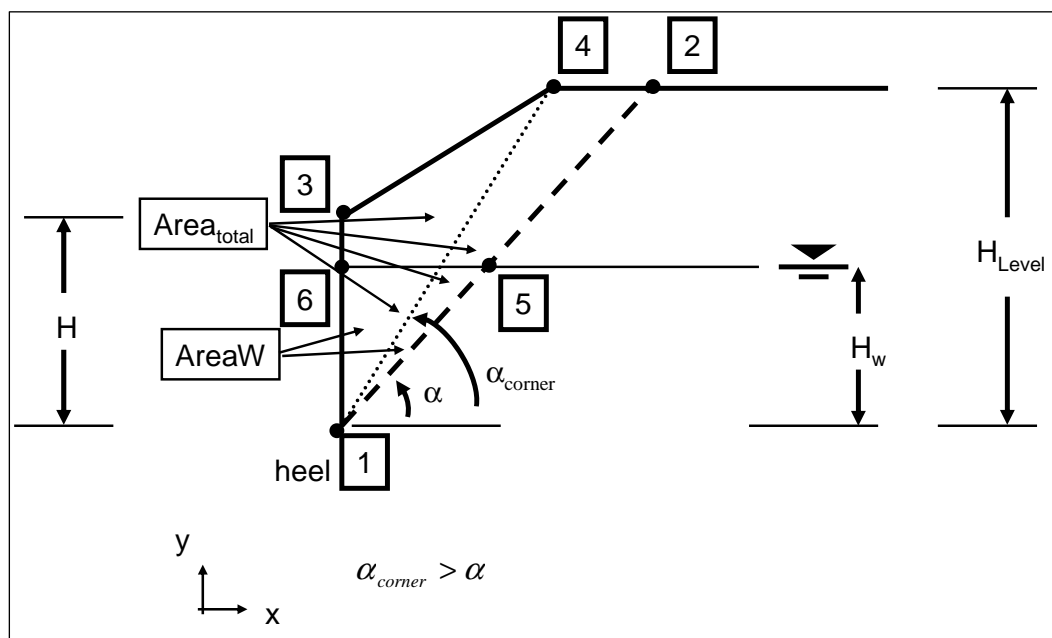


Figure A.9. Soil wedge defined by a bilinear ground surface with  $\alpha_{\text{corner}}$  greater than  $\alpha$ .



### A.6.2.1 $d_{crack} > \Delta_{4to9}$

Figure A.10 extends the Figure A.9 case to consider a crack within a retained (cohesive) soil. Note the depth of cracking extends from the ground surface to a depth,  $d_{crack}$ , below the sloping ground surface as well as below the level portion of the retained soil. The case shown is for a crack depth that intersects the planer trial slip plane (extending from points 1 to 2) below the sloping ground surface of slope  $\beta$  (versus below the level ground surface region). This intersection point is designated as point 7 in this figure, corresponding to the case of  $d_{crack} > \Delta_{4to9}$ . Point 9 defines the point along the planar trial slip surface (extending from point 1 to point 2) that is below point 4. The case shown in Figure A.10 is for point 7 above the hydrostatic water table. Points 7, 2, 4, and 8 delineate a region of the trial soil wedge that is fully contained within the depth of cracking (i.e.,  $Area_{crack}$ ).

$$Area_{crack} = \left[ \frac{(x_4 - x_8) + (x_9 - x_7)}{2} \right] \cdot \left[ \frac{(y_4 - y_9) + (y_8 - y_7)}{2} \right] + \frac{1}{2} \cdot \{ x_9 \cdot (y_2 - y_4) + x_2 \cdot (y_4 - y_9) + x_4 \cdot (y_9 - y_2) \} \quad (A.46)$$

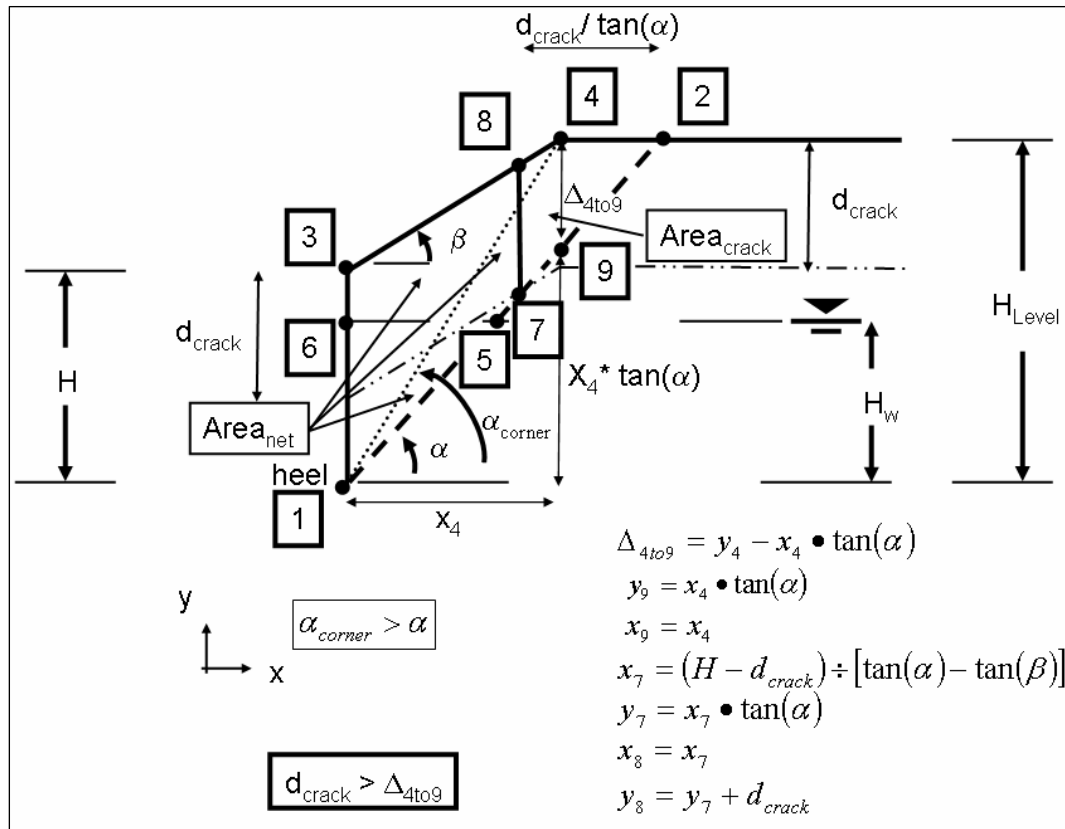


Figure A.10. Soil wedge defined by a bilinear ground surface with  $\alpha_{corner}$  greater than  $\alpha$  and crack depth,  $d_{crack}$ , that extends below the water table ( $d_{crack} > \Delta_{4to9}$ ).

The total soil wedge area less this triangular zone of cracking ( $Area_{crack}$ ) is designated as the  $Area_{net}$  in Figure A.10 and is computed to be

$$Area_{net} = Area_{total} - Area_{crack} \quad (\text{bis A.37})$$

The cross-sectional area of the entire submerged portion of the trial soil wedge, designated  $AreaW$ , is given by Equation A.38. Figure A.11 extends Figure A.10 so as to distinguish the moist net area, designated  $Area_{moist-net}$ , from the submerged net area, designated  $AreaW_{net}$ .

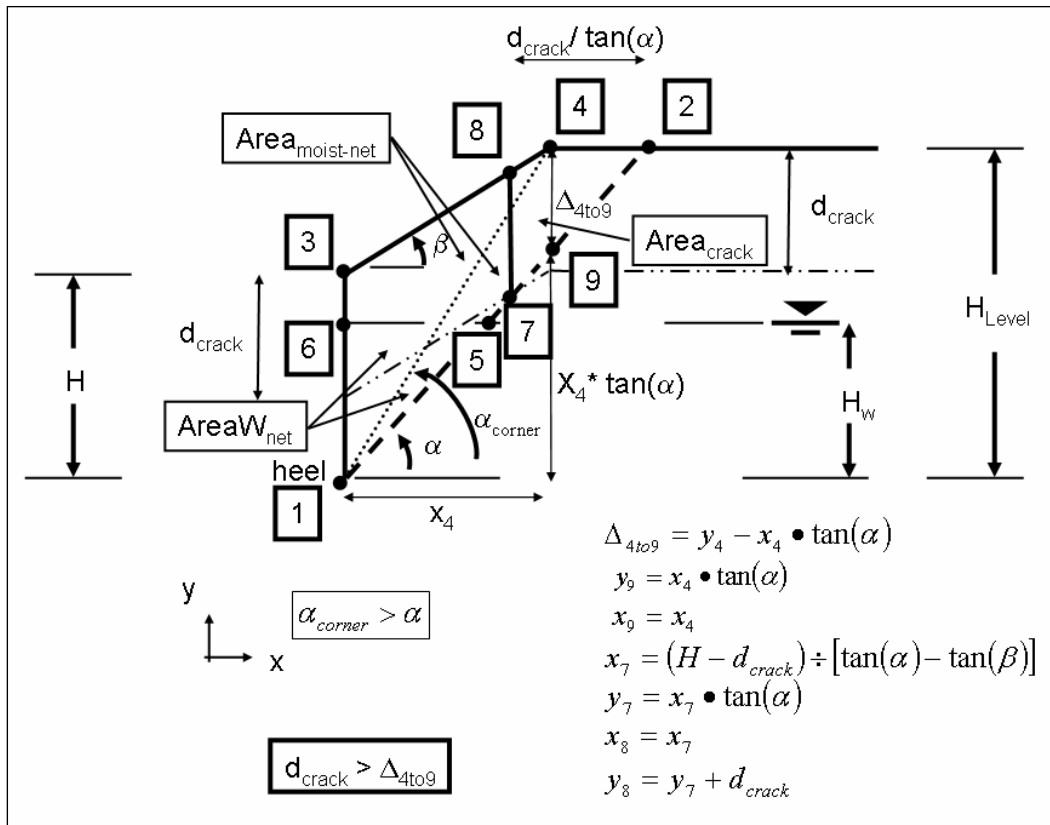


Figure A.11.  $Area_{moist-net}$ ,  $AreaW_{net}$ , and  $AreaW_{crack}$  within the soil wedge defined by a bilinear ground surface with  $\alpha_{corner}$  greater than  $\alpha$  and crack depth,  $d_{crack}$  ( $d_{crack} > \Delta_{4to9}$ ).

In the Figures A.9 through A.10 case, the zone of cracking is above the hydrostatic water table. Should the crack zone include a region of cracking below the water table as is the case for Figure A.8 when  $y_7$  is less than  $H_w$ , the total cross-sectional area of the submerged portion of the trial soil wedge (with crack) less the triangular zone of cracking below the water table is equal to  $AreaW_{net}$  and is given by

$$AreaW_{net} = AreaW - AreaW_{crack} \quad (\text{bis A.40})$$

$AreaW_{crack}$  is given by Equation A.39. Consequently, the net moist cross-sectional area of the trial soil wedge above the water table is equal to

$$Area_{moist-net} = Area_{net} - AreaW_{net} \quad (\text{bis A.41})$$

and identified in Figure A.11.

The weight of the net submerged portion of the trial soil wedge,  $W_{saturated}$ , is

$$W_{saturated} = \gamma_{saturated} \bullet Area W_{net} \quad (\text{bis A.42})$$

with the weight of the net moist portion of the soil wedge

$$W_{moist} = \gamma_{moist} \bullet Area_{moist-net} \quad (\text{bis A.43})$$

The total weight for the net trial soil wedge, considering a depth of crack,  $d_{crack}$ , is equal to

$$W = W_{saturated} + W_{moist} \quad (\text{bis A.44})$$

This and the other relationships given in this subsection are also valid in the case of  $d_{crack}$  equal to zero, i.e., cohesionless soils.

#### A.6.2.2 $d_{crack} < \Delta_{4to9}$

Figure A.12 extends the Figure A.9 case to consider a crack within a retained (cohesive) soil and for a crack depth that intersects the planer trial slip plane (extending from points 1 to 2) below the level ground surface region of retained soil (versus below the sloping ground surface retained soil region). This intersection point is designated as point 7 in this figure, corresponding to the case of  $d_{crack} < \Delta_{4to9}$ . Point 9 defines the point along the planar trial slip surface (extending from point 1 to point 2) that is below point 4. The case shown in Figure A.10 is for point 7 above the hydrostatic water table. Points 7, 2, and 8 delineate a triangular region of the trial soil wedge that is fully contained within the depth of cracking (i.e.,  $Area_{crack}$ ). The portion of the total cross-sectional area (i.e.,  $Area_{total}$  by Equation A.45) entirely contained within the depth of cracking zone is given by

$$Area_{crack} = \frac{1}{2} \bullet \{x_7 \bullet [y_2 - y_8] + x_2 \bullet [y_8 - y_7] + x_8 \bullet [y_7 - y_2]\} \quad (\text{bis A.36})$$



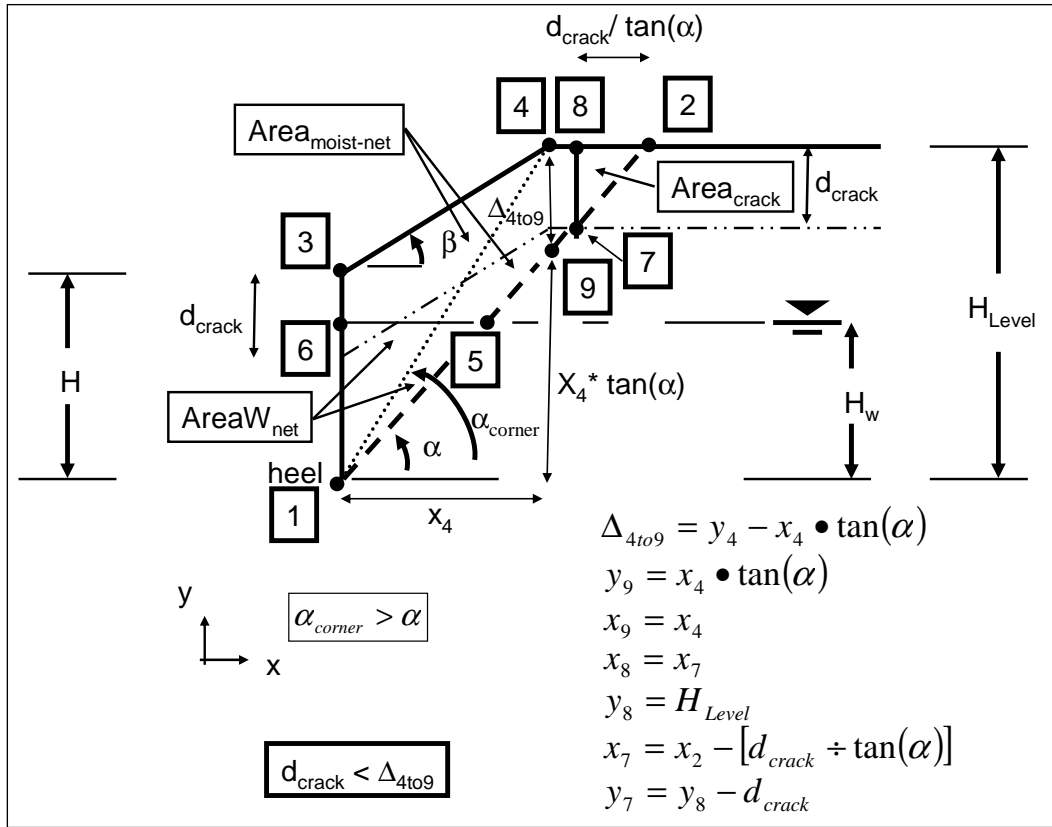


Figure A.13.  $Area_{moist-net}$ ,  $AreaW_{net}$ , and  $AreaW_{crack}$  within the soil wedge defined by a bilinear ground surface with  $\alpha_{corner}$  greater than  $\alpha$  and crack depth,  $d_{crack}$  ( $d_{crack} < \Delta_{4to9}$ ).

In the Figures A.12 and A.13 case, the portion of the soil wedge contained within the zone of cracking (designated  $Area_{crack}$ ) is above the hydrostatic water table. Should this crack zone include a region of cracking below the water table as is the case for Figure A.8 when  $y_7$  is less than  $H_w$ , the total cross-sectional area of the submerged portion of the trial soil wedge (with crack) less the triangular zone of cracking below the water table is equal to  $AreaW_{net}$  and is given by

$$AreaW_{net} = AreaW - AreaW_{crack} \quad (\text{bis A.40})$$

$AreaW_{crack}$  is given by Equation A.39. Consequently, the net moist cross-sectional area of the trial soil wedge above the water table is equal to

$$Area_{moist-net} = Area_{net} - AreaW_{net} \quad (\text{bis A.41})$$

and identified in Figure A.11.

The weight of the net submerged portion of the trial soil wedge,  $W_{\text{saturated}}$ , is

$$W_{\text{saturated}} = \gamma_{\text{saturated}} \bullet \text{Area} W_{\text{net}} \quad (\text{bis A.42})$$

with the weight of the net moist portion of the soil wedge

$$W_{\text{moist}} = \gamma_{\text{moist}} \bullet \text{Area}_{\text{moist-net}} \quad (\text{bis A.43})$$

The total weight for the net trial soil wedge, considering a depth of crack,  $d_{\text{crack}}$ , is equal to

$$W = W_{\text{saturated}} + W_{\text{moist}} \quad (\text{bis A.44})$$

This and the other relationships given in this subsection are also valid in the case of  $d_{\text{crack}}$  equal to zero, i.e., cohesionless soils.

## Appendix B: Dynamic Active Earth Pressure Force, $P_{AE}$ and its Point of Application, $h_{PAE}$

This appendix summarizes the procedure used to compute the point of application of  $P_{AE}$ , designated  $h_{PAE}$ . The sweep-search wedge solution is used to compute the values for  $P_{AE}$ , as outlined in Appendix A.

Figure 2.2 shows an idealized structural wedge containing a cantilever retaining wall retaining moist backfill with externally applied forces acting on it during the seismically induced translation of the wall. One of the forces identified in this figure is the dynamic active resultant earth pressure force exerted by the driving soil wedge on the structural wedge,  $P_{AE}$ . Rather than relying on the Mononobe-Okabe relationship, a sweep-search wedge formulation within the retained soil is used to determine the value of  $P_{AE}$ . Recall that the Mononobe-Okabe relationship is valid for a retained soil with a constant surface slope (including the case of a level backfill) and whose strength is characterized by the Mohr-Coulomb shear strength parameter  $\phi$  (e.g., refer to Equations 33 through 35 in Ebeling and Morrison (1992)). The computed value for  $P_{AE}$  via the Figure B.1.a sweep-search method in a cohesionless backfill will agree with the value computed using the Mononobe-Okabe relationship. The advantage of the sweep-search method, as formulated in this report and implemented in CorpsWallSlip, is that it allows for (1) the analysis of the more practical case of the bilinear ground surface depicted in Figure B.1.b and/or (2) the analysis of “cohesive” ( $S_u$ ) soils. Sufficient wall movement during earthquake shaking to fully mobilize the shear resistance within the retained soil as per Table 1.1 criteria is assumed in this formulation. The sweep-search formulation implemented within CorpsWallSlip is given in Appendix A for effective shear strength ( $c'$ ,  $\phi'$ ) and for undrained ( $S_u$ ) shear strength soil parameters.



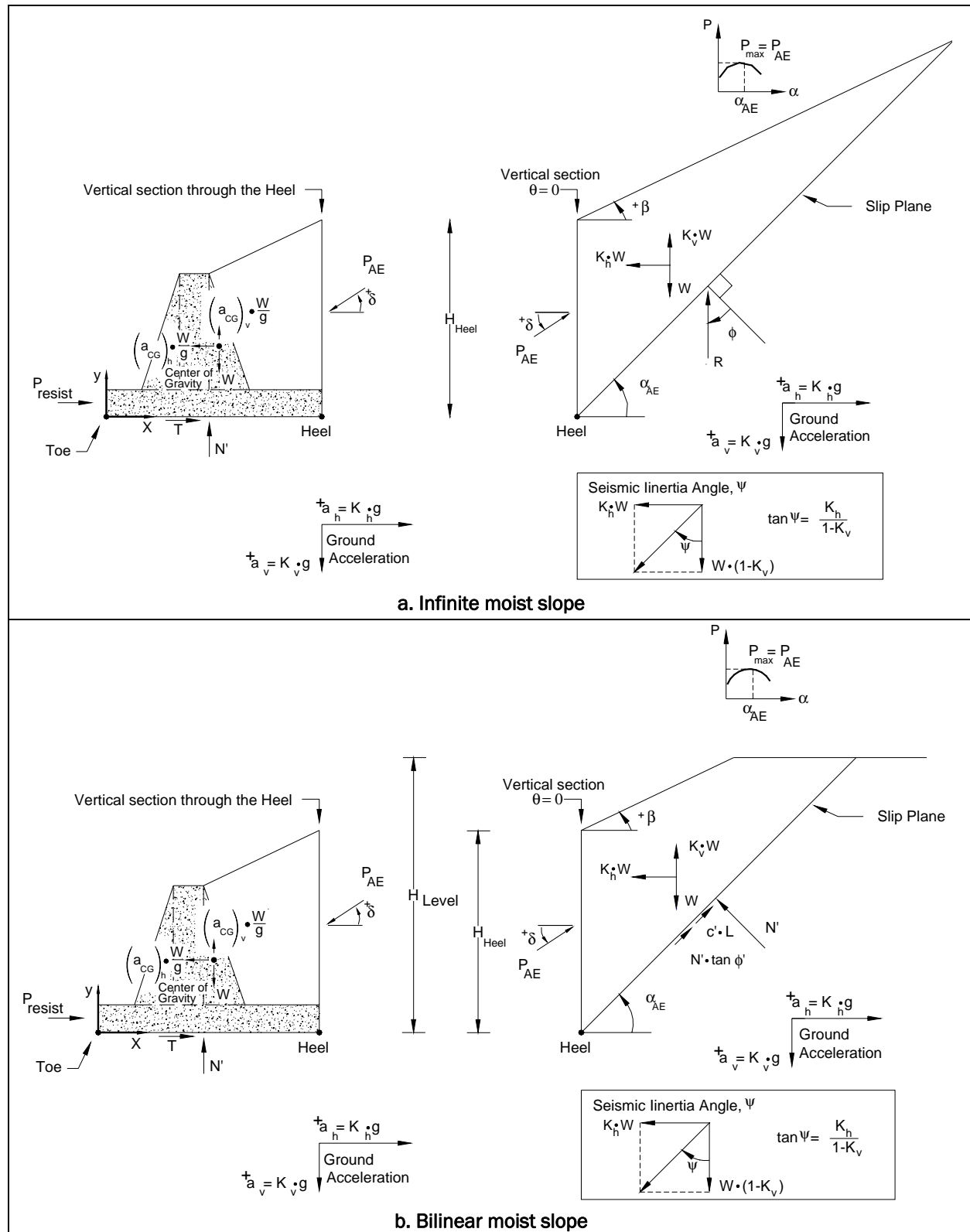


Figure B.1. Structural wedge with toe resistance retaining a driving soil wedge with a moist slope (i.e., no water table) analyzed by effective stress analysis with full mobilization of  $(c', \phi')$  shear resistance within the backfill.

The effect of an earthquake on the driving soil wedge is incorporated through the use of the user-specified horizontal and vertical components of the ground acceleration time-histories,  $a_h (= k_h g)$  and  $a_v (= k_v g)$ , respectively. Recall that  $g$  is the universal gravitational constant while  $k_h$  and  $k_v$  are the respective *time-histories* of the horizontal and vertical ground accelerations, expressed in decimal fraction. No potential site amplification effects are considered in this simplified formulation so the ground acceleration time-histories are assumed to act within the driving soil wedge as well. So, at each instant in time during earthquake shaking, the horizontal and vertical inertia forces ( $k_h$  times soil wedge weight,  $W$ , and  $k_v$  times soil wedge weight  $W$ , respectively) acts at the center of mass of the soil wedge and in the direction opposite to that in which their respective component ground acceleration acts (refer to the right-hand side of Figures B.1.a and B.1.b).

The Mononobe-Okabe analysis procedure does not provide a means for calculating the point of action of the resulting force  $P_{AE}$ , nor does the sweep-search soil wedge method of analysis. Limited test results involving dry sands (as discussed on page 63 in Ebeling and Morrison (1992)) indicate that the vertical position of  $P_{AE}$  ranges from 0.4 to 0.55 times the height of the wall (above the heel).  $P_{AE}$  acts at a higher position along the back of the wall than the static active earth pressure force due to the concentration of soil mass comprising the sliding wedge above the mid-wall height (Figure B.2). With the static force component of  $P_{AE}$  acting below mid-wall height and the inertia force component of  $P_{AE}$  acting above mid-wall height, the vertical position of the resultant force,  $P_{AE}$ , will depend upon the magnitude of the accelerations applied to the mass comprising the soil wedge. Following the approach taken by Seed and Whitman (1970),  $P_{AE}$  is defined as the sum of the initial static active earth pressure force,  $P_A$ , and the dynamic active earth pressure force increment,  $\Delta P_{AE}$ ,

$$P_{AE} = P_A + \Delta P_{AE} \quad (B.1)$$

as depicted in Figure B.2. The sweep-search method is also used in CorpsWallSlip to compute the resultant static active earth pressure force,  $P_A$ . After reviewing the various results, Seed and Whitman (1970) suggested applying the dynamic force component  $\Delta P_{AE}$  at 0.6 times  $H$ . Based on this recommendation, computation of the location of the resultant force  $P_{AE}$  along the imaginary vertical section extending upwards from the heel of the wall is made using

$$h_{PAE} = \frac{P_A \cdot \left(\frac{H}{3}\right) + \Delta P_{AE} \cdot (0.6 \cdot H)}{P_{AE}} \quad (B.2)$$

with  $P_A$  acting at  $H/3$  for moist, *level*, granular (with  $c' = 0$ ) backfill.<sup>1</sup> Note that the magnitude of  $P_{AE}$  and thus, the magnitude of  $h_{PAE}$  is a function of the seismic coefficient used in the driving wedge seismic analysis. The solution process implemented in CorpsWallSlip is to first compute  $P_{AE}$  and  $P_A$ , solve for  $\Delta P_{AE}$  using Equation B.1, then solve for  $h_{PAE}$  using Equation B.2.

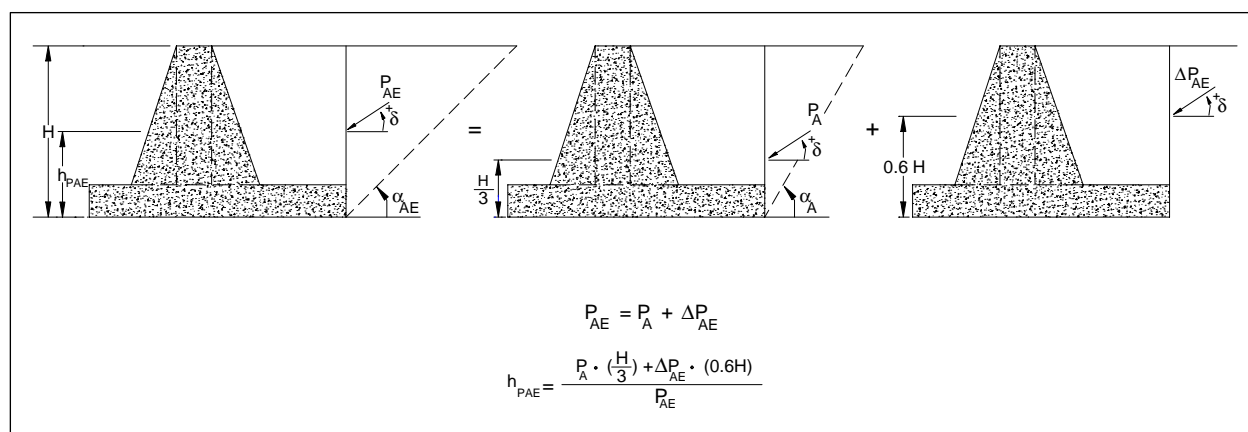


Figure B.2. Resultant location of  $P_{AE}$  based on the positions and magnitudes of the static active earth pressure force,  $P_A$ , and incremental dynamic active earth pressure force,  $\Delta P_{AE}$ , of a moist, level, backfill (after Ebeling and Morrison 1992).

Once the magnitude and location of  $P_{AE}$  that act on the back of the rigid block model of the structural wedge are determined, an approach such as the procedure described in Ebeling and Morrison (1992) and shown in Figure B.3 may be used to convert this force into equivalent pressure diagram. Key to this Ebeling and Morrison approach is the use of *pressure distributions* for each of the static  $P_A$  and for  $\Delta P_{AE}$  force components that are consistent not only in their magnitudes but also consistent with their Figure B.2  $P_A$  and  $\Delta P_{AE}$  force positions. The resulting total pressure distribution acting on the structural wedge is the sum of the triangular distribution of static active earth pressures that are consistent with  $P_A$  for

<sup>1</sup> Appendix C outlines procedures for determining the point of application of  $P_A$  for other backfill cases. Appendix H discusses two example computations of static, active earth pressure distributions and depth of cracking in cohesive soils.

the moist granular backfill shown in the figure plus the trapezoidal stress distribution consistent with  $\Delta P_{AE}$  acting at 0.6 times  $H$ .<sup>1</sup>

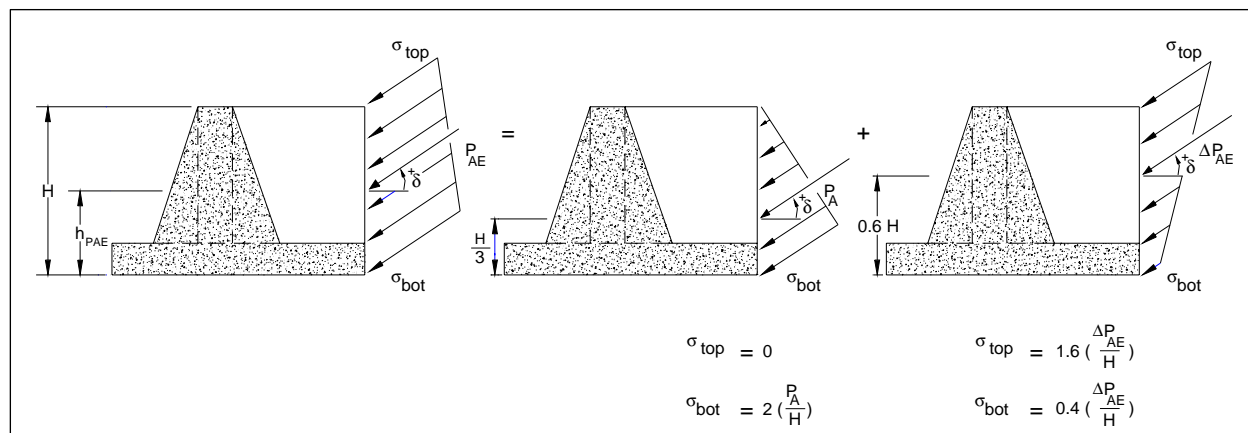


Figure B.3. The computation of equivalent earth pressures acting on a rigid block model of a cantilever wall retaining moist, level, granular (with  $c' = 0$ ) backfill (after Ebeling and Morrison 1992).

A key item is the selection of suitable shear strength parameters. In an effective stress analysis, the issue of the suitable friction angle is particularly troublesome when the peak friction angle is significantly greater than the residual friction angle. In the displacement-controlled approach examples given in Section 6.2 of Ebeling and Morrison (1992), effective stress based shear strength parameters (i.e., effective cohesion  $c'$  and effective angle of internal friction  $\phi'$ ) were used to define the shear strength of the dilative granular backfills, with  $c'$  set equal to zero in all cases due to the level of deformations anticipated in a sliding block analysis during seismic shaking. In 1992 Ebeling and Morrison concluded that it is conservative to use the residual friction angle in a sliding block analysis, and this should be the usual practice for displacement based analysis of granular retained soils. The primary author of this report would broaden the concept to the assignment of effective (or total) shear strength parameters for the retained soil to be consistent with the level of shearing-induced deformations encountered for each design earthquake in a rotational analysis and

<sup>1</sup> In the case of a water table and an effective stress analysis in which the effective shear strength parameters  $c'$  and  $\phi'$  are assigned to the (granular) retained soil, this approach is altered by changing the distribution of equivalent static earth pressures representing  $P_A$  to account for pore water pressures in the backfill in the usual manner for geotechnical engineering. This is demonstrated in Figure 7.10 in Ebeling and Morrison (1992) and discussed in Appendix C of this report. In the case of a total stress analysis, boundary water pressures (due to the presence of a water table in the retained soil) are not applied along the imaginary interface between the driving (soil) wedge and the structural wedge.

note that active earth pressures are used to define the loading provided to the structural wedge by the driving soil wedge. (Refer to Table 1.1 for guidance regarding wall movements required to fully mobilize the shear resistance within the retained soil during earthquake shaking.)

## Appendix C: An Approach for Computing the Dynamic Active Earth Pressure Distribution for a Partially Submerged Retained Soil

This appendix provides an approach for computing the dynamic active earth pressure distribution equivalent to the pseudo-static force  $P_{AE}$  and its corresponding point of application. The computation of the resultant location of  $P_{AE}$  and a corresponding pressure distribution for a granular backfill is discussed in Section C.1 in which Mohr-Coulomb effective stress shear strength parameter  $\phi'$  (with  $c'$  set equal to zero) is used to characterize the shear strength of the retained soil. Wall movements sufficient to fully mobilize the shear strength of the backfill are assumed in the formulation, thus allowing for the use of active earth pressures. A hydrostatic water table is assumed in this formulation. Section C.2 discusses the computation of the resultant location of the static  $P_A$  force component of  $P_{AE}$  and a corresponding pressure distribution for a granular backfill with a non-level backfill surface.

Section C.3 discusses the computation of the resultant location of  $P_{AE}$  and a corresponding pressure distribution for a backfill in which Mohr-Coulomb effective stress shear strength parameter  $\phi'$  and  $c'$  are nonzero. Section C.4 discusses the computation of the resultant location of  $P_{AE}$  and a corresponding pressure distribution for a backfill in which Mohr-Coulomb total stress shear strength parameter  $c$  is set equal to the undrained shear strength,  $S_u$ , and  $\phi$  is set equal to zero.

### C.1 Earth Pressure Distribution for the Dynamic Active Earth Pressure Force, $P_{AE}$ , of a Partially Submerged, Cohesionless, Level Backfill – Effective Stress Analysis with $c'$ Equal to Zero

In Appendix B an approach to convert the resultant active earth pressure force,  $P_{AE}$  (calculated using the approach outlined in Appendix A) into an equivalent pressure diagram for a wall retaining moist granular backfill was outlined. Key to this approach is the construction and use of *pressure distributions* for each of the two force components of  $P_{AE}$ ,

$$P_{AE} = P_A + \Delta P_{AE} \quad (\text{bis B.1})$$

The procedure was outlined in Figure B.3 for a *granular, moist backfill with a level ground surface*. This figure demonstrates that the resulting total pressure distribution acting on the structural wedge is the sum of the triangular distribution of static active earth pressures plus the trapezoidal stress distribution consistent with  $\Delta P_{AE}$ . For this moist backfill condition, the static pressures are consistent with  $P_A$  for the  $c' = 0$ , moist granular backfill (with no water table), the equivalent resultant force for the static active earth pressure distribution acts at a height of  $H/3$  and the equivalent resultant force for the incremental dynamic earth pressure distribution acts at a height equal to 0.6 times  $H$ . Equation B.2 is extended to partially submerged backfills by using the Ebeling and Morrison (1992) procedure for the case of a *level, granular backfill with a partially submerged backfill containing a hydrostatic water table*. This procedure is outlined below using a four-step computational process:

**Step 1: Convert the static active earth pressure force,  $P_A$ , into an equivalent active earth pressure diagram**

The active earth pressure coefficient,  $K_A$ , is first computed using the relationship

$$K_A = \frac{P_A}{\int_0^H \sigma'_{vertical} dh} \quad (C.1)$$

with  $P_A$  computed by the sweep-search method in CorpsWallSlip (refer to Section A.3) and the denominator equal to the integral of the vertical effective stress (i.e., the effective overburden pressure distribution). For level backfill with a hydrostatic water table of height  $H_w$  above the heel of the wall (and no surcharge), the denominator of Equation C.1 is computed using the simplified relationship

$$\int_0^H \sigma'_{vertical} dh = \left\{ \frac{1}{2} \cdot \gamma_{moist} \cdot (H - H_w)^2 + \gamma_{moist} \cdot [(H - H_w) \cdot H_w] + \frac{1}{2} \cdot (\gamma_{saturated} - \gamma_w) \cdot (H_w)^2 \right\} \quad (C.2)$$

with

$\gamma_{\text{moist}}$  = moist unit weight of the retained soil (above the water table)

$\gamma_{\text{saturated}}$  = saturated unit weight of the retained soil (below the water table)

$H$  = height of the imaginary section as measured vertically from the heel of the wall to the horizontal ground surface (and equal to the height of the imaginary section taken at the interface of the driving soil wedge with the structural wedge)

$(H-H_w)$  = thickness of the backfill above the hydrostatic water table

Note that the height term  $H_w$  in Equation C.2 is used to denote the thickness of the submerged backfill above the heel of the wall.

The static active earth pressure  $\sigma_A$ , acting at an effective interface friction angle of  $\delta$  to the normal of the vertical imaginary section, is computed at any depth,  $d$ , below the ground surface as

$$\sigma_A = K_A \bullet (\gamma_{\text{moist}} \bullet d) \quad \text{with} \quad d \leq (H - H_w) \quad (\text{C.3.a})$$

above the water table, and

$$\sigma_A = K_A \bullet \left\{ \gamma_{\text{moist}} \bullet (H - H_w) + (\gamma_{\text{saturated}} - \gamma_w) \bullet [d - (H - H_w)] \right\} \quad (\text{C.3.b})$$

*with*  $d > (H - H_w)$

below the hydrostatic water table, as shown in Figure C.1.



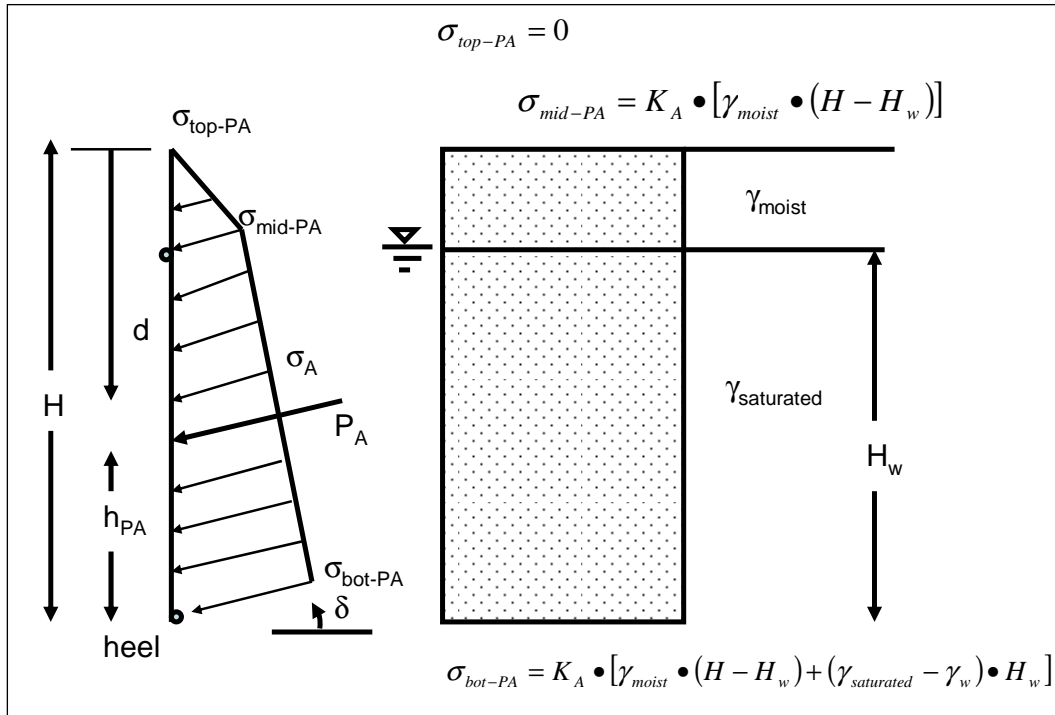


Figure C.1. Static active earth pressure  $\sigma_A$  distribution acting at an effective interface friction angle of  $\delta$  to the normal of the vertical imaginary section through the heel of the wall – effective stress analysis.

The area under the Figure C.1 active earth pressure diagram is equal to  $P_A$ .

The  $h_{PA}$  location of the equivalent resultant force ( $P_A$ ) for the Figure C.1 earth pressure distribution is computed in a two-step process: First, the active earth pressure distribution is converted into an equivalent set of Figure C.2 forces  $F_1$ ,  $F_2$ ,  $F_3$ , and  $F_4$

$$F_1 = \frac{1}{(H - H_w)} \cdot \left[ \frac{\sigma_{top-PA}}{3} + \frac{\sigma_{mid-PA}}{6} \right] \quad (C.4)$$

$$F_2 = \frac{1}{(H - H_w)} \cdot \left[ \frac{\sigma_{top-PA}}{6} + \frac{\sigma_{mid-PA}}{3} \right] \quad (C.5)$$

$$F_3 = \frac{1}{H_w} \cdot \left[ \frac{\sigma_{mid-PA}}{3} + \frac{\sigma_{bot-PA}}{6} \right] \quad (C.6)$$

$$F_4 = \frac{1}{H_w} \cdot \left[ \frac{\sigma_{mid-PA}}{6} + \frac{\sigma_{bot-PA}}{3} \right] \quad (C.7)$$

Secondly, from the moment equilibrium relationship for the horizontal components of the four forces about the heel,

$$\left\{ \sum_{i=1}^4 F_i \right\} \bullet \cos(\delta) \bullet h_{PA} = \{ F_1 \bullet H + (F_2 + F_3) \bullet H_w + F_4 \bullet 0 \} \bullet \cos(\delta) \quad (\text{C.8})$$

the  $h_{PA}$  location of the equivalent resultant active earth pressure force  $P_A$  is computed using

$$h_{PA} = \frac{F_1 \bullet H + (F_2 + F_3) \bullet (H - H_w) + F_4 \bullet 0}{\sum_{i=1}^4 F_i} \quad (\text{C.9})$$

Note that

$$\sum_{i=1}^4 F_i = P_A \quad (\text{C.10})$$

with  $P_A$  being the value computed by the sweep-search trial wedge solution discussed in Section A.3.

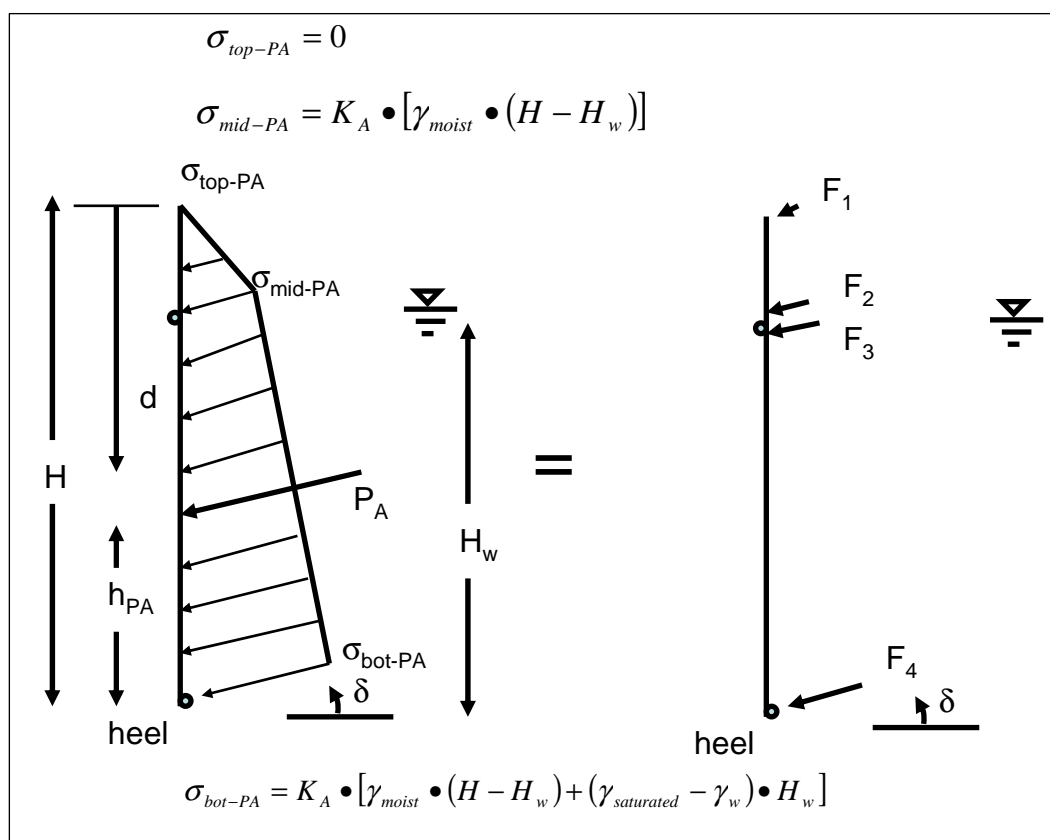


Figure C.2. The static active earth pressure distribution and its equivalent set of forces - effective stress analysis.

Observe in Figure C.2 that the location of the resultant force  $P_A$  for a level, granular ( $c' = 0$ ) backfill with a partially submerged backfill containing a hydrostatic water table is above the  $H/3$  height for a moist backfill (with no water table).

### Step 2: Create an incremental dynamic force component pressure diagram

The incremental dynamic force component  $\Delta P_{AE}$  is next converted into an equivalent earth pressure diagram. Using the relationship

$$\Delta P_{AE} = P_{AE} - P_A \quad (C.11)$$

and with values for  $P_{AE}$  and  $P_A$  provided by the dynamic and static sweep-search solutions made by CorpsWallSlip using the procedures outlined in Appendix A. The Ebeling and Morrison (1992) simplified procedure assumes a trapezoidal distribution for the corresponding incremental stress distribution, acting at an effective interface friction angle of  $\delta$  to the normal of the vertical imaginary section, as shown in Figure C.3. The

resulting force corresponding to the area under the pressure distribution is equal to  $\Delta P_{AE}$  and acts at a height to 0.6 times  $H$ .

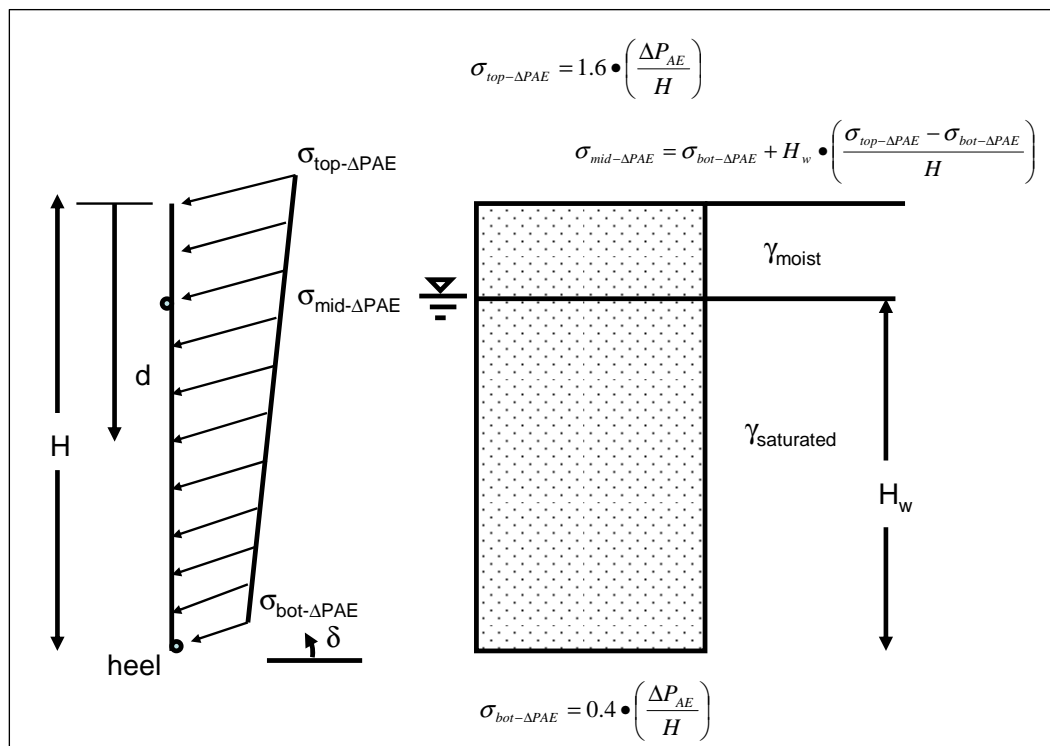


Figure C.3. The dynamic earth pressure distribution corresponding to the incremental dynamic force component  $\Delta P_{AE}$ , acting at an effective interface friction angle of  $\delta$  to the normal of the vertical imaginary section through the heel of the wall (after Ebeling and Morrison 1992).

### Step 3: Create the dynamic active earth pressure diagram

The dynamic active earth pressure diagram is created by adding the earth pressure diagrams created in Steps 1 and 2. The resulting force corresponds to the area under the combined pressure distribution and is equal to  $P_{AE}$  (recall  $P_{AE} = P_A + \Delta P_{AE}$ ). Its point of application above the heel of the wall is given by

$$h_{PAE} = \frac{P_A \cdot (h_{PA}) + \Delta P_{AE} \cdot (0.6 \cdot H)}{P_{AE}} \quad (C.12)$$

### Step 4: Complete the pressure diagram by adding in the pore water pressure distribution

In this effective stress analysis, pore water pressures will be added to the Figure C1  $P_A$  and Figure C3  $\Delta P_{AE}$  component earth pressure distributions

in order to obtain a total diagram of pressures acting on the structural wedge (and not to be confused with a total stress analysis). Pore water pressures act normal to the imaginary vertical section through the heel of the wall in this effective stress characterization of earth pressures acting on the structural wedge. For a hydrostatic water table, the pore water pressure at depth,  $d$ , below the ground surface is given by

$$u = 0 \quad \text{with} \quad d \leq (H - H_w) \quad (\text{C.13.a})$$

above the water table, and

$$u = \gamma_w \bullet [d - (H - H_w)] \quad \text{with} \quad d > (H - H_w) \quad (\text{C.13.b})$$

below the hydrostatic water table, as shown in Figure C.5.

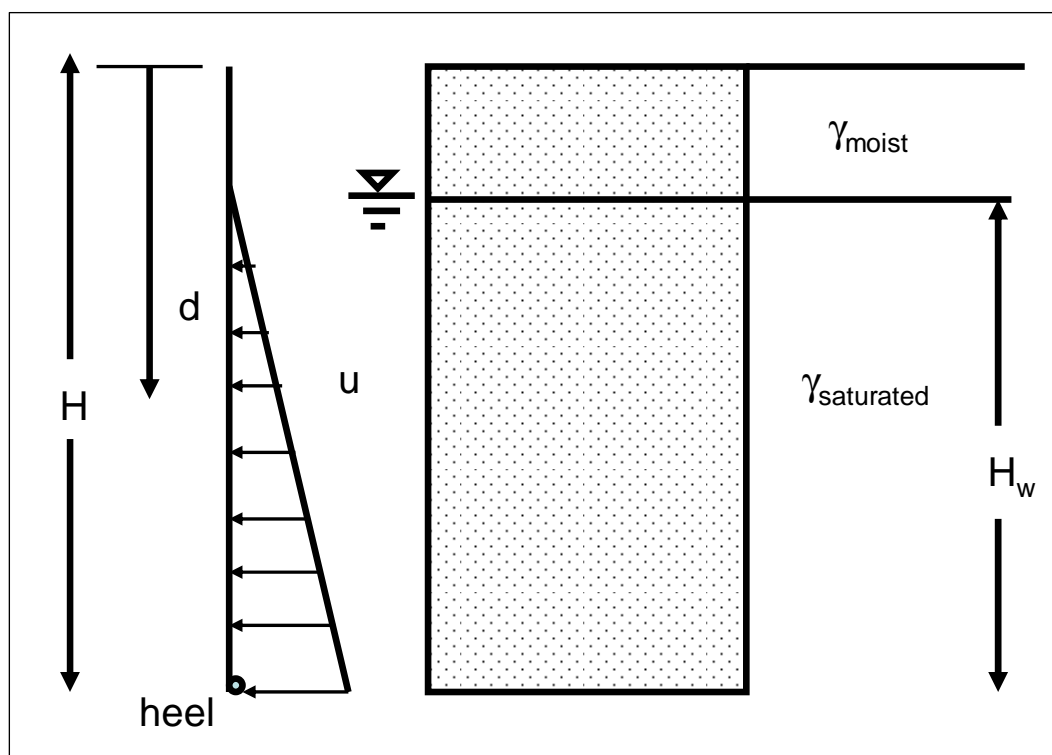


Figure C.5. Hydrostatic pore water pressure distribution acting normal of the vertical imaginary section through the heel of the wall.

Thus, a total diagram of pressures acting on the structural wedge consists of the Figure C.1  $P_A$  distribution, plus the Figure C.3  $\Delta P_{AE}$  distribution, plus the Figure C.5 pore water pressure distribution.

## **C.2 Earth Pressure Distribution for the Static Active Earth Pressure Force, $P_A$ , Component of $P_{AE}$ of a Cohesionless, Backfill with a Sloping or a Bilinear Ground Surface – Effective Stress Analysis with $c'$ Equal to Zero**

The previous section describes an approach to convert the resultant active earth pressure force,  $P_{AE}$  (calculated using the approach outlined in Appendix A), into an equivalent pressure diagram for a wall retaining moist granular backfill with  $c'$  equal to zero. This procedure starts with the computation of an equivalent static active earth pressure force  $P_A$  and an equivalent active earth pressure diagram for a *level* backfill ground surface. This section expands on the Section C.1 procedure for determining the distribution and resultant location of  $P_A$  for a sloping and a bilinear ground surface backfill following a procedure outlined in ETL 1110-2-322.

### **C.2.1 Basic Procedure to Compute the Active Effective Stress Distribution Corresponding to $P_A$ for a Moist Retained Soil with a Sloping Ground Surface**

The procedure to calculate the active earth pressure distribution for resultant static force  $P_A$  due to the geometry of the backfill is outlined using the information contained within Figure C.6 for a moist, granular frictional ( $\phi' > 0$  and  $c' = 0$ ) retained soil with a constant slope for the ground surface. The sweep-search wedge procedure described in Section A.3 is used to first compute the value for  $P_A$  as well as the orientation of the planar slip surface,  $\alpha_A$ , for the critical soil wedge that originates at point 1. The equation to compute the active earth pressure (designated as  $\sigma_A$ ) at key points is given in this figure and is equal to the active earth pressure coefficient,  $K_A$ , times the vertical effective stress at depth  $z$  in the moist retained soil. The key feature for this formulation is that at a given point along the vertical imaginary section through the heel of the structural wedge (and labeled in this figure), the effective vertical stress (designated as  $\sigma_{v-z}$  in the brackets) is computed *using a depth  $z$* , the depth below the ground surface as shown in this figure. A computation of  $\sigma_{v-z}$  and, subsequently,  $\sigma_A$  are made in this figure for point 1 (at the heel). Note that depth  $z$ , designated as  $z_1$  for point 1, is determined by extending the critical, planar slip plane from point 1 until it intersects the ground surface. This same procedure is followed to compute a different value for  $z$ ,  $\sigma_{v-z}$ , and for  $\sigma_A$  at any other point of interest along the imaginary vertical section of height  $H$ . To determine the value for the active earth pressure coefficient,  $K_A$ , the value for the force  $P_A$  from the sweep-search method of

analysis is divided by the integral of the  $\sigma_{v-z}$  distribution along the imaginary vertical section of height  $H$  (refer to the  $K_A$  equation given in this figure). For the case of a moist granular retained soil with a constant surface slope, the equation for  $\sigma_{v-z}$  and  $\sigma_A$  at key points and for  $K_A$  are straight-forward and given in this figure.

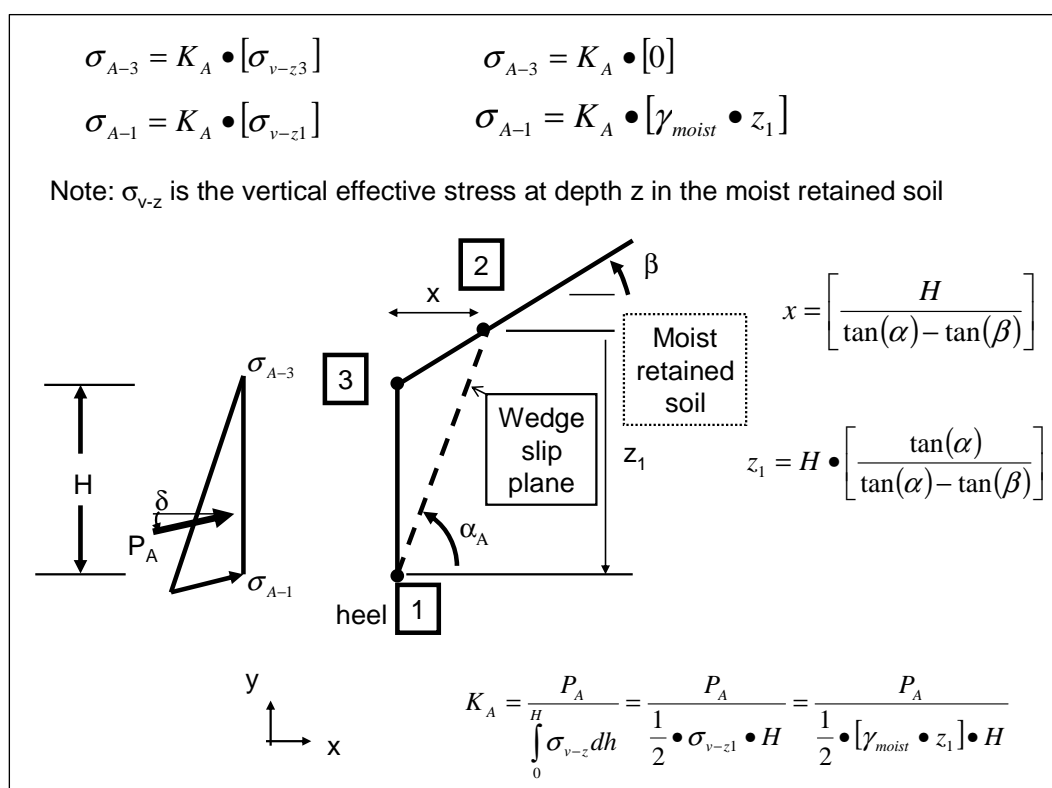


Figure C.6. The active earth pressure distribution corresponding to the incremental static force component  $P_A$ , acting at an effective interface friction angle of  $\delta$  to the normal of the vertical imaginary section through the heel of the wall – moist retained soil with  $\phi' > 0$  and  $c' = 0$ .

The procedure outlined in Step 1 in Section C.1 that converts the  $\sigma_A$  distribution into equivalent forces (see Figure C.2) is used to compute the resultant location  $h_{PA}$  of  $P_A$  for use in Equation C.12 for the resultant location  $h_{PAE}$  of  $P_{AE}$ . The procedure outlined in Step 2 and Step 3 in Section C.1 is used to compute the incremental dynamic force component  $\Delta P_{AE}$  and its corresponding equivalent earth pressure diagram.

### C.2.2 Basic Procedure to Compute the Active Effective Stress Distribution Corresponding to $P_A$ for a Partially Submerged Retained Soil with a Sloping Ground Surface

This section expands upon the procedure outlined in Section C.2.1 by including the case of a partially submerged granular backfill (with a hydrostatic water table). The procedure to calculate the active earth pressure distribution for resultant static force  $P_A$  due to the geometry of the backfill is outlined using the information contained within Figure C.7 for a granular frictional ( $\phi' > 0$  and  $c' = 0$ ) retained soil with the critical planar wedge slip plane that passes through point 1 (with  $\alpha_A > \alpha_{\text{corner}}$ ) and *intersects the sloping portion of the ground surface*. The sweep-search wedge procedure described in Section A.3 is used to first compute the value for  $P_A$  as well as the orientation of the planar slip surface,  $\alpha_A$ , for the critical soil wedge that originates at point 1. The equation to compute the active earth pressure (designated as  $\sigma_A$ ) at the key points identified in this figure as 1, 6, and 3, is equal to the active earth pressure coefficient  $K_A$  times the vertical effective stress at depth  $z$  in the retained soil. The key feature for this formulation is that at a given point along the vertical imaginary section through the heel of the structural wedge (identified in this figure as points 1, 6, and 3), the effective vertical stress (designated as  $\sigma'_{v-z}$  in the brackets) is computed using a depth  $z$ , the depth below the ground surface as shown in this figure. A computation of  $\sigma'_{v-z}$  and, subsequently,  $\sigma_A$  are made in this figure for point 1 (at the heel). Note that depth  $z$ , designated as  $z_1$  for point 1, is determined by extending the critical, planar slip plane from point 1 until it intersects the ground surface (at point 2). This same procedure is followed to compute the value for  $z$ ,  $\sigma'_{v-z}$ , and  $\sigma_A$  at the other key point 6 (and point 3) along the imaginary vertical section of height  $H$ . A plane oriented at  $\alpha_A$  from horizontal is projected from the point of interest, e.g., point 6, up through the retained soil until it intersects the sloping ground surface.  $\sigma'_{v-z6}$  is computed using the resulting vertical height  $z_6$  of this planar surface, as shown in this figure. Moist unit weights above the water table and buoyant unit weights below the water table (assuming a hydrostatic water table in the retained soil) are used to compute the vertical effective stress  $\sigma'_{v-z}$ . To determine the value for the active earth pressure coefficient,  $K_A$ , the value for the force  $P_A$  from the sweep-search method of analysis is divided by the integral of the  $\sigma'_{v-z}$  distribution along the imaginary vertical section of height  $H$  (refer to the equation given in this figure). [ $\sigma'_{v-z}$  is contained within the brackets of the  $\sigma_A$  relationships in this figure.] For the case of a granular retained soil with a constant surface slope, the



equation for  $\sigma'_{v-z}$  and  $\sigma_A$  at key points and for  $K_A$  is straight-forward and given in this figure.

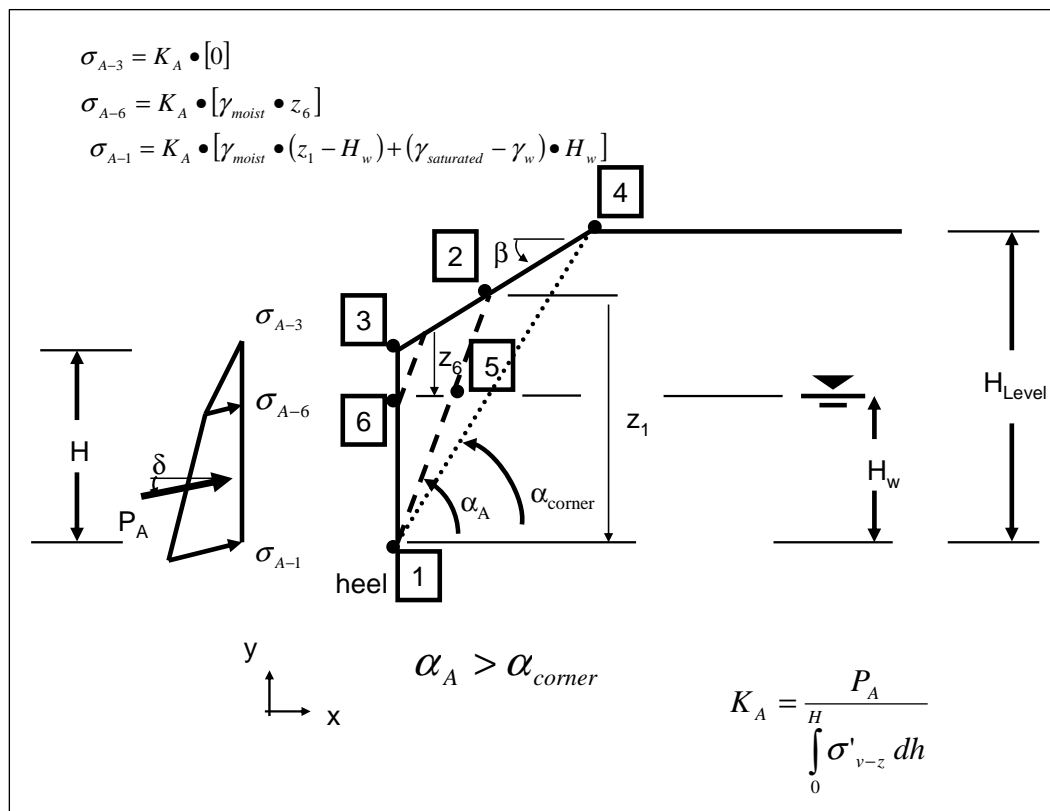


Figure C.7. The active earth pressure distribution corresponding to the incremental static force component  $P_A$ , acting at an effective interface friction angle of  $\delta$  to the normal of the vertical imaginary section through the heel of the wall – partially submerged backfill with  $\phi' > 0$  and  $c' = 0$ .

The procedure outlined in Step 1 in Section C.1 that converts the  $\sigma_A$  distribution into equivalent forces (as generalized in Figure C.8) is used to compute the resultant location  $h_{PA}$  of  $P_A$  for use in Equation C.12 for the resultant location  $h_{PAE}$  of  $P_{AE}$ . The procedures outlined in Step 2 and in Step 3 in Section C.1 are used to compute the incremental dynamic force component,  $\Delta P_{AE}$ , and its corresponding equivalent earth pressure diagram.

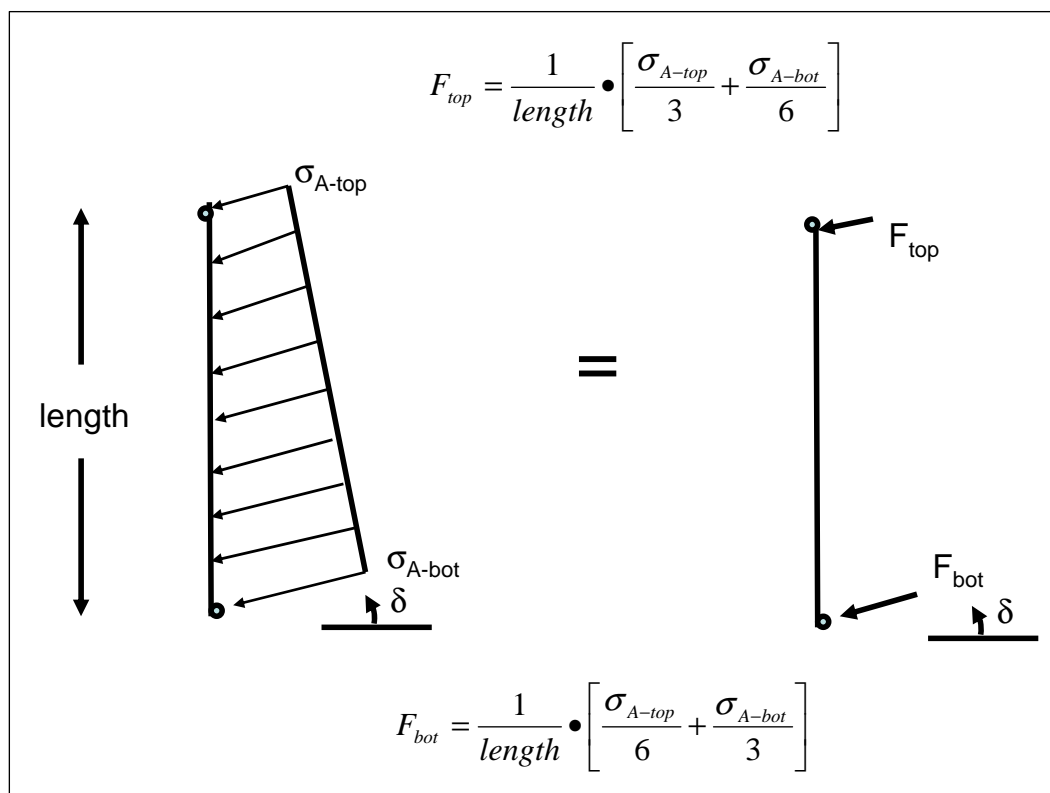


Figure C.8. Conversion of a linear stress distribution into an equivalent set of forces.

### C.2.3 Basic Procedure to Compute the Active Effective Stress Distribution Corresponding to $P_A$ for a Partially Submerged Retained Soil with a Bilinear Ground Surface

This section expands upon the procedure outlined in Section C.2.2 in the case of a partially submerged granular backfill. The procedure to calculate the active earth pressure distribution for resultant static force  $P_A$  due to the geometry of the backfill is outlined using the information contained within Figure C.9 for a granular, frictional ( $\phi' > 0$  and  $c' = 0$ ) retained soil for which the critical planar wedge slip plane that passes through point 1 (with  $\alpha_{corner} > \alpha_A$ ) and intersects the horizontal portion of the bilinear ground surface. The sweep-search wedge procedure described in Section A.3 is used to first compute the value for  $P_A$  as well as the orientation of the planar slip surface,  $\alpha_A$ , for the critical soil wedge that originates at point 1. The equation to compute the active earth pressures (designated as  $\sigma_A$ ) at the Figure C.9 key points 1, 12, 6, and 3 is equal to the active earth pressure coefficient,  $K_A$ , times the vertical effective stress at depth  $z$  in the moist retained soil. The key feature for this formulation is that at a given point along the vertical imaginary section through the heel of the structural wedge (identified in this figure as points 1, 12, 6, and 3), the effective

vertical stress (designated as  $\sigma'_{v-z}$  in the brackets) is computed using a depth  $z$ , the depth below the ground surface as shown in this figure. A computation of  $\sigma'_{v-z}$  and, subsequently,  $\sigma_A$  are made in this figure for point 1 (at the heel). Note that depth  $z$ , designated as  $z_1$  for point 1, is determined by extending the critical, planar slip plane from point 1 until it intersects the *horizontal* ground surface. This same procedure is followed to compute the value for  $z$ ,  $\sigma'_{v-z}$ , and  $\sigma_A$  at the other key points 12, 6, and 3 along the imaginary vertical section of height  $H$ . A plane oriented at  $\alpha_A$  from horizontal is projected from the point of interest (e.g., point 6) up through the retained soil until it intersects the *sloping* ground surface.  $\sigma'_{v-z_6}$  is computed using the resulting vertical height  $z_6$  of this planar surface, as shown in this figure. The computations outlined in Figure C.9 differ from the Figure C.7 computations because the deepest soil wedge slip plane (originating at point 1) intersects the horizontal rather than the sloping portion of the ground surface. Thus an additional key point 12 is needed to define the  $\sigma_A$  distribution. Moist unit weights above the water table and buoyant unit weights below the water table (assuming a hydrostatic water table in the retained soil) are used to compute the vertical effective stress  $\sigma'_{v-z}$ . To determine the value for the active earth pressure coefficient,  $K_A$ , the value for the force  $P_A$  from the sweep-search method of analysis is divided by the integral of the  $\sigma'_{v-z}$  distribution along the imaginary vertical section of height  $H$  (refer to the equation given in this figure). [ $\sigma'_{v-z}$  is contained within the brackets of the  $\sigma_A$  relationships given in this figure.] For the case of a granular retained soil with a bilinear ground surface, the equation for  $\sigma'_{v-z}$  and  $\sigma_A$  at key points and for  $K_A$  is straight-forward and given in this figure.

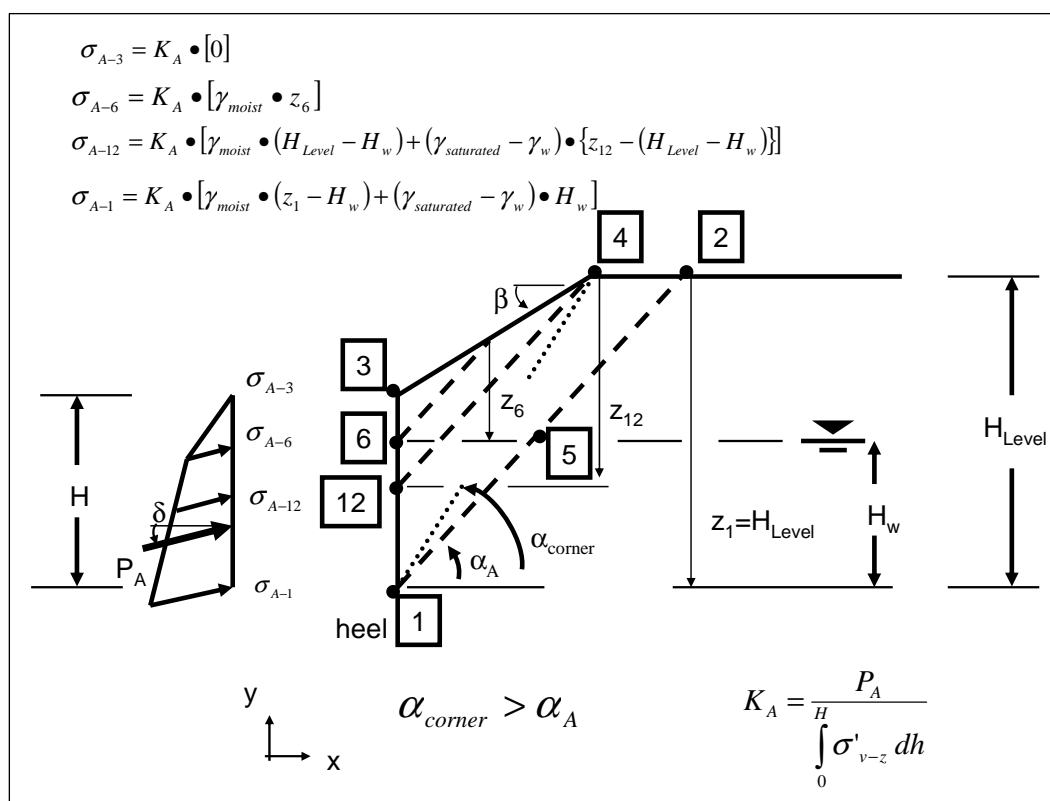


Figure C.9. The active earth pressure distribution corresponding to the incremental static force component  $P_A$ , acting at an effective interface friction angle of  $\delta$  to the normal of the vertical imaginary section through the heel of the wall for a bilinear ground surface – partially submerged backfill with  $\phi' > 0$  and  $c' = 0$ .

The procedure outlined in Step 1 in Section C.1 that converts the  $\sigma_A$  distribution into equivalent forces (see Figure C.8) is used to compute the resultant location  $h_{PA}$  of  $P_A$  for use in Equation C.12 for the resultant location  $h_{PAE}$  of  $P_{AE}$ . The procedure outlined in Step 2 and Step 3 in Section C.1 is used to compute the incremental dynamic force component  $\Delta P_{AE}$  and its corresponding equivalent earth pressure diagram.

### C.3 Earth Pressure Distribution for the Dynamic Active Earth Pressure Force $P_{AE}$ for a Backfill with Mohr-Coulomb Shear Strength Parameters $c'$ and $\phi'$ - Effective Stress Analysis

This section discusses the computation of the resultant location of  $P_{AE}$  and a corresponding pressure distribution for a backfill in which Mohr-Coulomb effective stress shear strength parameter  $\phi'$  and  $c'$  are both

nonzero.<sup>1</sup>  $P_{AE}$  is equal to the sum of  $P_A$  plus  $\Delta P_{AE}$  by Equation B.1. The same four-step computational process outlined in Section C.1 is used to determine the earth pressure distribution and resultant location for  $P_{AE}$  for a backfill with nonzero  $c'$  and  $\phi'$  effective stress based Mohr-Coulomb shear strength parameters assigned to the backfill:

*Step 1: Convert the static active earth pressure force,  $P_A$ , into an equivalent active earth pressure diagram*

Equation A.25 of the sweep-search wedge solution method described in Section A.3 demonstrates that  $P_A$  is made up of two forces, (1) a frictional and weight force component and (2) a cohesive force component. The frictional/weight resultant force component is reduced by the cohesion force component. The subtraction of the cohesion force component in Equation A.25 reflects a cohesion force component for a *tensile stress* distribution component of the resulting (effective) active earth pressure  $\sigma_A$  distribution of stresses with depth,

$$\sigma_A = K_{A-\phi-\text{weight}} \bullet \sigma'_{v-z} - SIGc \quad (C.14)$$

The component of (effective) active earth pressure distribution due to cohesion is designated as  $SIGc$  in this report and is of constant magnitude with depth.  $SIGc$  is computed by

$$SIGc = \frac{P_{A-C}}{H} \quad (C.15)$$

---

<sup>1</sup> A key item is the selection of suitable shear strength parameters. In an effective stress analysis, the issue of the suitable friction angle is particularly troublesome when the peak friction angle is significantly greater than the residual friction angle. In the displacement controlled approach examples given in Section 6.2 of Ebeling and Morrison (1992), effective stress based shear strength parameters (i.e., effective cohesion  $c'$  and effective angle of internal friction  $\phi'$ ) were used to define the shear strength of the dilative granular backfills, *with  $c'$  set equal to zero in all cases due to the level of deformations anticipated in a sliding block analysis during seismic shaking*. In 1992 Ebeling and Morrison concluded that it is conservative to use the residual friction angle in a sliding block analysis, and this should be the usual practice for displacement-based analysis of granular retained soils. The primary author of this report would broaden the concept to the assignment of effective (or total) shear strength parameters for the retained soil to be consistent with the level of shearing-induced deformations encountered for each design earthquake in a rotational analysis and note that active earth pressures are used to define the loading imposed on the structural wedge by the driving soil wedge. (Refer to Table 1.1 for guidance regarding wall movements required to fully mobilize the shear resistance within the retained soil during earthquake shaking.) Therefore, engineers are cautioned to carefully consider the reasonableness of including a nonzero value for effective cohesion  $c'$  in their permanent deformation and permanent rotation analyses.

with  $P_{A-C}$  corresponding to the cohesion component of  $P_A$  computed using Equation A.25 in the sweep-search wedge method of analysis with a critical wedge oriented at angle  $\alpha_A$ . The active earth pressure coefficient  $K_{A-\phi\text{-weight}}$  is computed using

$$K_{A-\phi\text{-weight}} = \frac{P_{A-\phi\text{-weight}}}{H \int_0^{\sigma'_{v-z}} dh} \quad (C.16)$$

with  $P_{A-\phi\text{-weight}}$  corresponding to the frictional/weight component of  $P_A$  computed using Equation A.25 in the sweep-search wedge method of analysis. The effective vertical stress  $\sigma'_{v-z}$  is computed using a depth  $z$ , the depth below the ground surface using the procedure outlined in the Section C.2. In a moist backfill (i.e., with no water table) the depth to zero stress (i.e., depth of cracking) is computed as

$$d_{crack} = \frac{S/Gc}{\gamma_{moist} \bullet K_{A-\phi\text{-weight}} \bullet \left[ \frac{\tan(\alpha_A)}{\tan(\alpha_A) - \tan(\beta)} \right]} \quad (C.17)$$

The effective vertical stress at the deepest point in the crack in moist soil (and above a water table) is computed equal to

$$\sigma'_{v-z-dcrack} = \gamma_{moist} \bullet z_{dcrack} \quad (C.18)$$

which, for a plane at angle  $\alpha_A$  (from horizontal) intersecting the sloping ground becomes

$$z_{dcrack} = d_{crack} \bullet \left[ \frac{\tan(\alpha)}{\tan(\alpha) - \tan(\beta)} \right] \quad (C.19)$$

and  $\sigma_{A-dcrack}$  is equal to zero at the crack tip

$$\sigma_{A-dcrack} = 0 = K_{A-\phi\text{-weight}} \bullet \sigma'_{v-z-dcrack} - S/Gc \quad (C.20)$$

In the case of a crack extending below a hydrostatic water table within a retained soil, the effective vertical stress at the deepest point in the crack in Equation C.20 is computed using







$$Z_{dcrack} = Z_{12} + (x_{11} - x_4) \bullet \tan(\alpha) \quad \text{with} \quad x_{11} > x_4 \quad (\text{C.29})$$

Equations C.20 and C.21 are used in a trial-and-error procedure to compute the value of  $d_{crack}$  (and  $y_{dcrack}$ ). The following relationships, based on the Figure C.10.b geometry, are also used in the solution process,

$$x_{11} = Z_{dcrack} / \tan(\alpha) \quad (\text{bis C.22})$$

$$Z_{12} = x_4 \bullet \tan(\alpha) \quad (\text{C.30})$$

$$Z_{11toWT} = Z_{dcrack} - Z_{WTto crack} \quad (\text{bis C.23})$$

with

$$Z_{WTto crack} = y_6 - y_{dcrack} \quad (\text{bis C.24})$$

substituting

$$y_6 = H_w \quad (\text{bis C.25})$$

and for  $y_3$  equal to H,

$$y_{dcrack} = H - d_{crack} \quad (\text{bis C.27})$$

Recognizing that  $z_{11toWT}$  is a constant, equal to the difference between  $H_{Level}$  and  $H_w$  (in the case of  $x_{11} > x_4$ ), the variable  $z_{WTto crack}$  is also expressed as

$$Z_{WTto crack} = Z_{dcrack} - (H_{Level} - H_w) \quad (\text{bis C.26})$$

Another useful geometrical Figure C.10.b relationship is

$$y_{12} = y_3 - \left\{ \frac{Z_{12}}{\left[ \frac{\tan(\alpha)}{\tan(\alpha) - \tan(\beta)} \right]} \right\} \quad (\text{C.31})$$

CorpsWallSlip performs a permanent displacement analysis of a retaining wall due to earthquake shaking. Reversal in the direction of the horizontal

component of the time-history of earthquake ground shaking occurs many times during the typical tens of seconds of ground motion. Consequently, a reversal in direction of the inertial force imparted to the structural wedge and to the soil driving wedge occurs many times during the course of the analysis using CorpsWallSlip. In a traditional soil wedge formulation for static loading, a crack is typically considered to exist within the upper regime of the soil driving wedge for a cohesive soil and the planer wedge slip surface is terminated when it intersects the zone of cracking at a depth  $d_{\text{crack}}$  below the ground surface (e.g., see Appendix H in EM 1110-2-2502). This assumption is not made the CorpsWallSlip formulation for dynamic loading. Instead, it is assumed that in the dynamic wedge formulation, the crack within the “zone of cracking” at the top of the retained cohesive soil of the driving wedge will not remain open during earthquake shaking *due to the inertial load direction reversals*. So even for cohesive soils, the Figure A.1 planar slip surface obtained from the sweep-search method of analysis used by CorpsWallSlip to obtain a value for the earthquake induced resultant driving force  $P_{\text{AE}}$  (acting on the structural wedge), extends uninterrupted within the driving soil wedge (in the retained soil) to the ground surface and is not terminated by a vertical crack face to the ground surface when it enters the zone of cracking. Since  $P_A$  is used solely to determine the value for  $h_{\text{PAE}}$ , the resultant location for  $P_{\text{AE}}$  with the procedure outlined in this appendix, a continuous planar slip surface is also assumed in  $P_A$  computations. A sweep-search wedge formulation is used to compute  $P_A$ . Equation C.17 for crack depth  $d_{\text{crack}}$  in moist backfill and Equation C.20 in partially submerged backfill are used solely to establish the static earth pressure diagram component of  $P_{\text{AE}}$  pressures along the imaginary vertical section passing through the heel of the wall, consistent with the Equation B.1 formulation. This assumption is made for the earth pressure distribution corresponding to  $P_A$  with consideration of  $d_{\text{crack}}$  because the permanent displacement of the structural wedge is away from the backfill and it is likely that at this vertical section a vertical crack may occur. Thus,  $d_{\text{crack}}$  is accounted for in the  $h_{\text{PAE}}$  computation using Equation C.12. The static tensile  $\sigma_A$  stresses along the driving soil wedge-to-structural wedge interface (i.e., located along the vertical imaginary section extending through the heel) are neglected over the depth of cracking due to the presence of the crack by CorpsWallSlip.

*Step 2: Create an incremental dynamic force component pressure diagram*

The incremental dynamic force component,  $\Delta P_{\text{AE}}$ , is next converted into an equivalent earth pressure diagram using the relationship

$$\Delta P_{AE} = P_{AE} - P_A \quad (\text{bis C.11})$$

and with values for  $P_{AE}$  and  $P_A$  provided by the dynamic and static sweep-search solutions made by CorpsWallSlip using the procedures outlined in Appendix A (Sections A.4 and A.5). The Ebeling and Morrison (1992) simplified procedure assumes a trapezoidal distribution for the corresponding incremental stress distribution with an interface friction angle of  $\delta = 0$  to the normal of the vertical imaginary section in a total stress analysis (refer to Figure C.3). The resulting force corresponding to the area under the pressure distribution is equal to  $\Delta P_{AE}$  and acts at a height to 0.6 times  $H$ .

*Step 3: Create the dynamic active earth pressure diagram*

The dynamic active earth pressure diagram is created by adding the earth pressure diagrams created in Steps 1 and 2. The resulting force corresponds to the area under the combined pressure distribution and is equal to  $P_{AE}$  (recall  $P_{AE} = P_A + \Delta P_{AE}$ ). Its point of application above the heel of the wall is given by

$$h_{PAE} = \frac{P_A \bullet (h_{PA}) + \Delta P_{AE} \bullet (0.6 \bullet H)}{P_{AE}} \quad (\text{bis C.12})$$

In the special case of cohesive soils, the CorpsWallSlip analysis disregards the tensile stresses when defining the static active earth pressures and the corresponding resulting static active earth pressure force to be applied to the structural wedge, as well as when computing  $h_{PA}$  for this modified stress distribution. A trapezoidal earth pressure distribution is still used to define  $\Delta P_{AE}$ .

*Step 4: Complete the pressure diagram by adding in the pore water pressure distribution*

Refer to discussion in Step 4 of Section C.1.

### **C.3.1 Basic Procedure to Compute the Active Effective Stress Distribution Corresponding to $P_A$ for a Partially Submerged Retained Soil with a Sloping Ground Surface**

The procedure outlined in Section C.2.2 is expanded to consider the case of a partially submerged backfill with nonzero effective cohesion and

friction shear strength parameters (i.e.,  $c' > 0$  and  $\phi' > 0$ ). The procedure to calculate the active earth pressure distribution for resultant static force  $P_A$  due to the geometry of the backfill is outlined using the information contained within Figure C.11 for which the critical planar wedge slip plane that passes through point 1 (with  $\alpha_A > \alpha_{\text{corner}}$ ), intersects the sloping portion of the bilinear ground surface. The sweep-search wedge procedure described in Section A.3 is used to first compute the value for  $P_A$  as well as the orientation of the planar slip surface,  $\alpha_A$ , for the critical soil wedge that originates at point 1. The equation to compute the active earth pressures (designated as  $\sigma_A$ ) at the Figure C.11 key points designated as 1, 6,  $d_{\text{crack}}$ , and 3 is, by Equation C.14, equal to the active earth pressure coefficient,  $K_{A-\phi\text{-weight}}$ , times the vertical effective stress at depth  $z$  in the retained soil minus  $\text{SIGc}$ . The key feature for this formulation is that at a given point along the vertical imaginary section through the heel of the structural wedge (identified in this figure as points 1, 6,  $d_{\text{crack}}$ , and 3), the effective vertical stress (designated as  $\sigma'_{v-z}$  in the brackets and for a hydrostatic water table) is computed using a depth  $z$ , the depth below the ground surface as shown in this figure. A computation of  $\sigma'_{v-z}$  and, subsequently,  $\sigma_A$  are made in this figure for point 1 (at the heel). Note that depth  $z$ , designated as  $z_1$  for point 1, is determined by extending the critical, planar slip plane from point 1 until it intersects the *sloping* ground surface. This same procedure is followed to compute the value for  $z$ ,  $\sigma'_{v-z}$ , and  $\sigma_A$  at the other key points 6,  $d_{\text{crack}}$ , and 3 along the imaginary vertical section of height  $H$ . A plane oriented at  $\alpha_A$  from horizontal is projected from the point of interest (e.g., point  $d_{\text{crack}}$ ) up through the retained soil until it intersects the sloping ground surface.  $\sigma'_{v-z-d_{\text{crack}}}$  is computed using the resulting vertical height,  $z_{d_{\text{crack}}}$ , of this planar surface, as shown in this figure. The computations outlined in Figure C.11 differ from the Figure C.7 computations because of the depth of cracking. Thus an additional key point,  $d_{\text{crack}}$ , is needed to define the  $\sigma_A$  distribution. Moist unit weights above the water table and buoyant unit weights below the water table (assuming a hydrostatic water table in the retained soil) are used to compute the vertical effective stress  $\sigma'_{v-z}$ . To determine the value for the active earth pressure coefficient,  $K_{A-\phi\text{-weight}}$ , the value for the force component  $P_{A-\phi\text{-weight}}$  from the sweep-search method of analysis is divided by the integral of the  $\sigma'_{v-z}$  distribution along the imaginary vertical section of height  $H$  (refer to the equation given in this figure). [ $\sigma'_{v-z}$  is contained within the brackets of the  $\sigma_A$  relationships given in this figure.] For the Figure C.11 case of a granular retained soil with a constant surface slope (as far as this effective vertical stress computational procedure is

concerned), the equation for  $\sigma'_{v-z}$  and  $\sigma_A$  at key points and for  $K_{A-\phi\text{-weight}}$  is straight-forward and given in this figure.

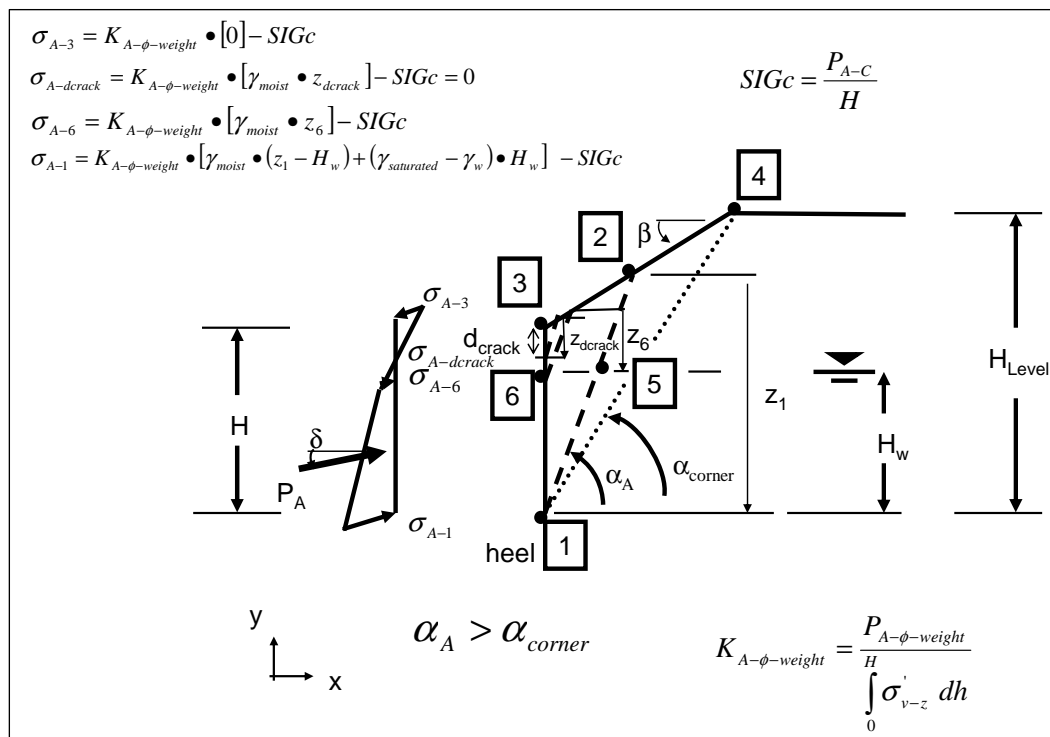


Figure C.11. The active earth pressure distribution corresponding to the incremental static force component,  $P_A$ , acting at an effective interface friction angle of  $\delta$  to the normal of the vertical imaginary section through the heel of the wall for a bilinear ground surface – partially submerged backfill with  $\phi' > 0$  and  $c' > 0$ .

The procedure outlined in Step 1 in Section C.1 that converts the  $\sigma_A$  distribution into equivalent forces (see Figure C.8) is used to compute the resultant location  $h_{PA}$  of  $P_A$  for use in Equation C.12 for the resultant location  $h_{PAE}$  of  $P_{AE}$ . The procedures outlined in Step 2 and Step 3 in Section C.1 are used to compute the incremental dynamic force component  $\Delta P_{AE}$  and its corresponding equivalent earth pressure diagram.

### C.3.2 Basic Procedure to Compute the Active Effective Stress Distribution Corresponding to $P_A$ for a Partially Submerged Retained Soil with a Bilinear Ground Surface

The procedure outlined in Section C.2.3 is expanded to consider the Figure C.12 geometry of a partially submerged backfill with nonzero effective cohesion and friction shear strength parameters (i.e.,  $c' > 0$  and  $\phi' > 0$ ). The procedure to calculate the active earth pressure distribution for resultant static force  $P_A$  due to the geometry of the backfill is outlined

using the information contained within Figure C.12 for which the critical planar wedge slip plane that passes through point 1 (with  $\alpha_A > \alpha_{\text{corner}}$ ), *intersecting the level portion* of the bilinear ground surface. The sweep-search wedge procedure described in Section A.3 is used to first compute the value for  $P_A$  as well as the orientation of the planar slip surface,  $\alpha_A$ , for the critical soil wedge that originates at point 1. The equation to compute the active earth pressures (designated as  $\sigma_A$ ) at the Figure C.12 key points designated as 1, 12, 6,  $d_{\text{crack}}$ , and 3 is, by Equation C.14, equal to the active earth pressure coefficient,  $K_{A-\phi\text{-weight}}$ , times the vertical effective stress at depth  $z$  in the retained soil minus  $\text{SIGc}$ . The key feature for this formulation is that at a given point along the vertical imaginary section through the heel of the structural wedge (identified in this figure as points 1, 12, 6,  $d_{\text{crack}}$ , and 3), the effective vertical stress (designated as  $\sigma'_{v-z}$  in the brackets and for a hydrostatic water table) is computed using a depth  $z$ , the depth below the ground surface as shown in this figure. A computation of  $\sigma'_{v-z}$  and, subsequently,  $\sigma_A$  are made in this figure for point 1 (at the heel). Note that depth  $z$ , designated as  $z_1$  for point 1, is determined by extending the critical, planar slip plane from point 1 until it intersects the horizontal ground surface. This same procedure is followed to compute the value for  $z$ ,  $\sigma'_{v-z}$ , and  $\sigma_A$  at the other key points 12, 6,  $d_{\text{crack}}$ , and 3 along the imaginary vertical section of height  $H$ . A plane oriented at  $\alpha_A$  from horizontal is projected from the point of interest (e.g., point  $d_{\text{crack}}$ ) up through the retained soil until it intersects the sloping ground surface.  $\sigma'_{v-z-d_{\text{crack}}}$  is computed using the resulting vertical height  $z_{d_{\text{crack}}}$  of this planar surface, as shown in this figure. The computations outlined in Figure C.12 differ from the Figure C.9 computations because of the depth of cracking. Thus an additional key point  $d_{\text{crack}}$  is needed to define the  $\sigma_A$  distribution. Moist unit weights above the water table and buoyant unit weights below the water table (assuming a hydrostatic water table in the retained soil) are used to compute the vertical effective stress  $\sigma'_{v-z}$ . To determine the value for the active earth pressure coefficient  $K_{A-\phi\text{-weight}}$ , the value for the force component  $P_{A-\phi\text{-weight}}$  from the sweep-search method of analysis is divided by the integral of the  $\sigma'_{v-z}$  distribution along the imaginary vertical section of height  $H$  (refer to the equation given in this figure). [ $\sigma'_{v-z}$  is contained within the brackets of the  $\sigma_A$  relationships given in this figure.] For the case of the Figure C.12 retained soil with a constant surface slope (as far as this effective vertical stress computational procedure is concerned), the equation for  $\sigma'_{v-z}$  and  $\sigma_A$  at key points and for  $K_{A-\phi\text{-weight}}$  is straight-forward and given in this figure.

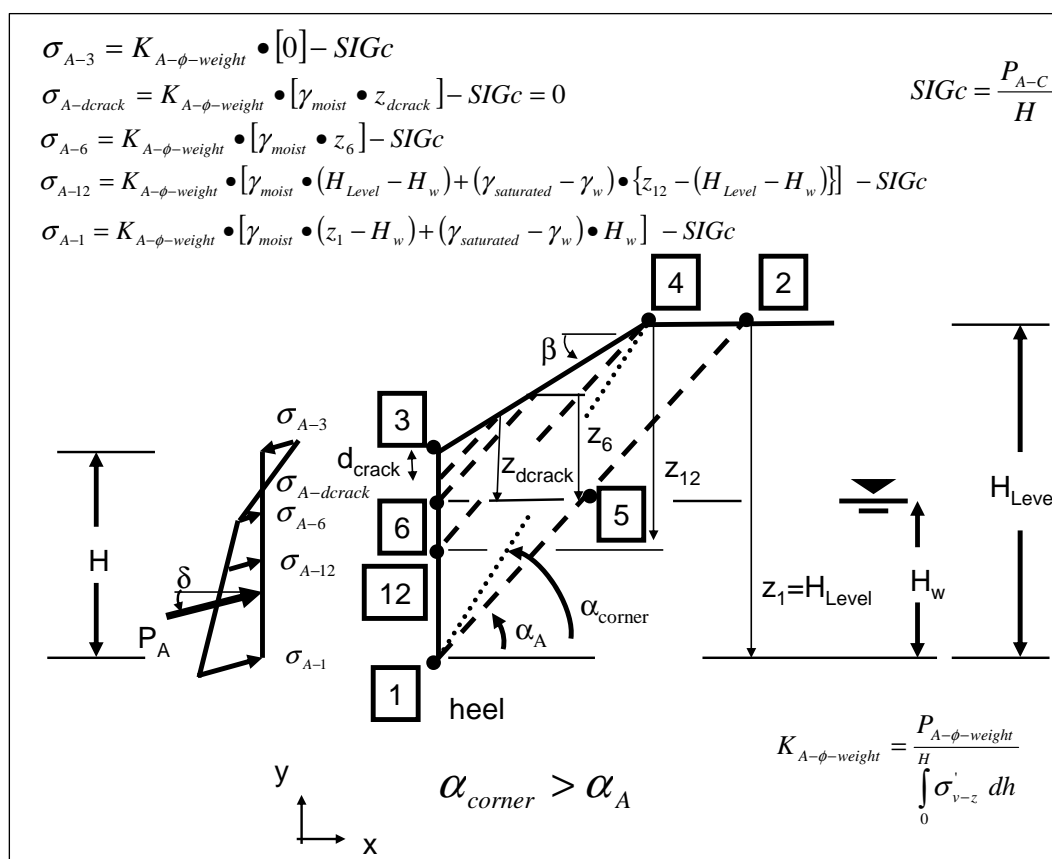


Figure C.12. The active earth pressure distribution corresponding to the incremental static force component,  $P_A$ , acting at an effective interface friction angle of  $\delta$  to the normal of the vertical imaginary section through the heel of the wall for a bilinear ground surface – partially submerged backfill with  $\phi' > 0$  and  $c' > 0$ .

The procedure outlined in Step 1 in Section C.1 that converts the  $\sigma_A$  distribution into equivalent forces (see Figure C.8) is used to compute the resultant location  $h_{PA}$  of  $P_A$  for use in Equation C.12 for the resultant location  $h_{PAE}$  of  $P_{AE}$ . The procedures outlined in Step 2 and Step 3 in Section C.1 are used to compute the incremental dynamic force component  $\Delta P_{AE}$  and its corresponding equivalent earth pressure diagram.

#### C.4 Earth Pressure Distribution for the Dynamic Active Earth Pressure Force, $P_{AE}$ , for a Backfill with Mohr-Coulomb Shear Strength Parameters, $S_u$ - Total Stress Analysis

This section discusses the computation of the resultant location of  $P_{AE}$  and a corresponding pressure distribution for a backfill in which Mohr-

Coulomb total stress (undrained) shear strength parameter,  $S_u$ , is non-zero.<sup>1</sup>  $P_{AE}$  is equal to the sum of  $P_A$  plus  $\Delta P_{AE}$  by Equation B.1. The first three steps of the computational process outlined in Section C.1 are used to determine the earth pressure distribution and resultant location for  $P_{AE}$  for a backfill with nonzero  $S_u$  total stress shear strength parameter assigned to the backfill:

*Step 1: Convert the static active earth pressure force,  $P_A$ , into an equivalent active earth pressure diagram*

Equation A.31 of the (total stress) sweep-search wedge solution method described in Section A.5 demonstrates that  $P_A$  is made up of two forces, (1) a force component due to the weight of the soil (driving) wedge and (2) a cohesive force component. The resultant force component due to the weight of the soil wedge is reduced by the cohesion force component. The subtraction of the cohesion force component in Equation A.31 reflects a cohesion force component for a *tensile stress* distribution component of the resulting (effective) active earth pressure  $\sigma_A$  distribution of stresses with depth,

$$\sigma_A = K_{A-weight} \bullet \sigma_{v-z} - SIG_{Su} \quad (C.32)$$

The component of (total) active earth pressure distribution due to cohesion is designated as  $SIG_{Su}$  in this report and is of constant magnitude with depth.  $SIG_{Su}$  is computed by

$$SIG_{Su} = \frac{P_{A-Su}}{H} \quad (C.33)$$

with  $P_{A-Su}$  corresponding to the cohesion component of  $P_A$  computed using Equation A.31 in the sweep-search wedge method of analysis with a critical wedge oriented at angle  $\alpha_A$ . The active earth pressure coefficient,  $K_{A-weight}$ , is computed using

---

<sup>1</sup> A key item is the selection of suitable shear strength parameters. The assignment of total (or effective) shear strength parameter(s) for the retained soil to be consistent with the level of shearing-induced deformations encountered for each design earthquake in a rotational analysis and note that active earth pressures are used to define the loading imposed on the structural wedge by the driving soil wedge. (Refer to Table 1.1 for guidance regarding wall movements required to fully mobilize the shear resistance within the retained soil during earthquake shaking.)



$$K_{A\text{-weight}} = \frac{P_{A\text{-weight}}}{H \int_0^H \sigma_{v-z} dh} \quad (\text{C.34})$$

with  $P_{A\text{-weight}}$  corresponding to the weight component of  $P_A$  computed using Equation A.31 in the sweep-search wedge method of analysis. The total vertical stress  $\sigma_{v-z}$  is computed using a depth  $z$ , the depth below the ground surface using the procedure similar to that outlined in the Section C.2. In a moist backfill (i.e., with no water table) the depth to zero stress (i.e., depth of cracking) is computed as

$$d_{\text{crack}} = \frac{S/G_{Su}}{\gamma_{\text{moist}} \bullet K_{A\text{-weight}} \bullet \left[ \frac{\tan(\alpha_A)}{\tan(\alpha_A) - \tan(\beta)} \right]} \quad (\text{C.35})$$

The total vertical stress at the deepest point in the crack in moist soil (and above a water table) is computed equal to

$$\sigma_{v-z\text{-dcrack}} = \gamma_{\text{moist}} \bullet z_{\text{dcrack}} \quad (\text{C.36})$$

which, for a slip plane intersecting the sloping ground is

$$z_{\text{dcrack}} = d_{\text{crack}} \bullet \left[ \frac{\tan(\alpha)}{\tan(\alpha) - \tan(\beta)} \right] \quad (\text{bis C.19})$$

and  $\sigma_{A\text{-dcrack}}$  is equal to zero at the crack tip

$$\sigma_{A\text{-dcrack}} = 0 = K_{A\text{-weight}} \bullet \sigma_{v-z\text{-dcrack}} - S/G_{Su} \quad (\text{C.37})$$

In the case of a crack extending below a hydrostatic water table within a retained soil, the total vertical stress at the deepest point in the crack in Equation C.37, is computed using

$$\sigma_{v-z\text{-dcrack}} = \gamma_{\text{moist}} \bullet z_{11\text{toWT}} + \gamma_{\text{saturated}} \bullet z_{\text{WTto crack}} \quad (\text{C.38})$$

with  $z_{11\text{toWT}}$  and  $z_{\text{WTto crack}}$  dimensions the same as were shown in Figures C.10.a and C.10.b for the effective stress based analysis. In retained soils with a hydrostatic water table an iterative approach, using Equations C.37 and C.38, is used by CorpsW<sub>allSlip</sub> to determine the value of

$d_{\text{crack}}$ . Note that pore water pressure internal to the soil wedge is not included in the Equation C.38 total vertical stress computation.

CorpsWallSlip performs a permanent displacement analysis of a retaining wall due to earthquake shaking. Reversal in the direction of the horizontal component of the time-history of earthquake ground shaking occurs many times during the typical tens of seconds of ground motion. Consequently, a reversal in direction of the inertial force imparted to the structural wedge and to the soil driving wedge occurs many times during the course of the analysis using CorpsWallSlip. In a traditional soil wedge formulation for static loading, a crack is typically considered to exist within the upper regime of the soil driving wedge for a cohesive soil and the planar wedge slip surface is terminated when it intersects the zone of cracking at a depth  $d_{\text{crack}}$  below the ground surface (e.g., see Appendix H in EM 1110-2-2502). This assumption is not made the CorpsWallSlip formulation for dynamic loading. Instead, it is assumed that in the dynamic wedge formulation, the crack within the zone of cracking at the top of the retained cohesive soil of the driving wedge will not remain open during earthquake shaking *due to the inertial load direction reversals*. So even for cohesive soils, the Figure A.1 planar slip surface obtained from the sweep-search method of analysis used by CorpsWallSlip to obtain a value for the earthquake induced resultant driving force  $P_{\text{AE}}$  (acting on the structural wedge) extends uninterrupted within the driving soil wedge (in the retained soil) to the ground surface and is not terminated by a vertical crack face to the ground surface when it enters the zone of cracking. Since  $P_{\text{A}}$  is used solely to determine the value for  $h_{\text{PAE}}$ , the resultant location for  $P_{\text{AE}}$  with the procedure outlined in this appendix, a continuous planar slip surface is also assumed in  $P_{\text{A}}$  computations. A sweep-search wedge formulation is used to compute  $P_{\text{A}}$ . Equation C.35 for crack depth  $d_{\text{crack}}$  in moist backfill and Equation C.37 in partially submerged backfill are used solely to establish the static earth pressure diagram component of  $P_{\text{AE}}$  pressures along the imaginary vertical section passing through the heel of the wall, consistent with the Equation B.1 formulation. This assumption is made for the earth pressure distribution corresponding to  $P_{\text{A}}$  with consideration of  $d_{\text{crack}}$  because the permanent displacement of the structural wedge is away from the backfill and it is likely that at this vertical section a vertical crack may occur. Thus,  $d_{\text{crack}}$  is accounted for in the  $h_{\text{PAE}}$  computation using Equation C.12. The static tensile  $\sigma_{\text{A}}$  stresses along the driving soil wedge-to-structural wedge interface (i.e., located along the vertical imaginary section extending through

the heel) are neglected over the depth of cracking due to the presence of the crack by  $C_{\text{orps}}W_{\text{allSlip}}$ .

*Step 2: Create an incremental dynamic force component pressure diagram*

The incremental dynamic force component,  $\Delta P_{\text{AE}}$ , is next converted into an equivalent earth pressure diagram using the relationship

$$\Delta P_{\text{AE}} = P_{\text{AE}} - P_{\text{A}} \quad (\text{bis C.11})$$

and with values for  $P_{\text{AE}}$  and  $P_{\text{A}}$  provided by the dynamic and static sweep-search solutions made by  $C_{\text{orps}}W_{\text{allSlip}}$  using the procedures outlined in Appendix A (Sections A.4 and A.5). The Ebeling and Morrison (1992) simplified procedure assumes a trapezoidal distribution for the corresponding incremental stress distribution with an interface friction angle of  $\delta = 0$  to the normal of the vertical imaginary section in a total stress analysis (refer to Figure C.3). The resulting force corresponding to the area under the pressure distribution is equal to  $\Delta P_{\text{AE}}$  and acts at a height to 0.6 times  $H$ .

In the case of a Figure A.4 water filled crack,  $\Delta P_{\text{AE}}$  is given by

$$\Delta P_{\text{AE}} = P_{\text{AE}} - P_{\text{A}} - \Delta U \quad (\text{C.39})$$

with values for  $P_{\text{AE}}$  and  $P_{\text{A}}$  provided by the dynamic and static sweep-search solutions made by  $C_{\text{orps}}W_{\text{allSlip}}$  using the procedures outlined in Appendix A (Sections A.4 and A.5).  $P_{\text{A}}$  is set equal to  $P_{\text{static-total stress}}$  (Equation A.31) for the critical slip plane (i.e., at angle  $\alpha = \alpha_{\text{A}}$ ),  $\Delta U$  (Equation A.34) is the difference in water pressure force within the cracks on both sides of the Figure A.4 driving soil wedge. Recall that in a total stress analysis, internal pore water pressures are not applied along the imaginary vertical sections and slip plane defining the driving soil wedge. However, should a crack extend to below the water table, the boundary water pressures and their resultant forces are included along the imaginary vertical sections in the free body diagram for the static soil wedge, as depicted in Figure A.4, and in the computation of  $P_{\text{A}}$ . Further, it is assumed that in the dynamic wedge formulation used to compute  $P_{\text{AE}}$ , the crack within the zone of cracking at the top of the retained cohesive soil of the driving wedge will not remain open during earthquake shaking *due to the inertial load direction reversals* during this time-history based

analysis. So, no crack depth is included in the CorpsWallSlip analysis of the dynamic resultant force,  $P_{AE}$ , for cohesive soils.

*Step 3: Create the dynamic active earth pressure diagram*

The dynamic active earth pressure diagram is created by adding the earth pressure diagrams created in Steps 1 and 2. The resulting force corresponds to the area under the combined pressure distribution and is equal to  $P_{AE}$  (recall  $P_{AE} = P_A + \Delta P_{AE}$ ). Its point of application above the heel of the wall is given by

$$h_{PAE} = \frac{P_A \bullet (h_{PA}) + \Delta P_{AE} \bullet (0.6 \bullet H)}{P_{AE}} \quad (\text{bis C.12})$$

In the case of a Figure A.4 water filled crack, the point of application of  $P_{AE}$  is

$$h_{PAE} = \frac{P_A \bullet (h_{PA}) + \Delta U \bullet h_{\Delta U} + \Delta P_{AE} \bullet (0.6 \bullet H)}{P_{AE}} \quad (\text{C.40})$$

with  $P_A$  set equal to  $P_{\text{static-total stress}}$  (Equation A.31) for the critical slip plane (i.e., at angle  $\alpha = \alpha_A$ );  $\Delta U$  (Equation A.34) the difference in water pressure force within the cracks on both sides of the Figure A.4 driving soil wedge, and  $h_{PA}$  and  $h_{\Delta U}$  are the resultant locations of these respective forces.

In the special case of cohesive soils, the CorpsWallSlip analysis disregards the tensile stresses when defining the static active earth pressures and the corresponding resulting static active earth pressure force to be applied to the structural wedge, as well as when computing  $h_{PA}$  for this modified stress distribution. A trapezoidal earth pressure distribution is still used to define  $\Delta P_{AE}$ .

#### **C.4.1 Basic Procedure to Compute the Active Total Stress Distribution Corresponding to $P_A$ for a Partially Submerged Retained Soil with a Sloping Ground Surface**

The procedure outlined in this subsection considers the case of a partially submerged backfill in which Mohr-Coulomb total stress (undrained) shear strength parameter,  $S_u$ , is nonzero (i.e., a nonzero cohesion). The procedure to calculate the active earth pressure distribution for resultant

static force,  $P_A$ , due to the geometry of the backfill is outlined using the information contained within Figure C.13 for which the critical planar wedge slip plane that passes through point 1 (with  $\alpha_A > \alpha_{\text{corner}}$ ) intersects the sloping portion of the bilinear ground surface. The sweep-search wedge procedure described in Section A.5 is used to first compute the value for  $P_A$  as well as the orientation of the planar slip surface,  $\alpha_A$ , for the critical soil wedge that originates at point 1. The equation to compute the active earth pressures (designated as  $\sigma_A$ ) at the Figure C.13 key points designated as 1, 6,  $d_{\text{crack}}$ , and 3 is, by Equation C.32, equal to the active earth pressure coefficient,  $K_{A\text{-weight}}$ , times the vertical total stress at depth  $z$  in the retained soil minus  $\text{SIG}_{\text{Su}}$ . The key feature for this formulation is that at a given point along the vertical imaginary section through the heel of the structural wedge (identified in this figure as points 1, 6,  $d_{\text{crack}}$ , and 3), the total vertical stress (designated as  $\sigma_{v-z}$  in the brackets) is computed using a depth  $z$ , the depth below the ground surface as shown in this figure. A computation of  $\sigma_{v-z}$  and, subsequently,  $\sigma_A$  are made in this figure for point 1 (at the heel). Note that depth  $z$ , designated as  $z_1$  for point 1, is determined by extending the critical, planar slip plane from point 1 until it intersects the *sloping* ground surface. This same procedure is followed to compute the value for  $z$ ,  $\sigma_{v-z}$ , and  $\sigma_A$  at the other key points 6,  $d_{\text{crack}}$ , and 3 along the imaginary vertical section of height  $H$ . A plane oriented at  $\alpha_A$  from horizontal is projected from the point of interest (e.g., point  $d_{\text{crack}}$ ) up through the retained soil until it intersects the sloping ground surface.  $\sigma_{v-z-d_{\text{crack}}}$  is computed using the resulting vertical height  $z_{d_{\text{crack}}}$  of this planar surface, as shown in this figure. Moist unit weights above the water table and submerged unit weights below the water table are used to compute the vertical total stress  $\sigma_{v-z}$ . To determine the value for the active earth pressure coefficient,  $K_{A\text{-weight}}$ , the value for the force component  $P_{A\text{-weight}}$  from the sweep-search method of analysis is divided by the integral of the  $\sigma_{v-z}$  distribution along the imaginary vertical section of height  $H$  (refer to the equation given in this figure). [ $\sigma_{v-z}$  is contained within the brackets of the  $\sigma_A$  relationships given in this figure.] For the Figure C.13 case of a retained soil with a constant surface slope (as far as this total vertical stress computational procedure is concerned), the equation for  $\sigma_{v-z}$  and  $\sigma_A$  at key points and for  $K_{A\text{-weight}}$  is straight-forward and given in this figure.

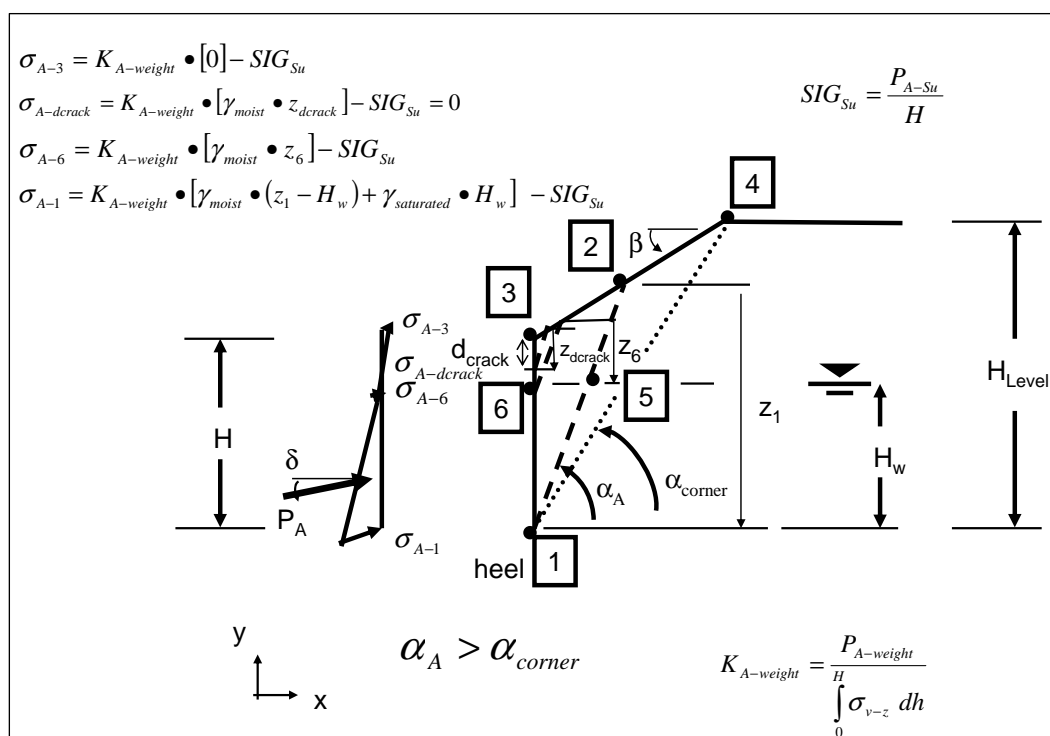


Figure C.13. The active earth pressure distribution corresponding to the incremental static force component,  $P_A$ , acting at an interface friction angle of  $\delta = 0$  to the normal of the vertical imaginary section through the heel of the wall for a bilinear ground surface – partially submerged backfill with  $S_u > 0$ .

The same procedure outlined in Step 1 in Section C.1 that converts the  $\sigma_A$  distribution into equivalent forces (see Figure C.8) is used to compute the resultant location  $h_{PA}$  of  $P_A$  for use in Equation C.12 for the resultant location  $h_{PAE}$  of  $P_{AE}$ . The procedure outlined in Step 2 and Step 3 in Section C.4 are used to compute the incremental dynamic force component,  $\Delta P_{AE}$ , and its corresponding equivalent earth pressure diagram.

#### C.4.2 Basic Procedure to Compute the Active Total Stress Distribution Corresponding to $P_A$ for a Partially Submerged Retained Soil with a Bilinear Ground Surface

The procedure used to calculate the active earth pressure distribution for resultant static force  $P_A$  due to the geometry of the backfill is outlined using the information contained within Figure C.14 for which the critical planar wedge slip plane that passes through point 1 (with  $\alpha_A > \alpha_{corner}$ ), *intersecting the level portion* of the bilinear ground surface. It considers the case of a partially submerged backfill in which Mohr-Coulomb total stress (undrained) shear strength parameter,  $S_u$ , is nonzero (i.e., a nonzero cohesion). The sweep-search wedge procedure described in Section A.5 is

used to first compute the value for  $P_A$  as well as the orientation of the planar slip surface,  $\alpha_A$ , for the critical soil wedge that originates at point 1. The equation to compute the active earth pressures (designated as  $\sigma_A$ ) at the Figure C.14 key points designated as 1, 12, 6,  $d_{\text{crack}}$ , and 3 is, by Equation C.32, equal to the active earth pressure coefficient,  $K_{A\text{-weight}}$ , times the vertical total stress at depth  $z$  in the retained soil minus  $\text{SIG}_{\text{Su}}$ . The key feature for this formulation is that at a given point along the vertical imaginary section through the heel of the structural wedge (identified in this figure as points 1, 12, 6,  $d_{\text{crack}}$ , and 3), the total vertical stress (designated as  $\sigma_{v-z}$  in the brackets) is computed using a depth  $z$ , the depth below the ground surface as shown in this figure. A computation of  $\sigma_{v-z}$  and, subsequently,  $\sigma_A$  are made in this figure for point 1 (at the heel). Note that depth  $z$ , designated as  $z_1$  for point 1, is determined by extending the critical, planar slip plane from point 1 until it intersects the horizontal ground surface. This same procedure is followed to compute the value for  $z$ ,  $\sigma_{v-z}$ , and  $\sigma_A$  at the other key points 12, 6,  $d_{\text{crack}}$ , and 3 along the imaginary vertical section of height  $H$ . A plane oriented at  $\alpha_A$  from horizontal is projected from the point of interest (e.g., point  $d_{\text{crack}}$ ) up through the retained soil until it intersects the sloping ground surface.  $\sigma_{v-z-d_{\text{crack}}}$  is computed using the resulting vertical height,  $z_{d_{\text{crack}}}$ , of this planar surface, as shown in this figure. Moist unit weights above the water table and submerged unit weights below the water table are used to compute the vertical total stress  $\sigma_{v-z}$ . To determine the value for the active earth pressure coefficient,  $K_{A\text{-weight}}$ , the value for the force component,  $P_{A\text{-weight}}$ , from the sweep-search method of analysis is divided by the integral of the  $\sigma_{v-z}$  distribution along the imaginary vertical section of height  $H$  (refer to the equation given in this figure). [ $\sigma_{v-z}$  is contained within the brackets of the  $\sigma_A$  relationships given in this figure.] For the case of the Figure C.14 retained soil with a constant surface slope (as far as this total vertical stress computational procedure is concerned), the equation for  $\sigma_{v-z}$  and  $\sigma_A$  at key points and for  $K_{A\text{-weight}}$  is straight-forward and given in this figure.

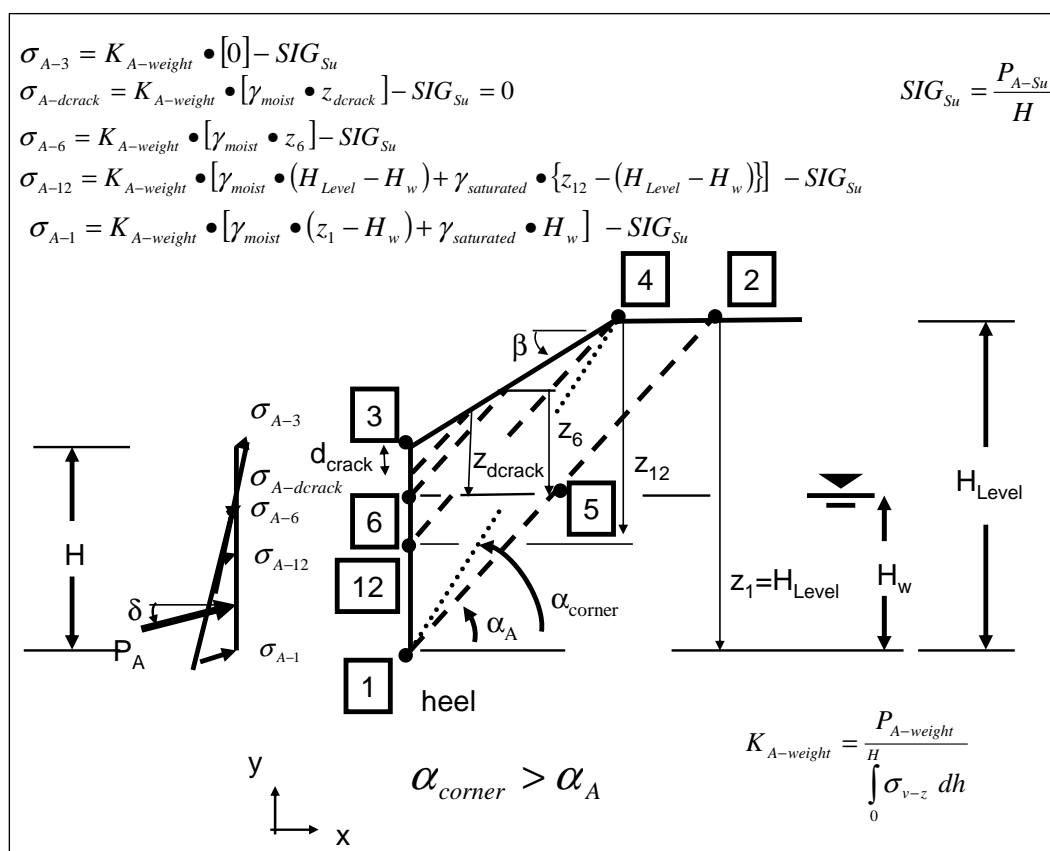


Figure C.14. The active earth pressure distribution corresponding to the incremental static force component,  $P_A$ , acting at an effective interface friction angle of  $\delta = 0$  to the normal of the vertical imaginary section through the heel of the wall for a bilinear ground surface – partially submerged backfill with  $S_u > 0$ .

The same procedure outlined in Step 1 in Section C.1 that converts the  $\sigma_A$  distribution into equivalent forces (see Figure C.8) is used to compute the resultant location  $h_{PA}$  of  $P_A$  for use in Equation C.12 for the resultant location  $h_{PAE}$  of  $P_{AE}$ . The procedure outlined in Step 2 and Step 3 in Section C.4 are used to compute the incremental dynamic force component,  $\Delta P_{AE}$ , and its corresponding equivalent earth pressure diagram.



## Appendix D: Water Pressures Acting on a Partially Submerged Structural Wedge

An earth retaining structure under investigation using CorpsWallSlip may retain a partially submerged backfill and may have a pool of water present in front of the structure. This appendix summarizes the computation of water pressures acting on a partially submerged structural wedge.

Dynamic considerations for the pool during earthquake shaking are accounted for in the analysis using hydrodynamic water pressures computed using the Westergaard (1931) procedure of analysis.

### D.1 Steady-State Water Pressures Acting on the Structural Wedge

**Effective Stress Analysis:** In an effective stress-based stability analysis, knowledge of the water pressures acting on the structural wedge is required. Figure D.1 shows key points and water pressures acting normal to the faces of the structural wedge that retains a partially submerged backfill and has a pool of water in front of the structure. Accounting for water pressures is an essential feature of an effective stress based stability analysis.

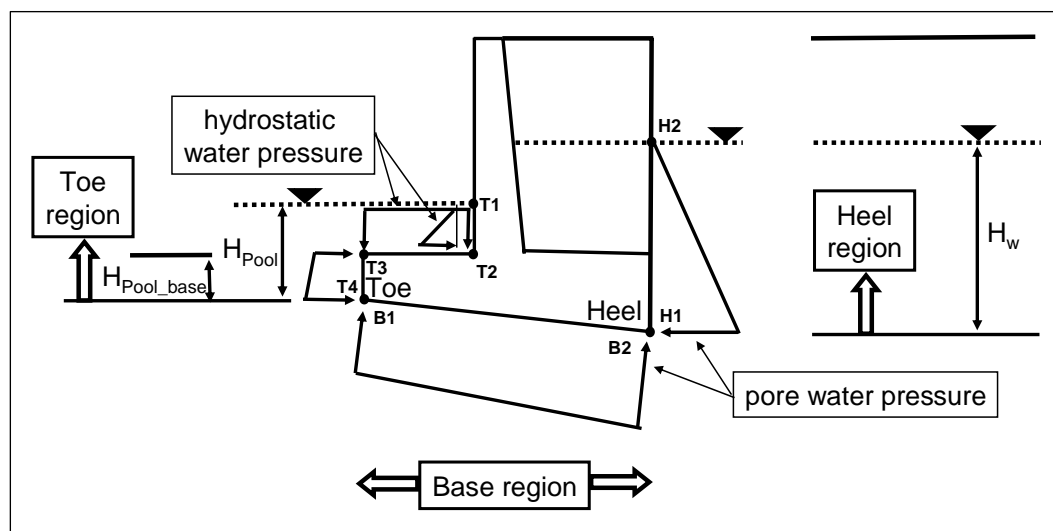


Figure D.1. Control points and steady-state water pressures acting normal to faces within the three regions of a structural wedge in full contact with the foundation – effective stress analysis.

Full contact between the base of the structural wedge and the foundation is assumed in Figure D.1. This is the situation for the sliding block method of analysis.

In CorpsWallSlip the faces of the structural wedge are divided into three regions: the toe region, the base region, and the heel region. Coordinates of key points defining these three regions are provided as input. These points are specified in a counterclockwise fashion progressing around the wetted perimeter of the structural wedge, as discussed in data input group 5 of Appendix F. For the structural wedge shown in Figure D.1, four points (designated points T1, T2, T3, and T4) define the wetted toe face, two points define the wetted base face (designated points B1 and B2), and two points define the wetted heel face (designated points T1 and T2). For the initial version of CorpsWallSlip, a simplified assumption is made that for steady-state conditions, hydrostatic water pressures exist within the heel region of the backfill. This implies that all head loss occurs due to flow within the foundation below the base of the structural wedge.<sup>1</sup> Thus, the pore water pressure at point H1 (also labeled as point B2) is equal to  $\gamma_w$  times  $H_w$ . Hydrostatic water pressures are also assumed within the pool at the toe region of the structural wedge. Consequently, the pore water pressure at point T4 (also labeled as point B1) is equal to  $\gamma_w$  times  $H_{Pool}$ . At points T2 and T3, the boundary water pressure is equal to  $\gamma_w$  times the depth to the point as measured from pool elevation. A linear variation in boundary water pressures is assumed along the base region, from point B1 to point B2. In this fashion, the steady-state boundary water pressures are assigned to the Figure D.1 idealized structural wedge.

CorpsWallSlip converts the Figure D.1 boundary water pressures into equivalent forces and points of application using the procedure outlined in Figure D.2 for the base region. The base region is defined by the two points B1 and B2. The pore water pressure at point B1 is designated  $u_{B1}$ , and the pore water pressure at point B2 is designated  $u_{B2}$ . A linear variation in pore water pressure exists between these two points and acts normal to this linear face. The pressure distribution acting normal to this linear face is then converted to equivalent forces (e.g., forces  $F_{B1}$  and  $F_{B2}$  at points B1 and B2, respectively) using the equations given in this figure. This same approach is used to compute equivalent point forces along each linear

---

<sup>1</sup> Future improvements to CorpsWallSlip will include other steady-state seepage conditions.

segment used to define all faces within the other two regions. Each region is reduced to linear segments of face geometry of constant or linear variation in pore water pressure with distance (e.g., three line segments are used to define the toe region while one line segment is used to define the heel region).

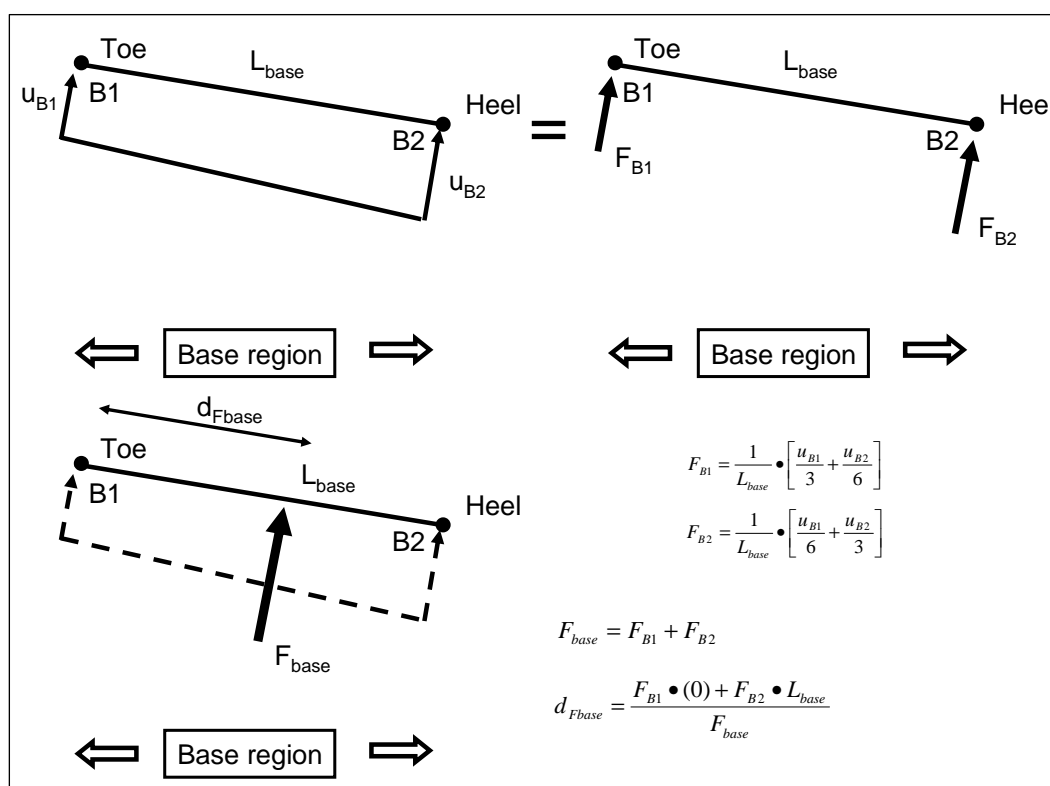


Figure D.2. Distribution of pore water pressures and its equivalent set of forces.

Also shown in Figure D.2 is a method for determining an equivalent resultant force, designated  $F_{base}$ , its point of application  $d_{Fbase}$  (as measured from the toe), and its point of application. An expanded variation on this procedure is used by CorpsWallSlip to compute the point of application of resultant force acting on each of the three regions identified in Figure D.1.

Global x- and y-coordinate forces are needed for the stability analysis of the structural wedge. They are computed for the equivalent point forces for each linear segment (defined by each adjacent pair of points) within each of the three regions. By specifying the Figure D.1 points in a counter-clockwise fashion around the wetted perimeter of the structural wedge, the equivalent point forces acting normal to the wetted perimeter face (refer to Figure D.2) may be converted into x- and y- global coordinates using the

procedure shown in Figure D.3. In this generalization, four hypothetical loaded faces, with each face defined by extending point I to point J, are shown. The face loaded by water pressure for each hypothetical line segment is identified in this figure. The procedure to convert a normal force, for example, at each point J into its x- and y- global force components is outlined using the equations given in this figure. Key to using the equations given in this figure is to determine for a given I-to-J line segment which quadrant this line segment falls into. For the toe region, the three line segments shown in Figure D.1 fall within quadrants IV and II. The single line segment defining the base region falls within quadrant IV and the line segment defining the heel region falls within quadrant I, along the positive Y axis.

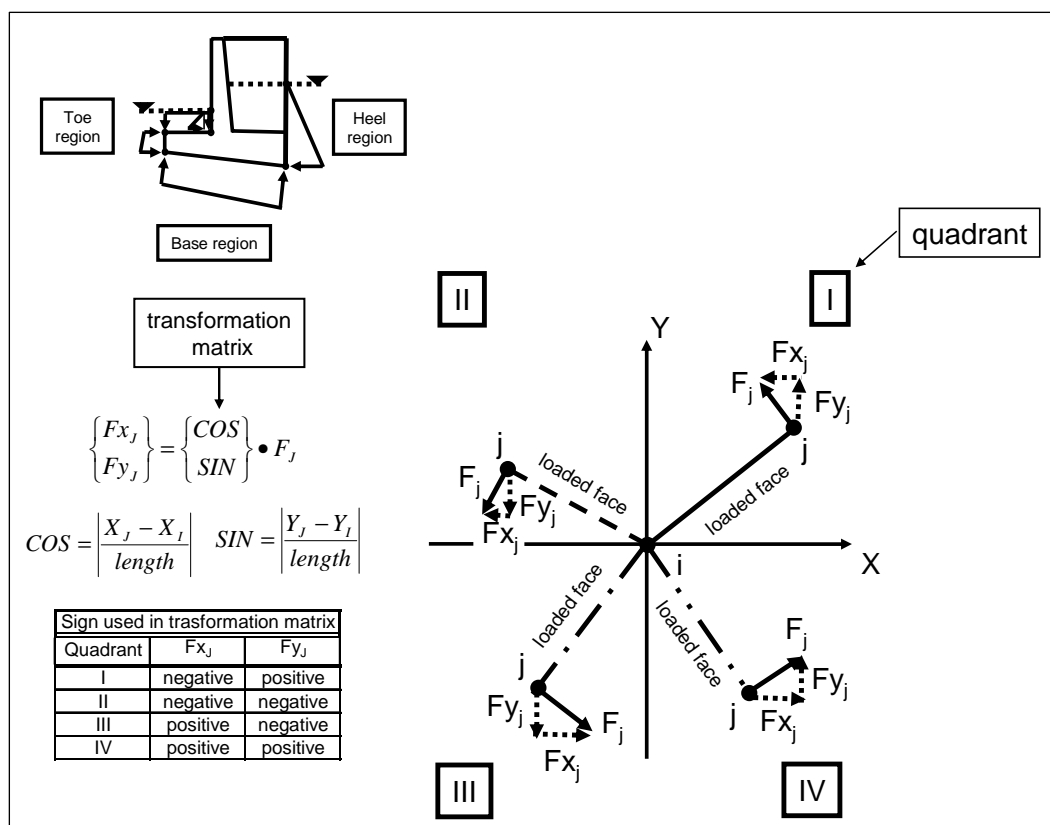


Figure D.3. Conversion of equivalent point forces at point J into global x- and y- coordinate forces.

In the case of rotation about the toe, contact between the base of the structural wedge and the foundation is lost sometime during earthquake shaking. Recall that a simplistic rigid base assumption is made in this formulation for rock-founded retaining structures. Due to the possible formation of a gap sometime during earthquake shaking, pore water

pressures along the base may differ from those shown in Figure D.1. (No excess pore water pressures due to earthquake-induced shear strains within the soils are included in the current  $C_{\text{orps}}W_{\text{allSlip}}$  formulation.) The exact pore water distribution within the structure-to-foundation gap is a complex problem and a subject for state-of-the-art research. In  $C_{\text{orps}}W_{\text{allSlip}}$ , a simplistic assumption of the hydrostatic pore water pressure at the heel of the wall is extended to along the entire base of the structure, as shown in Figure D.4. This assumes that a gap opens early on during earthquake shaking during rotation about the toe of the retaining wall.

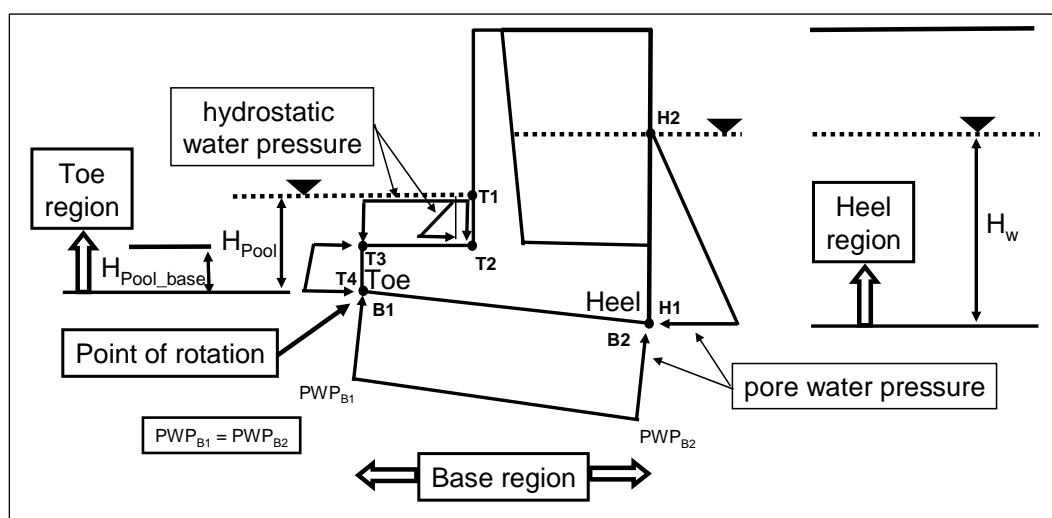


Figure D.4. Control points and water pressures acting normal to faces within the three regions of a structural wedge rotating about its toe – effective stress analysis.

**Total Stress Analysis:** In a total stress-based stability analysis, boundary water pressures are specified along the toe region only of the structural wedge. Knowledge of the internal (with respect to the soil and rock foundation) pore water pressures acting along/within the base region and the heel region of the structural wedge is not required in a total stress analysis.

Water pressure forces acting on the structural wedge are reported in the Workslide.TMP output file and the WORKslide.TMP output file generated in each  $C_{\text{orps}}W_{\text{allSlip}}$  analysis. These files may be viewed using the visual modeler boxes labeled **Show Sliding Evaluation** and **Show Lift-Off Evaluation** on the **Analysis** tab, respectively.

## D.2 Westergaard Procedure for Computing Hydrodynamic Water Pressures

Most Corps hydraulic structures that act as earth retaining structures possess a vertical face in contact with the pool (when present). The Westergaard procedure is used by CorpsWallSlip for computing the magnitude of the hydrodynamic water pressures along the idealized rigid walls during earthquake shaking. The solution developed by Westergaard (1931) is for the case of a semi-infinite long water reservoir retained by a concrete dam with a vertical face and subjected to a horizontal earthquake motion. The fundamental period of the concrete dam is assumed to be much smaller than the fundamental period of the earthquake so that the acceleration for the massive structure is approximated as the acceleration of the earthquake motion along the rigid base. This allows the problem of a very stiff concrete dam to be simplified to the case of a rigid vertical face moving at the same horizontal acceleration as the base horizontal acceleration. Using the equations of elasticity of a solid to describe the propagation of sounds in liquids (waves propagate without shear distortions) and with the water considered to compressible, a solution to the equation of motion of the water was developed for a harmonic motion applied along the base of the reservoir. This solution ignores the effects of surface waves and is valid only when the period of the harmonic excitation is greater than the fundamental natural period of the reservoir (Chopra 1967). The fundamental period for the reservoir,  $T_w$ , is equal to

$$T_w = \frac{4 \bullet H_p}{C} \quad (D.1)$$

where the velocity of sound in water,  $C$ , is given by

$$C = \sqrt{\frac{K}{\rho}} \quad (D.2)$$

And the mass density of water,  $\rho$ , is given by

$$\rho = \frac{\gamma_w}{g} \quad (D.3)$$

With the bulk modulus of elasticity of water,  $K$ , equal to  $4.32 \times 10^7$  lb/ft<sup>2</sup>, the unit weight for water,  $\gamma_w$ , equal to 62.4 lb/ft<sup>3</sup> and the acceleration due

to gravity,  $g$ , equal to 32.17 ft/sec<sup>2</sup>,  $C$  is equal to 4,720 ft/sec. For example, with a depth of pool of water,  $H_p$ , equal to 25 ft,  $T_w$  is equal to 0.02 sec (47 Hz) by Equation D.1.

The resulting relationship for hydrodynamic pressure on the face of the dam is a function of the horizontal seismic coefficient,  $k_h$  (expressed as a decimal fraction of acceleration of gravity,  $g$ ), the depth of water,  $Y_w$ , the total depth of the pool of water,  $H_p$ , the fundamental period of the earthquake, and the compressibility of the water,  $K$ . The hydrodynamic pressure is opposite in phase to the base application and for positive base accelerations the hydrodynamic pressure is a tensile. Westergaard proposed the following approximate solution for the hydrodynamic water pressure distribution: a parabolic dynamic pressure distribution,  $p_{wd}$ , described by the relationship

$$p_{wd} = \frac{7}{8} \cdot k_h \cdot \gamma_w \cdot \sqrt{y_w \cdot H_p} \quad (D.4)$$

The resultant dynamic water pressure force,  $P_{wd}$ , is equal to

$$P_{wd} = \frac{7}{12} \cdot k_h \cdot \gamma_w \cdot (H_p)^2 \quad (D.5)$$

acting at an elevation equal to 0.4  $H_p$  above the base of the pool as shown in Figure D.5. This dynamic force does not include the hydrostatic water pressure force acting along the face of the dam (refer to Figure D.5).

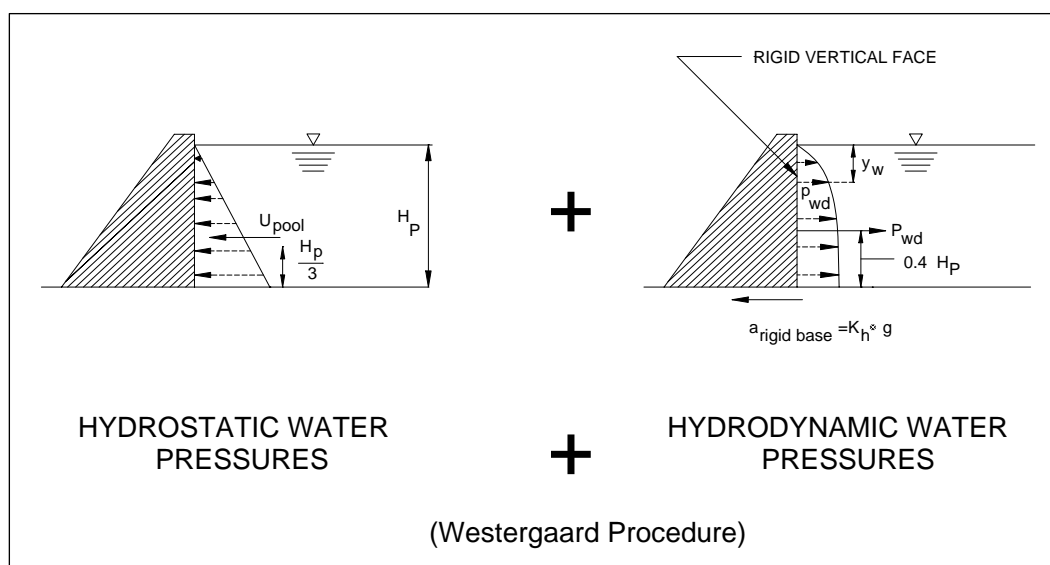


Figure D.5. Hydrostatic and Westergaard hydrodynamic water pressures acting along vertical wall during earthquakes.

Note that the value for  $P_{wd}$  is restricted to  $|P_{wd}| \leq U_{pool}$  in CorpsWallSlip when acceleration(s) induce a hydrodynamic water pressure  $P_{wd}$  force acting counter to the direction of the hydrostatic water pressure force,  $U_{pool}$ . This occurs in the case of the vector configuration for base acceleration(s) as shown in Figure D.5 (i.e., base acceleration(s) directed away from the body of the pool and towards the body of the dam).

In a maximum transmissible acceleration evaluation and during sliding in a Newmark sliding block time-history analysis of permanent displacement, the horizontal acceleration used to compute  $P_{wd}$  is a constant and equal to the value computed by Equation D.5 with  $k_h$  in this equation set equal to the maximum transmissible acceleration coefficient.  $H_p$  in Equation D.5 is set equal to the difference between the surface and the base height of the pool (i.e.,  $H_{Pool} - H_{Pool\_base}$ ) in CorpsWallSlip. The initial version of CorpsWallSlip implements the Westergaard hydrodynamic water pressure force Equation D.5 approximation in both the sliding and rotating block analysis. For a rigid block approximation and for the Corps hydraulic retaining structures with a vertical “wet” face (pool-side), the Westergaard procedure is considered a reasonable assumption by the primary author of this report. However, it is recognized that this assumption and approach is less accurate for the rotating block analysis than for the sliding block analysis because of the variation in horizontal accelerations along the wetted face of the structural wedge, as may be inferred by reference to the dependence of the horizontal acceleration on not only the



ground acceleration as well as the angular acceleration, rotational velocity and *position of the point of interest* as noted in Equation 3.6 for Figure 3.3. In this initial version of CorpsWallSlip, only the ground acceleration is used to compute  $P_{wd}$  using Equation D.5.<sup>1</sup> In a structural wedge analysis of incipient lift-off in rotation, the horizontal acceleration used to compute  $P_{wd}$  at incipient lift-off is another constant (of different value from the maximum transmissible acceleration value). Consequently, the value for  $P_{wd}$  is also a constant for the lift-off calculation. During a rotational time-history analysis, the magnitude of horizontal acceleration used to compute  $P_{wd}$  varies with time during rotation. So  $P_{wd}$  also varies in magnitude and direction with time in a rotational analysis in CorpsWallRotate.

---

<sup>1</sup> Future improvements will include the development of a more complete hydrodynamic water pressure force formulation that accounts for the variation in acceleration along the “wetted” face of the Corps hydraulic earth retaining structure during rotation by considering angular acceleration, rotational velocity, and *position of all points along the wetted face*.

## Appendix E: Structural Wedge Rigid Body Mass and Mass Moment of Inertia Computations

This appendix outlines the computation of the mass and center of gravity of the structural wedge and the computation of mass of its mass moment of inertia. Recall that the structural wedge is modeled as a rigid body.

### E.1 Mass and Center of Gravity of the Structural Wedge

The mass,  $m$ , per unit volume at any point within a body is given by

$$m = \frac{\gamma}{g} \quad (\text{E.1})$$

where at any point within the body  $\gamma$  is the total unit weight per unit volume, and  $g$  is the constant of acceleration due to gravity (equal to 32.174 ft/sec<sup>2</sup>, 386.086 in./sec<sup>2</sup>, 980.665 m/sec<sup>2</sup>, or 980.665 gal).

The total mass,  $M$ , of the planar rigid body is defined as

$$M = \iint_{\text{Area}} m \, dx \, dy \quad (\text{E.2})$$

Equivalently, this total mass  $M$  is

$$M = \frac{W}{g} \quad (\text{E.3})$$

where  $W$  is the total weight of the entire rigid body.

In order to compute the center of mass of a rigid body, it is often convenient to discretize the rigid body into regular geometrical and/or material regions (e.g., see Figure E.1), each with a constant material unit weight and thus a constant mass per unit volume. The mass for each region  $i$ ,  $\bar{m}_i$ , is

$$\bar{m}_i = \iint_{\text{Area } i} m \, dx \, dy \quad (\text{E.4})$$

and for regular geometry, its region mass center (denoted as  $x_i$  and  $y_i$ ) is easily computed.

For a rigid body comprised of regions of different masses, the center of mass (point G) of the rigid body is computed by

$$\bar{x} = \frac{\sum \bar{m}_i \cdot x_i}{\sum \bar{m}_i} \quad (\text{E.5})$$

and

$$\bar{y} = \frac{\sum \bar{m}_i \cdot y_i}{\sum \bar{m}_i} \quad (\text{E.6})$$

where  $\sum \bar{m}_i$  is equal to the sum of masses of each of the discretized regions, which is also the total rigid body mass  $M$ , and  $x_i$  and  $y_i$  are the individual coordinate centers of each mass region  $i$ .

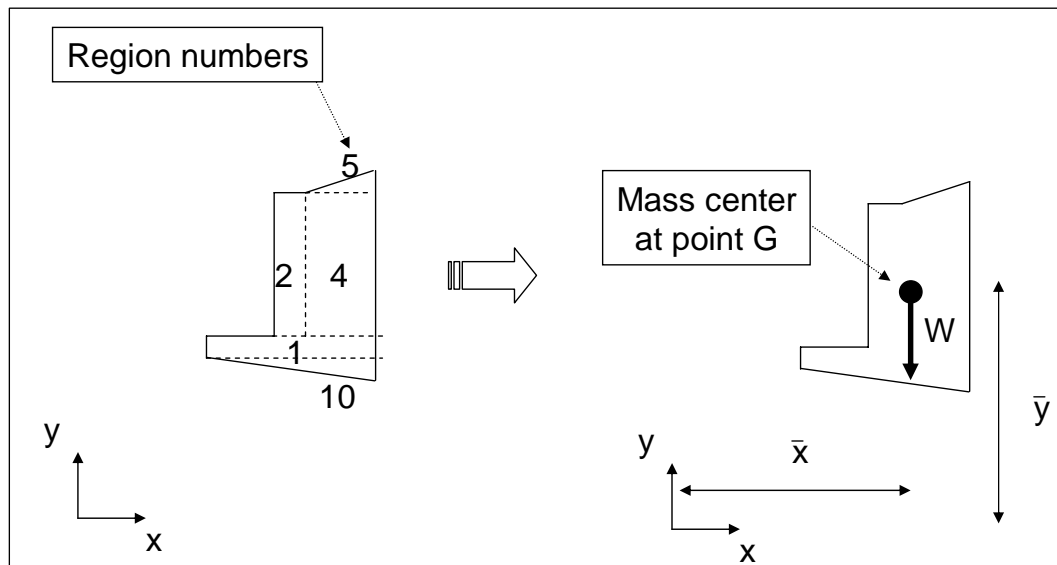


Figure E.1. Example discretization of a rigid body into regular geometrical and material regions.

## E.2 Mass Moment of Inertia of the Structural Wedge

Figure E.2 depicts the dynamic forces acting on the structural wedge as well as the ten material regions used to define this structural wedge that contains the retaining wall.

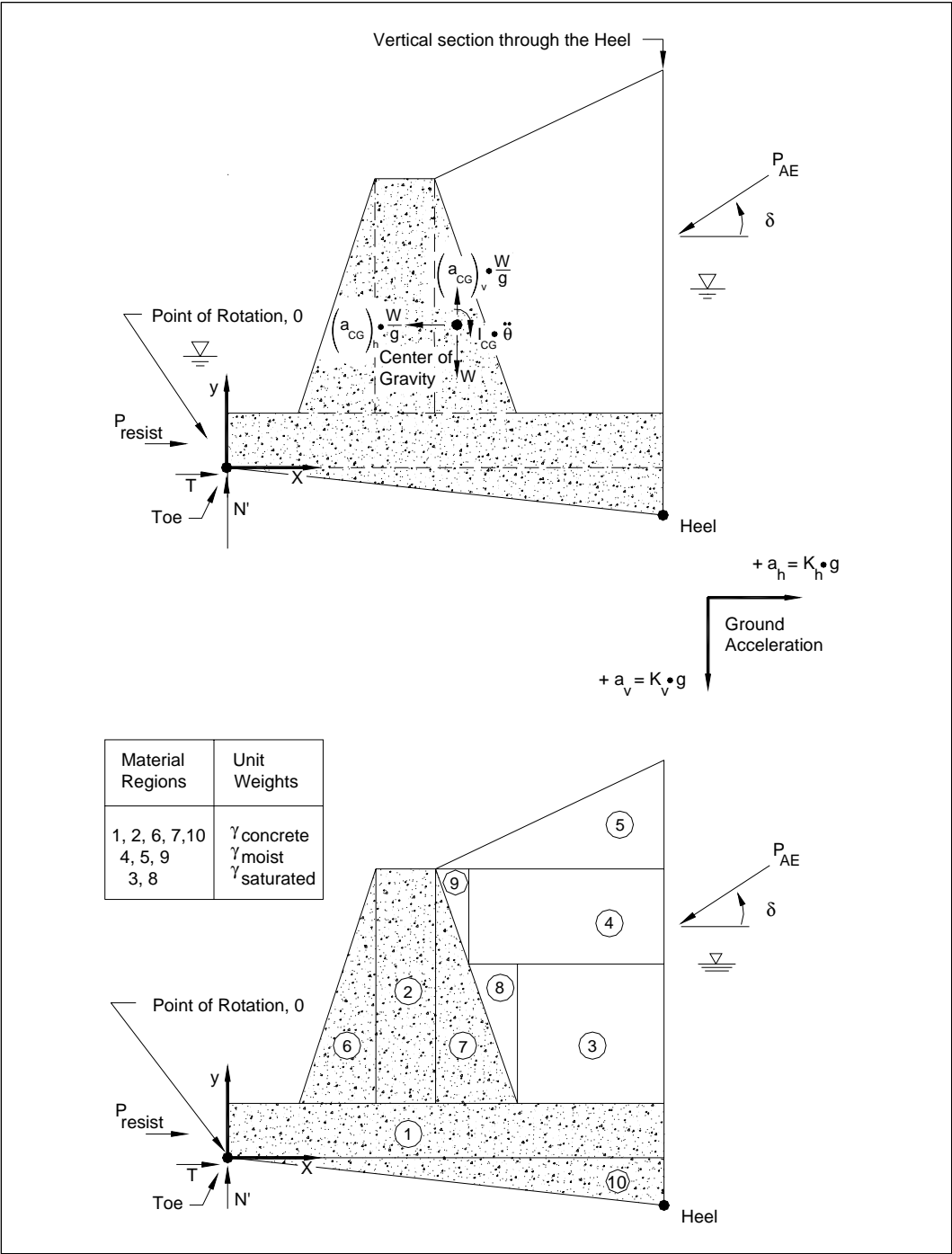


Figure E.2. Dynamic forces acting on the structural wedge and its material regions.

Each of the ten Figure E.3 material regions are labeled by a material region number and are either rectangular or triangular in shape. The user specifies the width and height of each of the ten material regions to define the geometry of the structural wedge. In the following two sections, the mass moments of inertia of a rectangle and a triangle are first derived. The mass moment of inertia of the entire structural wedge is then assembled from each of the ten material regions using one of these basic formulations.

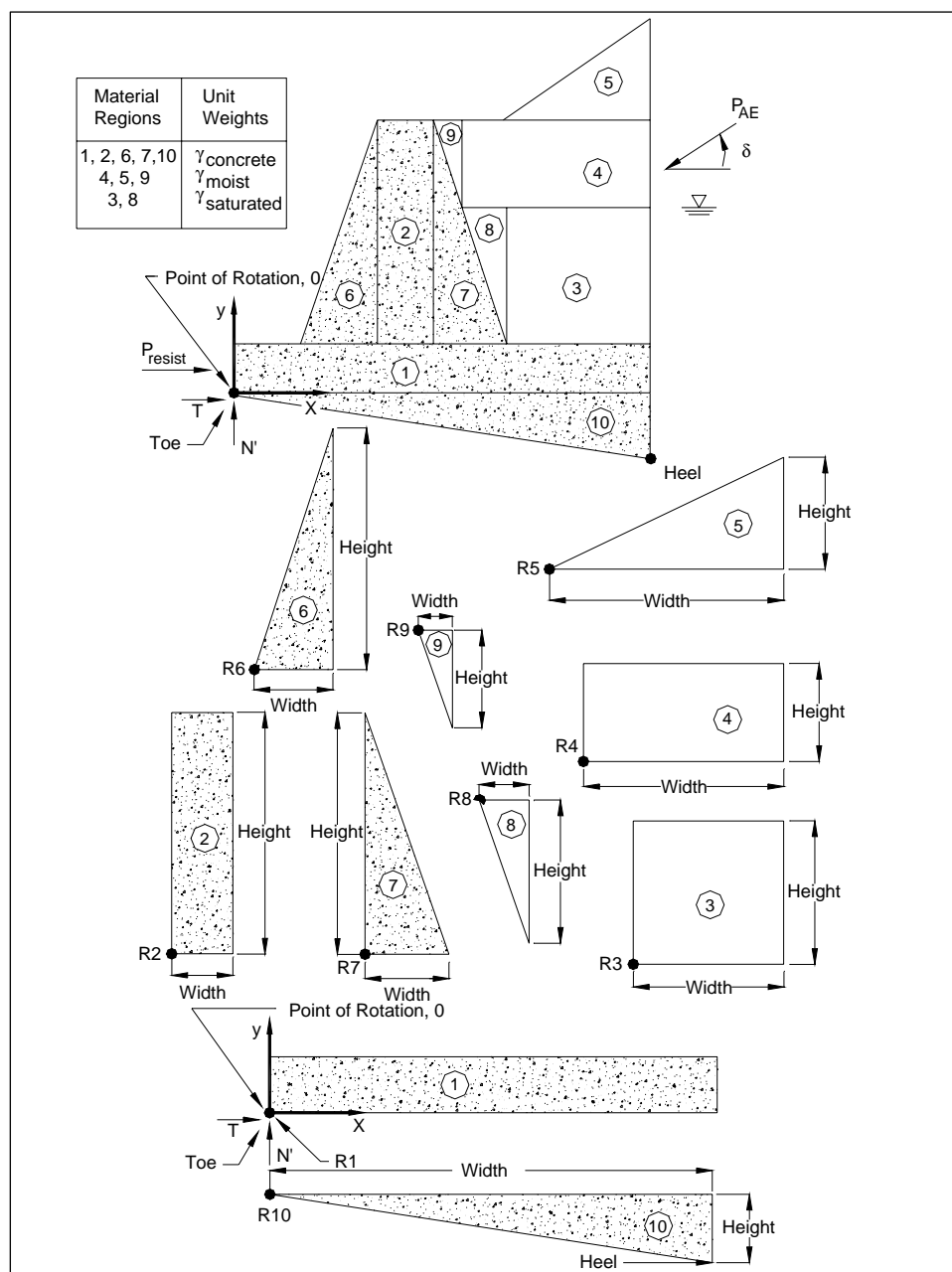


Figure E.3. The structural wedge comprises ten material regions.

Figure E.3 defines the reference points on each of the ten material regions. This point defines the left-most point on each material region. For rectangles and triangles with vertical left-hand sides, it is always the lower-most, left point. It is used to determine the position of each material region within  $C_{\text{orpsWallSlip}}$  and  $C_{\text{orpsWallRotate}}$ .

### E.2.1 Mass Moment of Inertia of a Rectangle

For a Figure E.4 rectangle of width  $b$  and height  $h$ , the cross-sectional area is

$$Area_{\text{rectangle}} = b \cdot h \quad (\text{E.7})$$

and with a mass of rectangle of

$$M_{\text{rectangle}} = \frac{\gamma \cdot Area_{\text{rectangle}}}{g} \quad (\text{E.8})$$

Note that the mass per unit volume is given by

$$m = \frac{\gamma}{g} \quad (\text{bis. E.1})$$

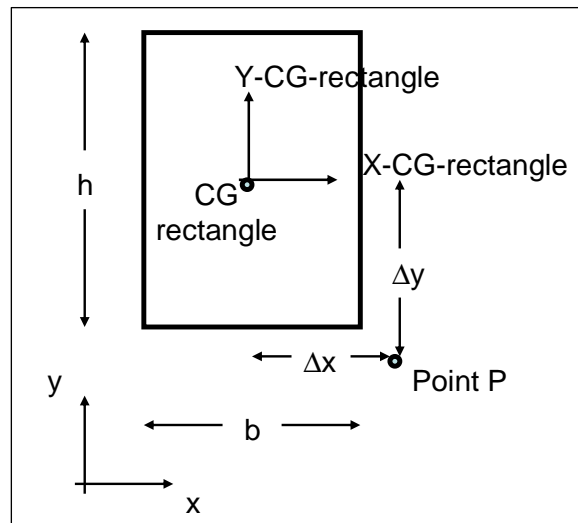


Figure E.4. Rectangle of width  $b$  and height  $h$ .

The  $x$ - and  $y$ - axes mass moments of inertia of the rectangle about its center of gravity, CG, are

$$I_{x\text{-CG-rectangle}} = \left( \frac{\gamma}{g} \right) \bullet \frac{1}{12} \bullet b \bullet (h)^3 \quad (\text{E.9})$$

and

$$I_{y\text{-CG-rectangle}} = \left( \frac{\gamma}{g} \right) \bullet \frac{1}{12} \bullet h \bullet (b)^3 \quad (\text{E.10})$$

Let the distance between the center of gravity of the rectangle to an arbitrary point P be equal to  $\Delta x$  and  $\Delta y$ .

The x- and y- axes mass moments of inertia of the rectangle about point O are

$$I_{x-P} = I_{x\text{-CG-rectangle}} + \left( \frac{\gamma \bullet \text{Area}_{\text{rectangle}}}{g} \right) \bullet (\Delta y)^2 \quad (\text{E.11})$$

and

$$I_{y-P} = I_{y\text{-CG-rectangle}} + \left( \frac{\gamma \bullet \text{Area}_{\text{rectangle}}}{g} \right) \bullet (\Delta x)^2 \quad (\text{E.12})$$

### E.2.2 Mass Moment of Inertia of a Triangle

For a Figure E.5 triangle of base width  $b$  and height  $h$ , the cross-sectional area is

$$\text{Area}_{\text{triangle}} = \frac{1}{2} \bullet b \bullet h \quad (\text{E.13})$$

and with a mass of triangle of

$$M_{\text{triangle}} = \frac{\gamma \bullet \text{Area}_{\text{triangle}}}{g} \quad (\text{E.14})$$

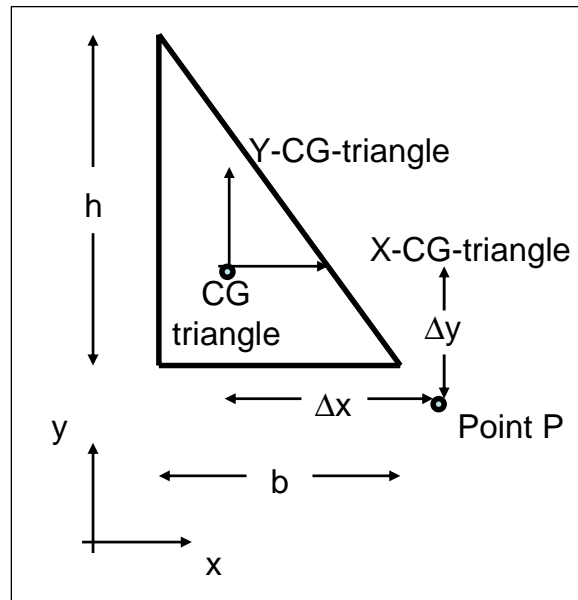


Figure E.5. Triangle of base width  $b$  and height  $h$ .

The  $x$ - and  $y$ - axes mass moments of inertia of the triangle about its center of gravity, CG, are

$$I_{x\text{-CG-triangle}} = \left( \frac{\gamma}{g} \right) \cdot \frac{1}{36} \cdot b \cdot (h)^3 \quad (\text{E.15})$$

and

$$I_{y\text{-CG-triangle}} = \left( \frac{\gamma}{g} \right) \cdot \frac{1}{36} \cdot h \cdot (b)^3 \quad (\text{E.16})$$

Let the distance between the center of gravity of the triangle to an arbitrary point  $P$  be equal to  $\Delta x$  and  $\Delta y$ .

The  $x$ - and  $y$ - axes mass moments of inertia of the triangle about point  $O$  are

$$I_{x-P} = I_{x\text{-CG-triangle}} + \left( \frac{\gamma \cdot \text{Area}_{\text{triangle}}}{g} \right) \cdot (\Delta y)^2 \quad (\text{E.17})$$

and



$$I_{y-P} = I_{y-CG-triangle} + \left( \frac{\gamma \bullet Area_{triangle}}{g} \right) \bullet (\Delta x)^2 \quad (E.18)$$

### E.2.3 Mass Moment of Inertia of the Structural Wedge

The center of gravity of the structural wedge is computed in CorpsW<sub>allSlip</sub> and CorpsW<sub>allRotate</sub> following the procedure described in Section E.1. The mass moment of inertia about this center of gravity is computed using either Equations E.11 and E.12 for a rectangle or Equations E.17 and E.18 for a triangle, for each of the ten material regions and with point P assigned to the coordinate of the center of gravity of the structural wedge. The mass moment of inertia about the center of rotation of the structural wedge, point O in Figure E.2, is computed using Equation E.19.

$$I_o = I_{CG} + \frac{W}{g} \bullet (r_{CG/O})^2 \quad (E.19)$$

## **Appendix F: Listing and Description of CorpsWallSlip ASCII Input Data File (filename: CWROTATE.IN)**

This appendix lists and describes the contents of the ASCII input data file to the FORTRAN engineering computer program portion of CorpsWallSlip. This data file, always designated as CWROTATE.IN, is created by the graphical user interface (GUI), the visual modeler portion of CorpsWallSlip. The FORTRAN code of CorpsWallSlip evolved from CorpsWallRotate (Ebeling and White 2006). Both formulations share many engineering computations. So in order to facilitate the maintenance of both engineering formulations and corresponding software, the same FORTRAN code is used with the two visual modelers and post-processors. The first line of input is used to designate a CorpsWallSlip analysis. Other key codes are used in the input data to further distinguish between the two engineering formulations.

### **First line/First column – Designate this data input is for a CorpsWallSlip analysis:**

Type a capital **S** in the first column of the first line.

### **Second line – Designate the type of CorpsWallSlip analysis:**

#### **KEY\_CWSLIP\_analysis**

with

KEY\_CWSLIP\_analysis = 1      Simplified sliding block analysis in which acceleration time-histories are not required.

KEY\_CWSLIP\_analysis = 2      Complete Newmark sliding block time-history analysis in which acceleration time-histories are required.

The ASCII input data to CorpsWallSlip is provided in eight groups of data. They are as follows:

### Group 1 – Global Geometry of the Structural Wedge that Contains the Retaining Wall

<b>XTOE, YTOE</b>	X and Y coordinates of the toe of the wall.
<b>XROTATE, YROTATE</b>	Set equal to the X and Y coordinates of the toe of the wall.
<b>XHEEL, YHEEL</b>	X and Y coordinates of the heel of the wall.
<b>Gweight, Gmass, Gconstant</b>	Weight and mass of the structural wedge. The value for Gconstant identifies the units of length, density, force, and pressure being used according to the table below.
<b>GXCG, GYCG</b>	X and Y coordinates of the center of gravity.
<b>GIXmassptO, GIYmassptO, GjmassptO</b>	X-mass moment of inertia about the point of rotation, Y-mass moment of inertia about the point of rotation, and the mass moment of inertia about the point of rotation.

Value for Gconstant	Units of Length	Units of Soil and Concrete Densities	Units of Force	Units of Pressure
32.174	feet	lb/ft <sup>3</sup>	lb	lb/ft <sup>2</sup>
386.086	inches	lb/in <sup>3</sup>	lb	lb/in <sup>2</sup>
9.80665	meters	kN/m <sup>3</sup>	kN	kN/m <sup>2</sup> (=kPa)
980.665	centimeters	kN/cm <sup>3</sup>	kN	kN/cm <sup>2</sup>
9806.65	millimeters	kN/mm <sup>3</sup>	kN	kN/mm <sup>2</sup>

### Group 2 – Base of Structural Wedge

#### **PHIi, Ci, PHIf, Cf, ISTRENGTHsw**

Ci and PHIi are the Mohr-Coulomb shear strength parameters for the base of wall-to-foundation interface.

Cf and PHIf are the Mohr-Coulomb shear strength parameters for the foundation.

and

ISTRENGTHsw = 1 Strength definition below the structural wedge – Effective Stress

ISTRENGTHsw = 2 Strength definition below the structural wedge – Total Stress

Note: In a Total Stress Analysis PHI is set equal to zero and C is set equal to the value for the undrained shear strength,  $S_u$ , for the out base of wall-to-foundation interface and in the foundation, respectively. Internal pore water pressures are not considered explicitly in total stress analyses, but the effects of the pore pressures in the undrained tests are reflected in the undrained shear strength value, as discussed in Duncan and Buchignani (1975). Consequently, uplift pressures acting normal to the foundation interface are not included in the free-body force diagram of the structural wedge in a total stress analysis by CWSlip.

**Group 3 – Resisting Force Normal to a Vertical Plane Extending up Thorough the Toe of the Structural Wedge**

**XRESIST, YRESIST, FXRESIST** - X and Y coordinates of the resisting horizontal force, and the value of the horizontal force in consistent units.

**Group 4 – Driving Wedge in the Retained Soil**

**PHI, C, DELTA**

**H, HLEVEL, BETA**

**GAMAMOIST, GAMASAT**

**SLIPMIN**

**ISTRENGTHdw**

C and PHI are the Mohr-Coulomb shear strength parameters for the retained soil (i.e., the backfill), and DELTA is the interface friction along the vertical plane extending up thorough the heel of the structural wedge.

GAMAMOIST is the moist unit weight of the retained soil and GAMASAT is the saturated unit weight in consistent units (force/length<sup>3</sup>).

H is the height of the vertical plane extending up from the heel of the structural wedge to the ground surface ( $H \leq HLEVEL$ ).

BETA is the slope of the ground surface of the retained soil in degrees ( $BETA = 0$  if  $HLEVEL = H$ ).

HLEVEL is the height to level retained soil as measured from the heel of the wall/structural wedge ( $HLEVEL \geq H$ ).

Note: For the infinite slope problem, input a large value for HLEVEL such that the critical, planer slip surface computed within the retained soil does not intersect the fictitious level retained soil ground surface.

SLIPMIN is the shallowest planar slip surface that a potential slip surface can achieve in the retained soil. SLIPMIN is measured from horizontal and specified in degrees (a value between 1 and 89 degrees).

with

ISTRENGTHdw = 1 Soil Strength definition within retained soil – Effective Stress

ISTRENGTHdw = 2 Soil Strength definition within retained soil – Total Stress

Note: In a Total Stress Analysis PHI is set equal to zero and C is set equal to the value for the undrained shear strength,  $S_u$ , of the retained soil (i.e., the backfill). Internal pore water pressures are not considered explicitly in total stress analyses, but the effects of the pore pressures in the undrained tests are reflected in the undrained shear strength value, as discussed in Duncan and Buchignani (1975). Consequently, pore water pressures acting normal to the potential slip plane within the retained soil are not included in the free-body force diagram of the soil wedge in a total stress analysis by CWSlip.

#### **Group 5 – Water Table Height in the Retained Soil and Pool Height, with Input in Four Parts**

##### **Part 1: GAMAW**

##### **HW, HPool, HPool\_base**

with

GAMAW is the unit weight of water in consistent units (units of force/length<sup>3</sup>).

HW is the height of water table in the retained soil (i.e., the backfill) as measured from the heel of the wall of the structural wedge.

HPool is the height of pool in front of the wall as measured from the toe of the wall of the structural wedge.

and

HPool\_base is the height to the base of the pool as measured from the toe of the wall of the structural wedge ( $HPool\_base \leq HPool$ ).

Note: For no water table in the retained soil (i.e., a “dry” backfill), HW is set equal to zero.

For no pool in front of the wall, HPool and HPool\_base are equivalent and set equal to zero.

Data provided in subsequent three parts define points along each of the three wetted perimeter regions of the structural wedge. The first point specified is at the intersection of the pool with the exposed face of the wall. All subsequent points are specified in a counterclockwise fashion progressing around the wetted perimeter of the structural wedge (of toe region to base region to heel region).

*Special case; “dry” site: In the case of a “dry” site, HW, HPool, and HPool\_base are all set to zero. Skip Parts 2, 3, and 4 input.*

**Skip Part 2 input if HPool = 0.**

**Part 2: nWetToePTS**

**X\_Wet\_Toe<sub>i</sub>, Y\_Wet\_Toe<sub>i</sub> (i=1 to nWetToePTS)**

with

nWetToePTS is the total number of points defining the exposed wetted perimeter face of the wall and progressing from the pool of water to the toe of the wall, including the point defining the intersection of the base of the pool and the wetted wall face.

X\_Wet\_Toe<sub>i</sub>, Y\_Wet\_Toe<sub>i</sub> are the coordinates of the exposed wetted perimeter face of the wall and progressing from the pool of water to the toe of the wall.

Note: The coordinates of the point defined by the intersection of the exposed wetted perimeter and the base of the pool in to be included in the nWetToePTS points.

**Part 3: nWetBasePTS**

**X\_Wet\_Base<sub>i</sub>, Y\_Wet\_Base<sub>i</sub> (i=1 to nWetBasePTS)**

with

nWetBasePTS is the total number of points defining the wetted perimeter face of the base of structure-to-foundation interface and progressing from the toe the heel of the wall.

X\_Wet\_Base<sub>i</sub>, Y\_Wet\_Base<sub>i</sub> are the coordinates of the exposed wetted perimeter face of the base of structure-to-foundation interface and progressing from the toe to the heel of the wall of the structural wedge.

Note: nWetBasePTS is set equal to 2 and the coordinates of the toe and the heel of the wall are provided as input.

**Skip Part 4 input if HW = 0.**

**Part 4: nWetHeelPTS**

**X\_Wet\_Heel<sub>i</sub>, Y\_Wet\_Heel<sub>i</sub> (i=1 to nWetHeelPTS)**

with

nWetHeelPTS is the total number of points defining the wetted perimeter face of the structural wedge to soil driving wedge interface, progressing along a vertical imaginary section extending upwards from the heel of the wall to the surface of the water table in the retained soil.

X\_Wet\_Heel<sub>i</sub>, Y\_Wet\_Heel<sub>i</sub> are the coordinates of the wetted perimeter face of the structural wedge to soil driving wedge interface, progressing along a vertical imaginary section extending upwards from the heel of the wall to the surface of the water table in the retained soil.

Note: nWetHeelPTS is set equal to 2 and the coordinates of a line defined by two points: (1) the heel of the wall and (2) the point defined by the intersection of a vertical line extending from the heel to the surface of the water table.

**Group 6.1 – Simplified Sliding Block Analysis Input (when KEY\_CWSLIP\_analysis = 1), with Input in Four Parts:**

**Part 1: Key\_AandM\_50, Key\_AandM\_95, Key\_CandB\_FandC, Key\_CandB\_N, Key\_WandL\_FandC, Key\_WandL\_95, Key\_RandE\_FandC, Key\_MandS**

with

Key_AandM_50 = 0	Do not compute permanent displacement via the Ambraseys and Menu (1988) mean relationship
Key_AandM_50 = 1	Compute permanent displacement via the Ambraseys and Menu (1988) mean relationship
Key_AandM_95 = 0	Do not compute permanent displacement via the Ambraseys and Menu (1988) relationship - 95% confident that the computed displacement will not be exceeded

Key_AandM_95 = 1	Compute permanent displacement via the Ambraseys and Menu (1988) relationship - 95% confident that the computed displacement will not be exceeded
Key_CandB_FandC = 0	Do not compute permanent displacement via the Cai and Bathurst (1996) mean upper bound relationship for the Franklin and Chang (1977) data
Key_CandB_FandC = 1	Compute permanent displacement via the Cai and Bathurst (1996) mean upper bound relationship for the Franklin and Chang (1977) data
Key_CandB_N = 0	Do not compute permanent displacement via the Cai and Bathurst (1996) mean upper bound relationship for the Newmark (1965) data
Key_CandB_N = 1	Compute permanent displacement via the Cai and Bathurst (1996) mean upper bound relationship for Newmark (1965) data
Key_WandL_50 = 0	Do not compute permanent displacement via the Whitman and Laio (1985a, 1985b) mean relationship
Key_WandL_50 = 1	Compute permanent displacement via the Whitman and Laio (1985a, 1985b) mean relationship
Key_WandL_95 = 0	Do not compute permanent displacement via the Whitman and Laio (1985a, 1985b) relationship - 95% confident that the computed displacement will not be exceeded
Key_WandL_95 = 1	Compute permanent displacement via the Whitman and Laio (1985) relationship - 95% confident that the computed displacement will not be exceeded
Key_RandE_FandC = 0	Do not compute permanent displacement via the Richards and Elms (1979) upper bound to the Franklin and Chang (1977) data



- Key\_RandE\_FandC = 1      Compute permanent displacement via the Richards and Elms (1979) upper bound to the Franklin and Chang (1977) data
- Key\_MandS = 0              Do not compute permanent displacement via the Makdisi and Seed (1978 lower and upper displacement curves
- Key\_MandS = 1              Compute permanent displacement via the Makdisi and Seed (1978) lower and upper displacement curves

## Part 2: ACCMAX, GACC

with

ACCMAX is the peak horizontal ground acceleration.

The value for GACC identifies the units of ACCMAX.

Value for GACC	Units
32.174	ft/sec <sup>2</sup>
386.086	in/sec <sup>2</sup>
9.80665	m/sec <sup>2</sup>
980.665	cm/sec <sup>2</sup>
9806.65	mm/sec <sup>2</sup>
1.0	G
980.665	gal

## Part 3: VELMAX, VELACC

with

VELMAX is the peak horizontal ground velocity.

The value for VELACC identifies the units of the VELMAX velocity value.

Value for VELACC	Units of Acceleration	Units of Velocity
32.174	ft/sec <sup>2</sup>	ft/sec
386.086	in/sec <sup>2</sup>	in/sec
9.80665	m/sec <sup>2</sup>	m/sec
980.665	cm/sec <sup>2</sup>	cm/sec
9806.65	mm/sec <sup>2</sup>	mm/sec

Note: Part 3 data is required when Key\_CandB\_FandC, Key\_CandB\_N, Key\_WandL\_FandC, Key\_WandL\_95, Key\_RandE\_FandC, or Key\_MandS are nonzero. If Key\_AandM\_50 and/or Key\_AandM\_95 is set equal to 1 and all other simplified analysis keys are set equal to zero, then Part 3 data is not required.

#### **Part 4: EQMAG**

with

EQMAG the Local (Richter) magnitude for the earthquake and equal to 6.5, 7.5, or 8.25.

Note: Part 4 data is required when Key\_MandS is nonzero, otherwise Part 4 data is not required.

#### **Group 6.2 – Acceleration Time-Histories for the Complete Sliding Block Analysis (when KEY\_CWSLIP\_analysis = 2), with Input in Two Parts**

##### **Part 1: NOACC, DT, GACC, XSCALE, YSCALE, KEYACCY**

with

NOACC is the total number of acceleration time-history values.

DT is the time-step in seconds.

GACC is the constant of acceleration due to gravity as given in the table below.

XSCALE is the scale factor applied to the horizontal acceleration time-history (negative value to invert time-history).

YSCALE is the scale factor applied to the vertical acceleration time-history (negative value to invert time-history).

and

KEYACCY is set to 0 in the case of horizontal and vertical acceleration time-histories.

or

KEYACCY is set to 1 in the case of a horizontal acceleration time-history and a constant vertical acceleration value. (When KEYACCY = 1, KEYkv must be set equal to 3 in Group 7 Analysis control data.)

Value for GACC	Units
32.174	ft/sec <sup>2</sup>
386.086	in/sec <sup>2</sup>
9.80665	m/sec <sup>2</sup>
980.665	cm/sec <sup>2</sup>
9806.65	mm/sec <sup>2</sup>
1.0	G
980.665	gal

**Part 2:** In the case of KEYACCY = 0, input  
**T(i=1 to NOACC), ACCX(I=1 to NOACC), ACCY(I=1 to NOACC)**

or

In the case of KEYACCY = 1, input  
**T(i=1 to NOACC), ACCX(I=1 to NOACC)**

Note: Horizontal and vertical inertial forces act in the direction opposite to the direction of the horizontal and vertical accelerations.

All time-histories are required to have zero acceleration value(s) for T(1) = 0.0 in the data input file.

Values for the horizontal accelerations used in CWSlip are equal to ACCX(I) times XSCALE times GACC.

Values for the vertical accelerations used in CWSlip are equal to ACCY(I) times YSCALE times GACC.

#### **Group 7 – Analysis controls.**

##### **KEYkv, constACCY, KEYanalysis**

with

KEYkv = 0 Simplified Sliding Block Analysis – no vertical acceleration time-history is used.

And for a complete time-history analysis:

KEYkv = 1 Use the vertical acceleration time-history ACCY(I=1 to NOACC) to determine a representative constant value for the vertical acceleration during those time-steps when the structural wedge slides. This requires an iterative process involving sequential executions of CWSlip, during which an updated value for the constant constACCY is specified.

Note:

1. KEYanalysis (see input below) must be set equal to 1 in this case and value for constACCY (see input below) is required.
2. Recommendation: For the first evaluation, the value for constACCY is usually set equal to zero.
3. Recommendation: For the second evaluation, the value for constACCY may be set to the average value for the vertical acceleration computed during those time-steps when the structural wedge slides (reported in the CWSlip output), determined from the output from the first KEYkv = 1 analysis.
4. The KEYanalysis = 1 analysis is repeated using updated constACCY values until the change in constACCY value and the vertical acceleration computed during those time-steps when the structural wedge slides is sufficiently small.

KEYkv = 2 Evaluation using the current vertical acceleration time-history ACCY(I=1 to NOACC). <Not available>

Note: KEYanalysis (see input below) must be set equal to 2 in this case.

KEYkv = 3 Evaluation using a constant value for the vertical acceleration constACCY (see below).

Note: KEYkv must be set equal to 3 when KEYACCY = 1 (in Group 6.2 data).

with

constACCY = Constant value for the vertical acceleration (may be used in either a simplified sliding block analysis or a complete time-history analysis). This can be an average vertical acceleration during sliding or during rotation. Specified in the same units as the acceleration time-histories of Group 6 (Units consistent with the value of GACC).

Note: Value for constACCY is used to compute the value for the horizontal yield acceleration in a sliding analysis (designated as cofkhslide in the output file WORKslide.TMP) or to compute the value for the horizontal acceleration for which there is incipient lift-off of the structural wedge from its foundation in rotation (designated as cofkhrotate in the output file WORKrotate.TMP).

and

KEYanalysis = 1 Sliding analysis of the structural wedge.

**Group 8 – Units for Output of Acceleration, Velocity, and Displacement Time-histories.**

**DISPACC** - The value for DISPACC identifies the units of the scaled acceleration, computed velocity, and computed displacements according to the table below in a complete time-history analysis. For a simplified sliding block analysis, DISPACC designated the units for the computed permanent wall displacement.

Value for DISPACC	Units of Acceleration	Units of Velocity	Units of Displacement
32.174	ft/sec <sup>2</sup>	ft/sec	feet
386.086	in/sec <sup>2</sup>	in/sec	inches
9.80665	m/sec <sup>2</sup>	m/sec	meters
980.665	cm/sec <sup>2</sup>	cm/sec	centimeters
9806.65	mm/sec <sup>2</sup>	mm/sec	millimeters

## Appendix G: Listing of CorpsWallSlip ASCII Output Files

This appendix lists the CorpsWallSlip ASCII Output Files. Table G.1 lists the output box labels and corresponding (tape) files for the visual modeler **Analysis** tab and briefly describes the contents.

Table G.1. Output data files used by output boxes in the visual modeler **Analysis** tab.

Visual Modeler Output Box Label	Name of Tape	Description
Show Log of CWSlip Execution	CWSLIP.RUN	Summary of execution steps and limited results.
Show Input Echo of CWSlip Execution	CWSLIP.OUT	Echo of key input variables assigned by the visual modeler.
Plot AccX	PLOTaccX.TMP	Scaled horizontal acceleration time-history.
Show AccX	WORKaccX.TMP	Show data file of scaled horizontal acceleration time-history.
Plot AccY	PLOTaccY.TMP	Scaled vertical acceleration time-history.
Show AccY	WORKaccY.TMP	Show data file of scaled vertical acceleration time-history.
Plot AccYX	PLOTaccYX.TMP	Scaled X- and Y- time-histories and ratio of a scaled-ACCY divided by scaled-ACCX.
Show AccYX	WORKaccYX.TMP	Show data file of scaled X- and Y- time-histories and ratio of a scaled-ACCY divided by scaled-ACCX.
Show Sliding Evaluation	WORKslide.TMP	Iteration results for Maximum Transmissible Acceleration; yield acceleration (horizontal) for structural wedge slide limit state. Boundary water pressures to the structural wedge, when present, are listed in this file. When water is present, the resultant water pressure forces acting on the structural wedge are reported in this file. For the simplified sliding block analysis, the computed permanent displacements are reported in this file.
Show Lift-Off Acceleration	WORKSlip.TMP	Iteration results for Maximum Acceleration resulting in lift-off of the structural wedge from its foundation with rotation about its toe. Boundary water pressures to the structural wedge, when present, are listed in this file. When water is present, the resultant water pressure forces acting on the structural wedge are reported in this file.
Plot PA File	PLOTpa.TMP	Sweep-search wedge results of $\alpha$ versus P and the resulting static active earth pressure force $P_A$ . A single sweep-search wedge solution is contained in this file using $SMF = 1.0$ .

Visual Modeler Output Box Label	Name of Tape	Description
Show PA File	WORKpa.TMP	Sweep-search wedge results of $\alpha$ versus P and the resulting static active earth pressure force, $P_A$ . A single sweep-search wedge solution is contained in this file, calculated using $SMF = 1.0$ .
Plot PO File	PLOTpo.TMP	Sweep-search wedge results of $\alpha$ versus P and the resulting approximation for the static at-rest earth pressure force $P_o$ . A single sweep-search wedge solution is contained in this file, calculated using $SMF = 1/1.5=0.67$ . The value for $P_o$ is not used in the sliding nor rotational rigid block calculations of the initial version of CWSlip.
Show PO File	WORKpo.TMP	Sweep-search wedge results of $\alpha$ versus P and the resulting approximation for the static at-rest earth pressure force $P_o$ . A single sweep-search wedge solution is contained in this file, calculated using $SMF = 1/1.5=0.67$ . The value for $P_o$ is not used in the sliding nor rotational rigid block calculations of the initial version of CWSlip.
Plot PAE File	PLOTpae.TMP	Sweep-search wedge results of $\alpha$ versus P and the resulting dynamic active earth pressure force $P_{AE}$ . This file contains results from multiple analyses. When a rotational rigid block time-history analysis is conducted, this file can become quite large. Drop down menu options can be used to plot user-selected $P_{AE}$ plot numbers. $P_{AE}$ run numbers are identified in various output files.
Show PAE File	WORKpae.TMP	Sweep-search wedge results of $\alpha$ versus P and the resulting dynamic active earth pressure force $P_{AE}$ . This file contains results from multiple analyses. Drop down menu options can be used to view user-selected $P_{AE}$ analyses. $P_{AE}$ run numbers are identified in other output files.
Plot Sliding Time History	PLOTslideTH.TMP	Time-history of sliding block analysis.
Show Sliding Time History	PLOTslideTH.TMP	Show data file of time-history of sliding block analysis.
Plot Effective Vertical Acc.	PLOTKEYkv1TH.TMP	Time-history of effective vertical acceleration during sliding analysis with $KEYkv = 1$
Show Effective Vertical Acc.	PLOTKEYkv1TH.TMP	Show data file of time-history of effective vertical acceleration during sliding analysis with $KEYkv = 1$

A second table, Table G.2 lists other tape files generated in each Corps  $W_{allSlip}$  analysis and briefly describes the contents.

Table G.2. Output data files used by output boxes in the visual modeler **Analysis** tab.

Name of Tape	Description
–	Print to screen a summary of execution steps and limited results. Same information as is contained in CWSLIP.RUN.
OUTPUTpa.TMP	Summary of forces acting on each wedge in a sweep-search wedge analysis of $\alpha$ versus $P_A$ (static active earth pressure force). A single sweep-search wedge solution is contained in this file.
OUTPUTpo.TMP	Summary of forces acting on each wedge in a sweep-search wedge analysis of $\alpha$ versus $P_o$ (static at-rest earth pressure force). A single sweep-search wedge solution is contained in this file.
OUTPUTpae.TMP	Summary of forces acting on each wedge in a sweep-search wedge analysis of $\alpha$ versus $P_{AE}$ (pseudo-static active earth pressure force). This file contains results from multiple analyses.



## Appendix H: Earth Pressure Distribution and Depth of Cracking in a Cohesive Retained Soil – Static Active Earth Pressures

This appendix summarizes for static loading the results of sweep-search analyses of two types of cohesive soils, the first being an effective stress analysis with Mohr-Coulomb effective stress shear strength parameters  $c'$  and  $\phi'$  used to characterize the shear strength of the retained soil and the second case for a backfill in which Mohr-Coulomb total stress shear strength parameter  $c$  is set equal to the undrained shear strength,  $S_u$ , and with  $\phi$  is set equal to zero. The objective of this appendix is to demonstrate the trial-and-error procedure used to determine the depth of cracking in a cohesive soil as well as the resulting static active earth pressure distribution that is applied to the structural wedge in a CorpsWallSlip analysis.

Background: The sole purpose of a  $P_A$  computation in a CorpsWallSlip analysis is to determine the value for  $h_{PAE}$ , the resultant location for  $P_{AE}$ . The procedure used is outlined in Appendix C. The approach used can also be interpreted in terms of an equivalent earth pressure distribution applied to the structural wedge by the driving soil wedge in a CorpsWallSlip analysis that is made up of two components, the earth pressure distribution due to the static active earth pressures and a trapezoidal earth pressure distribution due to the incremental dynamic force component  $\Delta P_{AE}$  (with  $\Delta P_{AE} = P_{AE} - P_A$ ). The methodologies discussed in Appendix A are used by CorpsWallSlip to first determine the resultant earth pressure forces,  $P_A$  and  $P_{AE}$ , and then the methodologies discussed in Appendix C are used to compute the resulting earth pressure distributions for  $P_A$  and  $\Delta P_{AE}$ , respectively. In order to compute values of  $P_{AE}$  and  $P_A$  by the dynamic and static sweep-search solutions of trial soil wedges, a depth of cracking needs to be specified in each sweep-search analysis made by CorpsWallSlip of a cohesive soil. Initial sweep-search soil wedge solutions are always made assuming a zero depth of crack. This is sufficient for the  $P_{AE}$  computation, as discussed previously. However, an iterative procedure is used to determine the value for the depth of cracking in the analysis of  $P_A$  in cohesive soils and the corresponding earth pressure distribution (which includes both compression as well as tensile stresses). After the resulting static earth pressure force,  $P_A$ , computation is completed, a resulting earth

pressure distribution is constructed and new depth of cracking for static loading is determined. CorpsWallSlip then proceeds with second sweep-search trial wedge analysis of the retained soil for a new value for  $P_A$  corresponding to this new, nonzero crack depth value. A new static earth pressure distribution and new crack depth is determined. The process is repeated until the depth of cracking used in the sweep-search trial wedge analysis and the depth of cracking determined from the static active earth pressure distribution are nearly the same value. This iterative procedure is demonstrated for two examples in this appendix.

In the special case of cohesive soils, the CorpsWallSlip analysis disregards the tensile stresses when defining the static active earth pressures and the corresponding resulting static active earth pressure force to be applied to the structural wedge, as well as when computing the resulting force location,  $h_{PA}$ , of this modified stress distribution. A trapezoidal earth pressure distribution is used to define  $\Delta P_{AE}$  for cohesive as well as cohesionless soils.

## H.1 Example No. 1: Effective Stress Analysis of a Cohesive Soil

Consider the case of the Figure H.1 20-ft-high, moist, cohesive, retained soil with  $c' = 200$  psf,  $\phi' = 10$  degrees,  $\delta = 0$  degrees, and  $\gamma_{\text{moist}} = 110$  psf. The first step in the CorpsWallSlip analysis of this static earth pressure problem is a sweep-search trial wedge analysis starting with assumption that the depth of cracking is equal to zero. This results in a computed  $P_A$  value equal to 8,105.9 per ft run of wall using the method outlined in Section A.3 of Appendix A for a planar slip surface with  $\alpha_A$  computed to be 50 degrees from horizontal. The second step is to compute the corresponding earth pressure distribution and depth of cracking using the procedure outlined in Section C.3 of Appendix C. This active earth pressure distribution resulted in a depth of cracking equal to 4.767 ft. Ignoring the tensile stresses within the depth of cracking, as is done by CorpsWallSlip, the resultant net force,  $P_{\text{AstaticPOSa}}$ , corresponding to the computed triangular compressive earth pressure stress distribution, is equal to 8,985.9 lb per ft run of wall with a point of application at 5.078 ft at the end of this first iteration. These results are consistent with the results given in Example 6-4 of Bowles (1968). Since the depth of cracking from the active earth pressure distribution (i.e., 4.767 ft) is so different from the value assumed in the sweep-search trial wedge solution for  $P_A$  (i.e., 0 ft), additional analyses are required.

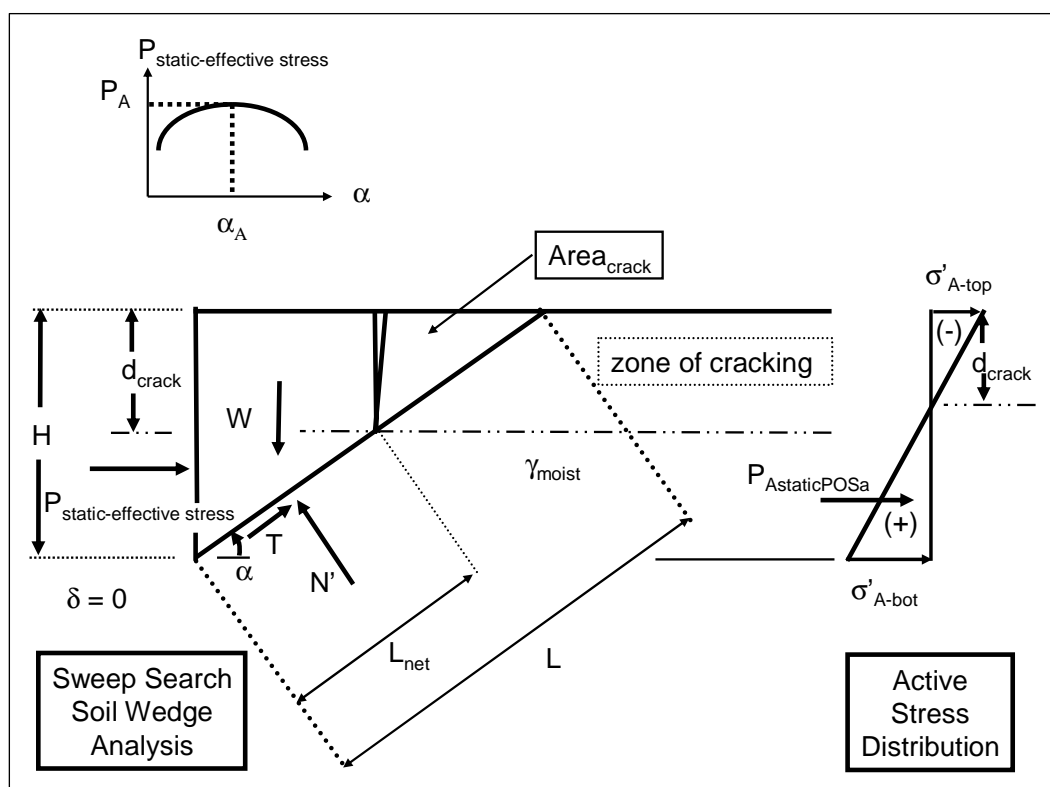


Figure H.1. Sweep-search trial wedge analysis of a cohesive retained soil and the corresponding active earth pressure distribution – effective stress analysis.

The second sweep-search trial wedge analysis starts with an assumption of 4.767 ft for the depth of cracking, as indicated in Table H.1. A total of four iterations are required to converge on a depth of cracking in which the depth of crack used in the sweep-search soil wedge analysis results are consistent with the depth of cracking resulting from the active stress distribution. In the final iteration (i.e., number 4), the net active force corresponding to the compressive stress distribution starting 3.973 ft below top of wall is equal to 9,549.7 lb per ft run of wall. Note that the sweep-search active soil wedge solution for  $\alpha_A$  equal to 50 deg is computed to be equal to 8,962.9 lb per ft run of wall. These two values differ because  $P_A$  is computed by the sweep-search (active) wedge solution and includes the contribution of tensile stresses due to cohesion in the retained soil (e.g., refer to Equation A.27).

Table H.1. Iterative results from the static sweep-search wedge analysis of a cohesive soil – effective stress.

Iteration No.	Depth of Crack Used in Sweep-Search Soil Wedge Analysis (ft)	$\alpha_A$ (deg)	$P_{AstaticMAXa}$ (lb per ft of run wall)	$\sigma'_{A-top}$ (psf)	$\sigma'_{A-bot}$ (psf)	$P_{AstaticPOSa}$ (lb per ft of run wall)	$H_{PAstatica}$ (ft)	Depth of Crack Resulting From Active Stress Distribution (ft)
1	0	50	8105.9	-369.2	1,179.80	8,985.9	5.078	4.767
2	4.767	50	8985.9	-281.2	1,179.80	9,527.1	5.384	3.849
3	3.849	50	8953.3	-298.1	1,193.40	9,549.2	5.334	3.998
4	3.998	50	8962.9	-295.4	1,191.70	9,549.7	5.342	3.973

## H.2 Example No. 2: Total Stress Analysis of a Cohesive Soil

Consider the case of the Figure H.2 20-ft-high, moist, cohesive, retained soil with  $S_u = 600$  psf (with  $\phi = 0$  degrees),  $\delta = 0$  degrees, and  $\gamma_{moist} = 130$  psf. The first step in the CorpsWallSlip analysis of this static earth pressure problem is a sweep-search trial wedge analysis starting with assumption that the depth of cracking is equal to zero. This results in a computed  $P_A$  value equal to 2,000 per ft run of wall using the method outlined in Section A.5 of Appendix A for a planar slip surface with  $\alpha_A$  computed to be 45 degrees from horizontal. The second step is to compute the corresponding earth pressure distribution and depth of cracking using the procedure outlined in Section C.4 of Appendix C. This active earth pressure distribution resulted in a depth of cracking equal to 9.231 ft. Ignoring the tensile stresses within the depth of cracking, as is done by CorpsWallSlip, the resultant net force,  $P_{AstaticPOSa}$ , corresponding to the computed triangular compressive earth pressure stress distribution, is equal to 7,538.5 lb per ft run of wall with a point of application at 3.59 ft at the end of this first iteration.

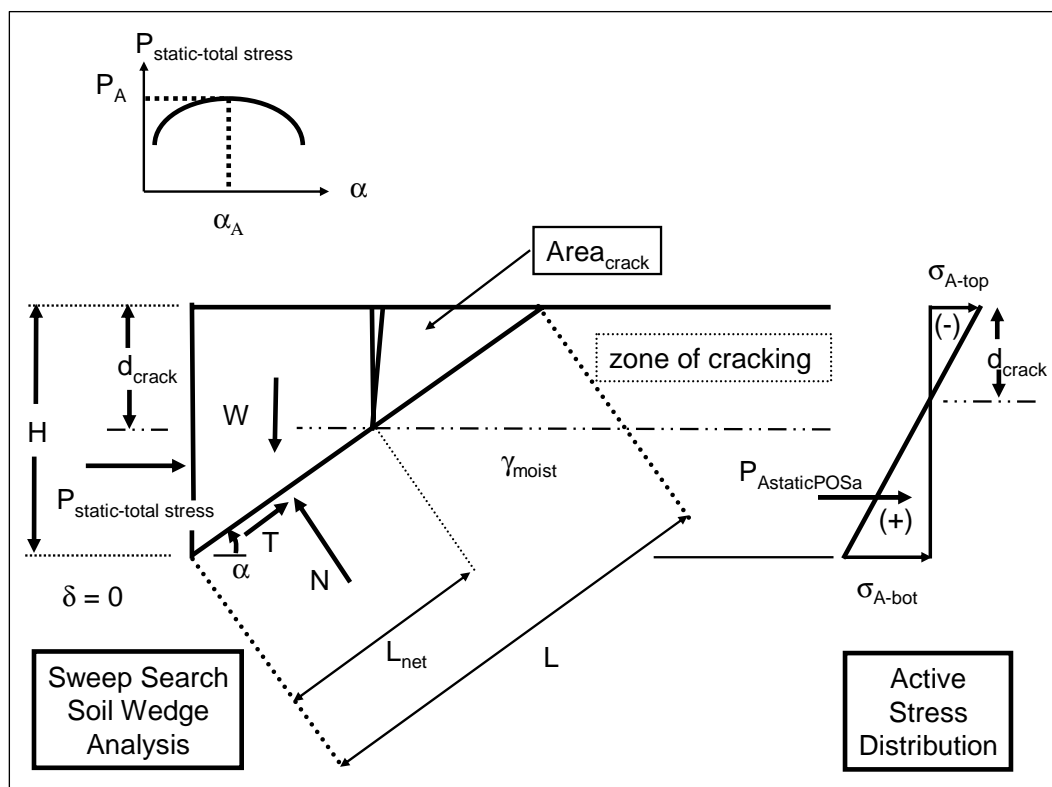


Figure H.2. Sweep-search trial wedge analysis of a cohesive retained soil and the corresponding active earth pressure distribution – total stress analysis.

These Corps *WallSlip* analysis results are consistent with the results for a Rankine active earth pressure distribution, for which the horizontal stress at any depth is given by

$$\sigma_a = K_A \cdot \gamma_{moist} \cdot \text{depth} - 2 \cdot c \cdot \sqrt{K_A} \quad (\text{H.1})$$

with

$$K_A = \tan^2 \left( 45 - \frac{\phi}{2} \right) \quad (\text{H.2})$$

Solving Equation H.1 for the depth of zero active horizontal earth pressure results in a depth of cracking of

$$d_{crack} = \frac{2 \cdot c \cdot \sqrt{K_A}}{K_A \cdot \gamma_{moist}} \quad (\text{H.3})$$

With  $\phi$  equal to zero and  $c$  set equal to  $S_u$  in this problem, Equations H.1 and H.3 simplify to

$$\sigma_a = \gamma_{moist} \bullet depth - 2 \bullet S_u \quad (H.4)$$

and

$$d_{crack} = \frac{2 \bullet S_u}{\gamma_{moist}} \quad (H.5)$$

With  $S_u$  equal to 600 psf and  $\gamma_{moist} = 130$  psf, the horizontal active earth pressure at the ground surface and at a 20-ft depth are computed to be -1,200 psf and 1,400 psf, respectively, by Equation H.4. Additionally, the depth of cracking is computed to be 9.231 ft below the ground surface. These results are consistent with those from the first iteration of the CorpsWallSlip analysis, summarized in Table H.2. Since the depth of cracking from the active earth pressure distribution (i.e., 9.231 ft) is so much greater than the value assumed in the sweep-search trial wedge solution for  $P_A$  (i.e., 0 ft), additional analyses are required.

Table H.2. Iterative results from the static sweep-search wedge analysis of a cohesive soil – total stress.

Iteration No.	Depth of Crack Used in Sweep-Search Soil Wedge Analysis (ft)	$\alpha_A$ (deg)	$P_{AstaticMAXa}$ (lb per ft of run wall)	$\sigma_{A-top}$ (psf)	$\sigma_{A-bot}$ (psf)	$P_{AstaticPOSa}$ (lb per ft of run wall)	$H_{PAstatica}$ (ft)	Depth of Crack Resulting from Active Stress Distribution (ft)
1	0	45	2000.0	-1200.0	1,400.0	7,538.5	3.590	9.231
2	9.231	45	7538.5	-646.2	1,400.0	9,578.9	4.561	6.316
3	6.316	45	6986.1	-821.1	1,519.7	9,866.1	4.328	7.015
4	7.015	45	7219.4	-779.1	1,501.0	9,881.4	4.389	6.834
5	6.834	45	7165.0	-790.0	1,506.5	9,882.5	4.373	6.880

The second sweep-search trial wedge analysis starts with an assumption of 9.231 ft for the depth of cracking, as indicated in Table H.2. A total of five iterations are required to converge on a depth of cracking in which the depth of crack used in the sweep-search soil wedge analysis results are consistent with the depth of cracking resulting from the active stress distribution. In the final iteration (i.e., number 5), the net active force

corresponding to the compressive stress distribution starting 4.373 ft below top of wall is equal to 9,882.5 lb per ft run of wall. Note that the sweep-search active soil wedge solution for  $\alpha_A$  equal to 45 deg is computed to be equal to 7,165 lb per ft run of wall. These two values differ because  $P_A$  is computed by the sweep-search (active) wedge solution and includes the contribution of tensile stresses due to cohesion in the retained soil (e.g., refer to Equation A.31).

REPORT DOCUMENTATION PAGE				Form Approved OMB No. 0704-0188	
Public reporting burden for this collection of information is estimated to average 1 hour per response, including the time for reviewing instructions, searching existing data sources, gathering and maintaining the data needed, and completing and reviewing this collection of information. Send comments regarding this burden estimate or any other aspect of this collection of information, including suggestions for reducing this burden to Department of Defense, Washington Headquarters Services, Directorate for Information Operations and Reports (0704-0188), 1215 Jefferson Davis Highway, Suite 1204, Arlington, VA 22202-4302. Respondents should be aware that notwithstanding any other provision of law, no person shall be subject to any penalty for failing to comply with a collection of information if it does not display a currently valid OMB control number. PLEASE DO NOT RETURN YOUR FORM TO THE ABOVE ADDRESS.					
1. REPORT DATE (DD-MM-YYYY) June 2007		2. REPORT TYPE Final report		3. DATES COVERED (From - To)	
4. TITLE AND SUBTITLE  Transitional Response of Toe-Restrained Retaining Walls to Earthquake Ground Motions Using CorpsWallSlip (CWSlip)				5a. CONTRACT NUMBER	
				5b. GRANT NUMBER	
				5c. PROGRAM ELEMENT NUMBER	
6. AUTHOR(S)  Robert M. Ebeling, Amos Chase, and Barry C. White				5d. PROJECT NUMBER	
				5e. TASK NUMBER	
				5f. WORK UNIT NUMBER	
7. PERFORMING ORGANIZATION NAME(S) AND ADDRESS(ES) U.S. Army Engineer Research and Development Center Information Technology Laboratory 3909 Halls Ferry Road, Vicksburg, MS 39180-6199; Science Applications International Corporation 3532 Manor Drive, Suite 4, Vicksburg, MS 39180				8. PERFORMING ORGANIZATION REPORT NUMBER  ERDC/ITL TR-07-1	
9. SPONSORING / MONITORING AGENCY NAME(S) AND ADDRESS(ES) U.S. Army Corps of Engineers Washington, DC 20314-1000				10. SPONSOR/MONITOR'S ACRONYM(S)	
				11. SPONSOR/MONITOR'S REPORT NUMBER(S)	
12. DISTRIBUTION / AVAILABILITY STATEMENT Approved for public release; distribution is unlimited.					
13. SUPPLEMENTARY NOTES					
14. ABSTRACT  This research report describes the engineering formulation and corresponding software developed for the translational response of rock-founded retaining walls buttressed at their toe by a reinforced concrete slab to earthquake ground motions. The PC software CorpsWallSlip (sometimes referred to as CWSlip) was developed to perform an analysis of the permanent sliding displacement response for each proposed retaining wall section to either a user-specified earthquake acceleration time-history via a Complete Time History Analysis or to user-specified peak ground earthquake response values via a Simplified Sliding Block Analysis. The resulting engineering methodology and corresponding software is applicable to a variety of retaining walls that are buttressed at their toe by a structural feature (e.g., navigation walls retaining earth, spillway chute walls, spillway discharge channel walls, approach channel walls to outlet works structures, highway and railway relocation retaining walls, and floodwall channels). CorpsWallSlip is particularly applicable to L-walls and T-walls (usually referred to as cantilever retaining walls). It may also be used to predict permanent seismically induced displacements on retaining walls without a toe restraint. Companion PC software, CorpsWallRotate, was developed to perform an analysis of permanent wall rotation. Both CorpsWallSlip and CorpsWallRotate software perform engineering calculations that help the engineer in assessment of the tendency for a retaining wall to slide or to rotate during earthquake shaking. <div style="text-align: right;">(Continued)</div>					
15. SUBJECT TERMS		Earthquake ground motions		Seismic	
Displacement		Earth retaining structures		Soil dynamics	
Dynamic earth pressures		CorpsWallSlip		Translation	
16. SECURITY CLASSIFICATION OF:			17. LIMITATION OF ABSTRACT	18. NUMBER OF PAGES  272	19a. NAME OF RESPONSIBLE PERSON
a. REPORT UNCLASSIFIED	b. ABSTRACT UNCLASSIFIED	c. THIS PAGE UNCLASSIFIED			19b. TELEPHONE NUMBER (include area code)



#### 14. ABSTRACT (concluded)

Formal consideration of the permanent seismic wall displacement in the seismic design process for Corps-type retaining structures is given in Ebeling and Morrison (1992). The key aspect of the engineering approach presented in this 1992 document is that simplified procedures for computing the seismically induced earth loads on Corps retaining structures are also dependent upon the amount of permanent wall displacement that is expected to occur for each specified design earthquake. The Ebeling and Morrison simplified engineering procedures for Corps retaining structures, including waterfront retaining structures, are geared towards hand calculations. The engineering formulation and corresponding PC software  $C_{\text{corps}}W_{\text{allSlip}}$  discussed in this report extend these simplified procedures to walls that slide during earthquake shaking and make possible the use of acceleration time-histories in the Corps design/analysis process when time-histories are made available on Corps projects. The engineering methods contained in this report and implemented within  $C_{\text{corps}}W_{\text{allSlip}}$  allow the engineer to rapidly determine if a given retaining wall system has a tendency to slide or to rotate for a specified seismic event.